

This electronic thesis or dissertation has been downloaded from the King's Research Portal at <https://kclpure.kcl.ac.uk/portal/>



Cathepsin S and protease activated receptor-2 new players in the sensation of itch

Chung, Keshi

Awarding institution:
King's College London

The copyright of this thesis rests with the author and no quotation from it or information derived from it may be published without proper acknowledgement.

END USER LICENCE AGREEMENT



Unless another licence is stated on the immediately following page this work is licensed

under a Creative Commons Attribution-NonCommercial-NoDerivatives 4.0 International

licence. <https://creativecommons.org/licenses/by-nc-nd/4.0/>

You are free to copy, distribute and transmit the work

Under the following conditions:

- Attribution: You must attribute the work in the manner specified by the author (but not in any way that suggests that they endorse you or your use of the work).
- Non Commercial: You may not use this work for commercial purposes.
- No Derivative Works - You may not alter, transform, or build upon this work.

Any of these conditions can be waived if you receive permission from the author. Your fair dealings and other rights are in no way affected by the above.

Take down policy

If you believe that this document breaches copyright please contact librarypure@kcl.ac.uk providing details, and we will remove access to the work immediately and investigate your claim.

Cathepsin S and protease activated receptor-2: new players in the sensation of itch

Keshi Chung

Thesis presented for the degree of
Doctor of Philosophy
at King's College London

Wolfson Centre for Age Related Diseases
King's College London

2018

Abstract

Whilst acute itch is a beneficial sensation that serves to remove irritants and potentially harmful agents from the skin by eliciting a scratch reflex, chronic itch is a debilitating condition associated with a reduction in quality of life and the development of skin lesions that risk becoming infected. Moreover, few effective treatments exist for chronic itch conditions, particularly those associated with skin diseases such as atopic dermatitis.

Cathepsin S is a protease that has recently been demonstrated to be involved in pruritus. Preliminary work in our lab demonstrated that intradermal injection of Cathepsin S results in scratching behaviour in mice, while others have found that over-expression of Cathepsin S results in the development of atopic dermatitis-like conditions. However, the source of Cathepsin S in itch conditions, whether Cathepsin S directly activates sensory neurons and the receptors on which it acts to mediate its effects, and whether it causes the release of neurotransmitters from primary afferent fibres had not been addressed. We thus sought to further investigate Cathepsin S-mediated itch.

We found that skin keratinocytes are a potential source of Cathepsin S, expression of which is upregulated in inflammatory conditions similar to those found in atopic dermatitis. Furthermore, Cathepsin S can be released from these cells following stimulation of TRPV4, and propose that alterations in skin hydration and pH in conditions such as atopic dermatitis might result in increased activity of this channel and hence release of Cathepsin S. We established that Cathepsin S activates sensory neurons *in vitro* via protease activated receptor 2 (PAR2) and that Cathepsin S-responding neurons belonged to the TRPV1/TRPA1-expressing subset of neurons. Finally, we found that intraplantar Cathepsin S injection results in activation of neurons in the outer laminae of the dorsal horn of the spinal cord, although we could not demonstrate the occurrence of release of neurotransmitters or neuropeptides from the central terminals of primary afferent neurons.

In conclusion, we have identified a pathway for Cathepsin S-induced itch as release of this protease from keratinocytes activates TRPV1/TRPA1-expressing neurons via PAR2 activation, and engages neurons in the dorsal horn that likely comprise part of the central itch circuitry.

Acknowledgements

Firstly I would like to thank my primary supervisor, Prof. Marzia Malcangio, for her support, expertise, and patience throughout this challenging and fascinating PhD. I would also like to thank my second supervisors, Dr Andy Grant for all his help and guidance throughout my time at the Wolfson, and Dr Reggie Docherty who is much missed at the Wolfson and I hope is enjoying his retirement.

I must also thank our collaborators at Medivir, not only for working with us and providing us with Cathepsin S to use in our experiments but also for the opportunity to spend time with them during my PhD. I am especially grateful to Erik Lindstrom for his supervision, and Ian Henderson and Gun Stenberg for their help in making Cathepsin S.

I would also like to thank everyone in the Wolfson who made this PhD not only possible, but also an enjoyable experience. A big thanks to Karli, Anna, Liz, Yahyah, João, and Raf for teaching me many of the skills and techniques I required for my PhD. Thanks to Ben, Petra, Paco, Milena, Kelly, Egle, Rachel, Elin, Katja, and Leanne for their company in the lab and their friendship. A special thanks to Tom Pitcher for performing the scratching assays and his wisdom of behavioural studies, Stewart Bevan for assistance in calcium imaging and for providing us with transgenic mice, and Fran and Doug for help with qPCR. I must also thank Ping Yip at Queen Mary's for his help and guidance with in-situs.

Outside of the lab I would like to thank my family and all of my friends for their help and support in both science and non-science related matters. In particular I would like to thank my mum for her support and encouragement and for always believing in me, and my good friends Laura, Wendy, Polly, Louise, Michele, Nicos, Martin, Patrick, Richard, Angela, Judith, Jenna, Tim, Amanda, Charlie, and many others for making sure I had a life outside of the lab doing very important things. Finally, I would like to thank my partner Brendan for putting up with me for all of these years, for always being there, and for making sure dinner was ready on nights when I came home late from the lab.

Table of contents

Abstract	2
Table of contents	4
List of figures and tables	7
List of abbreviations.....	11
Chapter 1	17
1.1 The skin as a source of pruritogens	18
1.2 Peripheral itch pathways.....	32
1.2.1 Histaminergic itch and TRPV1.....	38
1.2.2 Non-histaminergic itch	43
1.2.3 Peripheral sensitisation of itch	47
1.3 Central itch pathways	48
1.3.1 Glutamate and itch.....	52
1.3.2 Neuropeptides in itch.....	54
1.3.3 Central sensitisation of itch	64
1.4 Pathology of itch and the role of Cathepsin S in chronic itch	64
1.5 Animal models of itch	70
1.5.1 Cathepsin S-induced itch	76
1.6 Protease activated receptors	79
1.6.1 Protease activated receptors and itch	89
1.6.2 Protease activated receptor 2 and Cathepsin S	92
1.7 Thesis aims.....	93
Chapter 2	95
2.1 Introduction	95
2.2 Methods.....	102
2.2.1 HaCaT cell line culture	102
2.2.2 Immunocytochemistry and image acquisition	102
2.2.3 Western blotting	104
2.2.4 Quantitative polymerase chain reaction (qPCR)	106

2.2.5 Cathepsin S activity assays	107
2.2.6 Statistical Analysis.....	110
2.3 Results	110
2.3.1 Expression of Cathepsin S protein and mRNA.....	110
2.3.2 Intracellular Cathepsin S activity	116
2.3.3 Extracellular Cathepsin S activity.....	118
2.4 Discussion	126
Chapter 3	135
3.1 Introduction	135
3.2 Methods.....	137
3.2.1 Production of human recombinant Cathepsin S in baculovirus.....	137
3.2.2 Isolation and culture of mouse dorsal root ganglia.....	141
3.2.3 Patch clamping.....	143
3.2.4 Calcium imaging	145
3.2.5 Quantitative Polymerase Chain Reaction (qPCR)	147
3.2.6 Data analysis and statistics.....	147
3.3 Results	148
3.3.1 Cathepsin S induces inward current in dorsal root ganglia	148
3.3.2 Cathepsin S-mediated calcium influx in dorsal root ganglia.....	152
3.4 Discussion	163
Chapter 4	173
4.1 Introduction	173
4.2 Methods.....	174
4.2.1 Quantitative polymerase chain reaction (qPCR)	174
4.2.2 Enzyme-linked immunosorbent assay (ELISA) for natriuretic polypeptide B.....	174
4.2.3 Immunohistochemical staining	175
4.2.4 In-situ hybridisation	176
4.2.5 Quantification of staining.....	179
4.2.6 Behavioural testing	180
4.2.7 Statistical analysis	181

4.3 Results	182
4.3.1 Intraplantar injection of Cathepsin S activates cells in the dorsal horn.....	182
4.3.2 Itch-related peptides are expressed in dorsal root ganglia and spinal cord	183
4.3.3 Release of natriuretic polypeptide B from sensory neurons	192
Chapter 5	207
References	217

List of figures and tables

Chapter 1: General introduction

Figure 1.1: Simplified schematic of the itch pathway

Figure 1.2: Schematic of the layers of the skin

Figure 1.3: Schematic of the corneocyte lipid envelope

Figure 1.4: Schematic of proposed itch theories

Figure 1.5: Schematic of targeted delivery of QX-314 following activation of neurons by a pruritogen

Figure 1.6: Characteristic wheal and flare response of skin following injection of histamine

Figure 1.7: Schematic of sensitisation of TRPV1 via histamine

Figure 1.8: Schematic of sensitisation of TRP channels via non-histaminergic pruritogens

Figure 1.9: Overview of itch circuitry in the dorsal horn

Figure 1.10: Behaviour observed following injection of hr-CatS into the cheek

Figure 1.11: Mechanism of PAR activation

Figure 1.12: Canonical and biased agonism of PAR2 by various proteases

Figure 1.13: Overview of hypothesised roles of MrgprC11 and PAR2 in itch and hyperalgesia

Table 1.1: Proteases found in skin keratinocytes

Table 1.2: Cytokines in skin conditions characterised by chronic itch

Table 1.3: Summary of neurotransmitters and neuropeptides in spinal cord itch circuitry

Table 1.4: Summary of animal models of chronic itch

Table 1.5: Cathepsin S-induced scratching behaviour in transgenic mice

Chapter 2: Cathepsin S in keratinocytes – intracellular expression and extracellular activity

Figure 2.1: Schematic of proposed mechanism of lysosomal Cathepsin S release from cells

Figure 2.2: Expression of Cathepsin S peptide and LAMP-1

Figure 2.3: Western blots for Cathepsin S and actin

Figure 2.4: qPCR products of mRNA extracted from HaCaT cells

Figure 2.5: Toll-like receptor-4 and Cathepsin S mRNA expression in HaCaTs is increased following incubation in LPS

Figure 2.6: Cathepsin S mRNA expression in HaCaTs is increased following incubation in IL-4 and IL-13

Figure 2.7: Cathepsin S activity is detected in HaCaT cell lysates and occurs at both acidic and neutral pH

Figure 2.8: Cathepsin S activity in HaCaT cell lysates is reduced by the Cathepsin S inhibitor MDV-590

Figure 2.9: LPS and ATP do not induce release of Cathepsin S from HaCaTs

Figure 2.10: IL-4 and IL-13 do not induce release of Cathepsin S from HaCaTs

Figure 2.11: Combined IL-4 and IL-13 treatment with LPS and ATP does not induce release of Cathepsin S from HaCaTs

Figure 2.12: TRPV4 activation induces the release of Cathepsin S from HaCaTs

Figure 2.13: Extracellular calcium is required for TRPV4-mediated release of Cathepsin S from HaCaTs

Table 2.1: List of primary and secondary antibodies used for immunocytochemistry

Table 2.2: Primers used for CA2, CCL26, NELL2, CatS, PAR2, TLR4, TRPV4 and 18S in qPCR

Table 2.3: Ct values for qPCR performed on HaCaTs following 3 or 6 hours incubation in vehicle (buffer) or LPS

Table 2.4: Ct values for qPCR performed on HaCaTs following 0, 24, Or 48 hours incubation in IL-4 and IL-13

Chapter 3: Activation of cultured sensory neurons by Cathepsin S

Figure 3.1: Comparison of human and mouse CatS (A) and PAR2 (B) peptide sequences

Figure 3.2: Dissection of DRGs from the spinal cord

Figure 3.3: Example current traces during patching of the neurons

Figure 3.4: Schematic of drug application and incubation protocol for calcium imaging experiments

Figure 3.5: Inward currents in neurons following direct application of capsaicin or KCl

Figure 3.6: Inward currents in neurons following direct application of Cathepsin S

Figure 3.7: Calcium increase in neurons following bath application of capsaicin and mustard oil

Figure 3.8: Calcium increase in neurons following bath application of Cathepsin S

Figure 3.9: Calcium increase in neurons following application of Cathepsin S (400 nM) in the presence of the Cathepsin S inhibitor MDV-590 or the PAR2 antagonist FSLLRY-NH₂

Figure 3.10: No calcium responses following application of the PAR2 agonist SLIGRL-NH₂

Figure 3.11: Reduction in response to Cathepsin S in TRPV1 KO and TRPA1 KO DRGs compared with WT controls

Figure 3.12: Most of the cells that responded to Cathepsin S also responded to capsaicin or mustard oil

Figure 3.13: Pre-application of Cathepsin S resulted in an increase in the percentage of cells that responded to either capsaicin or mustard oil

Table 3.1: Primers used for PAR2 and 18S in qPCR

Table 3.2: Data for Figure 3.5

Table 3.3: Data for Figure 3.6

Table 3.4: Data for Figure 3.7

Table 3.5: Data for Figure 3.8

Table 3.6: Data for Figure 3.9 A and B

Table 3.7: Data for Figure 3.11 C

Table 3.8: Ct values for PAR2 expression

Table 3.9: Data for Figure 3.10

Table 3.10: Data for Figure 3.11

Table 3.11: Increase in the number of cells that responded to capsaicin or mustard oil following pre-incubation with Cathepsin S

Chapter 4: Activation of dorsal horn neurons and release of itch-related peptides by intraplantar Cathepsin S

Figure 4.1: Schematic of fluorescent in-situ hybridisation staining protocol

Figure 4.2: Injection of Cathepsin S into the hindpaw resulted in an increase in the number of pERK positive cells in the ipsilateral side of the dorsal horn of the spinal cord

Figure 4.3: Expression of NPPB and GRP mRNA in mouse DRG tissues

Figure 4.4: Expression and quantification of NPPB mRNA in mouse TG

Figure 4.5: Expression of NPPB peptide in mouse TG, DRG, and spinal cord

Figure 4.6: Quantification of NPPB mRNA and NPPB peptide in mouse DRG

Figure 4.7: Quantification of NPPB mRNA and CGRP peptide in mouse DRG

Figure 4.8: Expression of NPPB, CGRP, and IB4 peptides in the spinal cord dorsal horn

Figure 4.9: NGF-induced thermal hyperalgesia

Figure 4.10: The effect of NGF on the expression of NPPB in DRGs

Figure 4.11: The effect of NGF on the expression of NPPB in the spinal cord

Figure 4.12: The effect of NGF on the expression of CGRP in the spinal cord

Figure 4.13: The release of NPPB was not detected from cultured DRGs

Figure 4.14: Cathepsin S induced mechanical hyperalgesia

Figure 4.15: No effect of Cathepsin S on staining for NPPB in the spinal cord

Figure 4.16: No effect of Cathepsin S on staining for CGRP in the spinal cord

Table 4.1: Primers used for NPPB, GRP, and β -actin in qPCR

Table 4.2: Table of primary and secondary antibodies used for immunocytochemistry

Table 4.3: Oligonucleotide probes used for in-situ hybridisation

Table 4.4: Ct values for NPPB and GRP expression

Chapter 5: General discussion

Figure 5.1: Activation of receptors and sensitisation of TRP channels by Cathepsin S

Figure 5.2: Proposed pathway of Cathepsin S-induced itch from the periphery to the brain

List of abbreviations

2-AG	2-arachidonoylglycerol
5-HT	5-hydroxytryptamine
5-HTR	5-hydroxytryptamine receptor
5-LO	5-lipoxygenase
12-HPETE	12-hydroxyeicosatetraenoic acid
12-LO	12-lipoxygenase
AA	Arachidonic acid
ABC	Avidin-biotin complex
ADA	Adenosine deaminase
APC	Activated protein C
AGR129	Type I (A) and type II (G) IFN receptor and recombination activating gene 2 deficient
AMPA	alpha-amino-3-hydroxy-5-methyl-4-isoxazolepropionic acid
ANOVA	Analysis of variance
APS	Ammonium persulfate
ATP	Adenosine triphosphate
BAM8-22	Bovine adrenal medulla 8-22 peptide
Bhlhb5	Basic helix loop helix transcription factor b5
BLAST	Basic local alignment search tool
BSA	Bovine serum albumin
CA2	Carbonic anhydrase II
Ca ²⁺	Calcium ions
CaCl ₂	Calcium chloride
cAMP	Cyclic adenosine monophosphate
CatS	Cathepsin S
CCL26	C-C motif chemokine ligand 26
CD4/8/90	Cluster of differentiation 4/8/90
cDNA	Complementary deoxyribonucleic acid
C/EBP	CCAAT-enhancer-binding protein
CGRP	Calcitonin gene related peptide
CNS	Central nervous system
CNQX	Cyanquixaline
CO ₂	Carbon dioxide

Ct	Cycle threshold
CXCR	C-X-C chemokine receptor
DAG	Diacylglycerol
DAPI	4',6-diamidino-2-phenylindole
DEFB4	Defensin beta-4
DEPC	Diethyl pyrocarbonate
DETC	Gamma delta T cells
Dix3	Dixin 3
DK-SFM	Defined keratinocyte serum-free medium
DMEM	Dulbecco's Modified Eagle Medium
DMSO	Dimethyl sulfoxide
DNA	Deoxyribonucleic acid
DRG	Dorsal root ganglia
DTT	Dithiothreitol
Dyn	Dynorphin
EC ₅₀	Half maximal effective concentration
EDTA	Ethylenediaminetetraacetic acid
EGF	Epidermal growth factor
EGFP	Enhanced green fluorescent protein
EGFR	Epidermal growth factor receptor
ELISA	Enzyme-linked immunosorbent assay
EP1	Prostaglandin E2 receptor 1
ERK1/2	Extracellular signal-regulated kinase 1/2
FITC	Fluorescein isothiocyanate
Foxn1	Forkhead box protein N1
FSLLRN-NH ₂	Phenylalanine-Serine-Leucine-Leucine-Arginine-Tyrosine-trifluoroacetate salt
FU	Fluorescence unit
GABA	Gamma-aminobutyric acid
Glu	Glutamate
Gly	Glycine
GM-CSF	Granulocyte-macrophage colony-stimulating factor
GPCR	G protein-coupled receptor
GRP	Gastrin releasing peptide
GRPR	Gastrin releasing peptide receptor

H1R	Histamine-1 receptor
H3R	Histamine-3 receptor
H4R	Histamine-4 receptor
HaCaT	Human adult low calcium high temperature cells
hBD2	Human beta-defensin 2
HBSS	Hank's balanced salt solution
HEK293	Human embryonic kidney-293
HEPES	4-(2-hydroxyethyl)-1-piperazineethanesulfonic acid
hr-CatS	Human recombinant Cathepsin S
HRP	Horseradish peroxidase
IB4	Isolectin B4
IC ₅₀	Half maximal inhibitory concentration
IFN γ	Interferon gamma
IgE	Immunoglobulin E
IL	Interleukin
ILC	Innate lymphoid cell
IMAC	Immobilised metal ion affinity chromatography
IP ₃	Inositol 1,4,5-trisphosphate
IR	Immunoreactivity
JAK	Janus kinase
KCl	Potassium chloride
Klf4	Kruppel-like factor 4
KNRK	Kirsten Murine Sarcoma Virus transformed rat kidney epithelial cells
KO	Knock-out
KOR	Kappa-type opioid receptor
LAMP-1	Lysosomal-associated membrane protein 1
LTB4	Leukotriene B4
LPS	Lipopolysaccharide
MafB	Musculoaponeurotic fibrosarcoma oncogene homolog B
MAPK	Mitogen-activated protein kinase
MCA	Methylcoumarin
Mg ²⁺	Magnesium ions
MgCl ₂	Magnesium chloride
MHC	Major histocompatibility complex
Mrgpr	Mas-related G-protein coupled receptor

mRNA	Messenger ribonucleic acid
Na ₃ VO ₄	Sodium orthovanadate
NaCl	Sodium chloride
NaF	Sodium fluoride
NaOH	Sodium hydroxide
NELL2	Neural epidermal growth factor-like 2
NF-200	Neurofilament 200
NGF	Nerve growth factor
NiSO ₄	Nickel(II) sulfate
NK1R	Neurokinin-1 receptor
Nkp44+	Natural killer p44+ cells
Nkx2.5	NK2 homeobox 5
NMB	Neuromedin B
NMBR	Neuromedin B receptor
NMDA	N-methyl-D-aspartate
NMF	Natural moisturising factor
nNOS	Neuronal nitric oxide synthase
NPPA	Natriuretic polypeptide A
NPPB	Natriuretic polypeptide B
NPRA	Natriuretic Peptide Receptor A
NPRB	Natriuretic Peptide Receptor B
NPRC	Natriuretic Peptide Receptor C
OCT	Optimum Cutting Temperature
PAR	Protease activated receptor
Pax2	Paired box gene 2
PBS	Phosphate buffered saline
PBS-T	Phosphate buffered saline with Triton X
PEG4000	Polyethylene glycol-4000
pERK	Phosphorylated extracellular signal-regulated kinase
PFA	Paraformaldehyde
PGE ₂	Prostaglandin E2
PI3	Peptidase inhibitor 3
PIP ₂	Phosphatidylinositol 4,5-bisphosphate
PKA	Protein kinase A
PKC	Protein kinase C

PLA2	Phospholipase A2
PLC	Phospholipase C
PMSF	Phenylmethane sulfonyl fluoride
PNS	Peripheral nervous system
PWT	Paw withdrawal threshold
qPCR	Quantitative polymerase chain reaction
RhoE	Ras homolog gene family, member E
RNA	Ribonucleic acid
rRNA	Ribosomal ribonucleic acid
SCID	Severe combined immunodeficiency
SDS	Sodium dodecyl sulfate
SDS-PAGE	Sodium dodecyl sulfate polyacrylamide gel electrophoresis
SEM	Standard error of the mean
Sf9	Spodoptera frugiperda 9 cell line
SKALP	Skin-derived antileukoprotease
SLIGKV-NH ₂	Serine-Leucine-Isoleucine-Glycine-Lysine-Valine-trifluoroacetate salt
SLIGRL-NH ₂	Serine-Leucine-Isoleucine-Glycine-Arginine-Leucine-trifluoroacetate salt
Som	Somatostatin
SSC	Saline-sodium citrate
STAT	Signal transducer and activator of transcription
TBS	Trisaminomethane buffered saline
TBS-T	Trisaminomethane buffered saline with Triton X
TEMED	N,N,N',N'-tetramethylethyldiamine
TFLLR-NH ₂	Threonine-Phenylalanine-Leucine-Leucine-Arginine-trifluoroacetate salt
TG	Trigeminal ganglia
TGFβ	Transforming growth factor beta
Th	T helper cell
TLR	Toll-like receptor
TNFα	Tumour necrosis factor alpha
Trf	Transferrin
TRIS-base	Trisaminomethane base
TRIS-HCl	Trisaminomethane hydrochloride
TRITC	Tetramethylrhodamine
TrkA	Tyrosine kinase receptor A
T _{RM}	Tissue-resident memory alpha beta T cells

TRP	Transient receptor potential
TRPA1	Transient receptor potential ankyrin 1
TRPV1	Transient receptor potential vanilloid 1
TRPV4	Transient receptor potential vanilloid 4
TSLP	Thymic stromal lymphopoietin
VEGF	Vascular endothelial growth factor
VGAT	Vesicular gamma-aminobutyric acid transporter
VGLUT2	Vesicular glutamate transporter 2
WT	Wild type

Chapter 1

General introduction

Itch is defined as an unpleasant cutaneous sensation associated with the urge to scratch (Steinhoff et al., 2006). Itch signals are generated following activation of a subset of sensory neurons (pruriceptors) by itch causing agents (pruritogens). The purpose of itch is to protect from potentially harmful agents that may enter the skin, such as following an insect bite or plant sting (Hoon, 2015; Green and Dong, 2016; Ross, 2011). Such itch-causing agents are referred to as pruritogens. The scratching reflex that accompanies itch serves to remove the potentially dangerous substance from the skin and relieves the itching sensation, ensuring it is short-lived and preventing tissue damage that would otherwise result from excessive scratching. This type of itch is known as acute itch, typically lasts for several minutes, and is normally alleviated by scratching at the site of itch. However, in some cases such as found in atopic dermatitis and psoriasis, itch can persist for several weeks or months. Itch that lasts for 6 weeks or longer is defined as chronic itch (Ständer et al., 2007). Furthermore, rather than being relieved by scratching, excessive scratching in chronic itch damages the skin and causes localised inflammation that exacerbates itching, resulting in an itch-scratch cycle (Steinhoff et al., 2006).

In both acute and chronic itch, transmission of itch signals via neurons can broadly be divided into a peripheral pathway, comprising primary sensory neurons of the peripheral nervous system (PNS) that detect pruritogens, and the central itch pathway, consisting of the central terminals of sensory neurons in the dorsal horn of the spinal cord that then relay the itch signal to interneurons and projection neurons in the central nervous system (CNS) where the sensation of itch is perceived and the behavioural scratching responses are initiated (Figure 1.1).

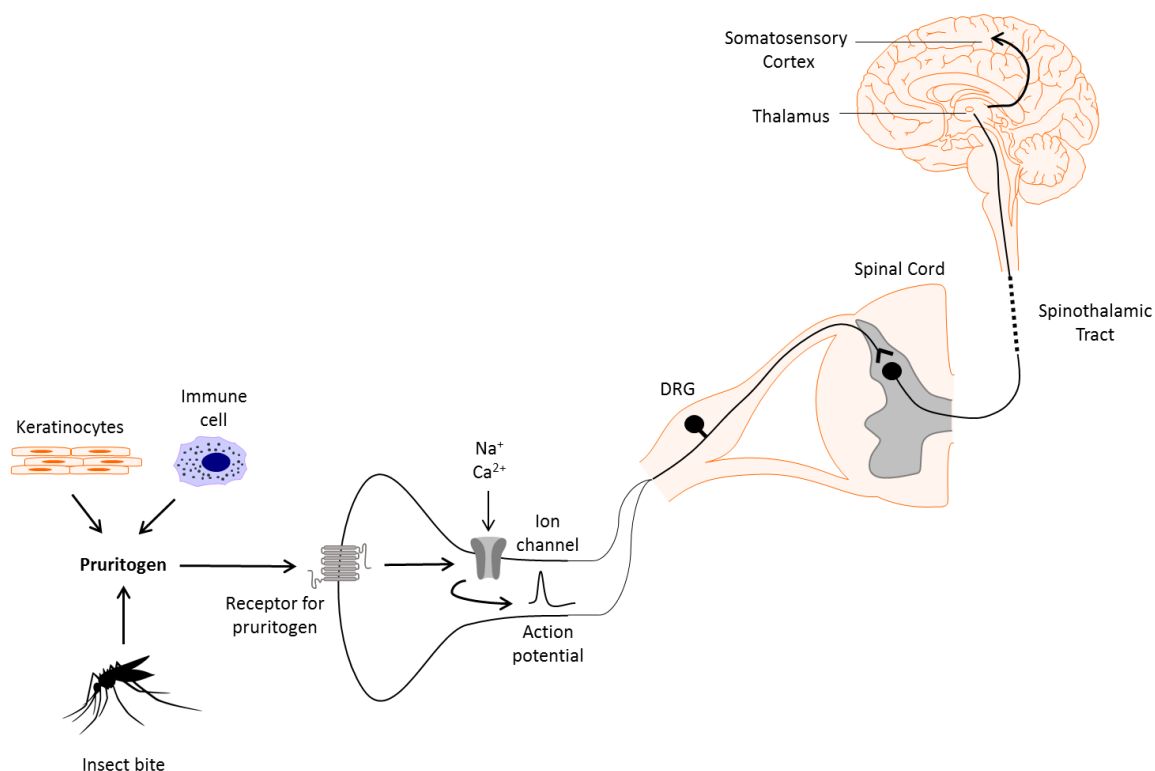


Figure 1.1: Simplified schematic of the itch pathway

Receptors on the endings of sensory neurons in the skin detect endogenous pruritogens released from cells in the skin such as keratinocytes or immune cells, or exogenous pruritogens from the environment. This results in the opening of ion channels, entry of cations into the neuron, culminating in propagation of action potentials and transmission of itch signals along the peripheral fibre, with the cell body located in the periphery in the dorsal root ganglia (DRG). Neurotransmitters and neuropeptides released in the dorsal horn of the spinal cord pass the signal to interneurons and eventually projection neurons which decussate and ascend along the spinothalamic tract to the thalamus of the brain, where the signal is relayed to higher brain centres.

1.1 The skin as a source of pruritogens

The free nerve endings of primary sensory neurons in the skin detect pruritogens. Pruritogens can be exogenous arising from the external environment, or they may come from our own cells and tissues, notably from the skin. Immune cells such as mast cells and basophils are known to release mediators that activate and sensitise pruriceptors especially during inflammation (Steinhoff et al., 2018). Skin keratinocytes are also known to release agents, often cytokines and proteases, which can act as pruritogens.

Overview of the skin

The skin itself is comprised of three layers – an outer epidermis, an underlying dermis, and an inner hypodermis. All layers serve a protective barrier function against injury, infection, and loss of fluids, with disruption of normal skin function associated with several chronic itch conditions, such as atopic dermatitis (Baroni et al., 2012). The free nerve endings of peptidergic and non-peptidergic sensory neurons are found in both the epidermis and dermis, where they are responsible for transmission of sensory information from the skin (Gibbins et al., 1987; Reinisch and Tschachler, 2012; Schuttenhelm et al., 2015; Taylor et al., 2009; Tobin et al., 1992). The epidermis is the first line of defence against foreign pathogens. Keratinocytes make up 95% of the cells found in the epidermis of the skin, where they synthesise and express many structural proteins and lipids essential to the function of the skin (McGrath et al., 2004). The majority of the remaining cells of the epidermis are melanocytes and Langerhans cells (Wickett and Visscher, 2006). The dermis is separated from the epidermis by the basement membrane. It contains blood vessels required for thermoregulation and providing the skin with nutrients, and lymphatic vessels where immune cells leave the skin and migrate to the lymph nodes (Mueller et al., 2014; Valladeau and Saeland, 2005). The dermis of the skin contains many different types of immune cells that help to ensure this layer serves as an immunological barrier to potential pathogens (Mueller et al., 2014). This includes dendritic cells, involved in presenting antigens to resident cells in the lymph nodes (Nestle et al., 1994; Valladeau and Saeland, 2005; Zaba et al., 2007), and macrophages, which are involved in the recruitment of neutrophils from circulation during infection (Abtin et al., 2014). Several different types of lymphocytes have been described in the dermis, including CD90hi innate lymphoid cell-2 (ILC2) that interact with mast cells and produce IL-13 and NKp44+ ILC3 cells that increase in the skin of patients with psoriasis (Roediger et al., 2013; Villanova et al., 2014). The dermis also contains many T cells, particularly Th1-polarised T cells, even in healthy, non-inflamed skin (Clark et al., 2006). These cells are thought to play a role in immune surveillance allowing a rapid response to antigens. The dermis additionally contains mast cells, which are more numerous at the junction with the epidermis and become less numerous deeper in the dermis (Cowen et al., 1979). As well as being involved in the release of histamine and inflammatory mediators following allergy, infection, and injury, mast cells may be important in the process of wound healing (Ng, 2010).

Keratinocytes

The epidermis itself is comprised of four to five layers or strata of keratinocytes at different states of maturation and differentiation (Baroni et al., 2012; Wickett and Visscher, 2006) (Figure 1.2). As keratinocytes mature, they migrate up through the layers of the epidermis.

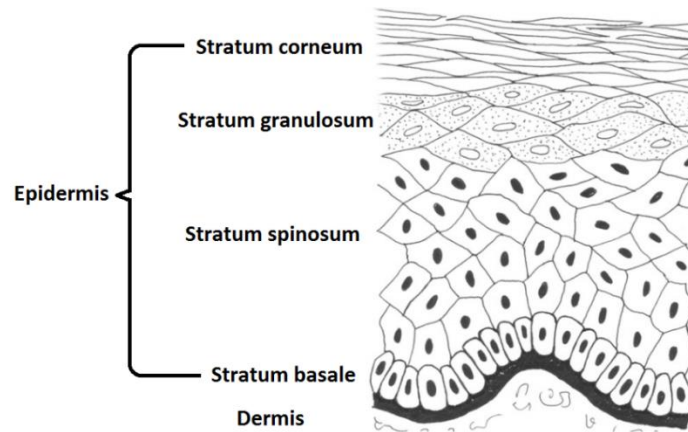


Figure 1.2: Schematic of the layers of the skin (adapted from Wickett and Visscher, 2006)

The stratum basale

The deepest layer of the skin, the basal layer, or stratum basale, consists of continually dividing keratinocytes that serve to replenish the cells shed from the outer layers of the skin during the process of desquamation or lost following injury. Keratinocytes typically require two weeks to leave the basal layer and a further two weeks to migrate through to the outermost layer, although the rate of replication and migration can be altered during inflammation or injury (Fenner and Clark, 2016). Rather than being a homogeneous population of stem cell progenitors, it is thought that the keratinocytes of the basal layer comprise a heterogeneous population of cells of different sizes and varying growth capabilities. For instance, one group of cells, which have a high tissue growth and regeneration potential, are found to express low levels of transferrin (Trf) receptor and epidermal growth factor (EGF) receptor, and may comprise mainly stem cells. In contrast, another group of cells expressing high levels of Trf receptor and EGF receptor are thought to be more mature and have less regeneration potential, and are likely to be progenitors that will eventually give rise to fully differentiated keratinocytes. Accordingly, keratinocytes expressing lower levels of Trf receptor have been found to be more competent in DNA repair, which is essential for the long-term maintenance of genomic integrity required for continuous generation of new stem cells (Fortunel and Martin, 2012).

When keratinocytes in the basal layer begin to migrate, intracellular expression of hemidesmosomal components increases as the hemidesmosomes connecting the keratinocytes to the basement membrane become internalised, allowing migration of these cells (Poumay et al., 1994). Integrin adhesion is reduced due to upregulation of RhoE, further allowing cells to migrate and become committed to differentiation (Liebig et al., 2009). In addition, a number of transcription factors, such as Nkx2.5, C/EBP α and β , and MafB are upregulated in keratinocytes as they mature, and are proposed to control expression of a number of genes involved in differentiation of keratinocytes (Hwang et al., 2009; Lopez et al., 2009; Miyai et al., 2017). A calcium and 1,25(OH)(2)D-3 (vitamin D metabolite) gradient may be important in keratinocyte differentiation, as cells leaving the basal layer become exposed to increasing concentrations of calcium and decreasing concentrations of 1,25(OH)(2)D-3 as they migrate and mature (Bikle, 2004; Menon et al., 1985). Furthermore, expression of the extracellular calcium-sensing receptor on keratinocytes is required for differentiation, since transgenic mice lacking this receptor have an increase in the number of proliferating cells in the basal layer and a decrease in the expression of keratinocyte differentiation markers in the epidermis (Komuves et al., 2002). Temperature and the presence of epidermal growth factor may also affect keratinocyte differentiation (Ponec et al., 1997).

The stratum spinosum

Keratinocytes that have left the basal layer of the epidermis begin to differentiate in the spinous layer, or strata spinosum, where the process of keratinisation begins through expression of keratins 1 and 10 (Dai and Segre, 2004; Poumay and Pittelkow, 1995). The transcription factors Klf4, Dlx3, and Foxn1 are predominantly expressed in the spinous layer of the epidermis, where they serve to establish a functional permeability barrier and ensure proper transcription of terminal differentiation markers (Baxter and Brissette, 2002; Dai and Segre, 2004; Jaubert et al., 2003; Morasso et al., 1996; Segre et al., 1999).

The stratum granulosum

During the final stages of differentiation, keratinocytes migrate to the granular layer, or stratum granulosum, so-called because of the appearance of granules in the cells of this layer. The granules are of two types – keratohyalin granules which contain proteins, and lamellar granules which contain layered stacks of lipids (Landmann, 1986; Suzuki and Kurosumi, 1972; Wickett and Visscher, 2006). The proteins of the keratohyalin granules include filaggrin and loricrin (Steven et al., 1990; Wickett and Visscher, 2006). Filaggrin

serves to aggregate keratin filaments and is also broken down to produce Natural Moisturising Factor (NMF) (Rawlings et al., 1994; Rawlings and Matts, 2005; Scott and Harding, 1986), while loricrin cross-links with involucrin to result in the formation of an insoluble envelope (Steinert and Marekov, 1997) (Figure 1.3). The profilaggrin N-terminal domain has also been found to interact with loricrin in addition to keratin, and may be required for terminal differentiation of keratinocytes (Yoneda et al., 2012). Lamellar bodies comprise about 20% of the cell volume and are polarised towards the apical border (Menon et al., 2012). In the upper granular layer of the epidermis, the lipid contents of lamellar bodies are extruded into the intercellular space, resulting in the formation of lipid sheets that act as a type of glue or paste between the cells and cross-linked proteins (Landmann, 1986; Nemes and Steinert, 1999).

The stratum corneum

Eventually the nucleus and organelles of the keratinocytes are digested and the cytoplasm disappears, leaving a flattened cell containing a dense network of proteins surrounded by covalently attached lipids that form a lipid envelope (Figure 1.3). These dead cells are known as corneocytes, and they comprise the outermost layer of the epidermis, known as the cornified layer or stratum corneum, forming a permeability barrier that prevents desiccation of the skin (Baroni et al., 2012; Wickett and Visscher, 2006). Lipids, including ceramides, cholesterol, and free fatty acids, comprise most of the intercellular space between corneocytes, and serve to prevent the loss of fluid from the skin (Feingold and Elias, 2014; Wertz and van den Bergh, 1998). The corneocytes themselves, which can be stacked up to 20 layers of cells, are held tightly together by a modified desmosome known as the corneodesmosome (Ishida-Yamamoto and Kishibe, 2011; Menon et al., 2012). As corneocytes mature, the corneodesmosomes are broken down by and eventually the dead corneocytes are shed from the skin, to be replaced by new terminally differentiating keratinocytes that have migrated from the basal layer.

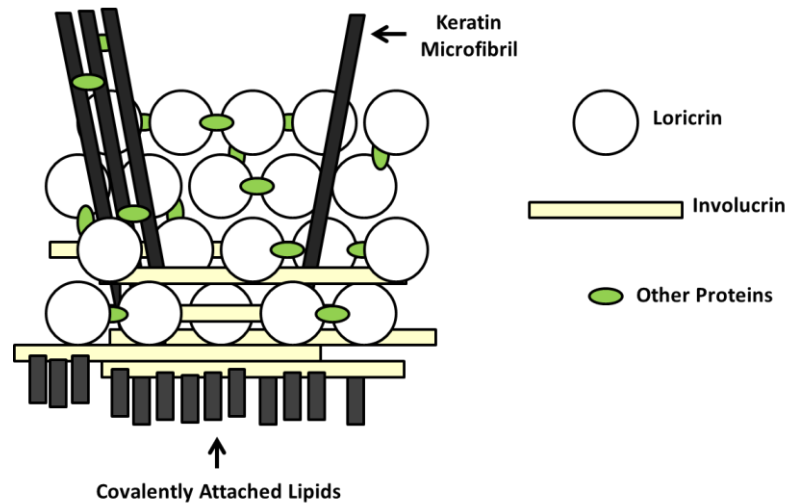


Figure 1.3: Schematic of the corneocyte lipid envelope (adapted from Wickett and Visscher, 2006)

The stratum lucidum

In the epidermis in the palms of the hands and soles of the feet, an additional epidermal layer, the clear layer or stratum lucidum, is found (Wickett and Visscher, 2006). This layer is likely involved in providing additional mechanical support to the skin in these locations. In transgenic mice lacking a gene required for the hydrolysis of sphingolipids, the epidermal structure was found to be altered (Doering et al., 1999). The clear layer was found to be thickened, likely as a result of unprocessed sphingolipids such as glucosylceramides in this layer. In contrast, partial loss of the cornified layer was observed, proposed to be due to reduced mechanical stability resulting from the loss of fully processed lipids normally found in the corneocyte lipid envelope.

Proteases in keratinocytes

Keratinocytes contain numerous proteases that are required for the normal functioning of the skin (Table 1.1). Several of these proteases have been proposed to act as pruritogens in addition to their normal functions (Andoh et al., 2015, Kim et al., 2012).

Table 1.1: Proteases found in skin keratinocytes

Protease	Function	References
Kallikrein 5	Degredation of skin corneodesmosomes	Caubet et al., 2004; Levi et al., 2008
Kallikrein 7	Degredation of skin corneodesmosomes	Caubet et al., 2004; Levi et al., 2008
Cathepsin V	Degredation of skin corneodesmosomes and melanosomes	Bernard et al., 2003; Homma et al., 2018
Cathepsin D	Degredation of skin corneodesmosomes; cross-linking involucrin and loricrin	Egberts et al., 2004; Horikoshi et al., 1999; Igarashi et al., 2004
Cathepsin B	Degradation of cell-cell contact in wound healing	Buth et al., 2004
Cathepsin S	MHC class II-mediated antigen presentation	Beers et al., 2005; Schonefuss et al., 2010; Schwarz et al., 2002

T cells

Various types of T cells can be found in the epidermis and dermis of the skin, particularly during and after infection, injury, and inflammation where they may provide protection against reinfection (Gebhardt et al., 2009). During infection, CD4+ and CD8+ T cells migrate to the dermis and epidermis of the skin to fight the infection, although CD4+ T cells eventually migrate back into circulation, while CD8+ T cells remain in the epidermis, with some becoming tissue-resident memory $\alpha\beta$ T cells (T_{RM}) (Gebhardt et al., 2011). After infection, T_{RM} cells predominate in the epidermis, while fewer numbers of $\gamma\delta$ T cells (DETC) are also to be found (Foster et al., 1990; Spetz et al., 1996). Indeed, T_{RM} cells and DETCs appear to compete with one another, with T_{RM} cells replacing DETCs over time (Zaid et al., 2014). Differentiation of CD8+ T cells to T_{RM} cells in the epidermis requires chemokine receptor signals such as CXCR3 and cytokines such as IL-15 and TGF- β released from keratinocytes or Langerhans cells in the epidermis (Mackay et al., 2013; Mackay et al., 2015).

CD4+ T cells are usually present in low numbers in the epidermis of the skin, although their numbers are reported to increase in atopic dermatitis and psoriasis (Bos et al., 1989; Bovenschen et al., 2006; Schon et al., 1997; Sinke et al., 1997). Following antigen recognition

in response to infection, allergens, or autoimmunity, CD4+ T cells undergo clonal expansion to differentiate into T helper (Th) cells that secrete cytokines thought to be specific to each Th subset (Bettelli et al., 2007; Clark and Schlapbach, 2017; Fujita, 2013; McGeachy, 2013; Nakayama and Yamashita, 2008; Plank et al., 2017; Raphael et al., 2015; Stockinger et al., 2004). Most of these cells undergo apoptosis when the antigen has been cleared, but a few become memory cells capable of lasting a long time and ready to respond following re-exposure specific to antigens. It is hypothesised that in skin conditions such as atopic dermatitis and psoriasis, there is an increase in the number and activity of these T helper cells and alteration in their balance in the skin, resulting in an increased production and release of cytokines that damages the structure of the skin, compromising its ability to serve as a physical barrier and prevent fluid loss and contributing to the release of pruritogens or sensitisation of neurons responsible for enhanced pruritus. Some cytokines involved in skin conditions characterised by chronic itch may act directly as pruritogens or cause the release of pruritogens from other cells (Table 1.2).

Table 1.2: Cytokines in skin conditions characterised by chronic itch

Cytokine	Condition	References
IFN γ	Psoriasis, atopic dermatitis (chronic phase)	Barker et al., 1991; Bjerke et al., 1983; Bockelmann et al., 2005; Grewe et al., 1994; Nattkemper et al., 2018; Schlaak et al., 1994; Zhu et al., 2010
IL-4	Atopic dermatitis	Pedrosa et al., 2017; Smits et al., 2017
IL-5	Atopic dermatitis	Simon et al., 2004
IL-12	Atopic dermatitis	Aral et al., 2006; Yoshizawa et al., 2002
IL-13	Atopic dermatitis	Smits et al., 2017
IL-17	Psoriasis	Kagami et al., 2010; Lowes et al., 2008; Ma et al., 2008
IL-18	Atopic dermatitis	Aral et al., 2006; Yoshizawa et al., 2002
IL-22	Psoriasis	Kagami et al., 2010; Ma et al., 2008
IL-31	Atopic dermatitis	Kato et al., 2014; Neis et al., 2006; Pitake et al., 2018; Raap et al., 2008; Raap et al., 2012; Sonkoly et al., 2006; Szegedi et al., 2012
TNF α	Psoriasis	Nattkemper et al., 2018; Portugal-Cohen et al., 2012
TSLP	Atopic dermatitis	Wilson et al., 2013

Th1 cells

Th1 cells are characterised by the production of IL-2, granulocyte-macrophage colony-stimulating factor (GM-CSF), interferon gamma (IFN γ), and tumour necrosis factor alpha (TNF α) (Raphael et al., 2015). These cells are involved in immunity to intracellular pathogens and cell-mediated immune responses, and IFN γ has also been implicated in autoimmune diseases including psoriasis (Barker et al., 1991; Bjerke et al., 1983; Bockelmann et al., 2005; Schlaak et al., 1994; Zhu et al., 2010). Polarisation of Th cells to Th1 cells and expression of IFN γ in these cells is proposed to be under the control of the transcription factor T-bet (Szabo et al., 2000). T-bet induces ectopic expression of IFN γ in a mouse thymal cell line that does not normally express this cytokine. Furthermore, T-bet can repress production of the Th2 cytokines IL-4 and IL-5 in Th2 cells and polarise these cells to Th1 cells capable of producing IFN γ and TNF α . Increased expression of T-bet might thus be responsible for the increase in Th1 cells characteristic of psoriasis and the subsequent increased production of IFN γ in this condition (Schlaak et al., 1994). In support of this, expression of T-bet mRNA in peripheral blood mononuclear cells is increased in patients with psoriasis compared with healthy controls. The number of T-bet positive cells in psoriatic lesions is also increased compared with healthy skin (Zhu et al., 2010).

TNF α is additionally involved in psoriasis. Increased levels of TNF α are reported in the skin of patients with psoriasis compared with atopic dermatitis or in healthy skin (Nattkemper et al., 2018; Portugal-Cohen et al., 2012). Inhibitors for this cytokine have been shown to improve symptoms of psoriasis (Mease et al., 2000). A more recent study found that a psoriasis patient treated with anti-TNF α showed a decrease in disease severity and a decrease in the number of innate lymphoid cell-3 (ILC3) that may be involved in TNF α -mediated symptoms of this disease (Villanova et al., 2014). However, these ILC3 are not known to produce TNF α , but instead have been reported to secrete IL-17 and IL-22 (Bernink et al., 2013). IL-17, a Th17 cytokine, and IL-22, a cytokine secreted by Th17 and Th22 cells, are both implicated in psoriasis (Kagami et al., 2010; Lowes et al., 2008; Ma et al., 2008). Thus, TNF α might be involved in the production of ILC3, contributing to the involvement of Th17 and Th22 cell types to psoriasis.

Stimulation of human skin cell lines and primary keratinocytes with the Th1 cytokines IFN γ , TNF α , and IL-1 α is reported to cause thickening of the corneal layer of these cultures, in a manner similar to that observed in psoriasis (Smits et al., 2017). Stimulation of these cells with these cytokines also resulted in increased expression of the psoriasis-related host

defence genes, peptidase inhibitor 3 (PI3) and defensin beta-4 (DEFB4), which encode for skin-derived antileukoprotease (SKALP)/elafin and human beta-defensin 2 (hBD2). SKALP/elafin is an elastase inhibitor reported to be present in the suprabasal layer of the skin in patients with psoriasis, but not in normal skin (Schalkwijk et al., 1993). SKALP/elafin mRNA is also upregulated in psoriatic skin compared with controls (Guttman-Yassky et al., 2008). Upregulation of this inhibitor following stimulation with Th1 cytokines suggests protection of elastin proteins from proteolytic cleavage in psoriasis. In a skin auto-fluorescence assay of patients with psoriasis and healthy controls, a small increase in the fluorescence spectra for elastin was observed in psoriatic lesional and non-lesional skin compared with the skin of healthy controls, however this difference was not significant, suggesting a lack of major changes in elastin cross-links in psoriasis (Portugal-Cohen et al., 2012). hBD2 is an antimicrobial peptide purified from psoriatic scales and may help to explain why patients with psoriasis present with a low incidence of skin infections compared with other skin conditions (Harder et al., 1997; Henseler and Christophers, 1995). Expression of hBD2 in keratinocytes can be upregulated following incubation in TNF α and expression of hBD2 mRNA is increased in the skin of patients with psoriasis (Guttman-Yassky et al., 2008; Harder et al., 1997), supporting a role for this peptide in psoriasis. However, hBD2 is a product of Th17 cells rather than Th1 cells, suggesting the involvement of both Th1 and Th17 cells in this condition.

Th2 cells

Cytokines produced by Th2 cells in response to allergy and parasite infestation include IL-4, IL-5, IL-9, IL-10, IL-13, and IL-31 (Castellani et al., 2010; Raphael et al., 2015; Nakayama and Yamashita, 2008; Stott et al., 2013). However, the presence of some of these cytokines appears to be involved in development of Th2 responses, resulting in a positive feedback loop whereby the production of cytokines from Th2 cells results in the further development of more cytokine-producing Th2 cells from CD4 $^{+}$ cells. For instance, it was recently reported IL-4 was required for the development of IL-4 and IL-4/IL-13-expressing Th2 cells in mouse (Prout et al., 2018). IL-4 was not, however required for the development of IL-13-expressing Th2 cells, suggesting that subsets of Th2 cells are differentially regulated. Indeed, secretion of IL-13 has been shown to require the release of IL-33 from resident lymphoid cells and the presence of epidermal growth factor receptor (EGFR) and its ligand amphiregulin on Th2 cells (Minutti et al., 2017). Thymic stromal lymphopoietin (TSLP), a cytokine released from keratinocytes (Wilson et al., 2013), may also be involved in the induction of IL-13-expressing Th2 cells. Ochiai et al. (2018) exposed naive CD4 $^{+}$ cells in culture to TSLP and observed the

development of a population of Th2 cells that expressed IL-13, IL-5, and IL-9, but not IL-4. *In vivo*, exposure of T cells in the lymph node to TSLP resulted in the development of two populations of Th2 cells, one expressing IL-13 but not IL-4, and the other population of Th2 cells expressing both IL-13 and IL-4 (Ochiai et al., 2018).

The acute phase of atopic dermatitis is characterised by a Th2 phenotype with T-cells that produce IL-4, IL-5, IL-13, and IL-31 cytokines (Mudde et al., 1992; Werfel, 2009). These cytokines have a variety of effects, particularly on immune cells and keratinocytes. IL-4 has been shown to induce apoptosis of eosinophils while enhancing survival of basophils (Reinhart and Kaufmann, 2018; Wedi et al., 1998). Apoptosis of eosinophils may serve to resolve chronic inflammation in atopic dermatitis. Basophils are a source of IL-4 and IL-13 (Redrup et al., 1998). In contrast, IL-5 promotes survival of eosinophils (Simon et al., 2004; Wedi et al., 1998; Yamaguchi et al., 1988). Increased numbers of eosinophils and eosinophil granule proteins are found in the skin and blood in patients with atopic dermatitis compared with healthy controls (Kiehl et al., 2001; Liu et al., 2011a; Simon et al., 2004; Schauer et al., 1995). Eotaxin-3, or C-C motif chemokine ligand 26 (CCL26), is a chemoattractant of eosinophils (Griffithsjohnson et al., 1993; Ponath et al., 1996) and is elevated in the serum and skin of patients with atopic dermatitis, but not in patients with psoriasis or healthy skin (Kagami et al., 2003; Nattkemper et al., 2018). Together with IL-5, CCL26 might be responsible for the increased number of eosinophils observed in the skin in atopic dermatitis. IL-4 stimulates expression of CCL26 in cultured human keratinocytes (Nishi et al. 2008), while IL-4 and IL-13 stimulate expression of CCL26 in HaCaTs (Bao et al. 2012, Bao et al., 2013, Kagami et al., 2005) and dermal fibroblasts (Banwell et al., 2002). Stimulation of primary keratinocytes and three-dimensional cultures of human skin equivalents with IL-4 and IL-13 also results in an increase in CCL26 mRNA (Serezani et al., 2017; Smits et al. 2017). Thus, expression of CCL26 has been used as a marker of atopic dermatitis (Smits et al. 2017).

Expression of carbonic anhydrase II (CA2) mRNA and protein is also upregulated in cultured human keratinocytes, N/TERT cells, and reconstructed human epidermis incubated with IL-4 and IL-13 (Kamsteeg et al. 2007; Kamsteeg et al. 2011; Pedrosa et al., 2017; Serezani et al., 2017; Smits et al. 2017). Similarly, expression of CA2 mRNA and protein is upregulated in the skin of patients with atopic and contact dermatitis (Kamsteeg et al. 2007; Kamsteeg et al. 2010). Expression of CA2 is greater in patients with atopic dermatitis than in patients with psoriasis (Kamsteeg et al. 2007; Kamsteeg et al. 2010; Nomura et al., 2003). Taken together, these studies support a role for the involvement of IL-4 and IL-13 cytokines in the

upregulation of CA2 in atopic dermatitis. CA2 is a member of the metalloenzyme family that catalyses the conversion of carbon dioxide and water to carbonate and hydrogen ions (Tashian, 1989). As a consequence of this, CA2 is involved in the maintenance of intracellular pH and ion homeostasis. Blocking carbonic anhydrase activity in *Xenopus* oocytes slows down the intracellular rate of pH change in response to addition of CO₂; conversely the rate of pH change is increased four-fold when oocytes are co-injected with CO₂ and carbonic anhydrase (Nakhoul et al., 1998). Furthermore, pharmacological inhibition of carbonic anhydrase in retinal neural cells and rat choroid plexus results in an increase in intracellular pH (Johanson et al., 1992; Kniep et al., 2006; Reber et al., 2003). However, the effects of inhibition of carbonic anhydrase may vary between different cell types, since a reduction in pH is observed in corneal endothelial cells in the presence of carbonic anhydrase inhibitors (Bonanno et al., 1995). This effect may be due to differences in the resting intracellular pH of these cells and variations in the expression of ion transporters in different cell types. In atopic dermatitis, the skin surface pH is reported to be increased compared with non-atopic skin and is correlated with dryness and itchiness (Eberlein-Konig et al., 2000; Sparavigna et al., 1999). This change in skin pH could be the result of increased CA2 expression in the skin, ultimately due to enhanced secretion of IL-4 and IL-13. Because synthesis of barrier lipids and barrier regeneration require acidic pH (Rippke et al., 2002), the increased pH in the skin in atopic dermatitis could be responsible for the impaired barrier function observed in this condition.

Neural epidermal growth factor-like 2 (NELL2), expressed in the developing and adult brain where it promotes the survival of neurons in the hippocampus and cerebral cortex (Aihara et al., 2003; Watanabe et al., 1996), is also implicated in the Th2 environment of atopic dermatitis. In addition to being expressed in neurons, expression of NELL2 has been reported in keratinocytes, where it could be responsible for post-natal survival of sensory neuron endings in the skin (Kamsteeg et al. 2011). Expression of NELL2 is increased in human skin equivalents following treatment with IL-4 or IL-13 and in the skin of patients with atopic dermatitis, but not contact dermatitis or psoriasis, supporting a role for IL-4 and IL-13 in increased expression of NELL2 specifically in atopic dermatitis (Kamsteeg et al. 2010; Kamsteeg et al. 2011; Pedrosa et al., 2017). It has been proposed that this increase in NELL2 expression in atopic dermatitis could be responsible for the increase in density of free nerve endings characteristic of this condition (Tobin et al., 1992; Tominaga et al., 2009; Urashima and Mihara, 1998).

In the skin keratinocytes of patients with atopic dermatitis, expression of filaggrin, loricrin, and involucrin mRNA and protein is reduced (Howell et al., 2007; Kim et al. 2008). Similarly, in primary keratinocytes, N/TERT cells, and Leiden epidermal models, expression of filaggrin, loricrin, and involucrin is down-regulated following incubation of cells in IL-4 and IL-13 (Danso et al., 2014; Howell et al., 2007; Kim et al. 2008; Smits et al. 2017), suggesting that release of Th2 cytokines in atopic dermatitis is responsible for downregulation of these structural proteins and disruption of the epidermal barrier in this condition. Furthermore, because filaggrin is broken down to form Natural Moisturising Factor (NMF) (Rawlings et al., 1994; Rawlings and Matts, 2005; Scott and Harding, 1986), and because extraction of NMF has been reported to increase the pH of the corneal layer of the skin (Nakagawa et al., 2004), downregulation of filaggrin as a result of IL-4 and IL-13 and the subsequent loss of NMF could contribute to the increased pH of the skin in patients with atopic dermatitis (Eberlein-Konig et al., 2000; Sparavigna et al., 1999).

IL-31 is another Th2 cytokine reported to be involved in atopic dermatitis. Expression of IL-31 and cells expressing it is increased in skin biopsies from patients with atopic dermatitis compared with patients with psoriasis and healthy individuals and is correlated with disease severity (Kato et al., 2014; Neis et al., 2006; Raap et al., 2008; Raap et al., 2012; Sonkoly et al., 2006; Szegedi et al., 2012). In mice, injection of IL-31 into the dermis results in infiltration of inflammatory cells into the skin, thickening of the skin, and scratching behaviour, while administration of IL-31 via an osmotic pump resulted in scratching behaviour and hair loss that was not reported in mice that received saline (Andoh et al., 2017; Arai et al., 2015; Cevikbas et al., 2014; Dillon et al., 2004; Pitake et al., 2018). Furthermore, transgenic mice over-expressing IL-31 developed severe pruritus, hair loss, increased infiltration of inflammatory cells and mast cells into the skin, and epidermal thickening (Dillon et al., 2004; Feld et al., 2016). Expression of IL-31 requires IL-4, since blocking IL-4 reduces the expression of IL-31 in Th2 clones and addition of IL-4 can induce expression of IL-31 in Th1 clones (Stott et al., 2013). The IL-31 receptor is expressed on several cell types, including keratinocytes, leucocytes, and neurons (Andoh et al., 2017; Arai et al., 2015; Cevikbas et al., 2014; Kato et al., 2014; Meng et al., 2018; Saleem et al., 2017; Zhang et al., 2008). The pruritic effects of IL-31 could thus be via direct action on neurons, or indirect via activation of cells that release pruritogens that then act on sensory neurons. Evidence for the direct activation of sensory neurons by IL-31 comes from the observation that application of IL-31 to cultured DRG neurons results in calcium fluxes and phosphorylation of extracellular signal-regulated kinase 1/2 (ERK1/2) in these cells (Cevikbas

et al., 2014; Pitake et al., 2018). Furthermore, IL-31 promotes the growth of cutaneous nerve fibres in transgenic mice over-expressing IL-31 (Feld et al., 2016). This effect is likely to be the result of direct activation of IL-31 receptors on these neurons, since neurite outgrowth of cultured DRG neurons in response to IL-31 was reduced in neurons cultured from IL-31 receptor deficient transgenic mice (Feld et al., 2016). A mechanism by which IL-31 might indirectly result in pruritus includes the release of the pruritogen leukotriene B4 (LTB4) from keratinocytes following application of IL-31 (Andoh and Kuraishi, 1998; Andoh et al., 2001; Andoh et al., 2017). Activation of the histamine receptor H4R on Th2 cells also causes increased expression of IL-31, resulting in a situation whereby release of histamine, for example during an allergic reaction, results in activation of H4R on these T cells and the subsequent release of IL-31 and induction of pruritus (Gutzmer et al., 2009).

The switch from Th2 to Th1

While the acute phase of atopic dermatitis is characterised by a Th2 phenotype, the chronic phase is characterised by a Th1 phenotype during which the expression of Th1 cytokines, including IFN γ , are increased in the skin (Grewe et al., 1998). Skin biopsies of lesions from patients with atopic dermatitis show increased expression of IFN γ mRNA and protein in addition to IL-4, suggesting the involvement of Th1 cytokines in this condition (Grewe et al., 1994; Nattkemper et al., 2018). In atopy patch tests, lesions from patients with atopic dermatitis show an increase in the production of IL-4 cytokines from T cells 24 hours after the patch test; however production of IFN γ from T cells dominates 48-72 hours after the patch test, suggesting the Th1 responses occur after onset of Th2 responses in this condition (Thepen et al., 1996). Whether this involves the conversion of Th2 cells already present in the lesions from a Th2 phenotype to a Th1 phenotype, or the infiltration of new Th1 cells into the lesions following signals released from Th2 cells, is not clear.

Release of IL-12 and IL-18 from dendritic cells is believed to polarise naïve T cells towards a Th-1 phenotype by increasing production of IFN γ from these cells (Grewe et al., 1995; Grewe et al., 1998; Stoll et al., 1998; Yoshimoto et al., 1998). In support of the involvement of IL-12 and IL-18 cytokines in atopic dermatitis, disease severity correlates with serum levels of IL-12 and IL-18 in children with atopic dermatitis, and patients with atopic dermatitis have increased serum IL-18 (Aral et al., 2006; Yoshizawa et al., 2002).

IFN γ upregulates expression of IL-4 receptor on keratinocytes, and pre-incubation of keratinocytes in IFN γ followed by IL-4 enhances the production of CCL26 (Nishi et al., 2008),

suggesting interactions between Th1 and Th2 responses in atopic dermatitis. Infiltration of IFN γ -releasing T cells in the dermis and epidermis in atopic dermatitis and allergic contact dermatitis results in upregulation of Fas receptors (CD95) on keratinocytes, causing them to be susceptible to apoptosis (Daehn et al., 2010; Trautmann et al., 2000; Trautmann et al., 2001). This in turn causes disruption of the epidermal barrier and development of eczematous lesions. Fas-induced apoptosis of keratinocytes may also be involved in the switch from the Th2 phenotype characteristic of acute phase atopic dermatitis to the Th1 phenotype characteristic of chronic-stage atopic dermatitis. Although Th1 cells can induce cell death in keratinocytes, Th2 cells are not able to induce apoptosis unless stimulated with IL-12, resulting in increased production of IFN γ from these cells (Trautmann et al., 2000). Furthermore, in a mouse model of atopic dermatitis in which mice lacked expression of Fas ligand or receptor, an increase in epidermal and dermal thickening, number of regulatory T cells, and mRNA expression of Th2 cytokines was observed compared with wild-type littermates, suggesting that Fas-induced apoptosis of keratinocytes is involved in the conversion of Th2 to Th1 phenotype in atopic dermatitis and lack of Fas-induced apoptosis results in worsening of atopic dermatitis symptoms including dermal thickening and Th2 inflammation (Bien et al., 2017).

1.2 Peripheral itch pathways

Pruritogens released from keratinocytes and immune cells in the skin activate receptors on sensory neurons (pruriceptors) resulting in transmission of itch signals (Bautista et al., 2014). These sensory neurons belong to the C-fibre and A δ -fibre classes (Johanek et al., 2008; Ringkamp et al., 2011; Schmelz et al., 1997). The cell bodies of these neurons are located in the dorsal root ganglia (DRG) or trigeminal ganglia (TG) (Akiyama and Carstens, 2013; Dhand and Aminoff, 2014), while the central terminals of these neurons are located in the CNS, where they release neurotransmitters and neuropeptides that then activate second-order interneurons in the dorsal horn of the spinal cord or spinal trigeminal nucleus in the medulla.

Pruriceptors are thought to belong to a subset of nociceptors that also convey noxious stimuli. In healthy volunteers, the cutaneous endings of sensory neurons that respond to application of pruritogens also respond to algogens, suggesting that the same sensory neurons are responsible for the transmission of both stimuli (Schmelz et al., 2003). Itch and pain signals may be conveyed by neurons that express the capsaicin receptor transient receptor potential vanilloid 1 (TRPV1), since ablation of TRPV1-expressing neurons results in

the abolition of both sensations (Imamachi et al., 2009). Furthermore, exposure to algogens and pruritogens does not always give the expected pain and itch responses, respectively, suggesting a degree of cross-talk during transmission of nociceptive and pruritic stimuli by sensory neurons, or during their perception in the cortex, allowing for noxious stimuli to be perceived as itch and pruritic stimuli to be perceived as painful. Alternatively, both stimuli are detected and conveyed by the same neurons but abnormalities in their perception in the brain result in these unexpected sensations. Although capsaicin, the pungent ingredient of chilli peppers is an algogen, punctate application of capsaicin via spicules to the skin of healthy volunteers results in itch sensations (Sikand et al., 2009). Moreover, noxious stimulation of the skin by electrical stimulation and injection of acidic solution in patients with atopic dermatitis evokes itch instead of pain (Ikoma et al., 2004; Vogelsang et al., 1995). In contrast, injection of histamine into the skin of patients with neuropathic pain is perceived as pain rather than itch (Baron et al., 2001). Thus, one possibility is that itch and pain stimuli are detected by the same sensory neurons and conveyed along the same spinothalamic tract neurons, with the distinction between itch and pain sensations occurring in the brain and the distinct scratching and withdrawal reflexes characteristic of itch and pain, respectively, occurring in the spinal cord (Davidson et al., 2007; Davidson et al., 2009; Davidson et al., 2012; Hachisuka et al., 2018; LaMotte et al., 2014). In this scenario, however, because the sensory neurons that detect and convey noxious and pruritic stimuli are the same, the abnormal perception of pruritic stimuli as painful or noxious stimuli as itch is the result of damage or abnormal activity in the spinal cord or brain, rather than the sensory neurons themselves. This would suggest that at least some itch and pain pathologies are the result of damage to the spinal cord or brain, rather than the pruriceptors or an increase in the exposure to pruritogens. However, because several chronic itch conditions arise due to pathologies in the skin, it is likely some other peripheral mechanism exists that distinguishes itch and pain sensations.

If itch and pain signals are mediated by the same group of sensory neurons, then the obvious question is how are they distinguished from one another? One hypothesis is that dedicated subsets of nociceptors act as pruriceptors that only respond to pruritogens and specifically convey information that is perceived as itch. In support of this, a number of studies have shown the existence of sensory neurons that are specifically involved in itch. A subset of TRPV1 neurons that express the Mas-related G-protein coupled receptor A3 (MrgprA3) has been shown to mediate itch and not pain. Ablation of these neurons in mice results in significant reduction of scratching behaviour in response to injection of

pruritogens, including histamine, chloroquine, and SLIGRL, although nocifensive behaviours in response to capsaicin are not affected (Han et al., 2013). Neurons that express MrgprA3 show reduced excitability and firing of action potentials compared with neurons that innervate the skin that do not express MrgprA3, likely due to the enhanced voltage-gated potassium current in MrgprA3-expressing neurons, suggesting these itch-specific neurons are less likely to fire than neurons that do not express MrgprA3 (Tang et al., 2016). In an animal model of allergic contact dermatitis, MrgprA3-expressing neurons had increased excitability and firing of action potentials, which may explain the increase in pruritus experienced in chronic itch conditions (Qu et al., 2014). Although neurons specific for itch have been described, it cannot be assumed that all itch stimuli are detected by neurons dedicated to transmission of only itch signals. Furthermore, itch sensations are sometimes accompanied by other sensations, particularly pain (Ross, 2011).

Models of itch coding

Several models have been proposed to explain how itch sensations may be conveyed, either via dedicated neurons specific for itch or neurons that can transmit both itch and pain signals (Bautista et al., 2014; LaMotte et al., 2014) (Figure 1.4).

One of the earliest models to explain the coding of stimuli to distinguish pruritic stimuli from noxious stimuli is **intensity coding** of the signals. This model proposes that the same polymodal neurons convey both itch and pain, and that it is the intensity of the stimulus which determines the sensation felt. Specifically, itch sensations occur when these neurons are weakly activated, while pain results from increased firing of action potentials in the same neurons in response to strong activation of these neurons. In support of this, using spicules to apply low doses of capsaicin to the skin of healthy volunteers resulted in itch sensations, while injection of high doses of capsaicin resulted in pain (Sikand et al., 2011b). However, in this study, similar sensations of itch and pain were reported following application of histamine whether injected or applied via spicules. It is likely that the itch sensations experienced following punctate application of capsaicin were due to activation of receptors on the terminals of sensory neurons in the outer epidermis of the skin, while activation of receptors of nociceptive-specific neurons located deeper within the dermis following injection of capsaicin resulted in pain. In contrast, because itch is only experienced at the body surface where scratching can occur (McMahon and Koltzenburg, 1992), activation of receptors on sensory neurons in the epidermis by pruritogens could be sufficient for itch sensation. Indeed, in healthy volunteers, transcutaneous electrical

stimulation of the skin was found to cause itch sensations, although, increasing the intensity of the stimulus did not result in pain, but instead resulted in increasing the intensity of the itch sensation (Ikoma et al., 2005; Tuckett, 1982). Thus, at the surface of the skin, activation of sensory neurons may elicit itch sensations only, regardless of the intensity of the stimulus used. This suggests the neurons for itch and pain respond to both pruritic and noxious stimuli but that activation of the receptors on nerve endings in the outer epidermis results in itch sensation, while activation of receptors deeper in the dermis causes pain.

It has also been proposed that punctate application of substances in the epidermis which results in the activation of one or a few nociceptors surrounded by inactivated nociceptors causes itch sensations (**spatial-contrast coding**), while simultaneous activation of a large number of pruriceptive and non-pruriceptive nociceptors in the skin following, for example, injection of an algogen, causes pain by inhibiting neurons conveying itch signals (**population or selectivity coding**) (Bautista et al., 2014; LaMotte et al., 2014).

The **pattern or frequency coding** model proposes that sensory neurons conveying itch are polymodal, rather than being specific for itch. In this model, itch is thought to arise from polymodal sensory capable of detecting a range of stimuli, but it is the temporal pattern or frequency discharge which determines whether itch is the sensation that arises (Bautista et al., 2014). In support of this, pruritogens were found to elicit lower rates of discharge than algogens in peripheral sensory neurons (Davidson et al., 2012). However, this could also reflect the fact that in human volunteers, algogens such as capsaicin have been reported to be perceived as producing more intense sensations than pruritogens such as histamine (Sikand et al., 2011b). Thus, the frequency of coding could reflect the intensity of the stimulus rather than whether the stimulus is perceived as itch or pain.

The **labelled-line coding** of itch, in contrast, proposes that the neurons responsible for itch are not polymodal, but instead specific for itch (Bautista et al., 2014; LaMotte et al., 2014). This would suggest that the itch and pain pathways are completely segregated and that activation of the neurons would result in a specific sensation, regardless as to the stimulus used. In support of this, a transgenic mouse model in which TRPV1 was expressed only in sensory neurons expressing MrgprA3 displayed scratching behaviour instead of nocifensive behaviour following injection of capsaicin, presumably because the nociceptive neurons that normally convey capsaicin-mediated pain had been effectively silenced and only the pruriceptive neurons could respond to application of capsaicin (Han et al., 2013). However,

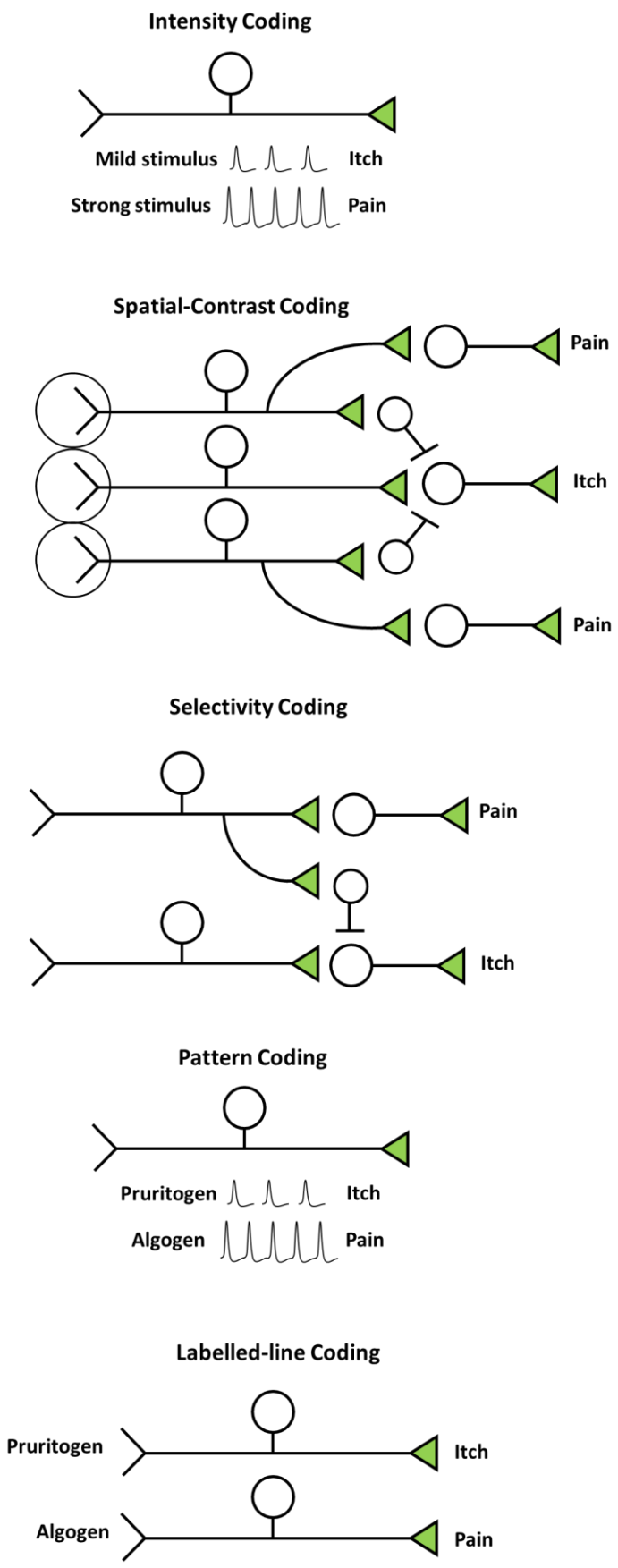


Figure 1.4: Schematic of proposed itch theories

this also agrees with the population or selectivity coding of itch, since simultaneous activation of both sets of neurons would have resulted in pain rather than itch.

Thus, it is likely that the different models for coding of itch information each play a role in conveying itch information and distinguishing itch and pain sensations from one another, possibly depending on the stimulus type and the neurons that are activated. However, whether the neurons responsible for itch are polymodal or specific remains to be further investigated.

Types of pruriceptors

It is generally accepted that sensory neurons of the peripheral itch pathways are likely subsets of the peripheral neurons responsible for the transmission of pain. In many cases the same receptors, ion channels, neurotransmitters and neuropeptides are utilised by sensory neurons that transmit itch and pain signals (Ikoma et al., 2006; Liu and Ji, 2013; Luo et al., 2015; Ross 2011). However, the existence of different subtypes of pruriceptors has also been proposed, which are thought to convey itch elicited by various pruritogens.

Itch is broadly subdivided into histaminergic or non-histaminergic itch, depending on whether pruritus is elicited following activation by histamine or other pruritogens. The existence of different types of itch might help to explain why the itch observed in chronic conditions, such as atopic dermatitis, is not treated by antihistamines, and that other pruritogens are likely to be involved in these types of itch (Klein and Clark, 1999; Rukwied et al., 2000; Wahlgren et al., 1990; Yarbrough et al., 2013). Distinct groups of pruriceptors are believed to be required for histaminergic and non-histaminergic itch, since most neurons respond to application of only one type of pruritogen (Roberson et al., 2013). Moreover, blocking one type of pruriceptor does not affect the itch responses observed following activation of other types of pruriceptors. This was recently demonstrated by Roberson et al. (2013) using the sodium channel blocker QX-314 to block specific subsets of neurons. Activation of G protein-coupled receptors (GPCRs) with a pruritogen results in the opening of large pore ion channel such as the transient receptor potential (TRP) channels, allowing the entry of sodium and calcium ions into the cell. However, when activated in the presence of QX-314, opening of the TRP channel allows the entry of QX-314 into the cell, where it then enters sodium channels in the cell membrane and blocks them, preventing further entry of sodium ions into the cells and hence activation of the cell (Figure 1.5). Using this technique, calcium responses of sensory neurons to application of pruritogens were

inhibited, and in mice scratching behaviour following intradermal injection of pruritogens was reduced, confirming the ability of this technique to block itch signalling. Furthermore, blocking activity of histaminergic pruriceptors did not prevent scratching behaviour following injection of non-histaminergic pruritogens, and vice versa. Importantly, blocking activity of these pruriceptors did not prevent behavioural responses to noxious heat, cold, mechanical, or painful stimuli. *This suggests pruriceptors, although comprising a subset of nociceptors, are not required for transmission of nociceptive stimuli and are therefore likely to comprise a distinct set of sensory neurons necessary for transmission of itch signals following activation by pruritogens.* Thus, although pruriceptors tend to be studied as a subset of nociceptors, by knowing the properties of the neurons thought to be responsible mediating itch signals, we can begin to characterise the neurons that respond to application of pruritogens, determine whether substances applied to the cells are likely to be pruritogens, and hence whether itch is the sensation experienced following application of these substances. Neurons that respond to application of pruritogens can be further characterised as mediating **histaminergic or non-histaminergic itch**, and the receptors and ion channels involved and specific to those pathways can also be investigated.

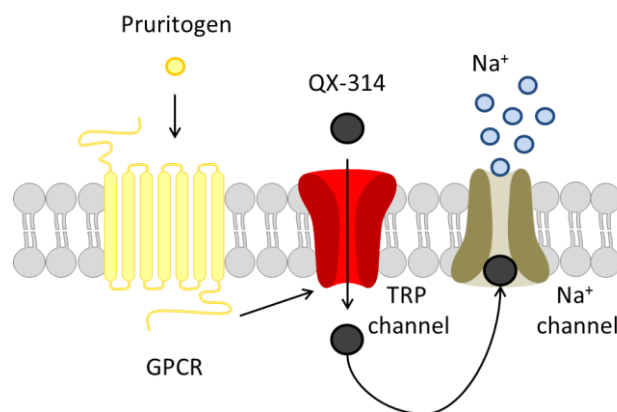


Figure 1.5: Schematic of targeted delivery of QX-314 following activation of neurons by a pruritogen (adapted from Roberson et al., 2013)

The sodium channel blocker QX-314 is unable to pass through the cell membrane to enter the cell. Pruritogens acting on GPCRs cause opening of TRP channels in the cell membrane, allowing for entry of QX-314 into the cell. Once inside the cell, the pores of sodium channels in the cell membrane become blocked, preventing conduction of action potentials.

1.2.1 Histaminergic itch and TRPV1

The most well-studied of the itch pathways is the histaminergic itch pathway. In addition to causing itch sensations in healthy human volunteers, intradermal injection of histamine into

the skin results in the development of localised oedema known as a wheal, surrounded by an area of erythema known as a flare (Figure 1.6) (Simone et al., 1991). Histaminergic itch is thought to be conveyed by the histamine 1 receptor (H1R), a GPCR coupled to Gq (Gutowski et al., 1991). Antihistamines acting on H1R have long been used to treat itch, particularly in allergic conditions such as urticaria, where histamine thought to be released from mast cells and basophils acts on pruriceptors (Kaplan 2002; Schwartz, 1991; Simons, 2004).

Histamine 1 receptor

Histaminergic itch involves the coupling of H1R to TRPV1 by several different intracellular signalling pathways. Evidence for the coupling of H1R and TRPV1 comes from studies in which mechanically insensitive C fibres that responded to histamine were also found to respond to the TRPV1 agonist capsaicin (Schmelz et al., 1997). Furthermore, expression of both H1R and TRPV1 are required for histaminergic responses, as inward currents in response to application of histamine are reported only in HEK293 cells expressing both receptors (Shim et al., 2007). In DRGs, responses to histamine can be prevented by using an antagonist to TRPV1 (Kim et al., 2004; Shim et al., 2007), and histamine-induced scratching behaviours are reduced in TRPV1 KO mice (Imamachi et al., 2009; Shim et al., 2007), suggesting activation of TRPV1 is required for histamine-mediated responses.

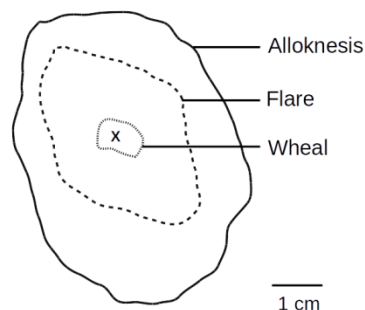


Figure 1.6: Characteristic wheal and flare response of skin following injection of histamine (adapted from Simone et al., 1991)

Intradermal injection of 1 µg histamine dihydrochloride into the skin at site X causes formation of a wheal at the site of injection due to increased permeability of small blood vessels. Surrounding the wheal is an area of erythema (flare) caused by vasodilation of the blood vessels. The wheal and flare are encompassed in an area of alopecia, or skin that is reported to be itchy when non-pruritic stimuli, such as gentle tactile stimuli, are applied.

Phospholipase A2 signalling

Histamine-mediated calcium responses in DRG neurons and HEK cells transfected with H1R and TRPV1 were reduced in the presence of inhibitors of phospholipase A2 (PLA2) and 12-

lipoygenase (12-LO), while intraperitoneal injection of these inhibitors prior to intradermal injection of histamine prevented histamine-induced scratching behaviour in mice, suggesting the involvement of these molecules in the coupling of H1R to TRPV1 (Kim et al., 2004; Shim et al., 2007). It has been hypothesised that activation of H1R by histamine results in activation of PLA2, which cleaves membrane phospholipids resulting in the production of arachidonic acid (AA) (Leurs et al., 1994), which is then metabolised by 12-LO to form 12-hydroxyeicosatetraenoic acid (12-HPETE) (Figure 1.7). In support of this, histamine was found to cause a 2.5-fold increase in the production of 12-HPETE in sensory neurons (Shim et al., 2007). Furthermore, 12-HPETE has been found to have a three-dimensional structure similar to that of capsaicin (Hwang et al., 2000) and to elicit scratching behaviour when intradermally injected into mice (Kim et al., 2007). It is thus plausible that 12-HPETE, produced following H1R activity, could activate TRPV1 directly, allowing for entry of calcium and other cations into the cell.

Similarly, LTB4, a product of AA metabolism by 5-LO, can also activate TRPV1-mediated currents (Hwang et al., 2000), while intradermal injection of LTB4 causes scratching behaviour in mice (Andoh and Kuraishi, 1998; Kim et al., 2007). However, whether activation of H1R results in production of LTB4 and itch sensations via activity at TRPV1 remains to be determined. Rather, it is more probable that LTB4 exerts its pruritic effects by acting on specific LTB4 receptors, since blocking these receptors with co-injection of antagonists reduces LTB4-mediated scratching behaviours in mice (Andoh and Kuraishi, 1998). Furthermore, keratinocytes are a potential source of LTB4, which could act on LTB4 receptors on sensory neurons to result in itch sensations (Andoh et al., 2001; Andoh et al., 2017).

Phospholipase C signalling

Activation of H1R additionally activates phospholipase C (PLC) and increases production of inositol 1,4,5-trisphosphate (IP₃) in cells in both neuronal and non-neuronal cells, suggesting the existence of multiple signalling pathways by H1R (Leurs et al., 1994; Nicolson et al., 2002). Inhibition of PLC reduced calcium responses to histamine and transgenic mice lacking the PLCβ3 isoform showed reduced scratching behaviour in response to injection of histamine, highlighting the importance of this particular isoform in histamine-induced itch (Han et al., 2006; Nicolson et al., 2002). In non-neuronal cells, activation of H1R and subsequent activation of PLC and production of IP₃ causes calcium fluxes as a result of calcium released from intracellular stores, since the responses to histamine remained when

stimulated in a calcium-free medium (Leurs et al., 1994). However, in neuronal cells, responses to histamine are reduced when cells are stimulated in a calcium-free medium, suggesting extracellular calcium is required for histamine-induced responses in neurons (Kim et al., 2004; Nicolson et al., 2002). Because histamine-mediated calcium fluxes are absent in TRPV1 KO mice and can be blocked by a TRPV1 antagonist, entry of extracellular calcium ions and other cations through activated TRPV1 is the likely mechanism by which histamine binding to H1R results in calcium fluxes (Shim et al., 2007).

Phosphatidylinositol 4,5-bisphosphate (PIP₂) inhibits TRPV1 (Chuang et al., 2001), however hydrolysis of PIP₂ to IP₃ and diacylglycerol (DAG) by PLC removes this inhibition from TRPV1 (Prescott and Julius, 2003), providing a mechanism by which activation of H1R could sensitise TRPV1 via PLC signalling. Furthermore, DAG and metabolites of DAG such as 2-arachidonoylglycerol (2-AG) can behave as endogenous agonists of TRPV1 (Woo et al., 2008; Zygmunt et al., 2013). Another product of PLC signalling is protein kinase C (PKC), which sensitises and activates TRPV1, likely via phosphorylation of the receptor (Premkumar and Ahern, 2000). Responses to histamine, but not to other pruritogens or capsaicin, were reduced in DRGs cultured PKC δ KO mice, suggesting the role of this PKC isoform in histamine-mediated itch (Valtcheva et al., 2015a). PKC δ is dependent upon DAG, but not calcium, for its activation (Exton, 1996), and is phosphorylated in response to histamine (Hao et al., 2008; Mizuguchi et al., 2011). In mouse DRG cultures, histamine also potentiates TRPV1-mediated calcium responses and membrane depolarisation to acid, the effect of which can be reduced in the presence of inhibitors for PLC and PKC (Kajihara et al., 2010). This supports the notion that activation of the histamine receptor sensitises TRPV1-mediated responses via PLC and PKC.

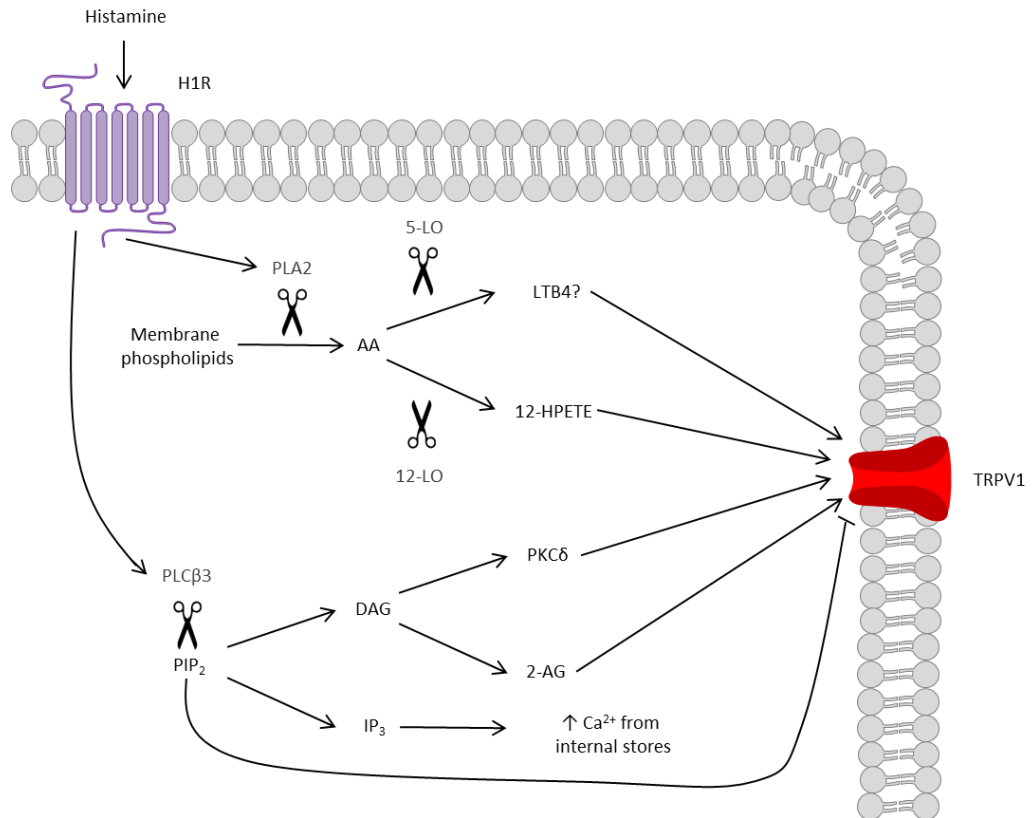


Figure 1.7: Schematic of sensitisation of TRPV1 via histamine

Activation of H1R by histamine activates PLA2 and PLCβ3 pathways to result in activation and sensitisation of TRPV1.

Histamine 3 and 4 receptors

The histamine 3 receptor (H3R) and histamine 4 receptor (H4R) have also been proposed to play a role in itch (Bell et al., 2004; Rossbach et al., 2011).

Rossbach et al. (2011) reported that sensory neurons innervating that skin could be activated by agonists of H4R in addition to H1R agonists. Dunford et al. (2007) observed that administration of an agonist selective for H4R elicited scratching behaviour in mice that was significantly reduced in the presence of a H4R antagonist or in H4R knockout mice. In healthy human volunteers, a H4R antagonist was found to be effective in reducing histamine-induced pruritus (Kollmeier et al, 2014), and H4R antagonists were found to improve symptoms in a clinical trial of patients with atopic dermatitis (Murata et al., 2015). However, other studies have found that H4R antagonists were ineffective in animal models of atopic dermatitis (Bäumer et al., 2011; Kamo et al., 2014). The reasons for this discrepancy are unclear, although concerns have been raised about expression of H4R in neuronal cells, off-target effects of histamine receptor agonists and antagonists, and lack of reproducibility of results from other groups (Schneider and Seifert, 2016). The mechanisms

by which activation of H4R would mediate itch are not fully known, although TRPV1 may mediate downstream signalling of H4R via PLC activity (Jian et al., 2016).

Expression of H3R has been detected in rodent DRGs, suggesting activity of this receptor on sensory neurons could be involved in transmission of itch signals (Cannon et al., 2007; Heron et al., 2001; Kajihara et al., 2010). However, Rossbach et al. (2011) reported that intradermal injection of an inverse agonist to H3R resulted in scratching behaviour in mice and increased calcium in cultured DRG cells, suggesting that activation of these receptors normally inhibits transmission of itch signals and may have a protective role in reducing itch.

1.2.2 Non-histaminergic itch

In addition to histamine, itch resulting from other pruritogens is known to occur via receptors other than the histaminergic receptors. Plant-derived proteases, such as papain from papaya, ficin from figs, bromelain from pineapples, and mucunain from cowhage, have all been reported to cause pruritus by acting on protease activated receptors (Papoiu et al., 2011; Reddy and Lerner, 2010; Reddy et al., 2008). The antimalarial drug chloroquine and bovine adrenal medulla 8-22 peptide (BAM8-22), a cleaved product of proenkephalin A, are also non-histaminergic pruritogens (Liu et al., 2009; Sikand et al., 2011a).

MrgprA3 and MrgprC11-mediated itch

Non-histaminergic itch is thought to be conveyed by pruriceptors expressing GPCRs such as MrgprA3, MrgprC11, and PAR2, as well as the ion channel transient receptor potential ankyrin 1 (TRPA1) in polymodal C-fibres (Johanek et al., 2008; Liu et al., 2009; Ross, 2011; Ru et al., 2017; Wilson et al., 2011). These fibres comprise a subset of TRPV1-positive neurons, since a subset of TRPV1 neurons that express MrgprC11 and MrgprA3 is reported to be activated by the pruritogens BAM8-22 and chloroquine, respectively (Liu et al., 2009). However, unlike with histaminergic itch, TRPV1 is not required for BAM8-22 and chloroquine signalling in neurons, as neurons from TRPV1 deficient animals demonstrate similar calcium activity and action potential firing in response to application of BAM8-22 or chloroquine as neurons from control wild-type littermates do (Wilson et al., 2011). Rather, TRPA1 is thought to be necessary for this type of itch (Figure 1.8), since scratching observed in wild type (WT) mice injected with BAM8-22 or chloroquine is significantly reduced in TRPA1-deficient mice (Wilson et al., 2011). Furthermore, in a neuroblastoma cell line transfected with MrgprA3 or TRPA1 alone, chloroquine failed to trigger calcium responses, instead requiring expression of both MrgprA3 and TRPA1 (Wilson et al., 2011). BAM8-22 did

result in calcium responses in cells transfected only with MrgprC11, although greater calcium responses occurred in cells transfected with both MrgprC11 and TRPA1 (Wilson et al., 2011). This suggests that expression of both GRPRs and TRPA1 is required for robust responses to pruritogens and that they are functionally coupled.

Both MrgprA3 and MrgprC11 are coupled to the $G\alpha_q/11$ signalling pathway where they can elicit calcium responses in transfected HEK cells (Han et al., 2002). These calcium responses were inhibited in the presence of a PLC inhibitor, suggesting activation of PLC downstream of $G\alpha_q/11$ signalling and supporting a role for PLC in the coupling of MrgprA3 and MrgprC11 to TRPA1. Similarly, Wilson et al. (2011) reported a reduction in the amplitude and percentage of mouse DRG neurons that responded to BAM8-22 in the presence of a PLC inhibitor, while Ru et al. (2017) found that neurons from transgenic mice lacking PLC β 3 lacked action potential discharges following application of chloroquine. In contrast, Wilson et al. (2011) reported that neuronal chloroquine-mediated calcium responses were not reduced by the addition of a PLC inhibitor, and Imamachi et al. (2009) observed that chloroquine-mediated scratching behaviours were not altered in transgenic mice lacking PLC β 3, suggesting MrgprA3 couples to TRPA1 via an additional mechanism. Indeed, pre-treatment of neurons with an inhibitor of the $G\beta\gamma$ subunits resulted in a decrease in both the amplitude of calcium responses and percentage of neurons that responded to chloroquine (Wilson et al., 2011). $G\beta\gamma$ has also been shown to be required for activation of TRPA1 via the GPCR bile acid receptor 1 (Lieu et al., 2014), suggesting that activation of TRPA1 by the $G\beta\gamma$ subunit of MrgprA3 as a plausible pathway. $G\beta\gamma$ subunits can bind to ion channels including inwardly-rectifying potassium channels and voltage-gated calcium channels and modulate their activity (Dascal, 2001), although whether direct binding of $G\beta\gamma$ subunits to TRPA1 is also responsible for their opening and the transmission of itch signals remains to be investigated. However, chloroquine-mediated activation of MrgprA3 can also result in sensitisation of TRPV1 via the PLC-PKC pathway, providing an additional mechanism by which Mrgprs could transmit itch signals (Than et al., 2013).

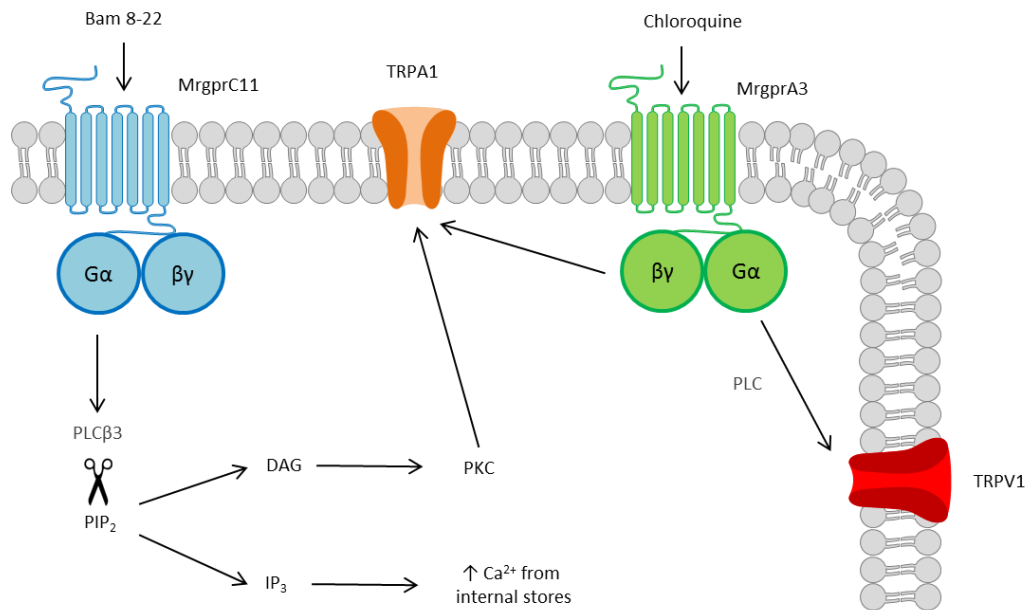


Figure 1.8: Schematic of sensitisation of TRP channels via non-histaminergic pruritogens
 Activation of *MrgprC11* and *MrgprA3* by *BAM8-22* and *chloroquine*, respectively, results in activation of *TRPA1* via *PLCβ3* and *Gβγ* signalling. *MrgprA3* can additionally sensitise *TRPV1* via *PLC* signalling.

Serotonergic itch

As well as being a neurotransmitter, serotonin (5-hydroxytryptamine or 5-HT) can act as a pruritogen that causes scratching behaviour when injected intradermally in mice and rats (Akiyama et al., 2016b; Imamachi et al., 2009; Jinks and Carstens, 2002; Klein et al., 2011; Morita et al., 2015; Nojima and Carstens, 2003; Ostadhadi et al., 2015; Shim et al., 2007; Thomsen et al., 2001; Yamaguchi et al., 1999). Along with other pruritogens, serotonin can be released from resident immune cells and keratinocytes in the skin, where it acts on receptors expressed on sensory neurons (Green and Dong, 2016). Release of serotonin from platelets has also been proposed to be involved in a mouse model of dry skin itch and allergic itch (Luo et al., 2018).

Serotonergic itch likely occurs via a different intracellular signalling pathway to histaminergic itch, as application of serotonin into the skin via iontophoresis of human volunteers does not result in the development of a localised wheal that is observed following application of histamine, and antihistamines do not significantly reduce serotonin-induced itch sensations (Hosogi et al., 2006). However, serotonin is also not known to activate Mrgprs (Liu et al., 2009), suggesting serotonergic itch is mediated either by direct opening of ionotropic serotonergic receptors or via coupling of metabotropic serotonergic

receptors to second messenger signalling systems where they can interact with other receptors expressed by sensory neurons.

5-HTR7

Despite being transmitted by TRPV1-expressing neurons, serotonin-mediated scratching behaviour is not reduced in TRPV1 KO mice (Akiyama et al., 2016b; Imamachi et al., 2009; Shim et al., 2007). Moreover, the percentage of neurons that demonstrate calcium responses to agonists of the 5-HTR7 serotonergic receptor is not decreased in DRGs cultured from TRPV1 KO mice, suggesting TRPV1 is not required for itch mediated by this serotonergic receptor (Morita et al., 2015). In contrast, there is evidence suggesting TRPA1 is required for serotonergic itch mediated by the 5-HTR7 receptor. In sensory neurons innervating the skin, expression of 5-HTR7 occurs in a subset of fibres that express TRPA1 (Morita et al., 2015). Furthermore, TRPA1 KO mice spend less time scratching following injection of the 5-HTR7 agonist and DRGs cultured from these mice demonstrate fewer calcium responses to application of 5-HTR7 agonists than DRGs from wild-type mice (Morita et al., 2015). 5-HTR7 is thought to activate TRPA1 by G β γ -mediated activation of adenylate cyclase and the production of cyclic adenosine monophosphate (cAMP), as inhibition of these pathways reduces serotonin-mediated calcium signals in cultured DRGs (Morita et al., 2015). TRPA1 is not required for all serotonergic itch responses, however. For example, scratching behaviour is not reduced in TRPA1 KO mice injected with serotonin (Akiyama et al., 2016b), suggesting activation of additional serotonergic receptors not linked to TRPA1 is sufficient to induce scratching behaviour. Indeed, different types of itch have been demonstrated to be mediated by activation of different serotonergic receptors (Luo et al., 2018).

5-HTR2

The 5-HTR2 receptor is also involved in pruritus (Akiyama et al., 2016b; Imamachi et al., 2009; Luo et al., 2018; Wilson et al., 2011; Yamaguchi et al., 1999). 5-HT-induced scratching behaviour is reduced in mice pre-treated with the 5-HT_{2R} antagonist ketanserin (Akiyama et al., 2016b). Moreover, activation of 5-HTR2 by α -methyl 5-HT results in scratching behaviour in both wild-type mice (Yamaguchi et al., 1999) and TRPA1 KO mice (Wilson et al., 2011). PLC β 3 may be involved in mediating serotonergic itch through 5-HTR2, as scratching in response to injection of the 5-HTR2 agonist α -methyl 5-HT was also significantly reduced in mice lacking the PLC β 3 receptor (Imamachi et al., 2009).

5-HTR3

The ionotropic 5-HTR3 serotonin receptor may additionally be involved in pruritus. In mice, scratching behaviour following intradermal injection of serotonin is reduced when mice are pre-treated with 5-HTR3 antagonists (Ostadhadi et al., 2015) and there are case studies of 5-HTR3 antagonists being effective in treating cholestatic pruritus (Raderer et al., 1994; Schwörer and Ramadori, 1993). However, other studies did not report scratching behaviour in rodents following injection with a 5-HTR3 agonist, or a reduction of serotonin-mediated scratching when mice were treated with 5-HTR3 antagonists or in 5-HTR3 deficient mice (Imamachi et al., 2009; Yamaguchi et al., 1999). Thus, whether serotonin-mediated itch occurs through activation of 5-HTR3 is unresolved, although it is likely serotonin normally acts through more than one receptor to result in activation of pruriceptors.

MrgprD-mediated itch

Some forms of non-histaminergic appear to be mediated by pruriceptors that do not express TRPA1 or MrgprA3, but instead express MrgprD. Despite belonging to a subpopulation of nociceptive neurons, these pruriceptors do not express TRPV1 or produce neuropeptides, but instead belong to the IB4-expressing subpopulation of nociceptors (Zylka et al., 2005). They respond to β -alanine, a supplement used for muscle building that often induces itch and tingling sensations (Décombaz et al., 2012; Liu et al., 2012), and increased sensitivity to heat and mechanical noxious stimuli, suggesting that these neurons can function as both pruriceptors and nociceptors, although they do not respond to all pruritogens (Imamachi et al., 2009; Liu et al., 2012). Indeed, it was observed in MrgprD knockout mice that scratching behaviour in response to oral administration of β -alanine was abolished, while scratching behaviour in response to administration of histamine was unaffected (Liu et al., 2012). The mechanism of itch via MrgprD receptors has not yet been fully elucidated but may involve calcium-activated chloride channels and PLC-mediated cleavage of PIP₂ to form IP₃, as inhibitors to calcium-activated chloride channels and PLC inhibitors both reduced β -alanine-induced currents in MrgprD-expressing *Xenopus* oocytes (Zhuo et al., 2014).

1.2.3 Peripheral sensitisation of itch

The phenomena of allodynia (the perception of itch in response to non-pruritic stimuli) and hyperknesis (enhanced pruritus following application of a pruritic stimulus) during chronic itch suggest the existence of sensitisation mechanisms that result in overall enhanced pruritus (Schmelz, 2010). In the periphery, sensitisation may result from increased sprouting of nerve endings following enhanced expression of neurotrophins such as NGF and artemin

in the skin, as has been reported in atopic dermatitis conditions (Murota et al., 2012; Urashima and Mihara, 1998). This increased sprouting of nerve endings would increase the likelihood of a pruriceptor encountering a pruritogen and subsequent transmission of an itch signal. Moreover, NGF causes sensitisation of TRPV1 channels in neurons, proposed to occur following removal of inhibitory PIP2 signalling when NGF binds to TrkA receptors and PLC signalling is initiated (Chuang et al., 2001). Increased expression of TRPA1 in sensory neurons is also reported due to NGF-mediated activation of p38 MAPK signalling (Diogenes et al., 2007). Although sensitisation of TRPV1 and TRPA1 could play a role in peripheral sensitisation of itch signals, it does not explain why pruritus, and not pain, is increased in response to NGF in chronic itch conditions. It could be speculated that a specific subset of nociceptors that respond to pruritogens is sensitised by NGF in chronic itch conditions, although the mechanisms that would result in this are not clear. Alternatively, a combination of peripheral sensitisation that serves to enhance overall activity in the periphery, as well as altered signalling centrally such that pain signals and other non-pruriceptive sensations are reduced, could be responsible for increased pruriception in chronic conditions.

1.3 Central itch pathways

Sensory neurons that respond to pruritogens in the skin release neurotransmitters and neuropeptides at their central terminals in lamina I and II of the dorsal horn of the spinal cord or the corresponding area of the trigeminal nucleus. The signal then passes through a series of interneurons in the spinal cord to projection neurons that transmit the signal to higher centres. *Unlike nociceptive signalling in which there may be direct input of primary afferent fibres to projection neurons in the dorsal horn, pruriceptive signals are passed through a series of interneurons before reaching the projection neurons, where the signals may be modulated, interacting with nociceptive signals where transmission of pruriceptive signals may be prevented, or become enhanced by loss of inhibitory inputs.*

The most generally accepted pathway of itch transmission (Figure 1.9) is that, following activation of pruriceptors, neurotransmitters such as glutamate and neuromodulators such as substance P, calcitonin gene related peptide (CGRP), and natriuretic polypeptide B (NPPB) are released from the terminals of primary sensory neurons in the spinal cord. These bind to their respective receptors on interneurons in lamina I and II of the dorsal horn of the spinal cord, which release gastrin releasing peptide (GRP) from their terminals. GRP then binds to its receptor found on another group of interneurons in the spinal cord, and these neurons

are proposed to signal to projection neurons in lamina I responsible for transmitting the itch signal to higher areas in the CNS (Bautista et al., 2014; Braz et al., 2014b; Green and Dong, 2016; LaMotte et al., 2014). A separate population of neuromedin B (NMB)-expressing neurons are proposed to signal to GRP receptor-expressing interneurons (Wan et al., 2017; Zhao et al., 2014). Itch signals may be inhibited by inhibitory interneurons that release gamma-aminobutyric acid (GABA), glycine, somatostatin, and/or dynorphin (Akiyama et al., 2011; Braz et al., 2014b; Huang et al., 2018; Ross, 2011). These interneurons are proposed to be activated by noxious stimuli or other sensory modalities and may serve to inhibit transmission of itch signals, for example, as a result of scratching the affected area.

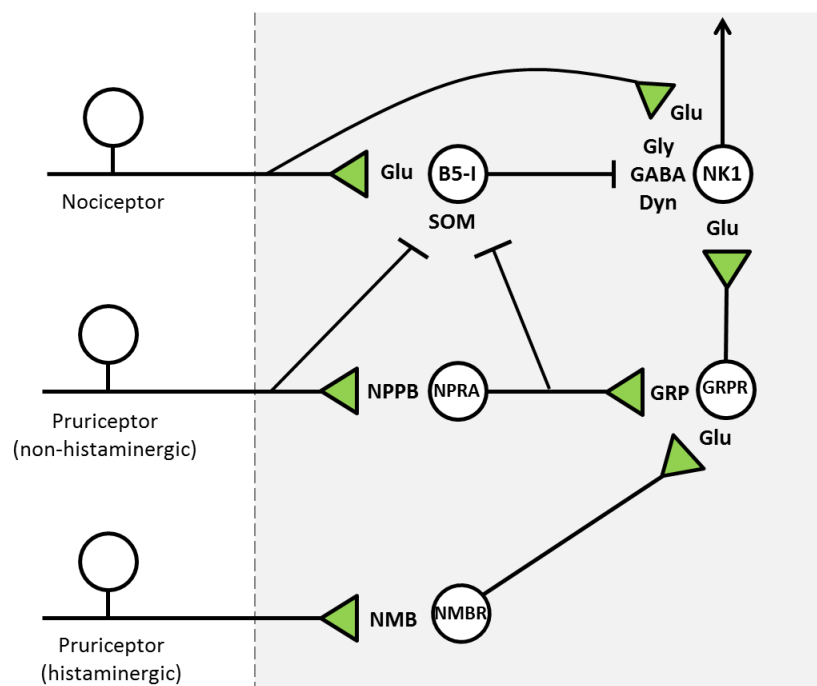


Figure 1.9: Overview of itch circuitry in the dorsal horn

Neuropeptides such as NPPB and NMB released from the terminals of pruriceptors bind to receptors expressed on interneurons in the dorsal horn, which in turn signal to NK1-expressing projection neurons in lamina I. Inhibitory circuits originating from nociceptors prevent transmission of itch signals in the spinal cord.

A population of interneurons in the dorsal horn that express the basic helix loop helix b5 (Bhlhb5) are known to belong to the itch circuitry. Transgenic mice lacking expression of Bhlhb5 display a loss of these neurons and development of spontaneous scratching behaviour and skin lesions. Compared with wild-type littermates, scratching behaviour in these transgenic mice is increased following intradermal injection of the mast cell degranulator compound 48/80 (Ross et al., 2010). Bhlhb5-expressing interneurons include a

population of excitatory glutamatergic neurons as well as inhibitory populations, known as B5-I neurons, expressing GABA, glycine, and dynorphin (Kardon et al., 2014; Ross et al., 2010; Sardella et al., 2011). To investigate whether loss of excitatory or inhibitory interneurons was responsible for increased scratching behaviour in mice, Bhlhb5 KO mice were crossed with Tlx3-cre mice, thereby abolishing the development of excitatory Bhlhb5 interneurons. Loss of Bhlhb5 inhibitory interneurons, but not excitatory interneurons expressing glutamate, increased compound 48/80-induced pruritus (Ross et al., 2010). This suggests a role for B5-I neurons in modulating scratching behaviour in acute and chronic itch. The roles of some of these neurotransmitters and neuropeptides in itch circuitry in the spinal cord is described in more detail below and in Table 1.3.

Transmission of the signals continues via projection neurons, which decussate the spinal cord and continue along the contralateral spinothalamic tract to the thalamus and parabrachial nucleus (Dong and Dong, 2018). Many of these projection neurons express the neurokinin-1 receptor (NK1R) (Carstens et al., 2010) and tracing experiments have shown that some of them do project to the brain (Akiyama et al., 2015). It has been observed that ascending spinothalamic tract neurons that respond to pruritogens such as histamine or cowhage also respond to noxious stimuli such as capsaicin, suggesting these two sensations share some common pathways to the brain (Davidson et al., 2007; Davidson et al., 2009; Davidson et al., 2012). Furthermore, different types of itch appear to be mostly mediated by different populations of spinothalamic tract neurons (Davidson et al., 2007; Davidson et al., 2012). Spinothalamic tract neurons terminate in the ventrobasal and posterior thalamus (Akiyama et al., 2015; Davidson et al., 2007; Davidson et al., 2009; Davidson et al., 2012; Moser and Giesler, 2014). Recent studies in anaesthetised rats have found a population of neurons in the thalamus, extending from the posterior triangular nucleus to the ventral posterior medial nucleus, that respond to intradermal injection of pruritogens including histamine, chloroquine, serotonin, and beta-alanine (Lipshetz et al., 2018). About half of the neurons in the thalamus were found to have mechanically defined receptive fields that corresponded to distal areas.

Table 1.3: Summary of neurotransmitters and neuropeptides in spinal cord itch circuitry

Neurotransmitter	Cell type	Receptor(s)	Function	Reference
Glutamate	Primary afferents and interneurons	AMPA, NMDA, kainate, mGlu1-8	Excitatory	Akiyama et al., 2014
GABA	Interneurons	GABA _A , GABA _B	Inhibitory	Braz et al., 2014a; Llewellyn-Smith et al., 2018; Ross et al., 2010
Glycine	Interneurons	GlyR	Inhibitory	Foster et al., 2015
CGRP	Primary afferents	Calcitonin receptor-like receptor and receptor activity-modifying protein 1 complex	Excitatory	Iyengar et al., 2017; McCoy et al., 2012
Substance P	Primary afferents	NK1-3	Excitatory	Steinhoff et al., 2014; Woolf et al., 1998
GRP	Interneurons, possibly some in primary afferents	GRPR/BB2	Excitatory	Aresh et al., 2017; Gutierrez-Mecinas et al., 2014; Zhao et al., 2014c
NMB	Primary afferents	NMBR/BB1	Excitatory	Fleming et al., 2012; Mishra et al., 2012
NPPB	Primary afferents	NPRA	Excitatory	Mishra and Hoon, 2013
Dynorphin	Interneurons	KOR	Inhibitory	Kardon et al., 2014; Sardella et al., 2011
Somatostatin	Primary afferents and interneurons	Sst1-5	Inhibitory	Huang et al., 2018; Kardon et al., 2014; Usoskin et al., 2015

From the thalamus, transmission of the itch signal is relayed to various other areas of the brain. Several imaging studies in healthy volunteers experiencing a pruritic stimulus have revealed activation of the primary somatosensory cortex corresponding to the location of the itch (Darsow et al., 2000; Drzezga et al., 2001; Herde et al., 2007; Ishiuchi et al., 2009; Papoiu et al., 2012; Schneider et al., 2008). Some studies have reported activation of secondary somatosensory cortex following an itch stimulus (Herde et al., 2007; Mochizuki et al., 2009; Papoiu et al., 2012), while others failed to detect activation of this area (Drzezga et al., 2001; Mochizuki et al., 2003), although differences in dosing and administration of

pruritogens as well as differences in imaging techniques could explain this discrepancy. Other areas of the brain that undergo changes during itch include areas involved with emotional processing and reward, such as the cingulate and prefrontal cortex, amygdala, and limbic systems, the insular cortex, which is involved in evaluation and self-awareness, and areas such as the motor, premotor, and supplementary motor cortex, which are involved in initiation of scratching behaviour (Darsow et al., 2000; Drzezga et al., 2001; Ishiiji et al., 2009; Leknes et al., 2007; Mochizuki et al., 2003; Mochizuki et al., 2009; Papoiu et al., 2012; Schneider et al., 2008; Valet et al., 2008). Different types of itch also appear to activate different regions of the brain. Compared with histamine-induced itch, itch induced by cowhage results in greater activation of the insular cortex, claustrum, and basal ganglia (Papoiu et al., 2012). Differences in regions of brain activity have also been observed in atopic itch compared with histamine-induced itch (Ishiiji et al., 2009; Leknes et al., 2007; Schneider et al., 2008).

1.3.1 Glutamate and itch

Glutamate is a neurotransmitter that is found in high concentration in the axons of neurons, where it is locally synthesised and packaged into vesicular glutamate transporters (VGLUTs) (Featherstone, 2010). VGLUT2 in particular is involved in transmission of itch and pain signals (Aresh et al., 2017; Lagerstrom et al., 2010; Liu et al., 2010; Scherrer et al., 2010). Different receptors for glutamate exist, which can be classified as fast-acting ionotropic ion channel receptors or G protein-coupled metabotropic receptors that are proposed to be involved in longer-term modulation of transmission of signals (Featherstone, 2010). The main ionotropic glutamate receptors are AMPA, NMDA, and kainate receptors. Both ionotropic and metabotropic types of receptors are located both on primary afferent neurons (Willcockson and Valtschanoff, 2008) and both pre- and post-synaptically in the dorsal horn of the spinal cord (Bardoni, 2013; Yung, 1998). The GluR2/4 subunits of the AMPA receptor and several kainate receptor subunits are pre-synaptically expressed on the terminals of GABAergic interneurons in the dorsal horn, where they are thought to be involved in the modulation of nociceptive signals, potentially by increasing the release of GABA from these interneurons thereby reducing transmission of nociceptive signals (Lu et al., 2005).

Histaminergic itch is mediated by glutamate, since firing of dorsal horn neurons in response to microinjection of histamine into the hindpaw is reduced when spinal cord sections are superfused with the AMPA/kainate receptor antagonist, CNQX, and scratching behaviour in

mice following intradermal injection of histamine in the skin is abolished when histamine was administered five minutes after injection of CNQX via lumbar puncture (Akiyama et al., 2014). Furthermore, around 80% of DRG cells that show calcium fluxes in response to histamine are positive for the VGLUT2 marker for glutamatergic neurons. Chloroquine-mediated scratching behaviour may also be mediated by glutamate, as chloroquine-mediated itch following intradermal injection of the pruritogen is partially reduced by CNQX injected into the cerebrospinal fluid, although antagonists of other receptors such as the NK1 and gastrin releasing peptide receptors are additionally required for complete inhibition of chloroquine-mediated itch (Akiyama et al., 2014).

As well as mediating pruriceptive signals, VGLUT2-expressing neurons have also been found to be involved in mediating nociceptive information. In conditional KO mice lacking expression of VGLUT2 in nearly all C fibres (peptidergic and non-peptidergic) and most A δ fibres, decreased firing of neurons in lamina I of the spinal cord to noxious mechanical and thermal stimuli was observed in compared with neurons from WT mice, suggesting noxious input to superficial dorsal horn lamina I neurons depends on glutamate release from VGLUT2-expressing nociceptors (Scherrer et al., 2010). These transgenic mice also displayed decreased nocifensive behaviour in response to noxious heat and injection of capsaicin, displaying longer response latencies, as well as increased mechanical pain threshold as measured using von Frey filaments (Scherrer et al., 2010). Furthermore, specific ablation of VGLUT2 in Nav1.8-expressing (Liu et al., 2010) or TRPV1-expressing (Lagerstrom et al., 2010) nociceptors results in reduced responsiveness to nociceptive stimuli but increased spontaneous scratching behaviours, suggesting these VGLUT2 nociceptors are also involved in the regulation of itch responses in the opposite direction to the regulation of nociception. A pathway is proposed in which activation of nociceptors, for example as a result of scratching, results in the release of glutamate from the central terminals of VGLUT2-expressing nociceptors, which in turn excites interneurons in the spinal cord that inhibit signalling along the itch pathway. Thus, when glutamate transmission is prevented in nociceptors, this inhibitory input to pruriceptive signalling is removed, causing activity of this pathway even in the presence of nociceptive stimuli that would otherwise normally inhibit transmission of itch signals.

1.3.2 Neuropeptides in itch

Gastrin releasing peptide

GRP is a 27-amino acid peptide that, although considered a gastrointestinal peptide, is also found in neuronal tissues (Weber, 2015). It is the mammalian homologue of the amphibian peptide bombesin, with similarities to other so-called gastrointestinal peptides including neuromedin B. The receptor for GRP, the gastrin releasing peptide receptor (GRPR) (sometimes known as BB2) is a GPCR expressed in many tissues including the the spinal cord and all brain regions, with highest expression reported in the hippocampus, hypothalamus, amygdala, and pons (Jensen et al., 2008). Activation of this receptor results in activation of PLC and the breakdown of phosphoinositides to generate DAG, resulting in the mobilisation of calcium and activation of PKC (Jensen et al., 2008). Serum GRP is correlated with disease severity in patients with atopic dermatitis, while an increase in GRP-expressing nerve fibres is reported in primates with chronic itch, suggesting a role for this neuropeptide in itch (Kagami et al., 2013; Nattkemper et al., 2013; Tirado-Sanchez et al., 2015). Using antibody staining, Kagami et al. also reported an increase in the number of GRP-positive fibres in the skin of patients with atopic dermatitis. Moreover, GRP peptide and mRNA is reported to be increased in DRG neurons a mouse model of dry skin itch (Barry et al., 2016). Intrathecal injection of GRP in rats, mice, and primates results in scratching behaviour, suggesting GRP acts centrally to mediate itch signals (Lee and Ko, 2015; Su and Ko, 2011; Sukhtankar and Ko, 2013).

GRP is reported to be expressed in approximately 8% of cells in the DRG which are likely to be neurons as expression of GRP peptide has been reported to co-localise with the neuronal marker NeuN in mouse DRG (Barry et al., 2016; Kiguchi et al., 2016). These neurons are proposed to belong to a subset of nociceptors since co-localisation with TRPV1 and neuropeptides including CGRP and substance P is reported (Barry et al., 2016; Sun and Chen, 2007). These neurons are also believed to be pruriceptors, since isolated GRP-expressing neurons in show calcium responses following application of pruritogens. Akiyama et al. (2013) found that 20-40% of DRG cells that exhibited calcium fluxes in response to pruritogens including histamine, chloroquine, and SLIGRL stained positively for GRP peptide. Expression of GRP peptide has also been reported in the dorsal horn, where it overlaps with expression of CGRP and TRPV1 (Barry et al., 2016; Sun and Chen, 2007).

However, conflicting evidence exists as to whether GRP is expressed in the central terminals of primary afferent neurons or in interneurons in the dorsal horn. Barry et al. (2016) could not find evidence of GRP-expressing cells in dissociated dorsal horn neurons but did find a reduction in GRP-expressing fibres in the dorsal horn following dorsal root rhizotomy. Sun and Chen (2006) did not find GRP mRNA in the dorsal horn and also found a significant reduction in GRP peptide in the dorsal horn following dorsal rhizotomy, suggesting GRP synthesised by the DRG was unable to be transported to the central terminals of primary afferents following rhizotomy. These studies suggest GRP is mostly synthesised by primary sensory neurons where it is subsequently transported to their terminals in the dorsal horn. In contrast, other studies have found that GRP peptide in the dorsal horn is mostly restricted to cell bodies and is likely to be synthesised locally. Indeed, while dorsal root transection results in a small reduction in the amount of GRP immunoreactivity in the dorsal horn, likely due to a reduction in the transport of GRP from a few cell bodies in the DRG to the dorsal horn, overall most of the GRP immunoreactivity remains as before rhizotomy, suggesting that a significant amount of GRP is synthesised and expressed locally by cells in the dorsal horn, allowing for most of the immunoreactivity to be retained. In contrast, compared with GRP, immunoreactivity of CGRP is more greatly reduced following dorsal root transection, as transport of CGRP from the DRG cell bodies to the terminals in the dorsal horn is impeded (Fleming et al., 2012).

Studies have also found expression of GRP mRNA in mouse spinal cord using in-situ hybridisation (Wang et al., 2013). The number of cells expressing GRP mRNA decreased more than 76% in conditional KO mice with selective deletion of testicular orphan nuclear receptor 4 in the CNS by crossing with Nestin-Cre mice, resulting in a reduction in the number of excitatory interneurons in the dorsal horn and a reduction in pain behaviours to the hotplate, von Frey test of mechanical pain, and capsaicin-induced licking and flinching behaviours. Scratching behaviours following intradermal injection of histamine, chloroquine, and serotonin are also reduced in these mice, supporting a role for GRP in pruritus (Wang et al., 2013).

GRP-expressing cells in the dorsal horn are mainly located in lamina II, with a small population found in lamina I, where they likely comprise interneurons rather than projection neurons. Transgenic mice in which GRP-expressing neurons were labelled with enhanced green fluorescent protein (EGFP) did not show co-localisation of GRP with the vesicular GABA transporter VGAT or Pax2, markers for inhibitory interneurons; however,

colocalisation with the vesicular glutamate transporter 2 (VGLUT2) was observed, suggesting many of the cells are excitatory neurons (Gutierrez-Mecinas et al., 2014). EGFP-positive cells were mostly restricted to lamina I and II of the dorsal horn, and fewer cells in deeper layers. Additionally, using retrograde tracers injected into the lateral parabrachial nucleus, Solorzano et al. (2015) were unable to observe double labelling of GRP with the tracer, in the spinal cord, suggesting these cells are likely to be interneurons rather than projection neurons.

Bell et al., (2016) observed that only 3-7% of GRP-expressing cells in the spinal cord were positive for Fos or phospho-ERK following injection of chloroquine in mice, while the majority of activated neurons in the dorsal horn did not express GRP, suggesting GRP is not critical for chloroquine-mediated itch, although it may be required for other types of itch. However, chloroquine-mediated scratching behaviour is found to be reduced following systemic or intrathecal administration of a GRP receptor antagonist (Akiyama et al., 2013). Furthermore, Wan et al. (2017) and Zhao et al. (2014c) found that scratching behaviour was reduced in GRP KO mice when injected with chloroquine, SLIGRL-NH₂, or BAM8-22. In contrast, no difference in scratching behaviour was observed following injection of compound 48/80 or histamine in GRP KO mice compared with wild-type mice. This suggests that GRP is not involved in histaminergic itch. However, both Sun and Chen (2007) and Zhao et al. (2014c) reported a small decrease in itch mediated by compound 48/80 in their GRPR KO mice, suggesting the GRP receptor may play a role in itch mediated by histamine released from mast cells. Sun et al. (2017) also reported a decrease in histamine and chloroquine-mediated scratching behaviours in mice following ablation of GRP-expressing neurons. Thus, the precise contribution of GRP signalling to histaminergic and non-histaminergic itch remains unclear, though it appears to at least contribute to transmission both types of itch signal.

GRP may also be involved in transmission of pain signals. Wan et al. (2017) reported that GRP KO mice had normal sensitivity to noxious mechanical, thermal, and chemical stimuli, suggesting GRP is not required for pain responses. In contrast, Sun et al. (2017) found that ablation of more than 95% of GRP-expressing neurons in transgenic mice expressing diphtheria toxin receptors in GRP-expressing neurons resulted in increased wiping behaviour following injection of capsaicin into the cheek and increased licking and flinching was noted following intraplantar injection of capsaicin into the hindpaw, while responses to tail immersion in hot water, hot plate, and Hargreaves were also increased. However, these

mice did not show increased sensitivity to von Frey, suggesting no change in mechanical sensitivity and that loss of GRP-expressing neurons enhances chemical and thermal pain only. This difference in response to noxious stimuli may be due to the different approaches used in these two studies (transgenic mice lacking expression of GRP versus ablation of GRP-expressing neurons), which may have off-target effects and differing degrees of compensation as a result of loss of GRP activity. Sun et al. (2017) also reported that GRP-expressing neurons received input from primary sensory neurons conveying both itch and pain information, with pruritogens and algogens capable of triggering action potentials in GRP-expressing neurons. Moreover, coding of pain by GRP-expressing neurons was intensity-dependent, with weak and strong activation of GRP-expressing neurons producing little nocifensive behaviour, and medium activation of GRP-expressing neurons producing greatest nocifensive behaviour. This intensity-dependence of activation of GRP-expressing neurons could explain why some studies have reported that GRP signalling is not involved in nociception, while other studies report a role for GRP in transmitting pain information. However, while the role of GRP in pain responses is unclear, expression of GRP in DRG neurons likely increases following injury. Peripheral nerve injury was reported to increase expression of GRP mRNA in DRGs by about 20-fold, while no change in GRP expression in the dorsal horn was observed (Solorzano et al., 2015). A quarter of these DRG neurons that expressed GRP following injury were positive for TRPV1, while a quarter were positive for the NF-200 marker of myelinated axons, suggesting that GRP is not restricted to pruriceptive or small diameter nociceptive neurons, and may have additional roles in the transmission of pruritic or nociceptive signals in chronic states following injury by upregulation or *de novo* expression in larger diameter cells.

Concerns about the GRP antibody have been raised, casting doubt on the interpretations of earlier studies investigating the expression and function of GRP signalling in neurons. Some studies use a GRP antibody raised against bombesin, which has a high affinity for the GRP receptor as well as the neuromedin B receptor (Jensen et al., 2008), and GRP antibodies may be able to cross react with neuromedin B and substance P (Goswami et al., 2014). Thus, studies examining the staining of GRP protein could potentially be looking at expression of neuropeptides other than GRP. Some studies have reported cross-reaction of GRP antibodies with other peptides (Gutierrez-Mecinas et al., 2014), while others have not found any cross-reactivity (Fleming et al., 2012). However, Solorzano et al. (2015) reported that the GRP antibody when used at low dilutions was non-specific, staining many DRG cells and terminals in the spinal cord in tissue sections from GRP KO mice. Staining of DRG cells and

terminals from GRP KO mice was prevented only when the antibody was used at 1:4000 dilution. However, at this dilution, cells in the DRG from WT mice did not stain for GRP, and only a few GRP-positive cells were observed in the dorsal horn. Rather than binding to GRP, it was reported that the GRP antibody could cross-react with substance P when used at higher concentrations, which could explain the presence of GRP-positive cells in DRG tissues and in the terminals of the dorsal horn reported in other studies using antibody staining. The GRP staining protocol has also been found to affect the outcome of GRP staining. Barry et al. (2016) reported that tissue sections mounted on slides prior to antibody staining resulted in a widespread staining pattern for GRP, while staining of free-floating sections resulted in a more specific pattern of staining with fewer numbers of cells stained. Such differences in staining protocol may also explain why some groups have reported expression of GRP in a substantial percentage of DRG cells, while other groups report only occasional numbers of GRP-positive cells in the DRG. Of the few cells that do appear to be positive for GRP, co-localisation with CGRP is reported, suggesting these cells belong to a subset of peptidergic sensory neurons (Fleming et al., 2012).

Expression of GRP mRNA has sometimes been reported in the DRG and spinal cord, although at very low levels. Using qPCR, expression of GRP mRNA has been reported to be very low in the mouse DRG (Fleming et al., 2012; Liu et al., 2014b; Mishra and Hoon, 2013; Solorzano et al., 2015), and Barry et al. (2016) reported that at least 32 cycles were required before GRP mRNA could be detected in the DRG using this technique. Using RNA-seq, Barry et al. (2016) detected low expression of GRP in murine DRGs, while Goswami et al. (2014) were unable to detect GRP in the DRG or TG in mouse, rat, or human, although expression of GRP in the spinal cord of all three species was confirmed. Solorzano et al. (2015) and Fleming et al. (2012) did not report expression of GRP mRNA in the DRG using in-situ hybridisation, while Barry et al. (2016) and Liu et al. (2014b) were able to successfully stain for GRP mRNA in DRG tissue sections. However, Barry et al. (2016) also found that GRP mRNA could be detected in DRG tissue sections only after several hours of incubation in substrate, likely reflecting the low copy number of GRP in these cells. This could also explain why some groups have been unable to find expression of GRP mRNA in the DRG using in-situ hybridisation. The low expression of GRP mRNA in the DRG makes it difficult to detect expression of this neuropeptide using certain methods, while more sensitive methods, such as qPCR, have been more successful in detecting the presence of GRP mRNA in tissues. However, expression of GRP mRNA can be increased under certain conditions. For instance, in a dry skin model of itch, Barry et al. (2016) detected an 8-fold increase in GRP mRNA in

the DRG using qPCR. GRP mRNA as well as peptide has been detected in spinal cord dorsal horn tissues, with expression being greater than that observed in DRG tissues (Fleming et al., 2012; Goswami et al., 2014; Mishra and Hoon, 2013; Zhao et al., 2013). As more GRP mRNA is detected in the spinal cord than in the DRGs, GRP mRNA is likely to be synthesised locally by cells in the dorsal horn rather than synthesised in the DRG cell body and transported to terminals the dorsal horn. This is also reflected in the difference in expression of GRP peptide in these tissues (Fleming et al., 2012; Solorzano et al., 2015).

The receptor for GRP, GRPR, is expressed in the outer laminae of spinal cord dorsal horn tissues (Aresh et al., 2017; Fleming et al., 2012; Nattkemper et al., 2013; Sun and Chen, 2007; Zhao et al., 2013; Zhao et al., 2014c). These GRPR-expressing neurons in the dorsal horn are likely to be excitatory interneurons, as they express VGLUT2 (Aresh et al., 2017; Zhao et al., 2014c). Expression of GRPR mRNA and protein is increased in a mouse model of chronic itch in which a constitutively active form of the serine/threonine kinase, BRAF, is expressed in Nav1.8 neurons, suggesting a role for GRP-GRPR signalling in chronic itch conditions (Zhao et al., 2013). In these transgenic mice, constitutively active BRAF in Nav 1.8 neurons enhanced signalling of the RAF/MEK/ERK cascade, as demonstrated by an increase in the phosphorylation of MEK and ERK in the DRGs, particularly in TRPV1-positive DRG neurons. Expression of BRAF and activation of the RAF/MEK/ERK signalling cascade is presumed to be involved in the development and projection of normal neuronal circuitry, as aberrant expansion of CGRP-expressing fibres deeper into the dorsal horn into lamina III and invasion of IB4-positive fibres into the outer parts of lamina II and lamina I is observed in these mice. Conversely, axon outgrowth is reduced in neurons from BRAF-deficient mice (Zhong et al., 2007). However, only pruritus appears to be affected in mice expressing constitutively active BRAF, as responses to noxious stimuli and motor behaviours are normal in these mice and comparable to those of WT littermates (Zhao et al., 2013). Furthermore, scratching behaviour following injection of pruritogens including compound 48/80, SLIGRL-NH₂, and chloroquine is significantly reduced in mice lacking the GRP receptor compared with wild-type littermates (Sun and Chen, 2007).

Neuromedin B

Like GRP, neuromedin B (NMB) is a bombesin-like peptide associated with itch. NMB injected intrathecally in rats or mice results in scratching behaviour, suggesting NMB has a role in transmission of itch signals in the CNS (Su and Ko, 2011; Sukhtankar and Ko, 2013). Wan et al. (2017) reported that, compared with wild-type mice, scratching behaviour was

reduced in NMB KO mice following injection of histamine, serotonin, chloroquine, SLIGRL-NH₂, or BAM8-22, suggesting NMB is involved in both histaminergic and non-histaminergic itch. Although mice lacking the NMB receptor do not display reduced scratching behaviour in response to injection of pruritogens, double KO mice lacking both NMB and GRP receptors show significant reduction of scratching behaviours to injection of histaminergic pruritogens that is not observed when only one of the receptors is missing (Zhao et al., 2014c). This suggests the NMB receptor acts synergistically with the GRP receptor to mediate transmission of histaminergic itch, and that some compensation may occur when signalling via one of the receptors is prevented. In support of this, GRP has been found to weakly activate the NMB receptor, and may account for the scratching behaviour observed in mice that lack functional NMB receptors (Zhao et al., 2014c). NMB is not required for pain behaviours, since NMB KO mice displayed normal sensitivity to noxious mechanical and thermal stimuli. However, injection of NMB has been reported to induce oedema and thermal and mechanical hypersensitivity, suggesting a role for NMB in nociception (Mishra et al., 2012).

Expression of NMB in DRG tissues has been reported using RNA-seq, qPCR, and in-situ hybridisation, where it is reported to be expressed in 50% of DRG neurons (Barry et al., 2016; Fleming et al., 2012; Goswami et al., 2014; Mishra et al., 2012; Zhao et al., 2014c). Most NMB-expressing neurons are small diameter, unmyelinated or thinly myelinated neurons of both peptidergic and non-peptidergic subsets (Fleming et al., 2012; Zhao et al., 2014c). These neurons are likely to be pruriceptive neurons, as many NMB-expressing neurons co-express TRPV1 and MrgprA3 (Fleming et al., 2012; Mishra et al., 2012). Co-expression of NMB and GRP has also been reported (Zhao et al., 2014c). The NMB receptor is expressed in cells in the dorsal horn of the spinal cord (Goswami et al., 2014; Zhao et al., 2014c). Most NMBR-positive cells are located in lamina I and II of the superficial dorsal horn, with a few cells found in the deeper layers (Zhao et al., 2014c). NMBR-positive cells do not express NK1 receptor, suggesting these cells are not projection neurons and are likely to be excitatory interneurons that form part of the spinal cord itch circuitry. Only 10% of NMBR-expressing neurons also expressed GRPR, suggesting NMBR and GRPR cells likely comprise distinct cell populations. Moreover, patch clamping experiments in spinal cord slice preparations have revealed that GRPR-expressing neurons in the spinal cord receive excitatory input from NMBR-expressing cells (Wan et al., 2017). Thus, although likely comprising distinct cell populations transmitting itch information from primary afferents, NMB and GRP signalling is also interconnected, with NMBR neurons relaying itch

information to GRPR neurons, and could help to explain the significant reduction in scratching behaviour in response to injection of histaminergic pruritogens that is observed only in mice that are lacking both receptors (Zhao et al., 2014c).

Natriuretic polypeptide B

The natriuretic peptides A, B, and C are a family of structurally related peptides containing the conserved sequence CFGXXDRXXXXGLGC, where X is any amino acid (Potter et al., 2006). Expression of natriuretic peptides was first described in heart tissues, but they have since been found to be expressed in other tissues, including the brain and sensory ganglia, where they have tissue-specific functions. They are synthesised in a pro-form that is subsequently proteolytically cleaved by corin and furin to form the mature peptides (Hall, 2004; Potter et al., 2006). Three receptors are known to exist for the natriuretic peptides. Natriuretic peptide receptor A (NPRA) is the receptor for both NPPA and NPPB, while natriuretic peptide receptor B (NPRB) is the receptor for NPPC (Potter et al., 2006). Both NPRA and NPRB are guanylyl cyclase linked receptors that results in the production of cyclic GMP when activated. The third receptor, natriuretic peptide receptor C (NPRC), in contrast, does not have guanylyl cyclase activity, and it thought to be involved in the clearance of natriuretic peptides through receptor-mediated internalisation and degradation (Potter et al., 2006).

Expression of NPPB is increased 3.5-fold in the sensory ganglia of a mouse model of atopic dermatitis (Meng et al., 2018). NPPB evokes scratching behaviour when injected into mice, which is reduced following ablation of NPPB-expressing cells or in the presence of antagonists to the NPPB or GRP receptors (Kiguchi et al., 2016; Mishra and Hoon, 2013). NPPB is also required for itch mediated by other pruritogens, since scratching behaviour following injection of histamine is reduced following ablation of neurons expressing the NPPB receptor via intrathecal injection of NPPB-saporin (resulting in death of NPRA-expressing cells) and scratching behaviour in response to injection of pruritogens including histamine, serotonin, chloroquine, and SLIGRL-NH₂ is reduced in NPPB KO mice compared with wild-type littermates (Mishra and Hoon, 2013). NPPB-induced scratching behaviour is also reduced in the presence of a GRP antagonist or following ablation of GRPR-expressing neurons by injection of GRP-saporin, suggesting NPPB is required for GRP-mediated scratching behaviours (Mishra and Hoon, 2013). NPPB is also likely to be required for IL-31-induced itch, since release of NPPB peptides from cultured mouse DRG cells is reported following stimulation with IL-31 (Pitake et al., 2018). In contrast, NPPB is not required for

responses to thermal and mechanical stimuli, as these responses were unaltered in NPPB KO mice, and nocifensive behaviours in inflammatory conditions are not affected in NPPB KO mice (Mishra and Hoon, 2013; Pitake et al., 2017), although Liu et al. (2014b) reported that in mice pain responses following intraplantar injection of capsaicin and the phase II response of formalin-evoked nocifensive behaviour were reduced when NPPB was administered intrathecally. Moreover, NPPB has been found to have reduced formalin-induced flinching behaviour in rats (Zhang et al., 2010). This suggests NPPB signally may additionally have a role in inhibition of nocifensive behaviours.

Expression of NPPB mRNA in cells of the DRG has been detected using in-situ hybridisation and qPCR (Li et al., 2016c; Mishra and Hoon, 2013; Pitake et al., 2017; Pitake et al., 2018; Solorzano et al., 2015). RNA-seq revealed that NPPB is highly expressed in mouse DRG, but to a lesser extent in rat and human sensory ganglia, suggesting species variation may exist in the expression of neuropeptides in these tissues (Goswami et al., 2014). Expression of NPPB was found to occur in a subset of neurons expressing TRPV1, suggesting these cells comprise a subset of nociceptors (Mishra and Hoon, 2013). All cells that were positive for NPPB mRNA were also positive for MrgprA, and MgrprC11, receptors for pruritogens such as chloroquine, and BAM8-22 and SLIGRL-NH₂, respectively (Mishra and Hoon, 2013). In contrast to NPPB mRNA, NPPB protein has been reported to be expressed in non-neuronal cells in mouse DRG and TG, using several different NPPB antibodies (Liu et al., 2014b; Vilotti et al., 2013). However, none of these studies verified the specificity of their antibodies in NPPB KO mice or by co-staining for NPPB mRNA. Furthermore, Zhang et al. (2010) and Li et al. (2016) both reported the presence of NPPB protein in small neurons in the rat DRG using antibody staining. NPPB was expressed in CGRP-positive and some IB4-positive cells, and expression in the DRG was increased following intraplantar injection of Complete Freund's Adjuvant and two days after injection of BmK I, a sodium channel modulator from the venom of Chinese scorpion (Li et al., 2016c; Zhang et al., 2010). Expression of NPPB peptide has also been reported in murine DRG cells in at least one study, where it co-localises with the neuronal marker NeuN (Kiguchi et al., 2016). As well as being expressed in the DRG, NPPB peptide is reported to be expressed in the outer laminae of the dorsal horn of the spinal cord, where it overlaps with CGRP-expressing fibres (Abdelalim et al., 2016; Kiguchi et al., 2016). Some NPPB-expressing cells are also found in the ventral horn of the spinal cord in rat, in what appear to be motor spinal neurons expressing choline acetyltransferase (Abdelalim et al., 2016).

Expression of the NPPB receptor natriuretic peptide receptor A (NPRA) has been reported in the dorsal horn of the spinal cord and overlaps with expression of cells positive for CGRP and GRP, suggesting GRP acts downstream of NPPB (Goswami et al., 2014; Kiguchi et al., 2016; Mishra and Hoon, 2013; Pitake et al., 2017; Zhang et al., 2010). Liu et al. (2014b) also observed expression of NPRA in the dorsal horn, although the staining patterns were different depending on the antibody used, sometimes appearing to stain individual cells throughout the entire dorsal horn and other times staining fibres restricted to the outer laminae, casting doubt on the actual distribution of NPRA-expressing cells and fibres in the spinal cord. Furthermore, NPRA-positive cells have also been reported in the DRG (Goswami et al., 2014; Li et al., 2016c; Liu et al., 2014b; Zhang et al., 2010).

Activation of primary sensory neurons by pruritogens is proposed to result in release of NPPB from the terminals of these neurons in the spinal cord dorsal horn. The released NPPB then binds to its receptor, NPRA, located on the dendrites of interneurons located mostly in lamina II of the dorsal horn. These interneurons, in turn, release GRP from their terminals, which binds to its receptor on additional interneurons or on projection neurons that transmit the itch signal to higher centres in the CNS. However, whether NPPB is upstream of GRP signalling in itch is disputed. Liu et al. (2014b) and Kiguchi et al. (2016) found that injection of NPPB did result in scratching behaviour in mice, but with a different timecourse to that observed following injection of GRP. Injection of GRP caused robust scratching behaviour shortly after injection, returning to baseline 40 minutes after injection. In contrast, injection of NPPB elicited very mild scratching behaviour that gradually increased over time, peaking at 40-50 minutes after injection. Furthermore, in contrast to Mishra and Hoon, 2013, scratching behaviour in response to injection of NPPB was not abolished in the presence of a GRP blocker (Liu et al., 2014b). Scratching responses were also unaffected in GRP KO mice and in GRPR KO mice (Liu et al., 2014b). If GRP signalling is downstream of NPPB, then it would be expected that preventing signalling of GRP would at least reduce scratching behaviour following injection of NPPB. One possible explanation for this is that some signalling of GRP occurs downstream of NPPB, but some signalling of GRP and NPPB also occurs independently of each other, and compensatory mechanisms may exist such that blocking of one pathway results in enhanced activity of another pathway, preserving transmission of the itch signal and the subsequent scratching behaviour. However, this does not explain the differences in scratching behaviour following injection of NPPB in the presence of a GRP antagonist as reported by Mishra and Hoon (2013), and Liu et al. (2014b).

1.3.3 Central sensitisation of itch

In addition to being involved in peripheral sensitisation, NGF may also play a role in central sensitisation of pruriceptors via upregulation of neuropeptides such as CGRP and substance P, resulting in their increased release from the central terminals of primary afferents in the spinal cord dorsal horn in response to pruritogens from the periphery (Verge et al., 1995). NGF may similarly increase expression of itch-related neuropeptides, such as NPPB and GRP. Increased release of neurotransmitters such as glutamate may further contribute to sensitisation via phosphorylation of the GluN2B subunit on post-synaptic NMDA receptors, resulting in enhanced activity of neurons in the dorsal horn circuitry (Inoue et al., 2016). Activation of glial cells and the subsequent release of inflammatory mediators such as TNF and IL-1 β in the spinal cord is known to be involved in central sensitisation in chronic pain, and may similarly do so for chronic itch (Ji, 2015). However, as for several of the proposed mechanisms of peripheral sensitisation in itch, the factors that determine sensitisation of itch signals over pain signals in the spinal cord remain to be further investigated.

1.4 Pathology of itch and the role of Cathepsin S in chronic itch

Although acute itch is a beneficial sensation, chronic itch is a detrimental condition that severely negatively impacts the quality of life of the sufferer (Erturk et al., 2012; Kini et al., 2011; Yosipovitch et al., 2000; Yosipovitch et al., 2001; Yosipovitch et al., 2002). Disorders of itch are classified into four different categories (Twycross et al., 2003):

- Pruritoceptive itch – Itch that originates in the skin, usually as a result of inflammation or damage to the skin. This type of itch is also a feature of conditions such as atopic dermatitis and psoriasis. Some forms of urticaria are also examples of pruritoceptive itch due to the release of histamine from cells in the skin.
- Neurogenic itch – Itch that originates in the CNS but without evidence of neuronal pathology. This type of itch is typically observed in liver disease with cholestasis and chronic kidney failure.
- Neuropathic itch – Itch due to disease or lesions of the afferent fibres, for example, as observed in postherpetic neuralgia, notalgia paraesthetica, and multiple sclerosis.
- Psychogenic itch – Itch resulting from a psychological disorder, such as delusions of parasitosis.

Atopic dermatitis

Atopic dermatitis is described as an inflammatory skin condition that usually develops during early childhood and is believed to affect up to 20% of the population (Bieber, 2010;

Leung and Soter, 2001). Pruritus is characteristic of atopic dermatitis and is used as a diagnostic criterion for this condition (Hong et al., 2011). Other features of atopic dermatitis include increased serum IgE and infiltration of mast cells and basophils (Ito et al., 2011; Leung and Soter, 2001; Sugiura et al., 1992) into the skin. Infiltration of T-cells, particularly of the Th2 phenotype, is also observed in the skin during the acute phase atopic dermatitis (Mudde et al., 1992; Werfel, 2009), although these appear to be replaced by Th1 cells that release interferon- γ (IFN γ) during the chronic phase of the disease (Grewe et al., 1998).

Increased infiltration of immune cells in this condition likely results in heightened inflammation in the skin and an increase in the release of mediators that could serve as pruritogens by acting directly on sensory neurons. For example, IL-31, a cytokine released by Th2 cells, causes scratching behaviour when injected into mice and was recently demonstrated to directly activate pruriceptors (Pitake et al., 2018). Alternatively, cytokines released from these cells may cause the release of pruritogens from other cells in the skin, such as keratinocytes. Increased inflammation is likely to be the cause of itch in atopic dermatitis, via the release of histamine and other pruritogens from mast cells and keratinocytes, rather than being a symptom of itch (Costa et al., 2008; Malaviya et al., 1996; Shimizu et al., 2015; Terakawa et al., 2008). However, the excessive scratching that accompanies chronic itch is likely to exacerbate inflammation, resulting in an itch-scratch cycle whereby scratching damages the skin and further worsens inflammation, resulting in the release of more pruritogens and continuation of the cycle.

As well as an increase in potential sources of pruritogens, the density of sensory nerve endings is increased in the skin of patients with atopic dermatitis, where they are more likely to come into contact with pruritogens (Horiuchi et al., 2005; Takano et al., 2005; Tobin et al., 1992). Sprouting of nerve fibres is likely to be due to NGF, which has been reported to be increased in atopic dermatitis conditions and correlates with disease severity (Horiuchi et al., 2005; Takano et al., 2005; Toyoda et al., 2002; Yamaguchi et al., 2009). NGF does not appear to sensitise neurons to histamine, suggesting the enhanced pruritus characteristic of atopic dermatitis is not caused by sensitisation of neurons to this pruritogen (Rukwied et al., 2013). However, NGF was found to sensitise neurons to other pruritogens, such as cowhage, providing a mechanism by which enhanced itch sensations could occur. Increased expression of receptors on sensory neurons, such as the receptor for cowhage, as well as TRP channels, may also contribute to pruritus (Nattkemper et al., 2018; Steinhoff et al., 2003).

Another interesting feature of this condition is that punctate application of pruritogens into lesioned skin results in much stronger pruritus than is reported by healthy controls (Andersen et al., 2017; Ikoma et al., 2003), and stimuli that would normally be felt as pain in healthy volunteers are felt as itch when applied to the lesioned skin of patients with atopic dermatitis, which is suggestive of sensitisation (Hosogi et al., 2006; Ikoma et al., 2004). Although histamine may play a role in scratching in atopic dermatitis, antihistamines have been shown to be ineffective in treating itch in this condition, suggesting other pruritogens are likely to be involved (Klein and Clark, 1999; Rukwied et al., 2000; Wahlgren et al., 1990; Yarbrough et al., 2013). Furthermore, in the lesioned skin of patients with atopic dermatitis, sensitisation to pruritogens is greater for non-histaminergic pruritogens such as cowhage than to histamine, further supporting a role for non-histaminergic pruritogens in this condition (Andersen et al., 2017).

Changes in the skin are also observed in patients with atopic dermatitis. In addition to the development of skin lesions, dry skin with increased transepidermal water loss is reported in this condition, suggestive of dysfunction of the epidermal barrier (Bieber, 2010; Leung and Soter, 2001). This dysfunction may be the result of loss of structural proteins in keratinocytes which contribute to barrier function. For instance, expression of filaggrin, loricrin, and involucrin proteins is reported to be reduced in the skin in atopic dermatitis and mutations in the filaggrin gene are often reported in patients with atopic dermatitis (Howell et al., 2007; Kim et al. 2008; Palmer et al., 2006). Increased skin pH is also found in atopic dermatitis, where it may contribute to barrier dysfunction by altering lipid organisation and metabolism and contribute to growth of bacteria in the skin (Rippke et al., 2004). This loss of integrity of the epidermal barrier and subsequent increase in bacterial colonisation of the skin may be responsible for the increased infiltration of immune cells into the skin of atopic dermatitis patients and the subsequent release of pruritogens, although at least some cases of atopic dermatitis are proposed to result from IgE-mediated autoimmunity (Bieber, 2010).

Oral administration of the μ -opioid receptor antagonist naltrexone has been found to be effective in reducing pruritus in atopic dermatitis, although topical administration of opioid antagonists does not relieve pruritus, suggesting centrally acting opioids can inhibit transmission of itch signals in this condition while pruritus in atopic dermatitis is unlikely to be mediated by peripheral opioid receptors (Herzog et al., 2011; Heyer et al., 2002; Malekzad et al., 2009). Nevertheless, expression of the μ -opioid receptor has been confirmed on sensory nerve fibres in the epidermis and dermis, and expression of both μ

and κ opioid receptors has been reported in skin keratinocytes, with greater expression of κ opioid receptors in the skin of patients with atopic dermatitis compared with healthy controls (Stander et al., 2002; Tominaga et al., 2007). Furthermore, in addition to improving skin symptoms in patients with atopic dermatitis, psoralen-ultraviolet A treatment also decreased expression of μ -opioid receptor in the skin (Tominaga et al., 2007). This suggests peripheral opioidergic activity may be responsible for some of the symptoms of atopic dermatitis, although not necessarily pruritus. Nevertheless, an indirect role of opioids acting on receptors on keratinocytes and sensory nerve endings in the skin may contribute to pruritus in this condition.

Cathepsin S

Cathepsin S (CatS) is a lysosomal protease that belongs to the cysteine family of proteases, and closely resembles Cathepsins K and L (Kirschke and Wiederanders, 1994; McGrath, 1999). The proteolytic functions of CatS have been well documented. CatS is expressed in the lysosomes of professional bone marrow-derived antigen presenting cells such as macrophages, microglia, B lymphocytes, and dendritic cells, as well as non-professional antigen presenting cells such as epithelial cells, where it is involved in major histocompatibility complex (MHC) class II-mediated antigen presentation by degradation of the invariant chain II and peptide loading (Bender et al., 2015; Chapman, 2006; Chapman et al., 1997; Clark et al., 2007; Clark et al., 2010; Hsing and Rudensky, 2005; Liuzzo et al., 1999; Petanceska et al., 1996; Shi et al., 1992; van Kasteren and Overkleeft, 2014). CatS can also cleave laminin, fibronectin, collagens I and IV, and chondroitin sulfate and heparan sulfate proteoglycans at both acidic and neutral pH, supporting a role for this protease in the degradation of extracellular matrix tissue remodelling following injury (Liuzzo et al., 1999; Petanceska et al., 1996). Moreover, endothelial cells from CatS KO mice have reduced proteolytic activity and impaired invasion into Matrigel and collagen gel, while development of microvessels during wound repair is defective in these mice (Shi et al., 2003). The CatS inhibitory antibody Fsn0503 also impaired the ability of endothelial cells to degrade extracellular matrix and blocked the development of tumour blood vessels in mice that received transplants of the HCT116 human colon cancer cell line (Ward et al., 2010). These findings suggest a role for CatS released from endothelial cells in angiogenesis following injury and in tumourigenesis.

Like the other cysteine proteases, CatS is synthesised as an inactive pre-pro-enzyme. Under reducing conditions and at acidic pH, inactive pre-pro-CatS synthesised in yeast and *E. coli* is

activated by self-cleavage, suggesting some CatS must exist in an active form (Bromme et al., 1993; Kopitar et al., 1996). CatS can also be activated following the addition of the non-specific serine protease subtilisin (Bromme et al., 1993), but not the aspartic protease Cathepsin D (Kopitar et al., 1996). In contrast, pro-CatS can be degraded by Cathepsin L (Maubach et al., 1997). Thus, other proteases may modulate activation of CatS, although whether they do so under physiological conditions remains to be determined. Activation of pro-CatS is accelerated by negatively-charged molecules such as glycosaminoglycans, chondroitin sulfates, dermatan sulfate, and dextran sulfate. Furthermore, while auto-activation of pro-CatS is greatest at acidic pH and decreases when the pH increases above 6, significant levels of auto-activation of pro-CatS can occur at neutral and mildly alkaline pH when in the presence of dextran sulfate (Vasiljeva et al., 2005). Auto-activation of CatS at neutral pH is affected by ionic strength, with increasing ionic strength resulting in a decrease in activation, suggesting negatively-charged glycosaminoglycans and polysaccharides interact with CatS via electrostatic interactions to accelerate auto-activation of this protease. The presence of a large number of positively-charged residues on pro-CatS supports this notion. The synthesis of lysosomal cathepsins as inactive zymogens that require activation serves two purposes. First, the N-terminal of the pro-peptide is required for correct folding of the peptide targeting to the lysosomal compartment (Turk et al., 2012). Second, production of cysteine proteases in an inactive pre-form, as well as peak activation at acidic pH, serves to protect in the event of accidental release or mistargeted release of proteases. However, because CatS can activate itself and has proteolytic activity at neutral pH, its release into the cytosol or extracellularly could potentially result in unwanted cleavage of proteins and tissue damage by the degradation of healthy tissues. Moreover, CatS can activate other cathepsins, such as Cathepsin C (Dahl et al., 2001). However, CatS is also regulated by the endogenous protein inhibitor, cystatin C, which reversibly binds to CatS and has been shown to regulate activity of CatS during maturation of dendritic cells (Bromme et al., 1991; Pierre and Mellman, 1998).

Cathepsin S in itch conditions

In addition to its proposed role in antigen presentation and degradation of extracellular matrix, CatS in the skin has been demonstrated to be involved in itch. Transgenic mice over-expressing CatS have increased expression of CatS in the skin and demonstrate spontaneous scratching behaviours, resulting in the formation of lesions, infiltration of mast cells, and thickening of the skin (Kim et al., 2012). CatS released from skin cells may be responsible for

pruritus by cleaving receptors on primary sensory neuron endings, or may result in pruritus via indirect mechanisms such as causing release of pruritogens from other cell types.

In a mouse model of **atopic dermatitis** in which transgenic mice over-expressed CatS, mRNA and protein expression of Th2 cytokines, including IL-4 and IL-10 was increased in the skin (Kim et al., 2012). Interestingly, however, compared with expression of Th2 cytokines, expression of Th1 cytokines, such as IL-2, IFN γ , and TNF α was even greater in transgenic mice compared with wild-type mice. This could reflect the development of chronic lesions in these mice, which were 16 weeks old at the time of the experiments, rather than the acute lesions associated with Th2 cytokines. However, because no time course was performed comparing the age of the mice, the development of lesions, and the cytokine profile, it is not possible to confirm whether younger mice with acute lesions would have had a dominant Th2 phenotype, or whether older mice with more advanced lesions would have had a complete Th1 phenotype. In a canine model of acute atopic dermatitis, gene expression of CatS, along with Th2 cytokines, was upregulated over 48 hours, supporting a role for CatS in the acute stage of this disease (Olivry et al., 2016).

CatS is also associated with itch conditions other than atopic dermatitis. Expression of CatS protein is increased in the lesions of patients with **seborrhoeic dermatitis** compared with healthy subjects (Viode et al., 2014). Moreover, Ainscough et al., (2017) and Schonefuss et al., (2010) both reported that CatS protein was upregulated in keratinocytes from patients with **psoriasis**. Furthermore, in HaCaT cultures, expression and release of CatS protein can be increased following incubation with Th1 cytokines, such as IFN γ and TNF α , while IFN γ upregulates expression of CatS in primary keratinocytes, further supporting a role for CatS in psoriasis (Ainscough et al., 2017; Schonefuss et al., 2010; Schwarz et al., 2002). In addition, a mechanism by which CatS activates IL-36 γ to mediate inflammation in psoriasis has been proposed (Ainscough et al., 2017). IL-36 γ is expressed in psoriatic lesions and serum levels are correlated with disease severity (D'Erme et al., 2015). However, IL-36 γ is expressed as an inactive precursor that must be cleaved in order to be active (Towne et al., 2011). CatS released from keratinocytes and fibroblasts or applied exogenously cleaves IL-36 γ at S18, resulting in secretion of IL-8 from keratinocytes (Ainscough et al., 2017). It is therefore likely that CatS is involved in both Th1 and Th2-mediated chronic itch conditions.

1.5 Animal models of itch

In order to study the mechanisms of itch, animal models are frequently employed. Mouse models in particular are often used due to the ease of handling and genetic manipulation, although rats, guinea pigs, dogs, and primates are also used. However, because pruritic stimuli elicit two responses – acknowledgement of the sensation and site directed scratching toward the stimulus site, the use of animal models to study itch is limited in that we can only measure scratching behaviour in animals (LaMotte et al., 2011). In contrast, studies in human volunteers typically use verbal reports acknowledging the onset, duration, and intensity of itch, and volunteers may be asked not to scratch. Scratching results in the generation of pain signals which can affect transmission of itch signals, potentially inhibiting it in the case of acute itch or exacerbating it in chronic and inflammatory itch, thereby affecting the duration and severity of itch that is being measured. However, animals are allowed to scratch in most models of itch, although their nails may be clipped to reduce skin damage and nociceptive effects. Elizabethan collars may be used to prevent scratching behaviour altogether, ensuring only pruriception and not nociception is being investigated, although this prevents the experimenter from determining the pruritic effects of the stimulus. Thus, when using animal models, there is a compromise between determining pruritogenicity of stimuli and examining pruritus without influence of nociception caused by scratching behaviour. Whether or not the animal is allowed to scratch is thus determined by the questions that are being addressed by the study.

Models of chronic itch

Because itch, like pain, exists in both acute and chronic forms, models for both acute and chronic itch have been developed. Animal models of chronic itch are usually based on clinical observations of diseases in which pruritus is a defining feature of the condition. Spontaneous scratching behaviour, often accompanied by the development of lesions on the skin, is characteristic of these models. Several animal models of chronic itch conditions exist, the most common being those that resemble atopic dermatitis, contact dermatitis, and psoriasis. There are also mouse models in which chronic itch develops due to defects in the central itch circuitry, which are thought to be applicable to most, if not all, cases of itch, rather than specific chronic itch conditions.

The NC/Nga inbred mouse strain is a spontaneous model of atopic dermatitis first described by Matsuda et al. (1997). When housed in conventional (non-sterile) conditions, these mice develop atopic dermatitis-like conditions, including chronic scratching behaviour, the

development of skin lesions, increased plasma IgE, infiltration of mast cells and eosinophils, thickening of the epidermis, and impaired skin barrier function (Aioi et al., 2001; Matsuda et al., 1997; Matsumoto et al., 1999). In contrast, NC/Nga mice kept in specific pathogen-free conditions do not develop these symptoms. Immunohistochemical analysis of the skin of these mice demonstrated the production of Th2 cytokines such as IL-4 and IL-5 from T cells and mast cells infiltrating the skin (Matsuda et al., 1997), a feature which is characteristic in the acute lesions of patients with atopic dermatitis and is thought to contribute to the pathogenesis of this disease by increasing production of IgE from B cells (Mudde et al., 1992; Werfel, 2009). Indeed, NC/Nga mice have a mutation resulting in constitutively active JAK3 on B cells, resulting in greater activity of these cells in response to IL-4 released from T cells, mast cells, and basophils (Matsumoto et al., 1999). Interestingly, constitutive activity of JAK3 is also observed from B cells from patients with atopic dermatitis, suggesting this mouse model mimics the disease in humans (Matsumoto et al., 1999). However, in signal transducer and activator of transcription 6 (STAT6)-deficient NC/Nga mice in which IL-4-mediated immune responses and production of IgE are prevented, atopic dermatitis-like conditions occur at a similar frequency, age of onset, and severity as reported in normal NC/Nga littermates (Yagi et al., 2002). This suggests that IL-4-mediated production of IgE via the STAT6 transcription factor is not required for the development of atopic dermatitis-like symptoms in these mice and that they are a symptom of disease progression, although whether this is also the case in humans with atopic dermatitis remains to be investigated. Nevertheless, STAT6 polymorphisms have been found to be associated with risk of developing atopic dermatitis, and synthetic double-stranded oligodeoxynucleotides which inhibit binding of STAT6 to its promoter regions have been demonstrated to improve pruritus and inflammation in patients with atopic dermatitis (Casaca et al., 2013; Igawa et al., 2009; Lee et al., 2015). Thus, IL-4-mediated production of IgE via STAT6 may be one of several means by which symptoms of atopic dermatitis develop, although other pathways may exist that can function independently of STAT6.

Other models of atopic dermatitis involve genetic manipulation of mediators known or proposed to be involved in this disease. For example, to investigate the involvement of CatS in atopic dermatitis, Kim et al. (2012) developed a transgenic mouse line in which **CatS was over-expressed**, and found that these mice displayed scratching behaviour and developed skin lesions, infiltration of mast cells into the skin, serum IgE levels, and increased proliferation of keratinocytes. However, the source of CatS responsible for these symptoms and whether CatS acts as a pruritogen or an inflammatory mediator was not addressed in

this study. Mice over-expressing Th-2 cytokines such as IL-4, IL-13, or IL-31 also develop atopic dermatitis-like symptoms, further supporting the role of these cytokines in the disease (Chan et al., 2001; Dillon et al., 2004; Zheng et al., 2009). However, the observation that increased expression of any one of these cytokines can result in atopic dermatitis-like symptoms suggests individual mediators can elicit these symptoms, although it is likely that clinically these mediators act together to result in the observed symptoms. Indeed, each mediator might contribute to different symptoms of the disease and work with other mediators to give the full range of symptoms. In support of this, transgenic mice over-expressing IL-4 or IL-13 in the skin have increased IgE serum, as is often reported in patients with atopic dermatitis; however, transgenic mice over-expressing IL-31 do not have increased serum IgE, suggesting this cytokine mediates other symptoms of the disease (Dillon et al., 2004). Another cytokine that is proposed to be involved in atopic dermatitis is TSLP, which is expressed in and released from keratinocytes (Wilson et al., 2013). Over-expression of this cytokine in the skin of mice also results in atopic dermatitis-like symptoms, supporting the role of TSLP in this disease (Yoo et al., 2005). However, when these mice were crossed with mice that lacked T cells, atopic dermatitis-like symptoms, including epidermal thickening and infiltration of mast cells and eosinophils into the skin, were still observed in these mice, although IgE levels were not increased compared with TSLP over-expressing mice that had T cells. This suggests T cells are not required for the development of skin inflammation in atopic dermatitis, although they do play a role in the production of IgE. Moreover, this supports the notion that increased IgE may be a symptom of atopic dermatitis but is not required for development or progression of the disease.

Some transgenic mouse lines also show spontaneous, chronic scratching behaviour without being linked to any specific disease. In these mice, signalling of itch is disrupted due to alterations in the activity of primary afferent neurons or neurons in the spinal cord circuitry. They are therefore applicable to itch in general and are useful for delineating itch transmission in the spinal cord. Such models include expression of constitutively active BRAF in sensory neurons, knocking out expression of VGLUT2 in Nav1.8-positive sensory neurons or TRPV1-positive neurons, and knocking out expression of the Bhlhb5 transcription factor in interneurons in the spinal cord (Lagerstrom et al., 2010; Liu et al., 2010; Ross et al., 2010; Zhao et al., 2013).

Not all animal models of chronic itch involve specific strains of mice that display spontaneous development of the disease or transgenic mice. Several models of atopic

dermatitis have been established in wild-type mice following repeated application of sensitisers including ovalbumin, house dust mite allergens, acetone/diethyl ether mixture, and haptens (Huang et al., 2003; Man et al., 2008; Miyamoto et al., 2002; Spergel et al., 1998), although it could be argued these more closely resemble contact dermatitis rather than atopic dermatitis. Nevertheless, these models are useful for studying many features of chronic itch associated with skin inflammation, without the need for acquiring specific breeds of mice. Moreover, these models can be applied to different areas of the animal, including the cheek, back of the neck, or hindpaw, and have additionally been performed in rats and dogs (Andoh et al., 2018; Olivry et al., 2016; Schuttenhelm et al., 2015; Valtcheva et al., 2015b). Similarly, psoriasis-like dermatitis can be induced in mice following daily topical application of the TLR7/8 ligand and immune activator, imiquimod, resulting in the development of psoriatic plaques and increased expression of IL-17 and IL-23 (van der Fits et al., 2009).

Transplantation models have been established to study chronic itch conditions. These models have been particularly well established for psoriasis, but not for other chronic itch conditions as of yet. In these models, donor skin from patients with psoriasis is transplanted onto immunodeficient mouse strains such as nude, SCID, or AGR129 mice to prevent rejection of the grafts (Boyman et al., 2004; Krueger et al., 1981; Villadsen et al., 2003). Importantly, transplantation from non-lesional and lesional skin can be used to study the development of psoriasis and established psoriasis, respectively. Although technically challenging to perform and requiring large amounts of donor tissue for the grafts, this model is believed to most closely resemble the disease, demonstrating the requirement of T cells and TNF α for the development of psoriasis in recipient mice and has been useful in validating drug targets, such as vitamin D and cyclosporin A (Boyman et al., 2004; Dam et al., 1999).

A table summarising different models of chronic itch is provided below. Each model has its own merits and limitations, which will affect the choice of model used. For instance, some models may mimic a disease state better than others but may also be more difficult to obtain or generate. The choice of model will also depend on whether a specific disease or more general features of pruritus are being investigated. Another important factor to consider is how accurately the model reflects the clinical observations. For instance, the IL-31 KO mouse, although displaying many symptoms of atopic dermatitis, does not have increased serum IgE, which is a feature of atopic dermatitis (Dillon et al., 2004). However, it

Table 1.4: Summary of animal models of chronic itch

Model	Disease	Reference
NC/Nga strain	Atopic dermatitis	Matsuda et al., 1997
DS-Nh strain	Atopic dermatitis	Hikita et al., 2002
Cathepsin S over-expression	Atopic dermatitis	Kim et al., 2012
IL-4 over-expression	Atopic dermatitis	Chan et al., 2001
IL-13 over-expression	Atopic dermatitis	Zheng et al., 2009
IL-18 over-expression	Atopic dermatitis	Konishi et al., 2002
IL-31 over-expression	Atopic dermatitis	Dillon et al., 2004
TSLP over-expression	Atopic dermatitis	Yoo et al., 2005
Caspase over-expression	Atopic dermatitis	Konishi et al., 2002
TRPV3 over-expression	Atopic dermatitis	Yoshioka et al., 2009
STAT3 over-expression	Psoriasis	Sano et al., 2005
TGF β over-expression	Psoriasis	Li et al., 2004
B1-integrin expression in epidermal suprabasal layers	Psoriasis	Carroll et al., 1995
Amphiregulin expression in epidermal basal layer	Psoriasis	Cook et al., 1997
BRAF over-expression in sensory neurons	General itch	Zhao et al., 2013
“Flaky tail” filaggrin knock-out	Atopic dermatitis	Oyoshi et al., 2009
Cathepsin E knock-out	Atopic dermatitis	Tsukuba et al., 2003
Serine palmitoyltransferase knock-out	Psoriasis	Nakajima et al., 2013
Interleukin-1 receptor antagonist-deficient	Psoriasis	Shepherd et al., 2004
VGLUT2 knock-out in sensory neurons	General itch	Lagerstrom et al., 2010; Liu et al., 2010
Bhlhb5 knock-out	General itch	Ross et al., 2010
Ovalbumin-induced	Atopic/Contact dermatitis	Spergel et al., 1998
House dust mite-induced	Atopic/Contact dermatitis	Huang et al., 2003
Acetone/diethyl ether mixture-induced	Atopic/Contact dermatitis	Miyamoto et al., 2002
Hapten-induced	Atopic/Contact dermatitis	Man et al., 2008
Trimellitic anhydride-induced	Urticaria/Contact dermatitis	Lauerma et al., 1997
Imiquimod-induced	Psoriasis	van der Fits et al., 2009
Delivery of VEGF to skin	Psoriasis	Xia et al., 2003
Xenotransplantation	Psoriasis	Boyman et al., 2004; Krueger et al., 1981; Villadsen et al., 2003

has also been reported that not all patients with atopic dermatitis have elevated IgE (Novak and Bieber, 2003). Thus, whether this model really reflects atopic dermatitis, or whether IL-31 is involved in other symptoms of the disease and this model is therefore more akin to atopic dermatitis as observed in a subset of patients, requires further investigation.

Models of acute itch

Models of acute itch tend to investigate the short-term effects of specific pruritogens or neurotransmitters of the itch pathway. Acute itch is typically induced following single injection of a pruritogen into the animal, and site-directed behaviour is measured usually as the amount of time spent scratching or the number of scratching bouts. Scratching behaviour is typically observed following intradermal or subcutaneous injection of pruritogens into the nape of the neck or the cheek, although site-directed biting and licking of the calf or hindpaw is observed following injection of pruritogens into these sites (Hoeck et al., 2016; LaMotte et al., 2011). Pruritogens may also be injected intrathecally to investigate the role of spinal neurotransmitters and neuropeptides in itch signalling (Hoeck et al., 2016).

For a long time, the Kuraishi model of subcutaneous injection of substances into the nape of the neck and observation of site-directed scratching behaviour as an indication of acute pruritus was used (Kuraishi et al., 1995). Both the number of scratching bouts and the total time spent scratching can be recorded, with stronger pruritogens resulting in increased scratching behaviour. However, injection of algogens such as capsaicin in this way also results in scratching behaviour, presumably as scratching is the only site-directed behaviour available at this site regardless of whether the stimulus is a pruritogen or algogen (Shimada and LaMotte, 2008).

The gold standard for measuring acute pruritus in mice is currently the “**cheek model**” developed by Shimada and LaMotte (2008), in which substances are injected intradermal into the cheek and two site-directed behaviours are observed – if the substance is a pruritogen, scratching with the hindpaw is observed, while wiping with the forepaw occurs if the substance is an algogen. Importantly, many substances act as both pruritogens and algogens and cause both scratching and wiping behaviours when injected into the cheek. Indeed, many TG neurons (the equivalent of DRG that innervates the cheek) that show calcium responses following application of pruritogens also respond to algogens (Akiyama et al., 2010b), although this may be due to the fact that pruriceptors comprise a subset of

nociceptors that also respond to algogens, and not necessarily be involved in the transmission of nociceptive signals or be felt as pain. Such differences in the activation of individual neurons *in vitro* and behavioural responses *in vivo* highlight the ongoing need for suitable animal models to study itch. The main drawback with the “cheek model” for investigating pruritus is that it is difficult to study the central effects of the pruritogen. Although the cheek is innervated by sensory neurons with cell bodies in sensory ganglia and central terminals in the spinal trigeminal nucleus, a structure in the medulla that is analogous to the dorsal horn where the terminals of sensory neurons innervating the skin in areas other than the face are located, the TG and nucleus have been less studied and are less well defined than their counterparts in the rest of the body. The spinal trigeminal nucleus is a continuation of the substantia gelatinosa and Lissauer tract of the spinal cord, and is rich in opioid receptors (Kam and Tan, 1996), although whether the itch circuitry in the spinal trigeminal nucleus is similar to that in the dorsal horn of the spinal cord has not yet been investigated. Furthermore, the sensory neurons innervating the skin of the cheek and face may be different to those innervating skin in other parts of the body. In healthy human volunteers, itch induced by histamine iontophoresis is stronger in the arm than in the face, while mechanically-evoked itch is observed in facial skin but not the arm when stimulated using a probe attached to a piezoelectric actuator (Fukuoka et al., 2013). This suggests there is less innervation of polymodal C fibre afferents in the skin of the cheek than in other body areas, while sensory neurons conveying mechanically-evoked itch signals may be more numerous in the face. Thus, this model of itch may not be completely representative of itch in other areas of the body, although it likely shares many similarities.

Pruritogens may also be injected into the skin of the calf or hindpaw, where biting and licking behaviours are used as indications of itch and pain, respectively (LaMotte et al., 2011). This allows for the effects of peripherally applied pruritogens to be investigated in the more familiar lumbar spinal cord. However, discrimination of biting and licking behaviours is difficult to perform, and in the case of injection into the hind limb, spontaneous behaviours are frequently reported.

1.5.1 Cathepsin S-induced itch

As well as belonging to the cysteine family of proteases, CatS also belongs to the papain superfamily of cysteine proteases (Turk et al., 2012). Papain is a plant cysteine protease found in papayas and was the first described protease of the superfamily which is called after it, although several papain-like proteases are now known to exist in many life forms

including protozoans, fungi, and animals (McGrath, 1999). Several members of the papain superfamily, including papain itself, elicit itch sensations in human volunteers when applied to the skin via a spicule (Arthur and Shelley, 1955). *More recently it has been shown that these cysteine proteases activate protease activated receptors (PARs) expressed on HeLa cells and it has been proposed that activation of these receptors on sensory neurons is responsible for the initiation of itch signals (Reddy et al., 2008; Reddy and Lerner, 2010). Furthermore, application of CatS to the skin via spicules also results in itch sensations in humans, and HeLa cells expressing PARs 2 and 4 similarly respond to CatS (Reddy et al., 2010).* These observations support a role for CatS in pruritus by activation of PARs expressed on sensory neurons, although this had not been demonstrated when the work in this thesis was begun.

To investigate whether CatS acts as a pruritogen *in vivo* and establish an animal model of CatS-induced acute itch, initial studies were conducted by our lab in which hr-CatS (Medivir, Sweden) was injected intradermal into the cheek of C57BL/6 mice as for Shimada and LaMotte (2008) and both wiping and scratching behaviours were observed. Injection of 4 $\mu\text{g}/10\ \mu\text{l}$ hr-CatS resulted in only minimal scratching and wiping behaviours. In contrast, injection of 20 $\mu\text{g}/10\ \mu\text{l}$ hr-CatS caused substantial scratching behaviour which persisted for about 20 minutes and some wiping behaviour which occurred within the first few minutes after injection before rapidly decreasing (Figure 1.10).

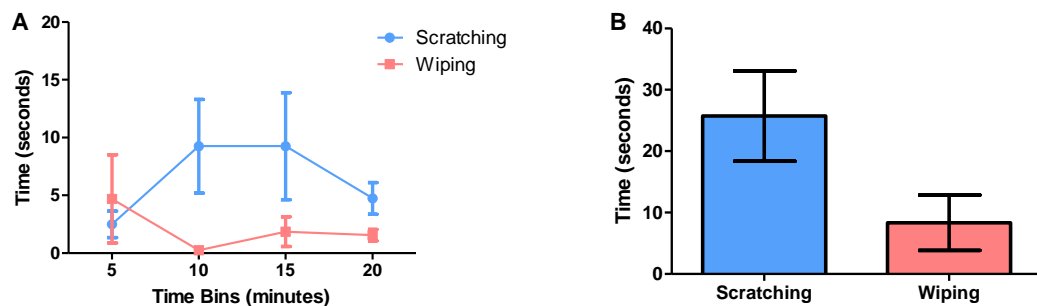


Figure 1.10: Behaviour observed following injection of hr-CatS into the cheek

Intradermal injection of 20 $\mu\text{g}/10\ \mu\text{l}$ hr-CatS into the cheek resulted in significant scratching behaviour and some wiping behaviour over a 20 minute observation period. Timecourse of scratching and wiping behaviours in 5 minute bins (A). Total time spent scratching and wiping (B). $n = 6$, data are mean \pm SEM. Experiment performed by Thomas Pitcher.

To investigate the roles of the TRP channels in CatS -induced scratching behaviour, hr-CatS was injected intradermal in transgenic mice lacking expression of TRP channels (Table 1.5). In TRPV1 KO mice, scratching behaviour was reduced, suggesting TRPV1 is required for CatS-mediated scratching behaviour. A slight reduction in scratching behaviour was observed following injection of CatS in TRPA1 KO mice, although this was not significantly different compared with the amount of time wild-type mice spent scratching. In TRPV1/TRPA1 double KO mice, scratching behaviour following injection of CatS was reduced similar to that observed in TRPV1 KO mice. No reduction in scratching behaviour was observed in transgenic mice lacking expression of TRPV4.

Injection of the PAR2 agonist SLIGRL-NH₂ (50 µg/10 µl) also causes scratching behaviour in a dose-dependent manner. Importantly, scratching induced by both SLIGRL-NH₂ and CatS can be inhibited with the PAR2 antagonist FSLRY-NH₂ (Pitcher et al., 2014). This suggests that CatS-induced scratching behaviour occurs via activation of PAR2. However, in contrast to CatS, SLIGRL-induced scratching behaviour was significantly reduced in TRPA1 KO mice, but not TRPV1 KO mice. In TRPV1/TRPA1 double KO mice, scratching behaviour was reduced as for TRPA1 KO mice. This suggests TRP channels contribute differently to itch elicited by different types of pruritogens, and also suggests CatS does not signal entirely via activation of PAR2. An alternative explanation is that activation of PAR2 by CatS is different to that by SLIGRL-NH₂, resulting in activation of different TRP channels and their involvement in transmission of itch signals and scratching behaviour. Indeed, PAR2 can be cleaved at different sites by various agonists as well as being activated by short synthetic ligands such as SLIGRL-NH₂ to result in activation of different downstream signalling pathways in a phenomenon known as biased agonism, which will be discussed in more detail later.

Table 1.5: Cathepsin S-induced scratching behaviour in transgenic mice

Data from Thomas Pitcher. NS = not significant.

	% Scratching Reduction	
	hr-CatS	SLIGRL-NH ₂
TRPV1 KO	50%	NS
TRPA1 KO	NS	80%
TRPV1/TRPA1 KO	50%	80%
TRPV4 KO	NS	-

These *in vivo* studies demonstrate that CatS is a pruritogen that causes scratching behaviour in mice, and also an algogen that causes some wiping behaviour. Scratching behaviour is mediated by the PAR2 receptor, as scratching is reduced following administration of a PAR2 antagonist. CatS-induced scratching requires expression of functional TRPV1, while TRPA1 appears to be dispensable, suggesting TRPV1, but not TRPA1, is required for CatS-mediated signalling of itch. Alternatively compensation may occur in TRPA1 KO mice such that signalling via other TRP channels, such as TRPV1, is sufficient to allow CatS-induced scratching behaviour to occur. The observation that scratching behaviour is not further reduced in TRPV1/TRPA1 double KO mice compared with TRPV1 KO mice also suggests that expression of TRPV1 is critical for CatS-induced scratching and that signalling via TRPA1, if it does occur, does not contribute additionally to this response. TRPV4 also is not required for CatS-induced scratching behaviour in these mice, as scratching behaviour is not reduced in TRPV4 KO animals. Although the expression of functional TRPV4 channels on sensory neurons in non-inflammatory pain has been questioned (Alexander et al., 2013), TRPV4-expressing sensory neurons are known to mediate nociceptive responses to hypotonic stimuli as well as inflammatory hyperalgesia (White et al., 2016). TRPV4 may also be involved in itch in inflammatory conditions, although it does not appear to be necessary for CatS-induced acute itch.

1.6 Protease activated receptors

Several proteases have been implicated in pruritus, particularly non-histaminergic itch and chronic itch, most of which act via the protease-activated receptors (PARs) (Briot et al., 2009; Reddy and Lerner, 2010; Reddy et al., 2008; Stefansson et al., 2008; Zhu et al., 2009; Zhu et al., 2015). In addition to their involvement in itch and inflammatory skin conditions, PARs have been reported to be involved in conditions including neurodegenerative diseases such as Alzheimer's disease and Parkinson's disease, respiratory diseases such as asthma, diseases of the gastrointestinal tract, and cancer (Amadesi and Bunnett, 2004; Ebrahimi et al., 2017; Kawabata and Kawao, 2005; Kularathna et al., 2014; Luo et al., 2007). Thus, PARs are involved in a range of physiological processes and diseases, which is made possible by the unique properties of these receptors.

The PAR family consists of four members – PAR1, PAR2, PAR3, and PAR4 (Macfarlane et al., 2001; Ossovskaya and Bunnett, 2004; Ramachandran and Hollenberg, 2008). There are two potential mechanisms by which PARs can be activated. The first and most physiologically relevant is following cleavage of the receptor extracellular domain by a protease, revealing a

tethered ligand at one end that then activates the receptor by binding on one of the extracellular loops (Macfarlane et al., 2001; Ossovskaya and Bunnett, 2004; Ramachandran and Hollenberg, 2008) (Figure 1.11). The second way PARs can be activated is by short synthetic peptide sequences that are derived from the sequences of the tethered ligand, such as the peptide SLIGRL-NH₂ which is derived from the trypsin cleavage site of mouse PAR2 (Nystedt et al., 1994). The human equivalent of this peptide is SLIGKV.

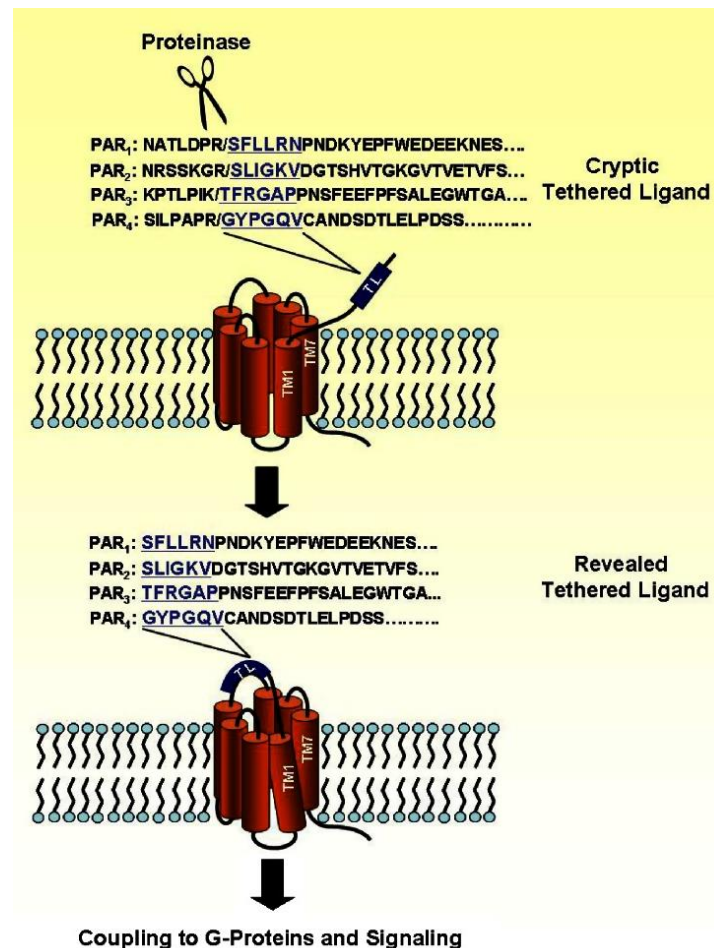


Figure 1.11: Mechanism of PAR activation (adapted from Ramachandran and Hollenberg, 2008)

PARs are activated when a protease cleaves the extracellular domain, revealing a tethered ligand. Synthetic ligands derived from the tethered ligand sequences (underlined in blue) can also activate the receptor.

The PARs are seven-transmembrane-spanning receptors coupled to G proteins, at the third intracellular loop and carboxyl terminus (Covic et al., 2002; Ramachandran et al., 2012).

Both PAR1 and PAR2 couple with G_{ai}, G_{αq}, and G_{α12/13} proteins (Coughlin, 2005;

Macfarlane et al., 2001; Ossovskaya and Bunnett, 2004; Russo et al., 2009; Steinhoff et al.,

2005). PAR3 is not known to signal via G proteins. PAR4 receptors activate calcium signalling via Gq and G12/13 (Coughlin, 2005; Russo et al., 2009). In addition to G proteins, PARs are also coupled to β -arrestins, increasing the number of downstream signalling pathways following activation of PARs (Ramachandran et al., 2012). β -arrestin-1 and 2 are involved in desensitisation but not internalisation of PAR1, while β -arrestin-1 and 2 are required for both desensitisation and internalisation of PAR2 (Dery et al., 1999; Kumar et al., 2007; Paing et al., 2002; Stalheim et al., 2005). β -arrestins are also involved in PAR2 intracellular targeting of activated ERK1/2 and chemotaxis (DeFea et al., 2000; Ge et al., 2003; Ge et al., 2003; Ge et al., 2004; Stalheim et al., 2005; Zoudilova et al., 2010).

PARs are expressed on many cell types, which in part may explain their different effects. They were first discovered on platelets as receptors for thrombin where they result in platelet activation and aggregation (Zhao et al., 2014b). PAR1 and PAR2 are expressed on the endothelium of blood vessels, where their activation results in nitric oxide-mediated vasodilation (Hamilton et al., 1998; Kawabata et al., 2004; Roy et al., 1998). In contrast, in the absence of functional endothelium, activation of PAR1 and PAR2 on vascular smooth muscle results in vasoconstriction (Laniyonu and Hollenberg, 1995; Moffatt and Cocks, 1998). PAR4 is not normally expressed in the vasculature in humans, but has been reported to be expressed during inflammation (Hamilton et al., 2001). PARs are also expressed on the epithelial and smooth muscle cells of the airways (Abey et al., 2006; Chambers et al., 2001; Kawabata and Kawao, 2005; Knight et al., 2001; Miotto et al., 2002). Activation of PARs in the epithelium results in the production of TSLP and development of Th2-type airway inflammation (Kouzaki et al., 2009). Expression of PARs on cells of the gastrointestinal system is thought to regulate neurotransmission, secretion, motility, mucosal permeability, and recruitment of immune cells (Amadesi and Bunnett, 2004). PARs are additionally expressed on primary sensory neurons and spinal cord, where they are proposed to be responsible for the sensations of itch and pain (Chen et al., 2015; Mrozkova et al., 2016a, b; Vellani et al., 2010; Zhu et al., 2005).

Responses of protease-activated receptors

PARs can be activated following cleavage by several proteases, resulting in different responses depending on the cell type and the receptor involved. For example, in platelets, activation of PAR1 and PAR4 by thrombin results in aggregation (Anderson et al., 1999; Hollenberg and Saifeddine, 2001; Hung et al., 1992). In human airway epithelial cells and astrocytoma cells, thrombin cleaves PAR3 to induce release of IL-8 (Ostrowska and Reiser,

2008). In vascular endothelial cells, trypsin is thought to cleave PAR2 resulting in hypotension (Cicala et al., 1999), while in a murine keratinocyte cell line trypsin cleaves PAR2 to cause inflammation and expression of chemokines (Meyer-Hoffert et al., 2004). In the pleural cavity of mice, trypsin cleaves PAR4 expressed on neutrophils and endothelial cells to mediate infiltration of neutrophils (Gomides et al., 2012). In human pulmonary epithelial cells, cleavage of PAR2 by neutrophil Cathepsin G (a serine protease) results in disarming of PAR2, such that the receptor can no longer be cleaved by trypsin (Dulon et al., 2003). In contrast, cleavage of PAR4 by Cathepsin G results in activation and aggregation of platelets (Sambrano et al., 2000).

Canonical signalling of protease-activated receptors

Canonical signalling of the PARs involves cleavage of the N-terminus of the receptor at defined sites by proteases, revealing tethered ligands that bind to a region in the second extracellular loop of the cleaved receptor, resulting in activation of the receptor and initiation of downstream signals (Zhao et al., 2014b). In the case of PAR1, canonical signalling occurs following cleavage of PAR1 at position R⁴¹/S⁴² by thrombin to reveal the tethered ligand SFLLRN (Vu et al., 1991). This results in the activation of G α q and G α 12/13 proteins, allowing for increased mobilisation of calcium via PLC signalling, and changes in endothelial cell barrier permeability and cell shape via Rho signalling, respectively (Barr et al., 1997; McLaughlin et al., 2005; Ossovskaya and Bunnett, 2004). Once thrombin has cleaved PAR1, it may remain bound to the receptor, where it facilitates the formation of PAR1 and PAR4 heterodimers and cleavage of PAR4 (Arachiche et al., 2013; Leger et al., 2006). The 41 amino acid peptide that is cleaved from the receptor, known as parstatin, has been reported to penetrate cells of the cardiovascular system and is an inhibitor of angiogenesis (Zania et al., 2009). Thus, canonical cleavage of PAR1 might result in numerous effects in addition to the effects mediated by activation of G proteins.

Canonical signalling of PAR2 involves cleavage of the receptor by trypsin at position R³⁶/S³⁷ (Figure 1.12 A), after which the ligand remains tethered to the receptor and interacts with the second extracellular loop of the receptor to exert its effects (Al-Ani and Hollenberg, 2003; Al-Ani et al., 1999; Al-Ani et al., 2002b). A number of pathways are activated following canonical activation of PAR2 (Figure 1.12 B, C), including G α q-mediated mobilisation of intracellular calcium via PLC and PIP₂ signalling, G α s-mediated elevation of cAMP, G α 12/13-mediated activation of Rho, and recruitment of β -arrestins resulting in receptor endocytosis and activation of ERK 1/2 (Böhm et al., 1996a, b ; DeFea et al., 2000; Dery et al., 1999; Ricks

and Trejo, 2009; Scott et al., 2003; Stalheim et al., 2005; Zhao et al., 2014a). Other serine proteases, including trypsin, acrosin, and membrane-type serine protease 1 also cleave PAR2 at the canonical site, although the potencies and kinetics of cleavage vary compared with trypsin (Molino et al., 1997; Smith et al., 2000; Takeuchi et al., 2000). For instance, the reduced potency of trypsin for PAR2 is thought to be due to a second cleavage site for trypsin at R⁴¹/S⁴², which prevents cleavage of the receptor at the canonical R³⁶/S³⁷ site (Molino et al., 1997). Following canonical activation of PAR2, calcium signalling is terminated by PKC acting on calcium release activated channels, and the receptor is internalised and degraded by lysosomes (Böhm et al., 1996a).

Thrombin may cleave PAR3 at K³⁸/T³⁹, resulting in hydrolysis of PIP₂ and generation of calcium (Ishihara et al., 1997). However, other groups have failed to observe thrombin signalling of PAR3 (Nakanishi-Matsui et al., 2000). Rather than being directly involved in cell signalling, PAR3 is thought to be a co-factor for the activation of other PARs, such as PAR1 and PAR4 (McLaughlin et al., 2007; Nakanishi-Matsui et al., 2000).

PAR4 is cleaved by both thrombin and trypsin at position R⁴⁷/G⁴⁸, although the EC₅₀ is much greater than for cleavage of PAR1 and PAR3 by thrombin (Xu et al., 1998). Cleavage of PAR4 at the canonical site results in activation of Gαq and signalling via PLC, hydrolysis of PIP₂, and increase in calcium (Bao et al., 2015; Xu et al., 1998). Following activation of PAR4, internalisation of the receptor occurs independently of β-arrestins and instead occurs via clathrin-mediated endocytosis (Smith et al., 2016).

Biased agonism of protease-activated receptors

In addition to the canonical signalling pathways, PARs can also be cleaved by proteases that act at sites other than the canonical sites cleaved by thrombin and trypsin. This phenomenon is known as biased agonism (or biased signalling) and has been proposed as a reason why cleavage of PARs can result in a variety of different responses. *A consequence of biased agonism is that different agonists or ligands acting on the same receptor can elicit different effects that may be different to the canonical signalling pathways* (Geppetti et al., 2015; Urban et al., 2007).

Several biased agonists have been identified for PAR1, which cleave the receptor at sites distinct from the canonical thrombin site. Activated protein C (APC) cleaves PAR1 both at the canonical R⁴¹/S⁴² site and a non-canonical R⁴⁶/N⁴⁷ site, resulting in activation of Rac1

mediated by β -arrestin, independent of G protein activity (Soh and Trejo, 2011). The neutrophil proteases elastase and proteinase-3 are also biased agonists of PAR1, cleaving at sites L⁴⁵/R⁴⁶ and A³⁶/T³⁷, respectively (Mihara et al., 2013). Rather than activation of G α q and G α 12/13 as would be observed following canonical activation of PAR1, cleavage of PAR1 by neutrophil proteases results in G α i-mediated activation of mitogen-activated protein kinase (MAPK) (Mihara et al., 2013).

Similarly, proteases cleaving at the non-canonical site of PAR2 can activate different signalling pathways to that observed following canonical cleavage of PAR2 by trypsin. For instance, while cleavage of PAR2 by trypsin results in G α s-mediated elevation of cAMP and increase in intracellular calcium (Böhm et al., 1996a, b; Scott et al., 2003; Zhao et al., 2014a), CatS, which cleaves PAR2 at E⁵⁶/T⁵⁷ (Figure 1.12 A), results in G α s-mediated formation of cAMP but not G α q-mediated mobilisation of intracellular calcium (Zhao et al., 2014a) (Figure 1.12 C). Activation of PAR2 is reported to sensitize TRPV4, resulting in inflammation and hyperexcitability of nociceptors. However, the mechanism by which PAR2 sensitises neuronal TRPV4 depends on the protease used to cleave PAR2. In the case of trypsin, PKC, PKA, and tyrosine kinases are reported to result in sensitisation of TRPV4 (Grace et al., 2014; Grant et al., 2007; Poole et al., 2013), while CatS-mediated activation of PAR2 causes sensitisation of TRPV4 mainly via the adenylyl cyclase/cAMP/PKA pathway (Zhao et al., 2014a). A further difference that occurs following canonical and non-canonical activation of PAR2 is that β -arrestins are recruited and PAR2 is endocytosed following cleavage with trypsin (DeFea et al., 2000; Dery et al., 1999; Ricks and Trejo, 2009; Zhao et al., 2014a), whereas no recruitment of β -arrestins is observed following cleavage of PAR2 with CatS and the receptor is not endocytosed, but instead remains on the surface of the cell (Zhao et al., 2014a). However, despite the different cleavage sites by CatS and trypsin, injection of both of these proteases results in similar scratching behaviours in mice and itch sensations in humans (Costa et al., 2008; Pereira et al., 2011; Reddy et al., 2010; Thomsen et al., 2002). This suggests a convergence of signalling in the sensory neurons following activation of PAR2 by several proteases, or that cleavage of additional receptors by both proteases is responsible for itch sensations.

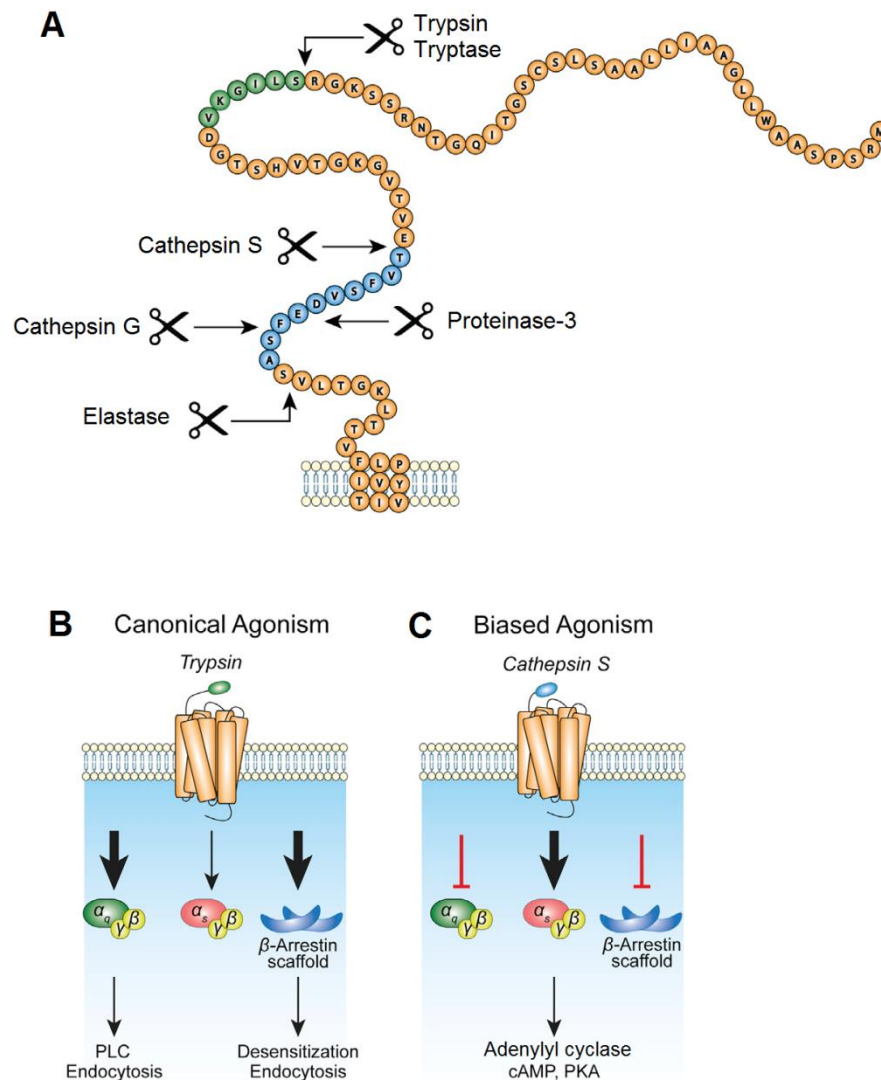


Figure 1.12: Canonical and biased agonism of PAR2 by various proteases (adapted from Geppetti et al., 2015; Zhao et al., 2014a and Zhao et al., 2014b)

The N-terminus of human PAR2 consists of 84 amino acids and can be cleaved by several proteases at the sites indicated (A). The green residues denote the canonical tethered ligand that is revealed following cleavage of the receptor by trypsin or tryptase; the blue residues show the tethered ligand revealed following cleavage by Cathepsin S. Canonical activation of PAR2 by trypsin (B) and non-canonical activation by CatS (C) result in activation of different downstream pathways and cell responses.

Unlike the other PARs, PAR3 and PAR4 do not appear to undergo biased agonism. Apart from thrombin, the only other protease to show activity at PAR3 is APC, which requires the formation of heterodimers with PAR1 (in mice) or PAR2 (in humans) (Burnier and Mosnier, 2013; Madhusudhan et al., 2012). APC cleaves PAR3 at the non-canonical R⁴¹/G⁴² site (Burnier and Mosnier, 2013). To date, no other proteases have been observed to cleave

PAR3. In addition to thrombin and trypsin, other proteases such as Cathepsin G and plasmin cleave PAR4 (Quinton et al., 2004; Sambrano et al., 2000). However, these appear to cleave PAR4 at the canonical site. Mannose-binding lectin-associated serine protease-1 has also been shown to cleave PAR4, but the exact cleavage site remains to be determined (Megyeri et al., 2009).

Disarming of protease-activated receptors

One of the consequences of biased agonism is that the canonical cleavage site for the PAR may be removed from the N-terminal if cleavage of the receptor occurs further from the N-terminal than the canonical site (Ramachandran et al., 2012; Zhao et al., 2014b). Thus, the receptor can no longer be cleaved at the canonical site. In this sense, proteases that disarm PARs can also be thought of as antagonists to the canonical signalling pathway, even if they are agonists for other non-canonical signalling pathways (Ramachandran et al., 2012).

Because *CatS cleaves the N-terminal of PAR2 further from the N-terminal than the canonical site for trypsin* (Figure 1.12), CatS can be considered to disarm the receptor for trypsin. In support of this, CatS has been reported to prevent trypsin-induced activation of PAR2. Zhao et al. (2014a) demonstrated that HEK cells pre-incubated with CatS showed reduced calcium activity in response to trypsin compared with cells that had been pre-incubated with vehicle, likely as a result of reduced trypsin-induced calcium signalling following disarming PAR2 by CatS. The neutrophil proteases Cathepsin G, which cleaves PAR2 at position P⁶⁵/S⁶⁶, elastase, which cleaves PAR2 at position S⁶⁸/V⁶⁹, and proteinase-3, which cleaves PAR2 at V⁶²/D⁶³, are also biased agonists of PAR2 that disarm the canonical cleavage site (Ramachandran et al., 2011; Zhao et al., 2014b) (Figure 1.12 A).

Post-translational modifications of protease-activated receptors

The activity of PARs can be affected by post-translational modifications, such as phosphorylation, ubiquitination, and glycosylation (Grimsey et al., 2011). It has been observed that, following activation of PAR1 by thrombin, PAR1 is phosphorylated by G-protein receptor kinases and subsequently inactivated (Ishii et al., 1994). Likewise, PAR2 is also phosphorylated following its activation. Phosphorylation of PAR2, resulting in uncoupling of the receptor with G-protein signalling, causes endocytosis of the receptor in a β -arrestin independent manner (Ricks and Trejo, 2009). Ubiquitination of PAR1 appears to prevent its internalisation (Paing et al., 2004; Wolfe et al., 2007), whereas it has been reported to be involved in internalisation and trafficking of PAR2 to the lysosome for degradation (Hasdemir et al., 2009; Jacob et al., 2005). Glycosylation is necessary for the

expression of PAR1 at the cell surface, and PAR1 mutants that are unable to be fully glycosylated show enhanced signalling compared with fully glycosylated PAR2, possibly as a result of conformational changes in the receptor (Soto and Trejo, 2010; Tordai et al., 1995). In contrast, glycosylation of PAR2 is not necessary for the expression of PAR2 at the cell surface, but does appear to be necessary for trypsin to activate the receptor (Compton et al., 2001; Compton, 2003). This suggests that glycosylation could play a role in protease specificity for PARs, adding to the signalling complexity of these receptors.

Synthetic and endogenous ligands of protease-activated receptors

In addition to proteases, the PARs can also be activated by short synthetic ligands (sometimes referred to as activating peptides) that correspond to the tethered ligands exposed following cleavage of the receptor by a protease, although these are unlikely to occur physiologically and are mostly of interest in experimental conditions (Ramachandran et al., 2012; Zhao et al., 2014b). Interestingly, the responses elicited following activation of a PAR by a synthetic ligand are not always the same as the responses following cleavage by a protease (Al-Ani et al., 2002b; Jiang et al., 2017b). This is another potential source of different responses following activation of PARs. For example, despite activating the same part of the receptor, activation of PAR1 by thrombin results in signalling via G α q and G α 12/13, while activation of PAR1 by the synthetic ligand SLLRN favours G α q over G α 12/13 signalling (McLaughlin et al., 2005). The hexapeptides SLIGRL-NH₂ and SLIGKV-NH₂ correspond to the mouse and human tethered ligands that are exposed following cleavage of PAR2 by trypsin, although they have been reported to have a relatively low potency compared with trypsin (Al-Ani et al., 2002b; Bohm et al., 1996; Nystedt et al., 1994). As with cleavage of PAR2 by trypsin, they have been reported to induce G α q-mediated increase in intracellular calcium and activation of ERK (Ramachandran et al., 2009; Sriwai et al., 2013; Stalheim et al., 2005). However, while cleavage of PAR2 by trypsin results in elevation of cAMP, activation of PAR2 by SLIGRL-NH₂ has been reported to result in an increase in cAMP on some occasions (Amadesi et al., 2006; Scott et al., 2003), but not in others (Sriwai et al., 2013), which may be dependent on the cell type being activated.

Activating peptides corresponding to the tethered ligands generated following non-canonical cleavage of PAR2 can also be used to activate the receptor. Zhao et al. (2014a) used the CatS activating peptide TVFSVDEFSA in HEK cells and observed a similar effect of G α s signalling and lack of receptor endocytosis as found following activation with CatS. The

CatS activating peptide acting on PAR2 was also able to sensitise TRPV4 in a similar manner to CatS in *Xenopus laevis* oocytes expressing TRPV4 and PAR2.

Interestingly, the synthetic peptide for PAR3 does not activate its receptor, although it can activate PAR1 and PAR2 (Hansen et al., 2004; Ishihara et al., 1997). This could be due to the fact that PAR3 on its own is unlikely to be involved in signalling (Nakanishi-Matsui et al., 2000). However, it does add further complexity to PAR signalling, since agonists could potentially activate more than one PAR on the same cell, resulting in complex responses that would not be detected following activation of just a single receptor. Furthermore, these synthetic peptides for PARs have been reported to act on receptors distinct from PARs (Liu et al., 2011b; McGuire et al., 2002).

Sensitisation of neurons by protease-activated receptors

The protease activated receptors have been reported to mediate several of their effects via sensitisation of TRP channels expressed on neurons, resulting in enhanced signalling, which is proposed to be responsible for sustained sensations of pain and hyperalgesia during inflammatory conditions (Amadesi et al., 2004; Amadesi et al., 2006; Chen et al., 2011; Dai et al., 2004; Dai et al., 2007; Geppetti et al., 2015; Grace et al., 2014; Grant et al., 2007; Lieu et al., 2016; Mrozkova et al., 2016b; Poole et al., 2013). Activation of PAR2 is known to cause sensitisation of TRPA1 via PLC and PIP₂ signalling (but not PKC) (Dai et al., 2007), TRPV1 via Gαq-mediated PKC and PKA phosphorylation of TRPV1 (Amadesi et al., 2004; Amadesi et al., 2006; Dai et al., 2004), and TRPV4 via PKC and tyrosine phosphorylation of TRPV4 (Grace et al., 2014; Grant et al., 2007; Poole et al., 2013). In a similar manner, activation of PAR2 by various pruritogens could also sensitise these channels to contribute to itch sensations (Davidson and Giesler, 2010). Indeed, co-application of trypsin, which cleaves PAR2, was found to potentiate responses to histamine and serotonin in calcium imaging experiments in human submucous plexus preparations (Ostertag et al., 2017). In mice, scratching behaviour in response to injection of chloroquine or BAM8-22 was increased if the mice were pre-treated with the PAR2 agonist SLIGRL-NH₂ first, and pre-treatment of DRG cells with SLIGRL-NH₂ resulted in an increase in the peak calcium response of cells to chloroquine and BAM8-22, suggesting cross-sensitisation had occurred, and possibly reflecting sensitisation of pruriceptors that convey non-histaminergic itch (Akiyama et al., 2012). Furthermore, in a rat model of liver disease, potentiation of TRPV1 by PAR2 was found to be responsible for enhanced scratching behaviour and increased responses of TRPV1 in calcium imaging experiments (Belghiti et al., 2013).

1.6.1 Protease activated receptors and itch

All of the PARs, apart from PAR3, are involved in itch (Tsuji et al., 2008; Akiyama et al., 2009b). There are many mechanisms by which activation of PARs could result in itch. For instance, direct activation of PARs expressed on sensory neurons might be responsible for the generation of action potentials, initiation of second messenger signalling and mobilisation of calcium, and the transmission of itch signals. Sensitisation of sensory neurons via PAR signalling could also be a mechanism by which stimuli, which would otherwise not normally activate the neuron, result in transmission of itch signals. Alternatively, indirect signalling via activation of PARs on other cell types, which release mediators that then act on neurons, could be responsible for itch sensations. In support of this, activation of PAR2 on keratinocytes has been found to cause the release of TSLP, an itch-related cytokine that acts on neurons (Wilson et al., 2013). Similarly, activation of PAR2 on mast cells in the skin could result in their degranulation and release of histamine and proteases, resulting in itch sensations (Sakai et al., 2016; Ui et al., 2006).

Protease-activated receptor 1 and itch

Injection of the synthetic ligand TFLLR-NH₂, which activates PAR1, has causes scratching behaviour in mice (Tsuji et al., 2008). This may be in part due to histamine release from cutaneous mast cells that express PAR1 (Moormann et al., 2006), and also due to direct activation of sensory neurons that express PAR1 (de Garavilla et al., 2001). Activation of PAR1 in corneal stromal cells with this synthetic ligand has also releases the itch-related cytokine TSLP and may be responsible for itch sensations in the cornea (Yin et al., 2017). TSLP is also released from keratinocytes where it causes itch sensations (Wilson et al., 2013). Whether release of TSLP from keratinocytes is also mediated by PAR1 remains to be elucidated.

Protease-activated receptor 2 and itch

Of the involvement of all the PARs in itch, most research has been carried out on PAR2. PAR2 is expressed in many cell types, including sensory neurons, keratinocytes, and mast cells (Steinhoff et al., 1999; Steinhoff et al., 2000; Steinhoff et al., 2003). Expression of PAR2 is increased in the nerve fibres and mast cells of patients with atopic dermatitis, and injection of the PAR2 agonist SLIGKV induces itch which is greatly enhanced when injected into the skin of patients with atopic dermatitis compared to control subjects (Steinhoff et al., 1999; Steinhoff et al., 2003). Moreover, mucunain, a protease which is the active ingredient of cowhage, produces itch in humans by acting on PAR2 (Reddy et al., 2008).

PAR2-mediated pruritus has also been reproduced in mice, in which injection of the PAR2 agonist SLIGRL-NH₂ causes scratching behaviour and activation of neurons in the superficial dorsal horn of the spinal cord in a histamine-independent manner (Akiyama et al., 2009a, b; Shimada et al., 2006; Tsujii et al., 2008). In addition to the numerous exogenous proteases and ligands for PAR2 that have been reported to cause itch sensations, several endogenous ligands that act on PAR2 to cause itch have been proposed. Tryptase and chymase, released from mast cells, have been reported to cause itch (Gordins et al., 2004; Tsujii et al., 2009), and may do so via activation of PAR2 (Ui et al., 2006). The kallikreins, a family of trypsin-like serine proteases that are expressed in the skin, are also potential candidates as endogenous agonists of PAR2 that cause itch (Komatsu et al., 2003; Komatsu et al., 2005). In support of this, kallikrein-5 and kallikrein-14 have been found to activate PAR2 (Oikonomopoulou et al., 2006; Stefansson et al., 2008), while expression of kallikrein-14 is increased in the skin in inflammatory skin conditions such as atopic dermatitis (Stefansson et al., 2008).

Exogenously applied CatS has also been reported to cause itch via cleavage of PAR2 (Reddy et al., 2010), although the endogenous source of CatS that directly cleaves PAR2 to cause itch sensations was not known and is a topic of investigation for this project. Furthermore, whether activation of neuronal PAR2 by pruritogens or release of pruritogens following activation of PAR2 on non-neuronal cells was responsible for itch was not determined.

Although there is much evidence for the involvement of PAR2 in itch, there remains controversy as to whether or not this receptor is responsible for itch sensations or whether it plays a role in pain. Activation of PAR2 by proteases such as CatS and the synthetic peptide SLIGRL-NH₂ has been reported to cause pain (Amadesi et al., 2004; Barclay et al., 2007; Vergnolle et al., 2001). Other studies found that the PAR2 agonist SLIGRL-NH₂ does evoke scratching behaviour, but that it is not abolished in PAR2 knockout mice, suggesting that PAR2 is not required for scratching behaviour (Liu et al., 2011b). Indeed, the role of SLIGRL-NH₂ in PAR2-mediated itch has been questioned. Liu et al. (2011b) reported that SLIGRL-NH₂ induces itch via MrgprC11, and not PAR2 (Figure 1.13).

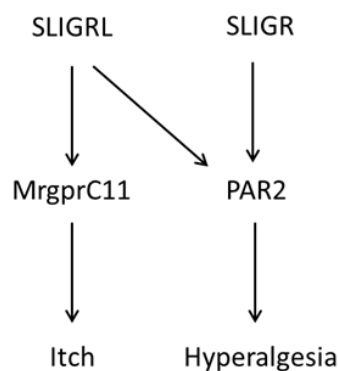


Figure 1.13: Overview of hypothesised roles of MrgprC11 and PAR2 in itch and hyperalgesia (adapted from Liu et al., 2011b).

SLIGRL activates both *MrgprC11* to cause itch and *PAR2* to cause hyperalgesia. The shortened peptide, *SLIGR*, is reported to only activate *PAR2*, causing hyperalgesia.

Protease-activated receptor 4 and itch

Whether *PAR2* is involved in itch and whether it does so via *SLIGRL* remains controversial (Liu et al., 2011b; Reddy et al., 2015; Reddy et al., 2018). However, one possibility is that cleavage of *PAR2* by other proteases results in itch, as a consequence of the effects of biased agonism. Another possibility is that activation of other receptors, such as *PAR4*, is also required for itch. Indeed, in humans, injection of mucunain acts on *PAR4* as well as *PAR2* to cause itch, and application of CatS elicits itch via *PAR4* and results in calcium transients in HeLa cells expressing *PAR2* or *PAR4* (Reddy et al., 2010; Reddy et al., 2018). Alternatively, activation of *PAR4* alone might be sufficient for itch. In support of this, injection of just *PAR4* agonists in mice also elicits scratching behaviour and activation of neurons in the superficial dorsal horn of the spinal cord in a *TRPV1/TRPA1*-dependent manner (Akiyama et al., 2009b; Patricio et al., 2015).

Itch induced by *PAR4* may or may not be dependent on histamine. Because *PAR4* is expressed on mast cells as well as neurons and injection of a *PAR4* agonist causes degranulation of mast cells, one hypothesis is that activation of *PAR4* on mast cells might result in the release of histamine (Han et al., 2012; Patricio et al., 2015; Russell et al., 2011). In support of this, Tsuji et al. (2008) reported that scratching behaviour in mice following injection of a *PAR4* agonist was partially but significantly attenuated by the *H1R* antagonist terfenadine, suggesting that this itch is at least partially dependent on histamine. However, Patricio et al. (2015) reported that *PAR4* mediated itch is independent of histamine, as injection of a *PAR4* agonist still induced scratching behaviour in mice treated with the mast cell stabiliser cromolyn and in mast cell-deficient mice. Because these studies used different

methods to investigate the contribution of histamine to PAR4 mediated itch, one explanation is that PAR4 mediated itch is partially dependent on histamine, which may or may not be observed, depending on the method used in the study.

1.6.2 Protease activated receptor 2 and Cathepsin S

CatS is a likely candidate for being involved in at least some instances of itch mediated by PAR2. First, the active site of CatS shares sequence homology with mucunain, the active component of cowhage, and both induce itch (Reddy et al., 2010). Furthermore, mucunain and CatS cleave PAR2 in transfected cells (Reddy et al., 2008; Reddy et al., 2010; Reddy and Lerner 2010). Second, CatS is expressed in keratinocytes and is upregulated under conditions of inflammation, especially in inflammatory skin conditions associated with chronic itch, such as seborrhoeic dermatitis, atopic dermatitis, and psoriasis, suggesting the involvement of CatS in chronic itch conditions (Ainscough et al., 2017; Olivry et al., 2016; Schönefuß et al., 2009; Schwarz et al. 2002; Viodé et al., 2014). Furthermore, transgenic mice over-expressing CatS develop a skin disorder similar to atopic dermatitis, characterised by chronic skin inflammation and increased scratching behaviour (Kim et al., 2012).

However, while there is some evidence supporting the involvement of CatS and PAR2 in itch, there remain a number of discrepancies. Although CatS does cleave PAR2, at E⁵⁶/T⁶⁷ (Figure 1.12 A), rather than mediating itch sensations, this appears to be involved in hyperexcitability of nociceptors and pain sensations (Zhao et al., 2014a). It is possible that cleavage of PAR2 at different sites is responsible for different sensations. An additional cleavage site for CatS on PAR2, G⁴¹/K⁴², has also been identified (Elmariah et al., 2014), but whether or not this is involved in itch is not known. Furthermore, SLIGRL and CatS still cause activation of sensory neurons and elicit scratching behaviour in PAR2 KO mice, suggesting that this pathway might not be involved in itch (Liu et al., 2011b; Reddy et al., 2015). However, it cannot be ruled out that a compensatory mechanism, such as enhanced signalling via PAR4 (Reddy et al., 2010) or MrgprC11 (MrgprX in humans) (Reddy et al., 2015; Reddy et al., 2018), is responsible for SLIGRL and CatS-mediated responses and scratching behaviour in these animals.

The role of PAR2 in CatS-mediated itch has recently been questioned. As with the recent reports that SLIGRL activates Mrgprs in addition to PAR2, (Figure 1.13), it has similarly been reported that *CatS and mucunain also activate Mrgprs in addition to PARs* (Reddy et al., 2015; Reddy et al., 2018). Sensory neurons from PAR2 KO mice were found to respond to

application of CatS or mucunain, and scratching behaviour was observed in PAR2 KO mice following injection of CatS or mucunain. As with PARs, proteases can activate Mrgprs by cleavage at the N-terminal. CatS has been reported to cleave MrgprC11 at site N¹⁶/E¹⁷ (Reddy et al., 2015). However, unlike the PARs, tethered or diffusible ligands of the cleaved region do not activate the receptor. Instead, it is proposed that cleavage of Mrgprs by proteases just results in a conformational change that causes activation of G-proteins and allows signalling to occur, likely via coupling to Gq and mobilisation of calcium, as has been reported for other agonists of these receptors (Robas et al., 2003; Subramanian et al., 2011; Subramanian et al., 2013). As well as activating mouse MrgprC11, CatS was also found to activate the human analogue MrgprX2, but not human MrgprX1 (Reddy et al., 2015). The role of Mrgprs in CatS-mediated itch would likely involve TRPA1-expressing neurons (Ross, 2011; Wilson et al., 2011). However, preliminary studies from our group found that scratching behaviour following injection of CatS was not significantly reduced in TRPA1 KO mice. While it is possible that compensatory mechanisms exist in transgenic animals that prevent overt changes in behaviour, another possibility is that CatS signals via several receptors, including PAR2 and Mrgprs, and potentially others that have yet to be discovered, and that activation of a number of different receptor types is required to induce itch. Knocking out one of the receptors may result in a small but unnoticeable reduction in scratching behaviour, which could be compensated for by increased expression of or activity at other receptors.

1.7 Thesis aims

The overall aim of the work in this thesis is to investigate the mechanisms underlying CatS - induced itch, from the periphery where CatS is released and itch signals are initiated in the endings of sensory neurons to the dorsal horn of the spinal cord where it becomes integrated with the spinal cord circuitry.

Chapter two concerns the source of CatS in itch; specifically we investigate whether skin keratinocytes are a potential source of endogenous CatS and the conditions under which they might release CatS. We proposed that the skin is an endogenous source of CatS, released from keratinocytes in inflammatory conditions, and that CatS may act on its own or in addition with other endogenous proteases to cause itch.

Given the observation that CatS may be involved in chronic itch conditions such as atopic dermatitis, we investigate whether CatS acts as a pruritogen by acting directly on primary

sensory neurons and whether they do so via PAR2, and we begin to characterise these neurons and whether they belong to the subset of TRPV1 and/or TRPA1 sensory neurons proposed to be involved in pruriception. This is addressed in chapter three.

The aim of chapter four is to determine whether peripherally applied CatS causes activation of neurons in the spinal cord dorsal horn via the release of neuropeptides from the central terminals primary afferent fibres.

By utilising *in vivo* and *in vitro* techniques including behavioural testing, release assays, immunohistochemical techniques, calcium imaging, and quantitative polymerase chain reactions, this work examines the hypothesis that in the skin endogenously-released CatS acting on PAR2 expressed on neurons is responsible for transduction of itch signals to the spinal cord and the release of neuropeptides involved in itch signalling.

Chapter 2

Cathepsin S in keratinocytes – intracellular expression & extracellular activity

2.1 Introduction

The HaCaT cell line as a keratinocyte model

To investigate the role of keratinocytes in releasing pruritogens such as CatS in atopic dermatitis-like conditions, we used the HaCaT (human adult low calcium high temperature) cell line (so-called after their origin and initial growth conditions, Boukamp et al., 1988) as an *in vitro* model system. This cell line is a spontaneously immortalised keratinocyte cell line that expresses keratins 1 and 10 as well as structural proteins such as filaggrin, loricrin, and involucrin (Boukamp et al., 1988; Seo et al., 2012). Importantly, HaCaTs also contain CatS, which is located primarily in the lysosomes, as is also reported in normal human keratinocyte cultures (Schonefuss et al., 2010; Schwarz et al., 2002). As a result of being immortalised, the cell line does not need to be replaced over time, reducing the variability that occurs with conventional primary keratinocyte cultures from multiple donors. From multiple donors. Thus, unlike primary keratinocyte cell lines which have a short window during which experiments must be performed (Choi and Lee, 2015; Lichti et al., 2008), experiments can be performed with immortalised cell lines such as HaCaTs for a longer period of time. Furthermore, unlike primary keratinocytes, HaCaTs do not require the use of a feeder layer to grow, which would add a further level of complexity to the system under investigation (Boukamp et al., 1988). Moreover, the use HaCaTs offers the advantage of a single cell type and avoids the risk of fibroblast contamination sometimes observed with primary keratinocyte cultures (Guo and Jahoda, 2009).

However, compared with normal human primary keratinocytes, the transcriptional profile of proteins such as filaggrin, loricrin, involucrin, and keratin-10 is abnormal (Seo et al., 2012). In addition, karyotyping of the cell line shows it is aneuploid, containing 72-88 chromosomes (Boukamp et al., 1988), although it has been suggested that aneuploidy may be necessary for the development of immortalised cell lines and cancerous cells from primary cells (Duesberg et al., 2001).

A low calcium concentration is used to maintain both primary keratinocytes and HaCaTs in a basal state *in vitro* (Boyce and Ham, 1983; Deyrieux and Wilson, 2007; Hennings et al., 1980;

Li et al., 2017). Increasing the calcium concentration inhibits cell growth and synthesis of DNA and induces differentiation of keratinocytes (Boyce and Ham, 1983; Colombo et al., 2017; Deyrieux and Wilson, 2007; Hennings et al., 1980; Li et al., 2017; Sakaguchi et al., 2003). This reflects the situation in the epidermis *in vivo*, whereby the calcium concentration increases towards the surface of the skin, apart from the corneal layer, which is almost completely devoid of calcium (Bikle, 2004; Menon et al., 1985). However, unlike primary keratinocytes which undergo irreversible terminal differentiation in the presence of increased calcium concentrations, HaCaTs are capable of reverting from a differentiated state back to an undifferentiated state then the calcium concentration is decreased (Deyrieux and Wilson, 2007). Furthermore, cell confluence affects the differentiation of keratinocytes including HaCaTs, with cells showing signs of differentiation when grown at high confluency, even in the presence of low calcium (Colombo et al., 2017; Deyrieux and Wilson, 2007; Lee et al., 1998). Cell density-mediated differentiation of normal human keratinocytes and HaCaTs is mediated by PKC, since blocking PKC activity decreases expression of filaggrin, involucrin, and loricrin in keratinocytes (Lee et al., 1998; Papp et al., 2003). Because the release of cytokines from HaCaTs maintained in low calcium and sub-confluent conditions is similar to that of normal keratinocytes (Colombo et al., 2017), we cultured our keratinocytes in defined keratinocyte serum-free medium (DK-SFM) which contains less than 0.1 mM calcium, and performed experiments before the cells reached full confluence.

Although typically grown in a basal-like, undifferentiated state as a monolayer in culture, HaCaTs can be made to differentiate and grow as a multilayered epithelium, for example, following transplantation onto nude mice or when grown at an air-liquid interface on collagen gels containing fibroblasts (Boelsma et al., 1999; Boukamp et al., 1988; Schoop et al., 1999). However, these cells do not undergo complete terminal differentiation and have a disorganised appearance, lacking a granular and cornified layer, and unable to synthesise lipids necessary for proper barrier formation (Boelsma et al., 1999). This could explain why HaCaTs, unlike normal keratinocytes, are able to revert back to a basal-like state after differentiation. Furthermore, additional keratins that are not normally expressed in the skin were found to be expressed in multilayered HaCaTs (Boelsma et al., 1999; Schoop et al., 1999). For these reasons, experiments were performed in HaCaTs that were cultured in a monolayer in a basal-like state rather than as a multilayer.

Release of Cathepsin S from antigen presenting cells

CatS released from cells in the skin could be responsible for pruritus. In addition to being expressed in skin keratinocytes, CatS is also expressed from immune cells, including microglia and monocytes/macrophages (Clark et al., 2007; Clark et al., 2010; Liuzzo et al., 1999; Petanceska et al., 1996), as well as vascular and cervical smooth muscle cells (Fonovic et al., 2013; Watari et al., 2000). Although not involved in itch, the mechanisms of release of CatS from these cells has been elucidated and likely share at least some similarities with the release of CatS from skin keratinocytes.

The expression and release of CatS from microglia in the spinal cord and its role in neuropathic pain has been well documented. CatS protein is expressed in microglia in the spinal cord of the rat, with the number of CatS -positive microglia increasing in the dorsal horn following peripheral nerve injury (Clark et al., 2007). CatS mRNA and protein is also expressed in primary microglia cultured from rat brain and spinal cord and in the N-13 microglia-like cell line (Clark et al., 2010; Liuzzo et al., 1999; Petanceska et al., 1996). Incubation of microglia-like cells in IFN γ for 5 hours does not increase release of CatS from these cells (Petanceska et al., 1996); in contrast, incubation in IFN γ for 24 hours increases release of CatS (Liuzzo et al., 1999), suggesting that IFN γ -mediated release of CatS from these cells requires a long incubation time. Furthermore, incubation of N-13 cells with TNF α for 24 hours induces the release of CatS (Liuzzo et al., 1999), suggesting that these cells can release CatS under inflammatory conditions, for example, following injury, and could be similar to the release of CatS from HaCaTs that is reported following 24-72 hours incubation with IFN γ and TNF α (Schonefuss et al., 2010; Schwarz et al., 2002). However, the mechanisms by which IFN γ and TNF α result in the release of CatS from cells is not yet understood.

Although Liuzzo et al., (1999) and Petanceska et al., (1996) observed release of CatS from N-13 cells following incubation in lipopolysaccharide (LPS), an activator of Toll-like receptor 4 (TLR4), incubation of primary microglia from rats with LPS alone did not result in the release of CatS from these cells (Clark et al., 2010). However, primary microglia cells incubated with LPS underwent morphological changes, and small increases in the intracellular expression of pre and mature forms of CatS protein were observed, suggesting microglia were primed by LPS. Following priming with LPS and stimulation with high concentration adenosine triphosphate (ATP) to activate the P2X $_7$ receptor, an increase in the release of CatS from

these microglia was observed. In contrast, ATP on its own was unable to induce release of CatS, indicating the requirement for LPS priming of these cells for CatS to be released.

ATP-induced release of CatS from primed microglia required the presence of extracellular calcium ions, since the release of CatS is halved when the cells are stimulated in the presence of a calcium-free buffer. Entry of extracellular calcium could be through P2X₇ channels, which allow conductance of calcium ions when expressed in gonadotropin-releasing hormone-secreting neurons (Koshimizu et al., 2000). Calcium release from intracellular stores also appears to be required for the release of CatS from microglia, since release of CatS is completely abolished when stimulated in the presence of dantrolene, an inhibitor of calcium release from stores in the sarcoplasmic reticulum (Clark et al., 2010). The increase in intracellular calcium ions promotes the trafficking of lysosomes to the cell membrane and release of lysosome contents, which would thus allow release of CatS from these cells (Andrews, 2002; Blott and Griffiths, 2002; Li et al., 2013).

As well as entry of calcium ions, potassium ions also appear to be involved in the release of CatS from microglia, since release of CatS is reduced in the presence of a high potassium buffer and increased in a potassium-free buffer (Clark et al., 2010). Activation of P2X₇ by ATP induces rapid efflux of potassium ions from the cell, possibly through P2X₇ channels themselves, which are permeable to potassium ions as well as calcium ions (Di Virgilio et al., 2001; Yaron et al., 2015). Thus, increasing the extracellular potassium concentration should reduce the efflux of potassium ions from the cell by reducing the potassium gradient across the cell; conversely reducing the extracellular potassium concentration would facilitate potassium efflux. Potassium efflux is upstream of calcium influx and may be required for the entry of extracellular calcium ions, since calcium chelation suppresses calcium fluxes without affecting ATP-induced potassium fluxes, while preventing efflux of potassium ions also prevents entry of extracellular calcium ions into the cell (Yaron et al., 2015).

Exocytosis of lysosomes also requires activity of PLC and calcium-dependent PLA2. Inhibitors of either PLC or PLA2 can prevent the lysosomal release of IL-1 β and caspase-1 from monocytes as well as the release of CatS from microglia following stimulation with ATP (Andrei et al., 2004; Clark et al., 2010). Activation of PLC is proposed to be required for the increase in intracellular calcium that follows activation of P2X₇ by ATP, since ATP-induced calcium fluxes are prevented by PLC inhibitors (Andrei et al., 2004). In contrast, ATP-induced calcium fluxes are not prevented by PLA inhibitors, suggesting PLA is downstream of PLC

activation or part of a parallel signalling pathway (Figure 2.1). Activation of PLC, which cleaves PIP_2 to form IP_3 , would result in the release of calcium from intracellular stores, thereby contributing to calcium-mediated exocytosis from cells. Furthermore, cleavage of PIP_2 by PLC to generate DAG has been shown to be required for exocytosis from mast cells (Hammond et al., 2006). This supports a role for PLC in the release of vesicles from cells, and may also apply to the exocytosis of lysosomes in other cell types. PLA2 has previously been shown to prime vesicles for fusion to plasma membranes (Karli et al., 1990), although whether PLA2 primes lysosomes in a similar manner for subsequent exocytosis remains to be investigated. Activation of PLC is thought to result in phosphorylation of MAPK, which in turn phosphorylates PLA2 (Figure 2.1), since incubation of microglia in LPS and ATP increases the presence of phosphorylated p38 MAPK in cultured microglia and inhibition of p38 MAPK prevents release of CatS from these cells (Clark et al., 2010).

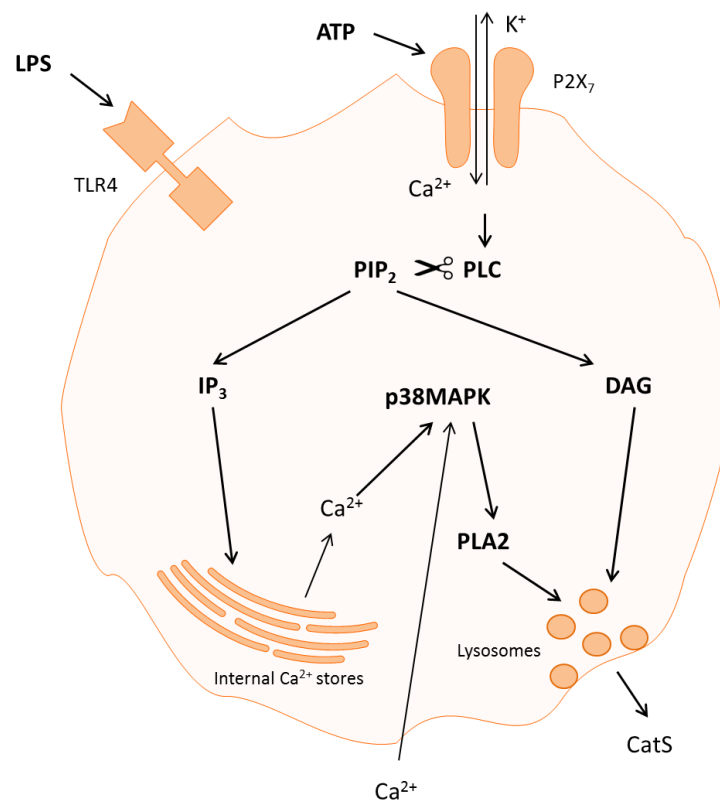


Figure 2.1: Schematic of proposed mechanism of lysosomal Cathepsin S release from cells (adapted from Clark et al., 2010)

We hypothesised that, similar to what has been reported in microglia, priming of HaCaT keratinocytes with LPS followed by stimulation with ATP could be a potential mechanism of CatS release from these cells. Although injured neurons might be a source of ATP for activation of microglia and subsequent release of CatS (Fields and Burnstock, 2006; Masuda

et al., 2016), keratinocytes themselves could be the source of ATP in skin inflammation (Mizumoto et al., 2003). Priming of keratinocytes for release of CatS could be due to LPS secreted by bacteria on the skin, although other inflammatory mediators present in the skin could also have a role in priming keratinocytes for release. Furthermore, the LPS receptor TLR4 is also expressed in neurons, and LPS has been found to enhance histamine-induced scratching behaviours in mice and the calcium responses of DRGs to histamine (Ji et al., 2018; Min et al., 2014). These support a role for LPS in the sensitisation of neurons to pruritogens as well as the release of CatS as a pruritogen from keratinocytes.

TRPV4-mediated release of Cathepsin S

An additional mechanism for the release of CatS from cells could be via activation of TRPV4 channels. TRPV4 is expressed in skin keratinocytes, where it is involved in barrier formation and recovery, cell-volume regulation, and UVB-induced pain (Becker et al., 2005; Denda et al., 2007; Kida et al., 2012; Moore et al., 2013). Furthermore, a role for TRPV4 in itch has been proposed, since injection of the TRPV4 agonist GSK1016790A (GSK101) results in scratching behaviours in mice (Chen et al., 2016). Importantly, this scratching behaviour is reduced in transgenic mice in which expression of TRPV4 was absent in keratinocytes, supporting a role for TRPV4 on keratinocytes in itch. TRPV4 appears to be involved in mediating histaminergic itch, as scratching behaviours in response to intradermal injection of histamine and histaminergic pruritogens is reduced in TRPV4 KO mice or when injected in wild-type mice in the presence of a TRPV4 antagonist (Chen et al., 2016). In contrast, compared with behaviours in wild-type mice, chloroquine-induced scratching behaviour is not altered in TRPV4 KO mice or in the presence of a TRPV4 antagonist. Furthermore, calcium fluxes in both murine and human keratinocytes in response to application of H1R, H3R, and H4R agonists were abolished when in the presence of TRPV4 inhibitors, suggesting TRPV4 mediates all forms of histaminergic itch signalling (Chen et al., 2016). TRPV4 may also be involved in chronic itch conditions, as expression of TRPV4 is increased in the skin in mouse models of dry skin and inflammatory itch and scratching behaviour is reduced when mice are given a TRPV4 antagonist (Luo et al., 2018).

Application of GSK101, exposure to warm temperatures (33°C), UVB, or swelling, all result in calcium transients in keratinocytes, suggesting involvement of calcium signalling in TRPV4-mediated responses (Becker et al., 2005; Kida et al., 2012; Moore et al., 2013). When activated, TRPV4 allows the entry of several cations, including calcium ions, into the cell (Nilius et al., 2003). Chen et al. (2016) reported that ERK signalling was downstream of

TRPV4-mediated calcium responses in skin keratinocytes, since phosphorylation of ERK was increased in both cultured keratinocytes and skin tissue in response to application of histaminergic pruritogens, and was reduced in the presence of a TRPV4 antagonist. Scratching behaviours in mice following injection of histaminergic pruritogens was also reduced following topical administration of an inhibitor of ERK, providing a role for ERK in the skin in histaminergic scratching behaviours, likely mediated by TRPV4 in keratinocytes. However, the signalling pathway downstream of ERK phosphorylation in keratinocytes that is responsible for transmission of the itch signal remains to be elucidated. We propose that activation of TRPV4 on keratinocytes culminates in the release of CatS from these cells, which then acts as a pruritogen on the endings of sensory neurons in the skin.

A recent study has reported that exposure of HaCaT cells and a melanoma cell line to the TRPV4 agonist GSK101 resulted in changes in cell morphology resembling apoptosis, detachment of cells, and cell death (Olivan-Viguera et al., 2018). Apoptosis was apparent as soon as after one hour incubation in GSK101 (10 nM). Co-incubation of cells with GSK101 and a TRPV4 antagonist reduced the morphological changes but the number of dead cells was not significantly reduced. The authors attributed these morphological changes and cell death to excessive entry of calcium and sodium into the cells following stimulation of TRPV4. However, a study by Fusi et al. (2014) reported that overnight incubation of HaCaTs in GSK101 (5 μ M), or other TRPV4 agonists, did not affect the viability of cells, despite using a greater concentration of GSK101. The reason for this discrepancy is not clear, although GSK101 has not been reported to affect cell viability in a number of cell types, including a hepatocellular carcinoma cell line and endothelial cells (Fang et al., 2018; Thoppil et al., 2015).

Chapter objectives

There is much evidence supporting the involvement of CatS in numerous skin conditions characterised by chronic itch. However, whether release of CatS from cells in the skin is directly responsible for signalling of itch by acting on receptors on the endings of sensory neurons in the skin, or whether CatS causes itch by indirect means, is not clear and is one of the questions addressed in this thesis. Furthermore, the mechanisms by which CatS is released from skin cells, particularly keratinocytes, in chronic skin conditions, is not fully understood and is addressed in this chapter.

Using the HaCaT keratinocyte cell line as a model system of the skin, the aims of this chapter were to investigate the expression of CatS in this cell line and to investigate the conditions under which CatS would be released. In particular, we wanted to determine whether these keratinocytes would release CatS following incubation in LPS and stimulation with ATP, as has been observed in microglia, and whether incubation with Th2 cytokines resulted in or modulated the release of CatS from these cells. Finally, we investigated whether stimulation of TRPV4 would cause release of CatS from HaCaT cells, establishing whether TRPV4 could potentially mediate its pruritic effects via the release of CatS.

2.2 Methods

2.2.1 HaCaT cell line culture

The immortalised HaCaT keratinocyte cell line, originally established by Dr Boukamp and Dr Fusenig (Boukamp et al., 1988) was supplied from Anthony Young. HaCaTs were grown in Defined Keratinocyte Serum-free Medium (DK-SFM) (Gibco, Life Technologies, UK) containing a growth supplement comprising bovine pituitary extract (BPE) (0.2% v/v), recombinant human insulin-like growth factor-1 (1µg/ml), hydrocortisone (0.18µg/ml), bovine transferrin (5µg/ml), and human epidermal growth factor (0.2 ng/mL), as well as penicillin-streptomycin (1%) (Gibco, Life Technologies, UK) and incubated in a humidified atmosphere of 5% CO₂ at 37°C. The culture medium was refreshed every 2-4 days. These adherent cells stick to the plastic on which they are cultured and so do not require a substrate on which to grow. When HaCaTs were between 80-100% confluent (approximately 8.4×10^6 cells per T75 tissue culture flask), they were split and sub-cultured to maintain optimal cell growth to plate for performing experiments. HaCaTs were split by removing DK-SFM from the flask and replacing with trypsin-EDTA containing 0.5 g/L porcine trypsin and 0.2 g/L EDTA•4Na (Sigma, UK). Once most of the cells had dislodged from the flask, trypsin was inactivated by addition of DMEM containing 10% serum. The cell suspension was then centrifuged, forming a pellet of cells. The liquid was aspirated and the pellet re-suspended in DK-SFM and added to a T75 tissue culture flask to maintain the culture, or plated onto 6-well tissue culture plates (35 mm diameter, Nunc, UK) or 24-well tissue culture plates (15.6 mm diameter, Nunc, UK) for use in experiments.

2.2.2 Immunocytochemistry and image acquisition

HaCaTs were seeded onto sterilised uncoated 13 mm diameter glass coverslips at 50,000 cells per coverslip and cultured in 5% CO₂ at 37°C until 50-60% confluent. Cells were fixed in

4% PFA (VWR, UK) for 30 minutes at 4°C. Cells were then washed 3 times with phosphate buffered saline (PBS). Single staining using antibodies from Wako or Abcam could be achieved without using the antigen retrieval method. However, preliminary experiments performed using antibodies from SantaCruz without using the antigen retrieval method did not produce reliable staining. Thus, for all co-staining experiments, the antigen retrieval method was used, followed by blocking in 2% milk, following a protocol adapted from Jio et al. (1999). Antigen retrieval was performed using citrate antigen unmasking solution (Vector Laboratories, USA) diluted 1:100 in H₂O, in which the cells were incubated at 80°C for 30 minutes. The cells were then left to cool at room temperature followed by blocking in 2% milk for 30 minutes and 3 washes with PBS. Primary antibodies (Table 2.1) were prepared in blocking buffer and cells were incubated in primary antibody dilutions for at least 2 hours at room temperature. This was followed by a further 3 washes in PBS and incubation in appropriate secondary antibodies diluted in blocking buffer (Table 2.1) for 2 hours at room temperature in the dark. Finally, cells were washed 3 times in PBS and mounted on a 25 mm x 75 mm x 1 mm glass slide in Vectashield mounting medium with DAPI (Vector Laboratories, USA).

The antibodies for CatS were also tested on mouse dorsal spinal cord. Mice were terminally anaesthetised with an overdose of sodium pentobarbital (Euthanol, 150 mg/kg body weight) and were transcardially perfused with 0.9% saline followed by 4% PFA. Spinal cords were removed and post-fixed in 4% PFA for 2 hours followed by dehydration and cryoprotection in 20% sucrose for 72 hours at 4°C, before being snap frozen and embedded in Optimum Cutting Temperature embedding medium (OCT) (VWR, UK). Transverse sections were cut to 20 µm thickness using a cryostat (Bright Instruments, UK) and sections were mounted on 25 mm x 75 mm x 1 mm microscopic glass slides (VWR, UK) and stored at -20°C. Before staining, sections were rehydrated in PBS for 10 minutes. Sections then underwent antigen retrieval, blocking, and incubation in primary and secondary antibodies as for above. All images were taken using a Zeiss Axioplan 2 fluorescent microscope and Axiovision version 4.8.2 software (Zeiss, UK).

Table 2.1: List of primary and secondary antibodies used for immunocytochemistry

Primary	Concentration	Secondary	Concentration
Goat anti-cathepsin S, M-19 (Santa Cruz Biotechnology Inc, UK)	1:100 – 1:500	Donkey-anti-goat IgG-conjugated AlexaFluor 546 or 488 (Molecular Probes, USA)	1:500
Mouse anti-cathepsin S, E-3 (Santa Cruz Biotechnology Inc, UK)	1:100 – 1:500	Goat-anti-mouse IgG-conjugated AlexaFluor 488 (Molecular Probes, USA)	1:500
Rabbit anti-Iba1, ab18207 (Wako Pure Chemical Industries, Germany)	1:1000	Donkey-anti-rabbit IgG-conjugated AlexaFluor 546 (Molecular Probes, USA)	1:500
Mouse anti-LAMP-1, H4A3 (Abcam, UK)	1:100	Donkey-anti-mouse IgG-conjugated AlexaFluor 488 (Molecular Probes, USA)	1:500

2.2.3 Western blotting

HaCaTs were cultured in 35 mm diameter wells until confluent. Cells were lysed by the addition of lysis buffer (TRIS-HCl pH7.5, 20 mM, Sigma, UK; NaF, 10 mM, Sigma, UK; NaCl, 150 mM, VWR, UK; NP-40, 1%, Sigma, UK; PMSF, 1 mM, Sigma, UK; Na₃VO₄, 1 mM, Sigma, UK) containing Complete Mini Cocktail Protease Inhibitor (Roche, UK) to each well. Cells were removed from the wells using a cell scraper, agitated at 12 rpm for 40 minutes, and centrifuged at 11,000 rpm for 15 minutes. The supernatant was then collected and stored at -20°C.

Protein concentration was determined using a Bradford assay and BSA standards. Samples were diluted 1:40 in water and loaded in duplicate into the wells of a clear-walled and clear-bottom 96-well plate. BSA standards (Sigma, UK) from 2 mg/ml to 15.625 µg/ml were also diluted 1:40 in water and loaded in duplicate. Bradford protein assay dye reagent (BioRad, UK) was added to the diluted samples and standards at 1:5 dilution, such that the final concentration of the samples and standards was at 1:50 dilution. Samples were read using a SpectraMax 340 PC platereader (Molecular Devices, USA) at 595 nm wavelength. A standard curve was generated using the BSA standards and from this the concentration of protein in the samples was calculated.

Samples were diluted in Laemmli sample buffer (BioRad, UK) to give an equal concentration of protein in each sample and incubated at 95°C for 5 minutes before loading into the gel. The gels for running the samples comprised of a 10% resolving gel (TRIS-HCl pH 8.8, 375 mM, Sigma, UK; acrylamide, 10%, BioRad, UK; SDS, 0.1%, Sigma, UK; ammonium persulfate (APS), 0.1%, Sigma, UK; N,N,N',N'-tetramethylethyldiamine (TEMED), 0.04%, Sigma, UK) with a stacking gel on top (TRIS-HCl pH 6.8, 125 mM, Sigma, UK; acrylamide, 5%, BioRad, UK; SDS, 0.1%, Sigma, UK; APS, 0.1%, Sigma, UK; TEMED, 0.01%, Sigma, UK). Gels were made at 1.5 mm thickness using BioRad (UK) moulds. Once the gels had set, they were placed inside an electrophorator (tank) filled with 1x SDS-PAGE running buffer (TRIS-base, 25 mM, Sigma, UK; glycine, 200 mM, Sigma, UK; SDS 10%, Sigma, UK). Precision Plus Protein Kaleidoscope ladder (BioRad, UK) was loaded onto each side of the gel, and the appropriate volumes of protein samples were loaded into the remaining wells of the gel. The electrophorator was run at 90V using a PowerPac200 (BioRad, UK) until the samples had run to the end of the stacking gel, and then run at 100V until the samples reached the end of the resolving gel.

The gels were cut to size and placed in a tray of ice-cold 1x TRIS-glycine transfer buffer (TRIS-base, 20 mM, Sigma, UK; glycine, 200 mM, Sigma, UK; methanol, 20% v/v, VWR, UK). For each gel, a cassette containing 0.2µm pore size nitrocellulose membrane (Amersham, GE Healthcare) was assembled and placed in the transfer chamber, which was run at 80V for 1 hour, or until the samples in the gel had transferred to the membrane. The membrane was then washed in 1x TBS-T at pH7.6 (TRIS-HCl, 50 mM, Sigma, UK; NaCl, 150 mM, VWR, UK; Tween-20, 0.1%, Sigma) and the presence of proteins was confirmed using a Ponceau red stain.

The membrane was washed twice in 1x TBS-T before being blocked in 5% milk prepared in 1x TBS-T for 45 minutes on a shaker. The membrane was then washed twice more in 1x TBS-T and cut according to the expected band size of interest. The primary antibody for CatS (M-19, goat, Santa Cruz, USA, and E-3, mouse, Santa Cruz, USA) was diluted 1:200 in 5% milk in 1x TBS-T, and the primary antibody for β-actin (rabbit, CST, USA) was diluted 1:1000 in 3% BSA in 1x TBS-T. The membrane was incubated in primary antibody solution overnight at 4°C on a shaker. The following day, the membranes were washed 3 times in 1x TBS-T. The secondary antibody for CatS, HRP-conjugated rabbit anti-goat (Dako, UK) for M-19 or goat-anti-mouse (Dako, UK) for E-3, was diluted 1:2000 in 5% milk TBS-T. The secondary antibody for β-actin, HRP-conjugated goat-anti-rabbit (Dako, UK), was diluted in 1:2000 dilution in 5%

milk TBS-T. The membrane was incubated in the secondary antibody solution for 1 hour at room temperature on a shaker, followed by 3 washes in 1x TBS-T.

To reveal the membrane, the membrane was covered in Luminata Forte Western HRP Substrate (Millipore) and agitated for 3 minutes on a shaker. The membrane was visualised using a BioSpectrum Imaging System (UVP, USA) and images were acquired using VisionWorks LS software (UVP, USA). Image acquisition times varied from 1 minute to 10 minutes exposure for CatS and from 10 seconds to 20 seconds exposure for actin.

2.2.4 Quantitative polymerase chain reaction (qPCR)

HaCaTs were cultured in 35 mm diameter wells until confluent. Total RNA was extracted from the cells using the RNeasy Mini Kit (Qiagen), according to the manufacturer's protocol. The total concentration of RNA was measured using the NanoDrop spectrometer. 1000 ng RNA was used to synthesise first strand DNA using the Superscript VILO cDNA Synthesis Kit (Invitrogen, UK) according to the manufacturer's protocol. Expression levels of CA2, CCL26, NELL2, CatS, PAR2, TLR4, and TRPV4 were analysed, with 18S rRNA used as a reference transcript. Amplification was performed with a LightCycler 480 (Roche, UK) using SYBR Green I Master (Roche, UK). The primers used are given in Table 2.2. The instrument was programmed as follows: 95°C for 5 minutes and 45 cycles of 3 steps of 10 seconds each, including denaturing at 95°C, annealing at 60°C, and primer extension at 72°C. Samples were run as duplicates, with 18S as the housekeeping gene. Samples in which the melting curve had more than one peak were excluded from analysis. Data was analysed using LightCycler 480 software (version 1.5.1). The relative gene expression level was calculated according to the $2^{-\Delta Ct}$ method and $2^{-\Delta\Delta Ct}$, where Ct represents the threshold cycle. The efficiency of the primers was confirmed using standard curves with cDNA concentrations of 15 ng/μl, 5 ng μl, 1.6 ng μl, 0.55 ng μl, and 0.185 ng μl. Efficiencies were required to be between 1.8 and 2.2. The qPCR products were added to 6x blue/orange loading dye (Promega, UK) and run on a 2% agarose gel containing ethidium bromide (0.01%, Sigma, UK) in TBE at 100V for one hour to confirm the presence of a single primer product. A 1 kb DNA ladder (Promega, UK) was run alongside to allow estimation of the band sizes, and band sizes obtained were compared with the predicted band sizes that would be obtained with the chosen primers.

Table 2.2: Primers used for CA2, CCL26, NELL2, CatS, PAR2, TLR4, TRPV4 and 18S in qPCR

Gene	Forward Sequence	Reverse Sequence	Reference
CA2	AACAATGGTCATGCTTTCAACG	TGTCCATCAAGTGAACCCCAG	Kamsteeg et al., 2010; Smits et al., 2017
CCL26	TCATTCAGTAAAGAGGCGAAGT ATTATC	CAGTTTTTTGGAGGGCATCTG	Smits et al., 2017
NELL2	TAAGGGTATAATGCAAGATGTCC AATT	AGATCTGGGCACTGAGCAATAA A	Kamsteeg et al., 2010
CatS	GCCTGATTCTGTGGACTGG	GATGTACTGGAAAGCCGTTGT	Fan et al., 2012, Wang et al., 2015
TLR4	CGATTCCATTGCTTCTTG	GCTCAGGTCCAGGTTCTT	Pivarsci et al., 2004
TRPV4	CTACGCTTCAGCCCTGGTCTC	GCAGTTGGTCTGGTCCTCATTG	Spinsanti et al., 2008
18 S	GCTGGAATTACCGCGGCT	CGGCTACCACATCCAAGGAA	Denning et al., 2008

2.2.5 Cathepsin S activity assays

HaCaTs were cultured in 15.6 mm or 35 mm diameter wells until confluent. Cells were stimulated according to several different paradigms. In all situations, the supernatant was transferred to 1.5 ml microfuge tubes (Starlab, UK) and snap frozen in liquid nitrogen and stored at -80°C, or used straight away to measure CatS activity.

To begin with, the culture media was removed from 15.6 mm diameter wells and replaced with warmed HEPES buffer at pH7.4 (HEPES, 10 mM, Sigma, UK; NaCl, 150 mM, Sigma, UK; KCl, 5 mM, Sigma, UK; MgCl₂, 1 mM, G Biosciences, USA; CaCl₂, 1 mM, Fisher Scientific, UK; glucose, 5.55 mM, Sigma, UK). Cells were incubated in HEPES with or without 1 µg/ml lipopolysaccharide (LPS) (*E. coli* 011:B4, Sigma, UK) for 3, 6, or 12 hours, followed by incubation with either 50 µM or 1 mM ATP (Sigma) or HEPES for 20 minutes. The rest of the incubations and stimulations were performed in HaCaTs cultured in 35 mm diameter wells. HaCaTs were incubated with the Th2 cytokines, IL-4 and IL-13, to investigate whether this would affect CatS activity. The culture media was replaced with fresh DK-SFM containing IL-

4 (50 ng/ml, BioLegend, UK) and IL-13 (50 ng/ml, Shenandoah, USA) or without any cytokines added, and incubated for 48 hours followed by collection of the media. To investigate whether additional stimulation was required for the release of CatS from these cells following incubation in Th2 cytokines, HaCaTs were also stimulated in IL-4 and IL-13 for 48 hours, followed by removal of the culture media and incubation in warmed HEPES containing LPS (1 µg/ml) for 6 hours and ATP (1 mM, ATP, Sigma) for 20 minutes. To determine whether stimulation of the TRPV4 channel could cause the release of CatS from HaCaTs, the culture media was replaced with warmed HEPES buffer, and cells were stimulated for 20 minutes with the TRPV4 agonist GSK1016790A (GSK101) (10 nM or 100 nM, Sigma) or with DMSO (0.001 %). To examine whether Th2 cytokines could enhance the release of CatS following stimulation of HaCaTs with GSK101, cells were stimulated in IL-4 and IL-13 for 48 hours, followed by removal of the culture media and incubation in warmed HEPES buffer containing GSK101 or DMSO for 20 minutes. To investigate the involvement of extracellular calcium in TRPV4-mediated release of CatS, the culture media was removed and replaced with standard warmed HEPES buffer or warmed HEPES buffer without any calcium ions added to it (HEPES, 10 mM, Sigma, UK; NaCl, 150 mM, Sigma, UK; KCl, 5 mM, Sigma, UK; MgCl₂, 1 mM, G Biosciences, USA; glucose, 5.55 mM, Sigma, UK), in which cells were stimulated with GSK101 (100 nM) or DMSO (0.001%) for 20 minutes. Samples were collected and the activity assay was then performed in standard HEPES buffer for the samples that had been incubated in standard HEPES buffer, while those that were incubated in HEPES buffer without any calcium ions added to it were had the activity assay performed in HEPES buffer containing double the concentration of calcium ions (HEPES, 10 mM, Sigma, UK; NaCl, 150 mM, Sigma, UK; KCl, 5 mM, Sigma, UK; MgCl₂, 1 mM, G Biosciences, USA; CaCl₂, 2 mM, Fisher Scientific, UK; glucose, 5.55 mM, Sigma, UK), such that the final concentration of calcium following the addition of the samples to the activity assay buffer was the same across all experiments to account for any effects that varying the calcium concentration may have had on CatS activity.

To investigate the activity of intracellular CatS in HaCaTs, total protein was extracted on ice as follows. The culture media was aspirated and cells were washed twice in cold, sterile PBS. An extraction buffer comprising sucrose (250 mM, Sigma, UK) in TRIS (10 mM, Sigma, UK) at pH7.2 was added to the cells, and using a cell scraper, cells were removed from the wells and transferred to 1.5 ml Eppendorf tubes. The samples were homogenised and agitated at 12 rpm at 4°C for 30 minutes. Finally, the samples were centrifuged at 11,000 rpm at 4°C for 15 minutes, and the top layer of supernatant was transferred to a new 1.5 ml Eppendorf

tube and snap frozen in liquid nitrogen and stored at -80°C or used straight away to measure CatS activity.

CatS is unique in that, unlike the other cathepsins, it retains activity at neutral pH, allowing it to function outside the acidic environment of lysosomes (Bromme et al., 1993; Shi et al., 1992; Vasiljeva et al., 2005). Thus, to examine whether the activity observed in the activity assay was due to the activity of CatS or due to other cathepsins and proteases, protein extraction and the activity assay were both performed at pH5 and pH7, using extraction buffers at pH5 and pH7 and HEPES buffer at pH5 and pH7, respectively. For some experiments, the activity of all proteases in the HaCaT cell lysates was inhibited by performing the protein extraction in a lysis buffer containing protease inhibitors (TRIS-HCl pH7.5, 20 mM, Sigma, UK; NaF, 10 mM, Sigma, UK; NaCl, 150 mM, VWR, UK; NP-40, 1%, Sigma, UK; PMSF, 1 mM, Sigma, UK; Na₃VO₄, 1 mM, Sigma, UK; Complete Mini Cocktail Protease Inhibitor, Roche, UK).

Samples that had been frozen were defrosted on ice; otherwise freshly prepared samples were used in the activity assays. The samples were added in duplicate to the wells of a black-walled and clear-bottom 96-well plate. To activate CatS, samples were incubated with dithiothreitol (DTT) (0.5 mM) at 37°C for 10 minutes. The Z-Val-Val-Arg-MCA substrate (50 µM in 0.01 potassium phosphate buffer and 5 mM disodium EDTA at pH7.5, Peptide Institute, Japan) was added to the samples. Fluorescence following cleavage of the Z-Val-Val-Arg-MCA substrate and liberation of 7-amino-4-methylcoumarin (Kirschke and Wiederanders, 1994) was measured using a FlexStation platereader (Molecular Devices, USA) at 360 nm excitation wavelength and 460 nm emission wavelength, and SOFTmax Pro software (Molecular Devices, USA). The assay was run for 2 hours in all conditions, with readings taken at 10-minute intervals. To investigate whether the increase in fluorescence was due to CatS or other cathepsins, extraction of the proteins and the activity assay were performed at pH5 and pH7. Proteins that had been extracted using an extraction buffer at pH5 underwent the activity assay in HEPES buffer at pH5, while those that had been extracted at pH7 underwent the activity assay at pH7. To further confirm that the increase in fluorescence was due to CatS activity, the activity assay was performed in the presence of the CatS inhibitor, MDV-590 ((S)-N-(1-((1-(2-amino-2-oxoacetyl)cyclobutyl)amino)-3-(1-fluorocyclopentyl)-1-oxopropan-2-yl)-3,3,3-trifluoro-2,2-dimethylpropanamide) (Medivir UK Ltd (2011), New Cathepsin S protease inhibitors, useful in the treatment of e.g. autoimmune disorders, allergy and chronic pain conditions. International Patent Application

WO2011/158197). HaCaT cell lysates that had been extracted as for above were loaded in duplicate in a 96-well plate and incubated with DTT (0.5 mM) at 37°C for 10 minutes. The Z-Val-Val-Arg-MCA substrate was then added, along with MDV-590 (10 µM) or DMSO (0.01%). The samples were incubated for a further 10 minutes in the dark prior to beginning the assay. Some HaCaTs were stimulated in GSK101 (100 nM) or DMSO (0.001%) in a HEPES buffer containing calcium ions (1 mM); others were stimulated in GSK101 or DMSO in a HEPES buffer without calcium ions added. However, for all activity assays, the final concentration of calcium in the supernatant and substrate mixture was 1 mM.

2.2.6 Statistical Analysis

Data were analysed and graphs generated using GraphPad Prism 5 (Graphpad Software Inc., USA). For qPCR experiments, data were analysed using one-way ANOVA followed by Bonferroni's multiple comparison tests when comparing multiple groups with each other or one-way ANOVA followed by Dunnett's multiple comparison test when comparing multiple groups against one control group. For the CatS activity assays, the kinetic time course data were analysed using two-way ANOVA followed by Bonferroni post hoc tests, while the changes in fluorescence were analysed using Student's t-tests when comparing just two groups, one-way ANOVA followed by Bonferroni's multiple comparison tests when comparing multiple groups with each other, or one-way ANOVA followed by Dunnett's multiple comparison test when comparing multiple groups against one control group. The n numbers are displayed within the figure legends of the results section. Data are presented as mean ± standard error of the mean (SEM). P≤0.05 was set as the level of statistical significance.

2.3 Results

To investigate whether the skin is a likely source of endogenous CatS, we first wanted to establish whether CatS is expressed in skin keratinocytes and if this CatS can be released from these cells. We then sought to investigate the mechanisms of CatS release from keratinocytes.

2.3.1 Expression of Cathepsin S protein and mRNA

To begin with, we wanted to establish whether the HaCaT keratinocyte cell line expressed CatS. This was investigated using qPCR for the expression of CatS mRNA, and antibody staining and Western blotting for the presence of CatS protein. We attempted to stain HaCaTs cells for CatS using two different antibodies against CatS. However, no positive

staining for was detected at any dilution used (Figure 2.2 A and B), although the lysosomal marker, LAMP-1, was expressed (Figure 2.2 C). However, as one of the antibodies to CatS (M-19) was able to detect the presence of CatS in mouse spinal cord, where it co-localised with Iba1 staining for microglia (Figure 2.2 D), suggesting that the antibody can detect protein and that perhaps insufficient CatS was expressed in HaCaTs to be able to detect using this method. Alternatively, the antibody does not recognise the CatS conformation in these cells.

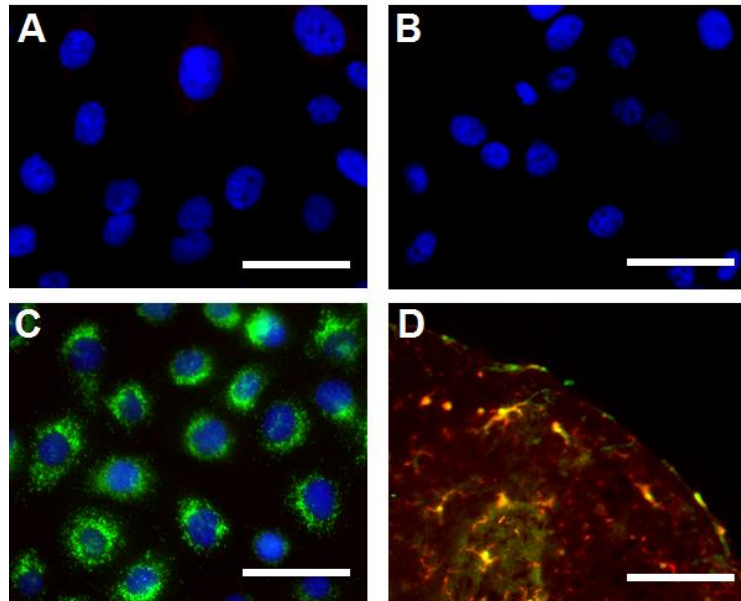


Figure 2.2: Expression of Cathepsin S peptide and LAMP-1

No expression of CatS in HaCaTs using M-19 (A) or E-3 (B) anti-CatS at 1:100 dilution. Staining for the lysosomal marker LAMP-1 in HaCaTs at 1:100 dilution (green) (C). Staining for CatS in mouse dorsal horn spinal cord using 1:100 M-19 anti-CatS (green) and 1:1000 Iba1 antibody (red) (D). Nuclei are stained blue using DAPI stain. Scalebar represents 50 μ m.

Using the same antibodies for CatS, we were unable to confirm expression of CatS protein in HaCaT cells using Western blotting (Figure 2.3 A), although actin could be detected (Figure 2.3 B). In the THP-1 cell line, which is also reported to express CatS (Pawar et al., 2016) we were unable to show expression of CatS in our Western blots. However, samples of active human recombinant CatS provided from Medivir run in a Western blot did produce a band at about 25 kDa (Figure 2.3 A), as well as the presence of a few smaller fragments. The predicted size for mature CatS is 24 kDa (Wiederanders et al., 1992).

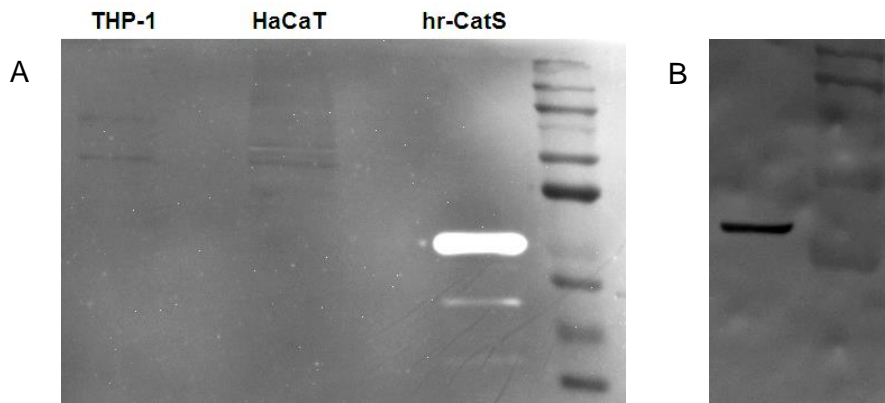


Figure 2.3: Western blots for Cathepsin S and actin

No bands for CatS in HaCaT or THP-1 samples were found. A band was observed for purified activated human recombinant CatS at about 25 kDa (A). Actin bands were observed in HaCaT samples at about 45 kDa, while the predicted size of actin is 42 kDa (B).

Although we could not detect expression of CatS protein in our HaCaTs, expression of CatS protein might not have been sufficient to be detected using this method. Using qPCR, however, we found expression of CatS mRNA in our cells. The qPCR products were also run on an agarose gel, which gave a band of about 250 base pairs, while the predicted band size was 232 base pairs for the primers for CatS that were used (Figure 2.4).

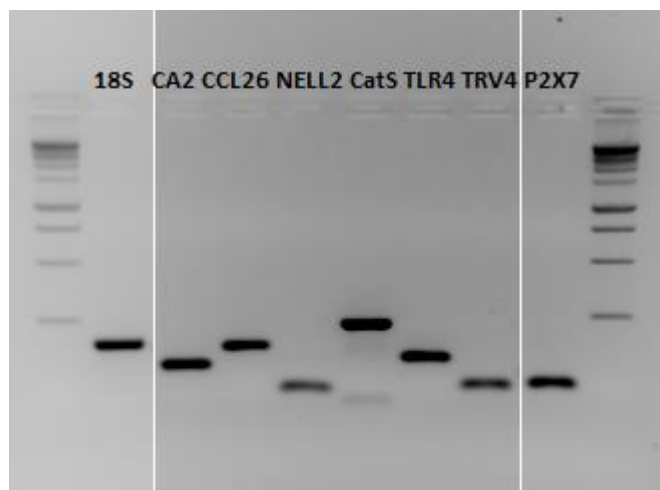


Figure 2.4: qPCR products of mRNA extracted from HaCaT cells

Image cropped from a gel containing several samples.

LPS has been reported to increase expression of CatS in cervical smooth muscle cells (Watari et al., 2000) and microglia (Tam et al., 2016). We thus hypothesised that LPS could also cause upregulation of CatS in skin keratinocytes. The receptor for LPS, TLR4, has been reported to be expressed in keratinocytes and HaCaT cells (Kollisch et al., 2005; Pivarcsi et

al., 2003; Pivarcsi et al., 2004; Song et al., 2002). We first confirmed the expression of TLR-4 on our HaCaT cell cultures using qPCR. Running the qPCR products on a gel gave a band of about 150 base pairs, while the predicted band size for this product was 137 base pairs based on the primers that were used (Figure 2.4). It has previously been reported that incubation of HaCaTs in LPS causes upregulation of TLR4 mRNA in these cells (Kollisch et al., 2005). We too observed an increase in the expression of TLR4 following 6 hours incubation in LPS (Figure 2.4 A). Although changes in the expression of TLR4 were found following incubation with LPS, we were mainly interested in investigating whether expression of CatS in these cells was also affected by incubation with LPS. Incubating HaCaTs in LPS for 6 hours resulted in an increase in the expression of CatS, compared with cells that had been incubated in buffer for the same length of time (Figure 2.5 B). No changes were reported after 3 hours incubation in LPS or buffer.

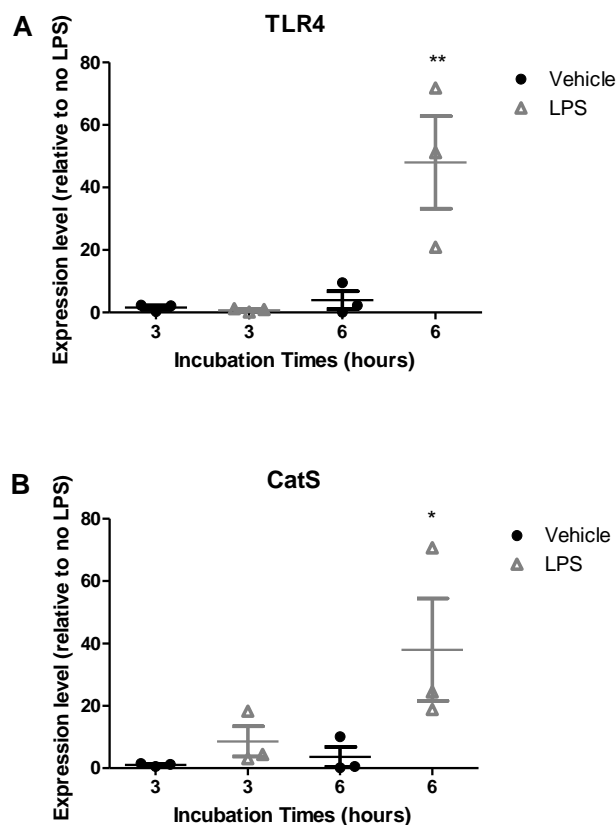


Figure 2.5: Toll-like receptor-4 and Cathepsin S mRNA expression in HaCaTs is increased following incubation in LPS

Incubation of HaCaTs in 1 $\mu\text{g/ml}$ LPS for 6 hours resulted in an increase in the expression of TLR4 (A) and CatS (B) mRNA in these cells compared with incubation in buffer. $n = 3$; 2 replicates per sample, data are mean \pm SEM. $**p \leq 0.01$, One-way ANOVA followed by Bonferroni's multiple comparison test vs HEPES incubations.

Table 2.3: Ct values for qPCR performed on HaCaTs following 3 or 6 hours incubation in vehicle (buffer) or LPS

Average Ct values of samples run as duplicates.

		18S		TLR4		CatS	
		Vehicle	LPS	Vehicle	LPS	Vehicle	LPS
3 hours	Sample 1	10.58	9.05	28.94	28.28	34.08	27.46
3 hours	Sample 2	14.63	7.135	32.895	27.235	36.95	27.595
3 hours	Sample 3	7.9	7.275	32.895	30.315	29.89	28.255
6 hours	Sample 1	7.085	8.835	35.105	26.295	28.395	27.335
6 hours	Sample 2	8.125	7.51	28.5	26.755	33.62	27.92
6 hours	Sample 3	8.365	7.635	30.85	25.585	35.49	27.665

IL-4 and IL-13 are proposed to be involved in the pathogenesis of atopic dermatitis (Danso et al., 2014; Kamsteeg et al., 2011; Smits et al., 2017; Werfel, 2009), and so we hypothesised they might do so by upregulating expression of CatS in keratinocytes. Incubation of HaCaTs in IL-4 and IL-13 (50 ng/ml) for 48 hours resulted in a two-fold increase in CatS mRNA (Figure 2.6 A). Similarly, the expression of CA2, CCL26, and NELL2 have been reported to be increased in the skin of patients with atopic dermatitis (Kagami et al., 2003; Kamsteeg et al., 2007; Kamsteeg et al., 2010), as well as following stimulation of keratinocytes with Th2 cytokines such as IL-4 and IL-13 (Kamsteeg et al., 2011; Smits et al., 2017). We therefore investigated whether our HaCaTs had similar changes in the expression of these genes following incubation with IL-4 and IL-13, and hence whether we were able to model an atopic dermatitis-like condition in our cells. Although we were able to confirm expression of CA2, CCL26, and NELL2 in our HaCaTs, no significant changes in their expression were observed following 24 or 48 hours incubation in IL-4 and IL-13 (Figure 2.6 B – D).

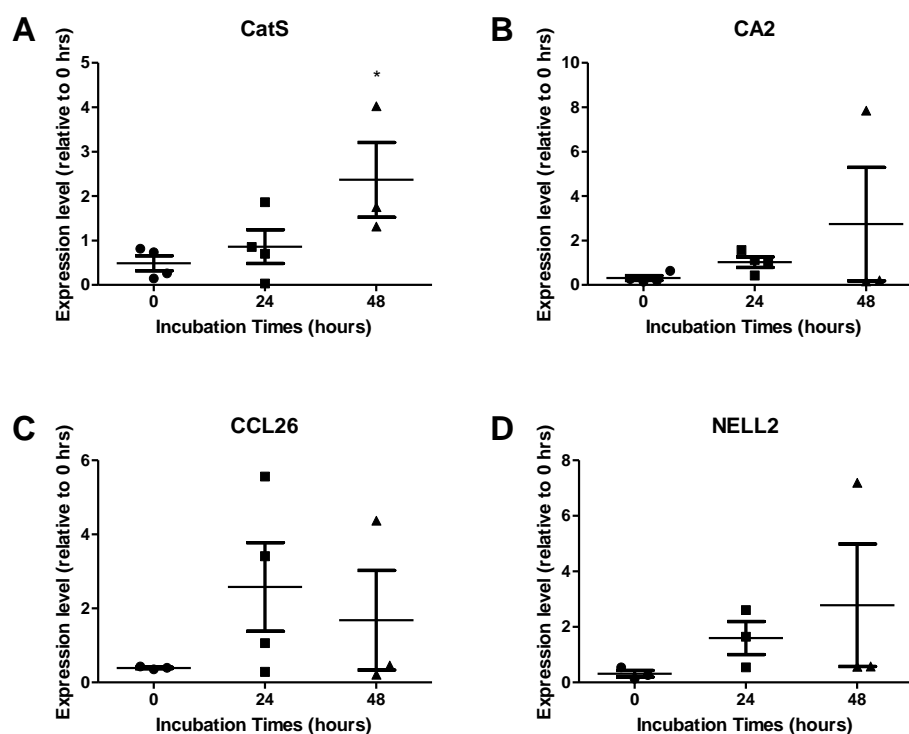


Figure 2.6: Cathepsin S mRNA expression in HaCaTs is increased following incubation in IL-4 and IL-13

mRNA expression of *CatS* (A), *CA2* (B), *CCL26* (C), and *NELL2* (D) for HaCaTs incubated in 50 ng/ml IL-4 and 50 ng/ml IL-13 for up to 48 hours. $n = 3, 4$; 2 replicates per sample, data are mean \pm SEM. * $p \leq 0.05$, One-way ANOVA followed by Dunnett's multiple comparison test vs no IL-4/IL-13.

Table 2.4: Ct values for qPCR performed on HaCaTs following 0, 24, Or 48 hours incubation in IL-4 and IL-13

Average Ct values of samples run as duplicates. X denotes missing data.

		18S	CatS	CA2	CCL26	NELL2
0 hours	Sample 1	7.695	28.32	25.1025	X	31.36
0 hours	Sample 2	7.9425	31.0425	23.245	35.43	X
0 hours	Sample 3	6.8425	29.12	23.3825	34.61	31.5025
0 hours	Sample 4	7.3025	28.0725	24.3175	34.91	29.9625
24 hours	Sample 1	9.015	34.1275	23.0225	32.815	30.0725
24 hours	Sample 2	8.9	29.745	24.7925	36.9625	X
24 hours	Sample 3	8.745	28.18	23.2275	33.25	29.14
24 hours	Sample 4	7.2875	27.845	21.96	33.475	29.94
48 hours	Sample 1	10.0475	28.37	21.735	34.195	28.98
48 hours	Sample 2	X	X	X	X	X
48 hours	Sample 3	7.0825	26.6025	24.2975	34.475	29.635
48 hours	Sample 4	7.315	27.2475	24.21	35.7925	29.8975

2.3.2 Intracellular Cathepsin S activity

Although we were unable to detect CatS peptide expression, mRNA expression suggested that the enzyme is present in HaCaT cells. Thus, we next investigated whether CatS activity could be detected in these cells, either in cell media or in cell lysates, incubated with a Z-Val-Val-Arg-MCA substrate that fluoresces following the liberation of 7-amino-4-methylcoumarin cleaved when by CatS (Kirschke and Wiederanders, 1994). Because the Z-Val-Val-Arg-MCA substrate can potentially be cleaved by cathepsin L and other cysteine lysosomal proteases, and because CatS, unlike other cathepsins, retains its activity at physiological pH, this assay was performed at both pH5 and pH7 to determine if the activity that was observed was due to CatS and not other proteases (Bromme et al., 1993; Kirschke and Wiederanders, 1994; Shi et al., 1992). High levels of fluorescence were detected in HaCaT cell lysates at both pH5 and pH7. Although the fluorescence level at pH7 was less than that at pH5, it was still significantly greater than the fluorescence in assay buffer alone without protein samples (Figure 2.7 A and B). Thus, most fluorescence changes observed in this assay at pH7 can be attributed to the cleavage of the Z-Val-Val-Arg-MCA substrate by CatS.

To further confirm that the fluorescence changes observed in HaCaT cell lysates, the activity assay was performed in the presence of a buffer containing protease inhibitors including PMSF and E-64. This resulted in almost a complete reduction of fluorescence and hence protease activity in the assay (Figure 2.7 A and B). To test more specifically for the activity of CatS, the assay was also performed at pH7 in the presence of the CatS inhibitor MDV-590. Pre-incubating the HaCaT cell lysate in MDV-590 for 10 minutes before performing the assay resulted in a significant decrease in fluorescence (Figure 2.8), suggesting much of the fluorescence is due the activity of CatS on the Z-Val-Val-Arg-MCA substrate.

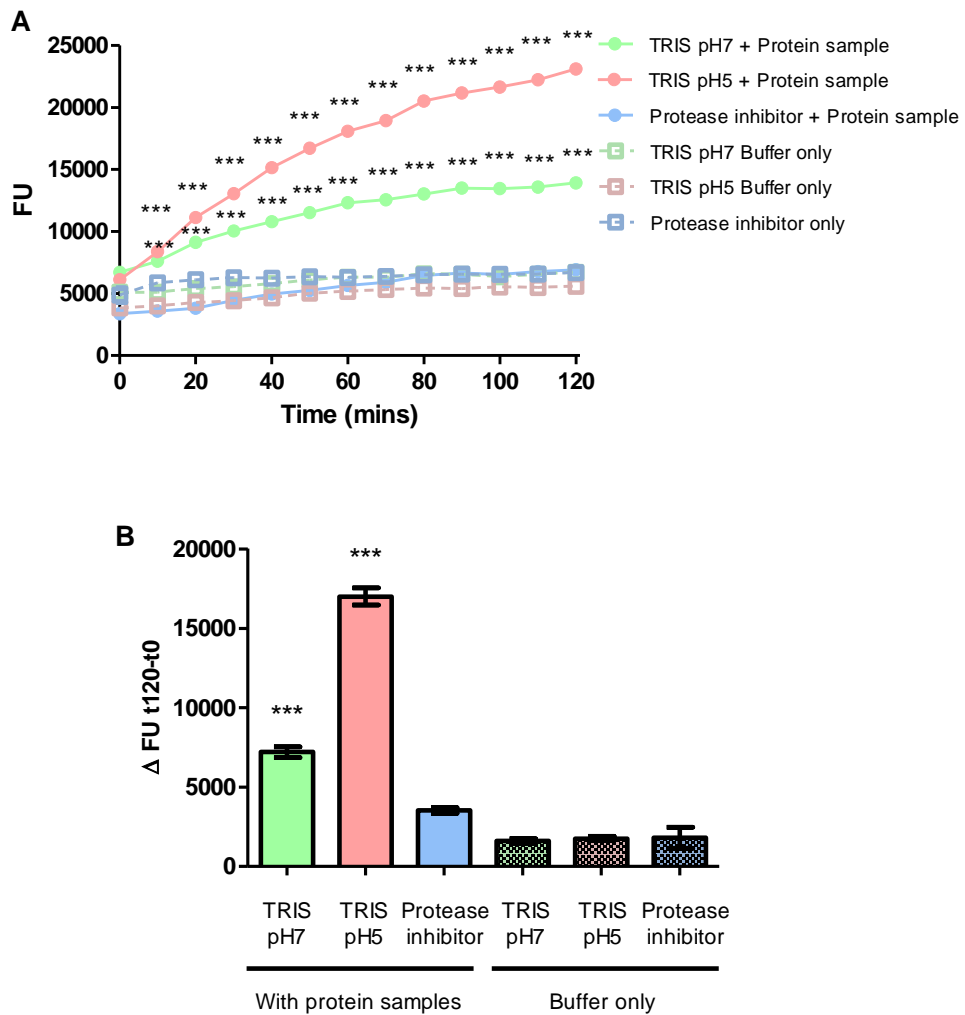


Figure 2.7: Cathepsin S activity is detected in HaCaT cell lysates and occurs at both acidic and neutral pH

*A. Time course of fluorescence changes over a 2 hour period when HaCaT cell lysates were incubated with the Z-Val-Val-Arg-MCA substrate at both pH5 and pH7 or in the presence of a lysis buffer containing protease inhibitors at pH7. $n = 3$; 2 replicates per sample, data are mean \pm SEM. $***p \leq 0.001$, Two-way ANOVA followed by Bonferroni post hoc test.*

*B. Quantification of changes in fluorescence at time point 120 minutes (t120) minus the initial reading at time point 0 (t0). $n = 3$; 2 replicates per sample, data are mean \pm SEM. $***p \leq 0.001$, One-way ANOVA followed by Bonferroni's multiple comparison test.*

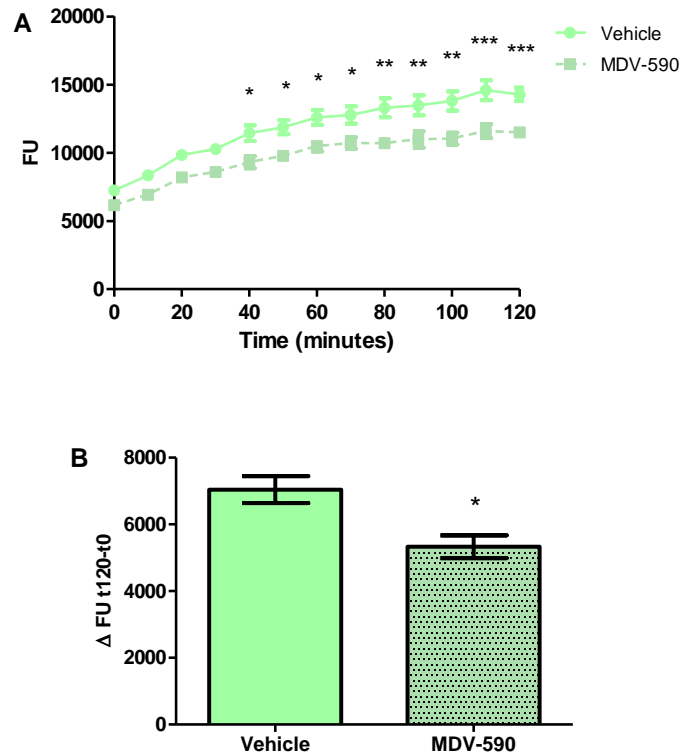


Figure 2.8: Cathepsin S activity in HaCaT cell lysates is reduced by the Cathepsin S inhibitor MDV-590

*A. Time course of fluorescence changes from HaCaT cell lysates incubated with the Z-Val-Val-Arg-MCA substrate in the presence of MDV-590 (10 μ M). $n = 4$; 2 replicates per sample, data are mean \pm SEM. * $p \leq 0.05$; ** $p \leq 0.01$; *** $p \leq 0.001$, Two-way ANOVA followed by Bonferroni post hoc test.*

*B. Quantification of changes in fluorescence. $n = 4$; 2 replicates per sample, data are mean \pm SEM. * $p \leq 0.05$, Student's *t*-test.*

2.3.3 Extracellular Cathepsin S activity

In addition to intracellular CatS activity of HaCaTs, we also wanted to demonstrate that HaCaTs could be made to release CatS. It has previously been shown that incubation of microglia with LPS and ATP results in the maturation and release of CatS from these cells (Clark et al., 2010). We therefore investigated whether stimulation of HaCaTs with LPS and ATP could also result in maturation and release of CatS. We first confirmed expression of TLR4 and P2X7, the receptors for LPS and ATP, respectively, using qPCR (Figure 2.4). HaCaTs were then incubated with LPS (1 μ g/ml) for 3 hours and stimulated with ATP (1 mM) for 20 minutes, and the culture medium was collected to test for CatS activity. However, no changes in fluorescence were observed, suggesting no release of CatS from these cells (Figure 2.9 A and B). To reduce the possibility that sub-optimal stimulation conditions was

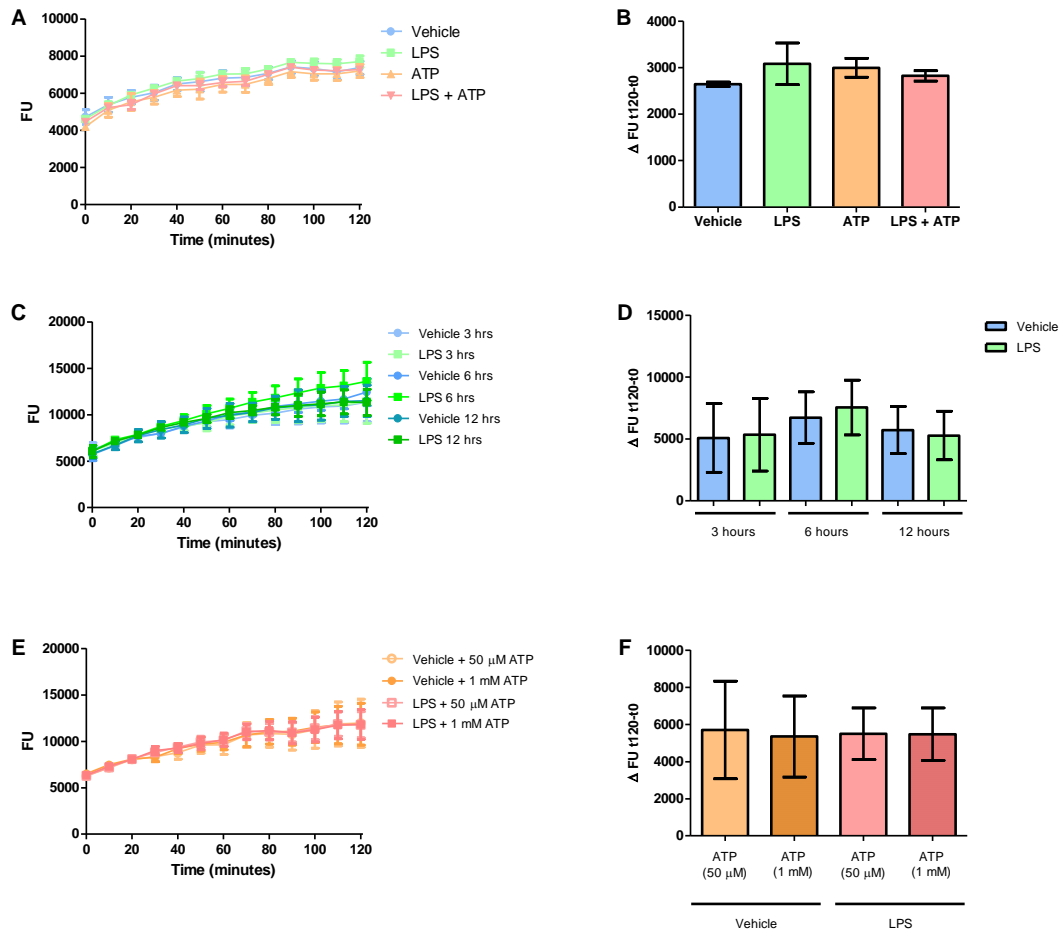


Figure 2.9: LPS and ATP do not induce release of Cathepsin S from HaCaTs

A, B. Time course and quantification of fluorescence changes of supernatant following incubation of HaCaTs in LPS (1 μg/ml) for 3 hours and stimulation in ATP (1 mM) for 20 minutes. n = 4; 6 replicates per sample, data are mean ± SEM. No significance, Two-way ANOVA followed by Bonferroni post hoc test (A) and One-way ANOVA followed by Dunnett's multiple comparison test vs HEPES (B).

C, D. Time course and quantification of fluorescence changes of supernatant following incubation of HaCaTs in LPS (1 μg/ml) for up to 12 hours. n = 3, 4; 4 replicates per sample, data are mean ± SEM. No significance, Two-way ANOVA followed by Bonferroni post hoc test (C) and Two-way ANOVA followed by Bonferroni's multiple comparison tests (D).

E, F. Time course and quantification of fluorescence changes of supernatant following incubation of HaCaTs in LPS (1 μg/ml) for 6 hours and stimulation in ATP (50 μM or 1 mM) for 20 minutes. n = 3, 4; 4 replicates per sample, data are mean ± SEM. No significance, Two-way ANOVA followed by Bonferroni post hoc test (E) and Two-way ANOVA followed by Bonferroni's multiple comparison tests (F).

responsible for the lack of CatS activity observed, HaCaTs were also incubated in LPS for up to 12 hours (Figure 2.9 C and D), and underwent stimulation with ATP (50 μ M or 1 mM) for 20 minutes following 6 hours incubation in LPS (Figure 2.9 E and F), although in all conditions no significant differences in fluorescence, and hence activity of extracellular CatS, were observed, suggesting that LPS and ATP do not play a role in the release of CatS from HaCaTs.

Because IL-4 and IL-13 have been proposed to be involved in the pathogenesis of atopic dermatitis, and because CatS is reported to be upregulated in the skin in atopic dermatitis conditions (Danso et al., 2014; Kamsteeg et al., 2011; Kim et al., 2012; Smits et al., 2017; Werfel, 2009), we hypothesised that these cytokines might regulate CatS expression in keratinocytes. Indeed, as 48 hours incubation with IL-4 and IL-13 resulted in an increase in CatS mRNA in our HaCaTs (Figure 2.6 A), we investigated whether this resulted in an increase in CatS protein as well, which would subsequently be released from the cells. A preliminary study was performed in which HaCaTs were incubated with IL-4 and IL-13 for 48 hours and release of CatS was measured. However, no changes in fluorescence, and hence CatS activity were observed (Figure 2.10 A and B), suggesting that IL-4 and IL-13 on their own are not involved in the release of CatS from HaCaTs. To exclude the possibility that IL-4 and IL-13 increased intracellular CatS without affecting release of CatS from the cells, CatS activity was also measured in the cell lysates. However, no significant changes were found in CatS activity of HaCaT cell lysates following stimulation with IL-4 and IL-13, (Figure 2.10 C and D) suggesting these cytokines do not cause an increase in intracellular CatS activity.

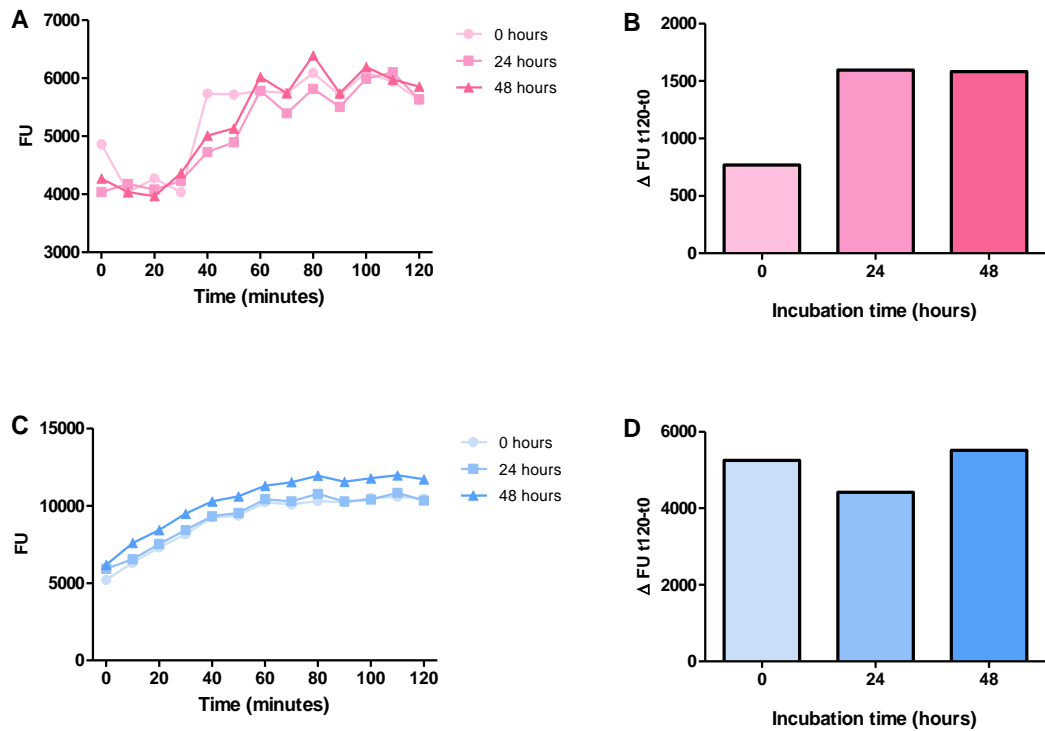


Figure 2.10: IL-4 and IL-13 did not induce release of Cathepsin S from HaCaTs

Preliminary data of time course of fluorescence changes in extracellular (A) and intracellular (C) solution of HaCaTs following incubation in IL-4 and IL-13 (50 ng/ml) for up to 48 hours. Quantification of changes in fluorescence from extracellular (B) and intracellular (D) samples. $n = 2$; 2 replicates per sample, data are mean. No statistics performed.

Since preliminary data suggested that IL-4 and IL-13 are not capable of causing release of CatS from these cells on their own, we tested the possibility that incubation with IL-4 and IL-13 along with LPS and ATP could cause release of CatS from these cells. HaCaTs were incubated with IL-4 and IL-13 for 48 hours, followed by incubation with LPS for 6 hours and ATP for 20 minutes. However, no significant differences in fluorescence from the extracellular buffer or cell lysates were observed (Figure 2.11).

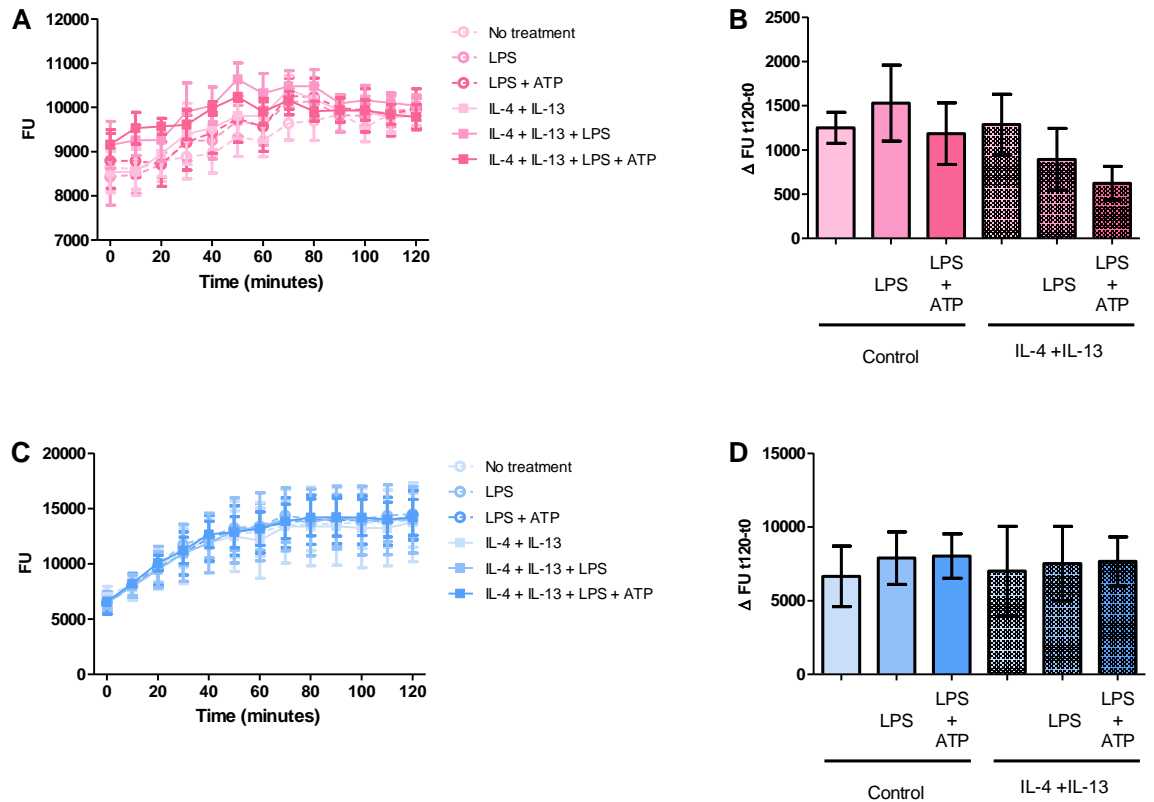


Figure 2.11: Combined IL-4 and IL-13 treatment with LPS and ATP does not induce release of Cathepsin S from HaCaTs

Time course of fluorescence changes in extracellular (A) and intracellular (C) solution of HaCaTs following incubation in IL-4 and IL-13 (50 ng/ml) for 48 hours, LPS (1 μ g/ml) for 3 hours, and stimulation in ATP (1 mM) for 20 minutes. $n = 4$; 2 replicates per sample, data are mean \pm SEM. No significance. Two-way ANOVA followed by Bonferroni post hoc test. Quantification of changes in fluorescence from extracellular (B) and intracellular (D) samples. $n = 4$; 2 replicates per sample, data are mean \pm SEM. No significance, One-way ANOVA followed by Dunnett's multiple comparison test vs HEPES.

Activation of TRPV4 on keratinocytes has been reported to cause itch sensations (Chen et al., 2016). We first confirmed expression of TRPV4 in our HaCaT cells using qPCR (Figure 2.4). Running the qPCR products on a gel gave a band of about 100 base pairs, while the predicted band size for this product was 76 base pairs based on the primers that were used. HaCaTs were incubated in the TRPV4 agonist GSK101 at 10 nM and 100 nM concentrations for 20 minutes and CatS activity was measured in supernatant and cell lysates. 100 nM GSK101 caused an increase in fluorescence, and hence CatS activity (Figure 2.12 A and B). No significant changes in intracellular CatS activity were observed following stimulation with GSK101 (Figure 2.12 C and D). To investigate if IL-4 and IL-13 could enhance TRPV4-mediated release of CatS, HaCaT were stimulated with GSK101 (10 nM and 100 nM) for 20 minutes following pre-incubation in IL-4 and IL-13 for 48 hours. Although a significant increase in fluorescence was observed following stimulation with 100 nM GSK101 compared with stimulation of 10 nM GSK101 or DMSO (Figure 2.12 E and F), it was not significantly enhanced compared with the activity observed following stimulation with 100 nM GSK101 in the absence of pre-incubation with IL-4 and IL-13. Furthermore, no significant increase in CatS activity was observed following stimulation of HaCaTs with 10 nM GSK101 in the presence of IL-4 and IL-13, suggesting no sensitisation of these cells to release CatS in response to these cytokines. No significant changes in intracellular CatS activity were observed following stimulation with GSK101 with pre-incubation in IL-4 and IL-13 (Figure 2.12 G and H).

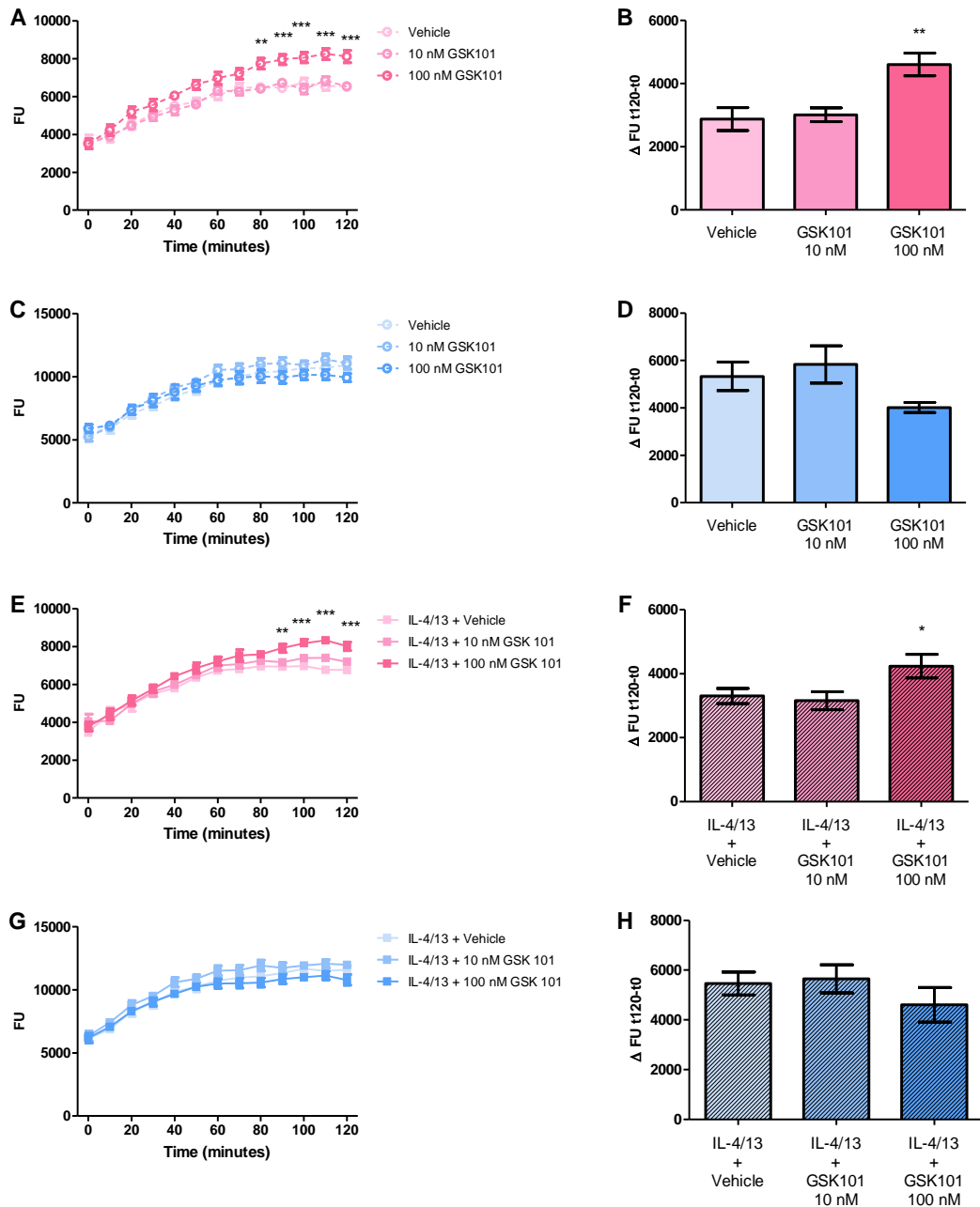


Figure 2.12: TRPV4 activation induces the release of Cathepsin S from HaCaTs

Time course of fluorescence changes in extracellular (A) or intracellular (C) solution of HaCaTs following 20 minute incubation in 0.001% DMSO (vehicle) or GSK101 (10 nM or 100 nM). Time course of fluorescence changes in extracellular (E) or intracellular (G) solution of HaCaTs following 48 hour incubation in IL-4 and IL-13 (50 ng/ml) and 20 minute incubation in DMSO or GSK101. $n = 6, 7$; 2 replicates per sample, data are mean \pm SEM. $**p \leq 0.01$; $***p \leq 0.001$, Two-way ANOVA followed by Bonferroni post hoc test. Quantification of changes in fluorescence from extracellular (B, F) and intracellular (D, H) samples. $n = 6, 7$; 2 replicates per sample, data are mean \pm SEM. $*p \leq 0.05$; $**p \leq 0.01$, One-way ANOVA followed by Dunnett's multiple comparison test vs DMSO.

Entry of calcium into keratinocytes, fibroblasts and epithelial cells induces exocytosis of lysosomes (Jans et al., 2004; Rodriguez et al., 1997). Since CatS is a lysosomal protease, we hypothesised that entry of calcium into HaCaTs might be responsible for the release of CatS. Furthermore, because TRPV4 channels allow for the entry of cations such as calcium ions into the cell (Nilius et al., 2003; Voets et al., 2002), we further hypothesised that the entry of extracellular calcium through these channels might be the mechanism by which CatS is released. We therefore incubated HaCaTs in GSK101 (100 nM) or DMSO in the presence of a buffer with 1 mM calcium and a buffer without calcium ions added to it. When it came to performing the activity assay, the supernatant from cells incubated in GSK101 or DMSO in buffer without calcium added to it had assay buffer containing 2 mM calcium, such that the final concentration of calcium was 1 mM, the same for all experiments, as initial experiments suggested that CatS activity may be affected by the concentration of calcium ions in the assay buffer. We observed that incubation of cells in GSK101 in the buffer containing 1 mM calcium resulted in significant CatS activity, while the activity from cells incubated in DMSO or GSK101 in the buffer without calcium ions added to it did not show any significant CatS activity (Figure 2.13 A and B), suggesting extracellular calcium ions are required for TRPV4-mediated release of CatS from these cells.

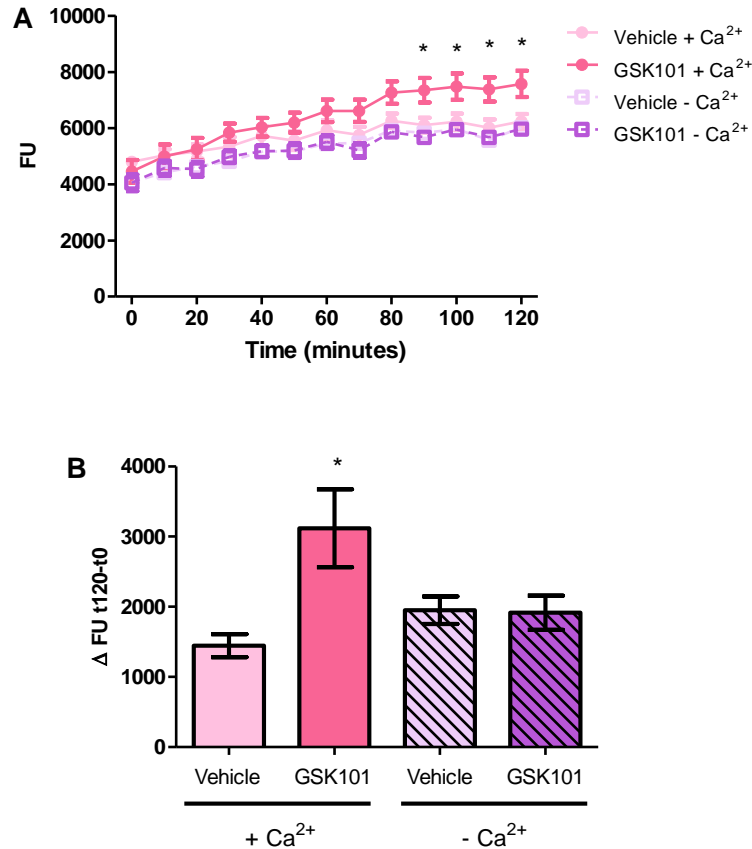


Figure 2.13: Extracellular calcium is required for TRPV4-mediated release of Cathepsin S from HaCaTs

A. Time course of fluorescence changes from the supernatant of HaCaT cells incubated with the Z-Val-Val-Arg-MCA substrate following stimulation with 100 nM GSK101 for 20 minutes prior to the assay being performed. $n = 5, 6$; 2 replicates per sample, data are mean \pm SEM.

* $p \leq 0.05$, Two-way ANOVA followed by Bonferroni post hoc test.

B. Quantification of changes in fluorescence. $n = 5, 6$; 2 replicates per sample, data are mean \pm SEM. * $p \leq 0.05$, One-way ANOVA followed by Bonferroni's multiple comparison test.

2.4 Discussion

Several findings relating to expression and release of CatS from skin keratinocytes were made in this chapter. We confirmed expression of CatS mRNA in the HaCaT cell line, and that incubation of these cells in LPS or IL-4 and IL-13 cytokines results in an increase in CatS mRNA. Furthermore, we demonstrated that HaCaTs contain intracellular active CatS protease that can cleave a substrate, emitting a fluorescent signal that can be measured as a proxy for CatS activity, and that stimulation of HaCaTs with the TRPV4 agonist GSK101 results in the release of CatS from these cells. This TRPV4-mediated release of CatS is dependent on the presence of extracellular calcium ions.

Although we could confirm expression of CatS mRNA in HaCaT cells using qPCR, we were unable to detect expression of CatS protein in our cells using either antibody staining of fixed cells or Western blotting. Staining of HaCaTs using the lysosomal marker LAMP-1 revealed punctate staining around the nucleus of the cell, similar to previous reports by other groups using primary human keratinocyte cell cultures (Jans et al., 2004; Sarafian et al., 2006). In primary microglia cultures, CatS protein is co-localised with LAMP-1 and can be visualised in cells stained with antibodies (Clark et al., 2010). However, we were unable to detect expression of CatS protein in our cells, despite using two different antibodies for CatS. Nevertheless, one of the antibodies used detected expression of CatS in mouse spinal cord tissue, which co-localised with Iba1, suggesting the antibody is able to detect CatS expressed in murine spinal cord microglia, but not in human keratinocytes. Although the antibody claims to be able to detect human CatS in addition to murine CatS, we were unable to detect staining for CatS in our human cell line. However, the same antibody for Western blotting detected bands for purified human recombinant CatS. The band sizes were at about 25 kDa, while mature CatS is predicted to be 24 kDa in size (Wiederanders et al., 1992). At least two faint bands of smaller sizes were detected in the purified CatS sample, although it is not known whether these are fragments of CatS protein in the sample or whether some non-specific staining has occurred. No bands of larger sizes were detected, suggesting the antibody does not detect unprocessed CatS or that insufficient quantities of unprocessed CatS were in our samples to be detected using this method. The same antibody for CatS used in other experiments was able to detect the presence of both pre-pro and pro-forms of CatS, as well as the mature form (Clark et al., 2010). This suggests the pre-pro and pro forms of CatS are also undetected in our samples. Despite the ability of the antibody to detect purified CatS, no bands were observed in either HaCaT or THP-1 positive control. It cannot be ruled out that HaCaTs do not normally express much CatS protein, as THP-1 cells, which are reported to express CatS (Pawar et al., 2016), also failed to show bands for CatS. Furthermore, bands for actin could be detected in our HaCaT samples, suggesting the presence of adequate concentrations of protein for Western blotting. Thus, it is likely that insufficient quantity of CatS protein is expressed in these cells to be detected using antibody staining and Western blotting techniques, while the activity assay may be sensitive enough for the low levels of CatS in our cells. Indeed, this is in agreement with other studies in which CatS protein was undetectable in healthy skin keratinocytes (Schonefuss et al., 2010). However, under certain conditions, such as those found in atopic dermatitis, keratinocytes may increase expression of CatS. Thus, to establish whether upregulation of CatS is required for its detection using antibody staining and Western blotting, future experiments should be

performed in which HaCaTs are incubated with LPS or IL-4 and IL-13 to determine if increased CatS mRNA corresponds with detection of CatS protein using these methods.

Despite being unable to detect expression of CatS protein in HaCaTs, HaCaT cell lysates demonstrated protease activity with the ability to cleave the Z-Val-Val-Arg-MCA substrate. This substrate can be cleaved by Cathepsins B and L as well as CatS, however most activity is reported with CatS compared with other cathepsins, and the activity of other cathepsins on this substrate is abolished at pH7 while CatS maintains 60-70% of its activity at this pH (Kirschke and Wiederanders, 1994). Thus, at pH7, this substrate is most specific for CatS. We observed that HaCaT cell lysates could cleave the Z-Val-Val-Arg-MCA substrate, resulting in a fluorescent signal that is taken as a readout of protease activity. Activity was observed at pH5 and pH7, although fluorescence at pH7 was about half that observed at pH5, which is less than what has previously been reported. Nevertheless, substantial fluorescence readouts were obtained at pH7 compared with buffer, suggesting the presence of active CatS in the HaCaT cell lysate. When the cells were lysed using a lysis buffer containing protease inhibitors, fluorescent readout was low, likely due to prevention of cleavage of the substrate by CatS. To further confirm that the fluorescence changes observed were due to the activity of CatS on the Z-Val-Val-Arg-MCA substrate, the assay was repeated in the presence of the CatS inhibitor MDV-590, resulting in a modest reduction in fluorescence readout. Cell lysates were incubated in MDV-590 for 10 minutes prior to the assay being performed, which may not have allowed sufficient time for maximal inhibition of CatS activity in the samples. Furthermore, the concentration of MDV-590 used may not have been enough to allow for complete inhibition of CatS activity. The concentration of MDV-590 used was based on the upper ranges of the preferable concentration for inhibition of physiological proteases (Medivir UK Ltd (2011), New Cathepsin S protease inhibitors, useful in the treatment of e.g. autoimmune disorders, allergy and chronic pain conditions. International Patent Application WO2011/158197). Furthermore, because MDV-590 is dissolved in DMSO, increasing the concentration of MDV-590 would have also increased the concentration of DMSO used in the assay, which could have resulted in unwanted effects. Addition of MDV-590 to the samples at earlier time points could also have been performed, but would have resulted in the samples being left on ice for long periods of time, potentially resulting in premature CatS activity, which could have affected overall CatS activity and prevented comparison of these results with other activity assays using cell lysate samples. Thus, further optimisation of the assay is still required to completely block the effects of CatS activity using MDV-590.

Incubating HaCaTs in LPS for 6 hours resulted in a 50-fold increase in the expression of TLR4, the receptor for LPS. Expression of TLR4 in HaCaTs and primary keratinocytes has previously been confirmed, with increasing expression as cells undergo differentiation and following incubation with LPS or LPS and IFN γ (Iotzova-Weiss et al., 2017; Kollisch et al., 2005; Pivarcsi et al., 2003; Pivarcsi et al., 2004; Song et al., 2002). Using 100 ng/ml LPS, Kollisch et al. (2005) found that TLR4 mRNA was maximal after 8 hours incubation in LPS and began to decline at 24 hours incubation in LPS, although TLR4 mRNA was still much greater than that from untreated cells. They also found that 2 hours incubation in LPS did not have any significant effects on TLR4 mRNA levels, which is similar to the lack of effect of 3 hours LPS incubation that we observed. Increased expression of TLR4 following incubation of cells in LPS would potentially result in a positive feedback loop, whereby cells become more responsive to LPS and further increase expression of TLR4. However, as expression of TLR4 mRNA was shown to decrease by 24 hours incubation in LPS, this likely acts as a mechanism to prevent excessive expression of TLR4 on keratinocytes and potential damage to cells in response to long-term exposure to LPS. TLR4 also suppresses proliferation of keratinocytes, with increased proliferation observed in HaCaTs in which TLR4 expression is knocked down, and decreased proliferation in a squamous cell carcinoma line over-expressing TLR4 (Iotzova-Weiss et al., 2017). In healthy skin, this could serve to prevent proliferation of differentiating cells that leave the basal layer, as expression of TLR4 increases.

Expression of CatS mRNA in HaCaTs was increased 40-fold following 6 hours incubation in LPS, compared with incubation in buffer. No increase in CatS mRNA was observed after 3 hours incubation in LPS. Incubation of human cervical smooth muscle cells in LPS for 12 hours has previously been shown to increase expression of CatS mRNA by 12.5-fold (Watari et al., 2000). Although we obtained a greater increase in CatS mRNA than Watari et al., despite the shorter incubation time in LPS, we also used a greater concentration of LPS (1 μ g/ml) than that used by Watari et al. (100 ng/ml). The LPS serotype that was used also differed, as we used serotype O11:B4 LPS, while serotype O55:B5 LPS was used by Watari et al. Furthermore, we detected changes in mRNA expression using qPCR, while Watari et al. detected mRNA changes using Northern blotting, which is less sensitive than qPCR. Finally, the difference in cell type (HaCaT versus cervical smooth muscle cell) could explain the observed differences in CatS mRNA changes in response to LPS. LPS has also been reported to result in upregulation of CatS mRNA in bipolar/rodshaped microglia that have been transformed into amoeboid microglia, as detected using qPCR (Tam et al., 2016). Upregulation of CatS in these experiments was much lower, at about 1.3-fold. However, as

with Watari et al., a different concentration (10 µg/ml) and serotype (O127:B8) of LPS was used by Tam et al. It is interesting to note that, despite using a greater concentration of LPS than in our experiments and incubating cells for the same length of time in LPS, Tam et al. reported a lower increase in CatS mRNA in their microglia than we did in HaCaTs. One possibility is that excessive LPS is suboptimal and impairs the upregulation of CatS mRNA following incubation in LPS. In support of this, Watari et al. found that incubating cervical smooth muscle cells in LPS for 48 hours resulted in a reduced upregulation of CatS mRNA, compared with incubation in LPS for 12 or 24 hours. Similarly, a reduction in the upregulation of CatS mRNA was observed when cervical smooth muscle were incubated in 1 µg/ml LPS compared with incubation in 100 ng/ml LPS.

LPS has previously been demonstrated to prime microglia to release CatS, causing slight increases in the expression of pre and mature forms of CatS protein (Clark et al., 2010). However, we did not observe an increase in CatS activity from HaCaT cell supernatant following incubation with LPS for up to 12 hours, suggesting LPS only upregulates the expression of CatS mRNA, and may or may not affect translation of CatS mRNA or processing of CatS into its mature form in our cell line. Although LPS was required for priming microglia to release CatS, release of CatS from these cells was observed only when followed by stimulation with high concentration ATP (Clark et al., 2010). Furthermore, significant increases in the expression of the pre- and mature forms of CatS protein were reported following treatment of microglia with both LPS and ATP (Clark et al., 2010). Thus, while LPS might increase the expression of LPS mRNA, ATP might be required for this to result in an increase in the release of active CatS from cells. However, in contrast to Clark et al., (2010), we were unable to observe any changes in CatS activity following stimulation of HaCaTs with high concentration ATP. To exclude the possibility that ATP activity might be modulated by P2X₄ activity on keratinocytes rather than P2X₇, HaCaTs were also stimulated with a lower concentration of ATP (50 µM). However, this also did not affect the release of CatS from these cells, even when primed with LPS prior to stimulation. This suggests that, in contrast to microglia, keratinocytes do not release CatS in response to LPS and ATP.

If LPS and ATP do not cause the release of CatS from HaCaTs, then what are the mediators that might enable the release of CatS from these cells? Following incubation of HaCaTs in the Th1 cytokines IFN γ and TNF α , the release of CatS has been reported (Schonefuss et al., 2010). In these experiments, CatS was detected in the supernatant of the cells following cytokine treatment. This suggests the release of CatS from keratinocytes in psoriasis and

other skin diseases characterised by Th1 cytokines. However, whether CatS is released from keratinocytes in other skin diseases, such as those mediated by Th2 cytokines, was one of the questions we aimed to address in this chapter. Expression of the Th2 cytokines IL-4 and IL-13 is reported to be increased in the skin of patients with atopic dermatitis, supporting a role for these cytokines in itch (Werfel, 2009). We hypothesised that release of these cytokines from T cells could result in increased expression and release of CatS from keratinocytes, which would be responsible for activating sensory neurons and transmission of itch signals in atopic dermatitis. To address this question, we first determined whether expression of CatS would be increased following incubation in the Th2 cytokines IL-4 and IL-13. Incubation of HaCaTs in these cytokines for 48 hours resulted in a 2.5-fold increase in CatS mRNA compared with untreated cells. However, expression of CA2, CCL26, and NELL2 was not significantly altered following incubation of cells in IL-4 and IL-13. CA2, CCL26, and NELL2 have all previously been used as *in vitro* markers for atopic dermatitis and have been reported to be increased in the skin of patients with this condition. Stimulation of primary keratinocytes, N/TERT keratinocytes, and HaCaTs with these cytokines has previously been shown to result in increased expression of CA2 and CCL26 (Bao et al. 2012, Bao et al., 2013, Kagami et al., 2005; Smits et al. 2017). This suggests we were unable to fully mimic atopic dermatitis conditions *in vitro*, although we were still able to observe upregulation of CatS. Compared with incubation in LPS, the increased expression of CatS mRNA following incubation in IL-4 and IL-13 is much lower, suggesting a much smaller effect with these cytokines. Thus, one possibility is that the cells have not been optimally treated to release CatS and express markers of atopic dermatitis in Th2 conditions. For example, Kagami et al. (2005) reported that incubation of HaCaTs with IL-4 and TNF α resulted in an increase in CCL26 that was larger than when either cytokines were used alone, suggesting they can act synergistically. This should not be so surprising, given that chronic atopic dermatitis lesions are associated with an increase in Th1 cytokines in addition to Th2 cytokines. Thus, a more accurate atopic dermatitis model *in vitro* might involve the presence of Th1 cytokines in addition to Th2 cytokines, and might be required for both upregulation and release of CatS and potentially other pruritogens from keratinocytes.

Since incubation of HaCaTs in IL-4 and IL-13 for 48 hours increased expression of CatS mRNA in HaCaTs, we investigated whether these cytokines would also affect the release of CatS. However, because incubation for 48 hours was required, the cells needed to be maintained in their culture medium to prevent cell death and other changes due to being outside of their normal growth conditions for long periods of time. This resulted in the protocol being

unsuitable for the assay for measuring CatS activity, as the HaCaT culture media contains phenol red, with no suitable phenol red-free alternative existing, and the activity assay measures changes in fluorescence that could be interfered with by the phenol red in the culture media. A preliminary trial measuring CatS activity in the supernatant of HaCaTs stimulated with IL-4 and IL-13 in their culture media yielded negative results, suggesting IL-4 and IL-13 do not cause the release of CatS from these cells, but it cannot be excluded that the presence of phenol red in the samples interfered with the fluorescence readings. As an alternative, we investigated whether incubation of HaCaTs with IL-4 and IL-13 would result in LPS and ATP-mediated release of CatS from these cells. However, IL-4 and IL-13 did not affect the release of CatS, with or without the addition of LPS and ATP. Furthermore, no differences in intracellular CatS were observed. We thus conclude that IL-4 and IL-13, on their own or in combination with LPS and ATP, do not affect the intracellular activity of CatS or the release of CatS from HaCaTs, despite increasing the expression of CatS mRNA. Nevertheless, it cannot be excluded that IL-4 and IL-13 are not involved in the release of CatS from keratinocytes in atopic dermatitis and other skin conditions. Since others have reported increased expression of markers of atopic dermatitis following incubation of cells with IL-4 and IL-13, and since we did not observe an increase in these markers in our experiments, it is possible that optimal conditions would allow for increased expression of these markers and even greater increase in the expression of CatS mRNA, as well as the release of CatS from cells and/or increased intracellular activity of CatS.

Treatment of HaCaTs with the TRPV4 agonist GSK101, on the other hand, resulted in a significant increase in extracellular CatS activity, indicative of an increase in the release of CatS following activation of TRPV4 on these cells. Incubation of keratinocytes with GSK101 has previously been shown to result in calcium transients (Moore et al., 2013). In keratinocytes, entry of calcium induces exocytosis of lysosomes. Jans et al., (2004) found that treating keratinocytes with ionomycin to raise intracellular calcium levels increased the appearance of LAMP-1 and LAMP-2 lysosomal markers at the surface of the cell. Thus, entry of calcium into the cell following activation of TRPV4 could also mediate exocytosis of lysosomes from the cell, resulting in the release of CatS. In support of this, we demonstrated that extracellular calcium was required for TRPV4-mediated release of CatS. This is also in agreement with the observations of Moore et al. (2013), who found that extracellular calcium was required for GSK101-mediated calcium transients in cultured keratinocytes. Similarly, extracellular calcium has been shown to be required for LPS and ATP-mediated release of CatS from microglia (Clark et al., 2010). However, the downstream mechanisms of

TRPV4-mediated release of CatS have yet to be explored. Release of calcium from intracellular stores may also be involved, as was reported for microglia by Clark et al. (2010), and should be addressed in future experiments to determine if release of calcium from intracellular stores can further enhance TRPV4-mediated release of CatS from keratinocytes.

Specificity of the action of GSK101 on the TRPV4 receptor should also be addressed in future experiments, for example, by stimulating release of CatS from cells in the presence of a TRPV4 antagonist such as HC067047. The specificity of molecules commonly used as TRPV4 agonists, such as 4 α PDD, has been questioned and it is reported to have off-target effects (Alexander et al., 2013). Likewise, GSK101 may have offtarget effects that should be addressed. Stimulation of TRPV4-mediated CatS release from keratinocytes could additionally be performed using other TRPV4 agonists, such as bisandrographolide A, a plant-based molecule reported to exclusively target TRPV4 (White et al., 2016).

It has recently been reported that GSK101 results in morphological changes and subsequent cell death of several different cell types, including HaCaT cells (Olivan-Viguera et al., 2018). This raises the possibility that the death of cells following treatment with GSK101 causes them to release their contents, and this could result in the increased CatS activity observed in our assay. However, no significant changes in intracellular CatS activity were observed following incubation with GSK101, suggesting the cells had not undergone apoptosis and had retained most of their intracellular contents during treatment. This is similar to other reports that incubation of HaCaTs and other cell lines in GSK101 for several hours does not affect cell viability (Fang et al., 2018; Fusi et al., 2014; Thoppil et al., 2015). Moreover, incubation of hepatic stellate cells with TRPV4 agonists results in a decrease in apoptosis in these cells, suggesting activation of TRPV4 prevents against apoptosis (Zhan et al., 2015).

To conclude, we have demonstrated that the HaCaT keratinocyte cell line express CatS mRNA, and although we were unable to detect CatS protein in our cells, it is likely that healthy keratinocytes do not normally express large quantities of CatS in any event. Furthermore, lysed HaCaT samples demonstrated protease activity at pH7, at which the activity of all other cathepsins is diminished, and could be reduced in the presence of a CatS inhibitor, suggesting these cells do contain active CatS, although at levels that cannot be detected using antibody staining of fixed cells or Western blotting techniques. Incubation of HaCaTs with Th2 cytokines did increase the expression of CatS mRNA, but did not result in the release of CatS from these cells, although additional cytokines may be required for

release, reflecting the complex nature of cytokine signalling during skin diseases such as atopic dermatitis. Further experiments should be performed to determine whether conditions which result in increased CatS mRNA in HaCaTs also results in increased expression of the protease that can be detected using antibody and Western blotting methods. Finally, activation of TRPV4 channels results in the release of CatS from HaCaTs, although whether this mechanism of CatS release from skin keratinocytes plays a role in chronic itch conditions remains to be addressed.

Chapter 3

Activation of cultured sensory neurons by Cathepsin S

3.1 Introduction

CatS is a pruritogen that causes itching sensations in healthy human subjects and scratching behaviour when injected into mice (Reddy et al., 2010). There are two main mechanisms by which CatS-mediated pruritus may be achieved. The first is direct activation of sensory neurons following cleavage of receptors such as PAR2. Alternatively, CatS may result in pruritus by activating receptors on non-neuronal cells, causing them to release pruritogens such as histamine that then activates sensory neurons or mediators that sensitise neurons and make them more likely to respond to pruritogens.

The similarity of the peptide sequences between human and mouse CatS and PAR2 underlies their importance throughout evolution and suggests the human analogue of the protease may be able to interact with receptors from the mouse and vice versa. Indeed, using NCBI Protein BLAST (National Center for Biotechnology Information, Bethesda, MD, USA) to compare human and mouse CatS protein sequences (GenBank accession numbers AAC37592.1 and BAE29827.1 respectively) and PAR2 sequences (GenBank accession numbers AAP97012.1 and NP_032000.3 respectively) revealed more than 70% similarity between proteins from the two species (Figure 3.1). It has also been previously published that the protein sequence of the PAR2 receptor for CatS is more than 80% similar between human and mouse (Böhm et al., 1996b). Furthermore, the use of human CatS on cells derived from mice has already been previously observed (Zhao et al., 2014a). Since human recombinant CatS was provided from Medivir as a purified and activated enzyme, unlike commercially supplied CatS which must first be activated and so contains DTT and EDTA, we therefore decided to investigate the effects of this human CatS on cells cultured from mouse DRGs which are more easily available than human-derived neuronal cells.

A		Score	Expect	Method	Identities	Positives	Gaps
		526 bits(1355)	0.0	Compositional matrix adjust.	244/324(75%)	282/324(87%)	1/324(0%)
Human	9	LVCSSAVAQLHKDPTLDHHHLWKKTYGKQYKEKNEEAVRRLIWEKNLKFVMLHNLEHSM					68
Mouse	3	LVCSSAAMEQLQRDPTLDYHWDLWKKTHEKEYKDKNEEVRRLIWEKNLKFIMIHNLLEYSM					62
Human	69	GMHSYDLGMNHLGDMTSEEVMSLMSLLRVPSQWQRNITYKSNPNRILPDSVDWREKGCVT					128
Mouse	63	GMHTYQVGMNDMGDMTNEEILCRMGALRIPRQSPKTVTFRSYSNRTPDVTVDWREKGCVT					122
Human	129	EVKYQSGCGACWAFSAVGALEAQLKLTGKLVLSAQNLDVDCST-EKYGNKGCNGGFMFT					187
Mouse	123	EVKYQSGCGACWAFSAVGALEQLKLTGKLVLSAQNLDVDCSNEEKYGNKGCNGGGMTE					182
Human	188	AFQYIIDNKGIDSDASYPYKAMDLCQYDSKYRAATCSKYTELPGREDVLKEAVANKGP					247
Mouse	183	AFQYIIDNNGGIEADASYPYKATDEKCHYNSKNRAATCSRYIQLPFGDEDALKEAVATKGP					242
Human	248	VSVGVDARHPSFFLYRSGVYEPSCQNVNHGVLVVGYGDLNGKEYWLKNSWGHNFGE					307
Mouse	243	VSVGIDASHSSFFFYKSGVYDDPSCQGNVNHGVLVVGYGDLGKDYWLKNSWGLNFGDQ					302
Human	308	GYIRMARNKGNHCGIASFPSYPEI					331
Mouse	303	GYIRMARN NHCGIAS+ SYPEI					326

B		Score	Expect	Method	Identities	Positives	Gaps
		660 bits(1703)	0.0	Compositional matrix adjust.	316/380(83%)	348/380(91%)	2/380(0%)
Human	1	MRSPSAAWLLGAAILLAASLSCSGT--IQGTNRSSKGRSLIGKVDGTSHTVTKGKVTETV					58
Mouse	1	MRSLSLAWLLGGITLLAASVSCSRTEENLAPGRNNSKGRSLIGRLETQPPITGKGVPEPG					60
Human	59	FSDVEFSASVLTGKLTTFVFLPIVYIVFVVLGSLPSNGMALWVFLFRTRKKKHPAVIYMANLA					118
Mouse	61	FS+DEFSAS+LTGKLTTFVFLP+VY IVFV+GLPSNGMALW+FLFRTRKKKHPAVIYMANLA					120
Human	119	LADLLSVIWFPLKIAYHIHGNNWYGEALCNVLIGFFYGNMYCSILFMTCLSVQRYWVIV					178
Mouse	121	LADLLSVIWFPLKISYHLHGNNWYGEALCKVLIGFFYGNMYCSILFMTCLSVQRYWVIV					180
Human	179	NPMGHSRKKANIAIGISLAIWLLILLVTIPLYVVKQTIIFIPALNITTCRHDVLPQELLVGD					238
Mouse	181	NPMGHPRKKANIAVGVSLAIWLLIFLVTIPLYVMKQTIYIPALNITTCRHDVLPQELLVGD					240
Human	239	MFNYFLSLAIGVFLFPAFLTASAYVLMIRLSSAMDESEKRRKRAIKLIVTVLAMYLI					298
Mouse	241	MFNYFLSLAIGVFLFPA LTASAYVLM+ LRSSAMDE+SEKRR+RAI+LI+TVLAMY I					300
Human	299	CFTPSNLLLHVHYFLIKSQGSHVYALYIVALCLSTLNSCIDPFVYVYFVSHDFRDHAKNA					358
Mouse	301	CF PSNLLLHVHYFLIK+Q QSHVYALY+VALCLSTLNSCIDPFVYVYFVSKDFRDHARNA					360
Human	359	LLCRSVRTVKQMVSLSK					378
Mouse	361	LLCRSVRTV +MQ+SL+S K					380

Figure 3.1: Comparison of human and mouse CatS (A) and PAR2 (B) peptide sequences
Human and mouse CatS protein sequences were determined from GenBank accession numbers AAC37592.1 and BAE29827.1, respectively, and PAR2 sequences from GenBank accession numbers AAP97012.1 and NP_032000.3, respectively.

Chapter objectives

Pruriceptors can be regarded as a subset of nociceptors, as determined by their response to the TRPV1 agonist capsaicin and other algogens, and are considered as being pruriceptors if they also respond to application of a pruritogen. In this regard, we assume for the purposes of this chapter that pruriceptors are polymodal, capable of responding to both algogens and pruritogens, but as to whether the sensation that would be experienced would be itch or

pain following activation of these neurons is beyond the scope of this chapter. Instead, we aimed to characterise the neurons that would respond to pruritogen CatS that likely underlie the itching and scratching behaviour observed *in vivo*.

The primary aim of this chapter therefore was to determine if sensory neurons could respond to direct application of CatS, and hence whether CatS itself can directly act as a pruritogen, rather than acting via an indirect mechanism. To investigate whether sensory neurons could respond directly to application of CatS and characterise these neurons, isolated mouse DRGs were exposed to human CatS and various other compounds in both patch clamping and calcium imaging experiments.

3.2 Methods

3.2.1 Production of human recombinant Cathepsin S in baculovirus

Human recombinant CatS was provided by our industrial collaborators at Medivir, produced using the methods detailed below, and was used in all subsequent experiments in this chapter and in chapter 4.

Human pro-CatS, with a hexa-histidine tag, was expressed in the Sf9 insect cell line using a FlashBAC One recombinant baculovirus (Oxford Expression Technologies, UK). Sf9 cells were grown in Insect-Xpres protein-free culture medium (Lonza, Switzerland) without antibiotics, incubated at 28°C and agitated at 100 rotations per minute. Cells were seeded at a density of 0.5×10^6 cell/ml and split every 3-4 days to maintain optimal growth conditions. Virus stock was maintained by infecting a culture of Sf9 cells at a density of 1×10^6 cells/ml, and was harvested after a few days in culture. An expression culture was established in a culture of Sf9 cells seeded at a density of 1×10^6 cells/ml and allowed to grow for 24 hours before addition of virus stock at a ratio of 1 part virus to 5 parts cell culture. Cells were counted and visually inspected every 24 hours to confirm infection of the cells by the virus, as indicated by a decrease in the rate of cell growth and the appearance of swollen and dead cells. Supernatant was collected 72 hours after infection and protein was harvested by centrifugation at 3,000 g for 10 minutes.

Harvested proteins were purified using immobilised metal ion affinity chromatography (IMAC) over a Ni Sepharose 6 Fast Flow column (GE Healthcare, USA). All steps were performed at 4°C. The nickel beads were equilibrated in a wash buffer (1x PBS at pH7.4–7.5,

containing NaCl, 0.36 M; glycerol, 10%; imidazole, 50 mM; PMSF, 0.2 mM) before use. The harvested supernatant containing proteins was then added to the equilibrated nickel beads, to which NiSO₄ (1 mM) was added. The suspension was mixed for 90 minutes at 70-80 rpm to prevent the nickel beads from sinking to the bottom and allow binding of the histidine-tagged proteins to the beads. The bead suspension was poured through a No.2 Pyrex filter and the beads were recovered and packed into an Econo-pac chromatographic column (Bio-Rad, USA). The beads were washed with wash buffer to remove any proteins that bound weakly to the beads. CatS was eluted using elution buffer (1x PBS at pH7.4–7.5, containing NaCl, 0.36 M; glycerol, 10%; imidazole, 250 mM; PMSF, 0.2 mM), the higher concentration of imidazole in this buffer displacing the histidine-tagged CatS from the beads, and a minimum of 10 fractions were collected. The purity of the collected fractions was checked by running an SDS-PAGE gel. Following purification, CatS was dialysed overnight to remove imidazole and EDTA was added for sequestering ions such as calcium, magnesium, and nickel that may be added during the purification process or derive from the culture medium. The purest fractions of CatS protein were pooled together and the concentration of protein was measured using a spectrophotometer. Dialysis was performed at 4°C using dialysis tubing cellulose membrane with a 14,000 Da cut-off (Sigma, UK). The pooled fractions of CatS protein were poured into the tubing and placed overnight in a beaker containing dialysis buffer (PBS at pH7.4–7.5, containing NaCl, 0.36 M; glycerol, 10%; EDTA, 2 mM; PMSF, 0.2 mM). Protein concentration was again checked the following day using dialysis buffer as a blank. The purified CatS is required to be concentrated to about 20 mg/ml, as this is the optimum concentration for activating it. This was performed by centrifuging the protein through an Amicon Ultra-15 centrifuge filter with a cut-off of 10,000 Da (Merck Millipore, UK) at 3,300 g for 25 minutes at 4°C. The concentration and purity of the concentrated CatS was then remeasured using a spectrophotometer and by running another SDS-PAGE gel to ensure successful concentration.

Because CatS was secreted from the cells in its pro-form, it is required to be activated before it can be used in experiments. However, before it can be activated, the activation time course of the pro-CatS needs to be measured to determine the optimal incubation time for activation of CatS. This assay requires 11 μM DTT to be made up in activation buffer (Na acetate, 1.1 M; NaCl 1.1 M; EDTA, 55 mM, at pH 4.5), and 1 part of this DTT to be added to 5 parts of the purified, concentrated pro-CatS. The CatS/DTT mixture is then placed on a heatblock at 37°C. Every 5 minutes, 1 μl of this mixture is diluted 1:10 in assay buffer (ADA, 100 mM; NaCl, 100 mM; PEG4000, 0.1%, at pH 6.5), after which 1 μl is then further diluted

1:250 in substrate buffer (ADA, 100 mM; NaCl, 100 mM; PEG4000, 0.1%; DTT, 1 mM; boc-val-leu-lys-AMC, 100 μ M, Bachem, Switzerland, at pH 6.5) in a white polystyrene round-bottom 96-well plate (Corning, UK). The plate was read using a CLARIOstar Spectrophotometer (BMG Labtech, UK) at excitation wavelengths of 360 – 390 nm and emission wavelengths of 450 – 470 nm every second for 10 seconds. Readings were taken after each 5-minute incubation period until the activity started to decrease. The peak of the time course, which represents optimum CatS activity where the pro form of CatS has been cleaved but non-specific cleavage that deactivates the protease has not yet occurred, is usually reached within 20 – 90 minutes. To activate CatS, 10 μ l of activation buffer is added for every 100 μ l of purified pro-CatS there is. Upon addition of the activation buffer, the pH will be reduced, allowing partial unfolding of CatS to open up the cleavage site for activation. The CatS and activation buffer mixture is then placed on a heat block at 37°C for the length of time that was required to reach peak activity during the activation time course. After heating, the mixture is centrifuged at 14,000 rpm for 5 minutes to remove any precipitates that may form during heating, and the CatS is transferred to a new microfuge tube kept on ice.

Activated CatS was buffer exchanged into 1x PBS (pH7.4) using an Econo-Pac 10DG column (Bio-Rad, USA). The column was first equilibrated with 1x PBS and the flow-through discarded. To ensure the highest concentrations of activated CatS were collected, the protein was passed through the column followed by 1x PBS, and the drops that came out of the column were collected one at a time into a UV-transparent 96-well plate (UVStar, Greiner Bio-One, Austria). The plate was centrifuged at 500 g for 30 seconds and the absorbance was measured at 280 nm wavelength using a CLARIOstar Spectrophotometer. The protein in the wells which contained the highest absorbance values was collected and pooled into a new microfuge tube on ice.

The active site concentration of CatS was determined by titration with cysteine protease inhibitor E-64. E-64 was diluted in DMSO to give 100 μ M stocks. The activated and desalted CatS was diluted 1:400 in assay buffer, to which DTT (1 mM) was added. 200 μ l of this CatS mixture was added to the first well in one row of a polystyrene 96-well plate, while 100 μ l was added to the remaining wells in that row. 2 μ l of the diluted E-64 was then added to the first well in the row (final E-64 concentration 1 μ M) and mixed. 100 μ l was then transferred from this first well to the next well in the row, resulting in “double dilution”, in which the concentration of E-64 was halved. This double dilution was carried out across the row of the

plate, discarding the last 100 μ l. The plate was then sealed and incubated at room temperature for at least one hour. Into each well of one of the rows of a new white 96-well plate, 100 μ l of substrate buffer was added. 1 μ l from each well of the first polystyrene plate was added to the corresponding wells of this new plate containing substrate buffer (i.e. 1 μ l from the well in row 1 of the first plate was added to the contents of the well in row 1 of this plate, etc.). The plate was then read at excitation wavelengths of 360 – 390 nm and emission wavelengths of 450 – 470 nm every 30 seconds for 31 to 61 cycles (i.e. for 15 to 30 minutes). The rate of activity was plotted against the E-64 concentration and linear regression of non-zero rates was performed. The concentration of active sites in the CatS was determined by multiplying the x-intercept by 400 (i.e. the amount by which the CatS was diluted for performing this assay). From this assay, the concentration of activated CatS stock in mg/ml was obtained. From this, CatS stocks were diluted to 2 mg/ml concentrations in 1x PBS and aliquoted at 50 μ l in cryovials. The aliquots were labelled with the batch number, concentration, volume, and dates, and stored at -80°C.

Before measuring the substrate kinetics of activated CatS, an initial dilution experiment is performed to find the optimal dilution of CatS to use for the kinetics assays. The initial dilution is performed by adding 200 μ l of substrate buffer to the first well in one row of a white 96-well plate and 100 μ l to the rest of the wells in that row. A 1:10 dilution of the activated CatS is made before starting the assay by diluting in assay buffer. 2 μ l of this diluted CatS was then added to the substrate buffer in the first well in the row of the plate. The contents of the well were mixed, and 100 μ l of this was transferred to the next well of the plate. This double dilution was performed across all wells in the row, such that the concentration of CatS in each well was halved each time, and the last 100 μ l was discarded to ensure the volume in all wells was the same. The plate was then read at excitation wavelengths of 360 – 390 nm and emission wavelengths of 450 – 470 nm every 30 seconds for 61 cycles. The well in which most CatS activity can be observed indicates the factor by which the activated CatS needs to be diluted for use in the kinetics assay.

The substrate kinetics of CatS were measured by adding 100 μ l of DMSO (12.5%, diluted in assay buffer) to wells 2 – 8 across one row of a polypropylene 96-well plate. A mixture of 179 μ l of assay buffer and 25 μ l of substrate buffer was mixed in the first well of the row, and 100 μ l was transferred to the second well containing DMSO. This double dilution was performed across all well in the row that contained DMSO, such that the concentration of substrate in each well was halved. 20 μ l of the contents of each well was then transferred to

three rows in a new 96-well plate, such that the reaction could be performed in triplicate to obtain an average value. To each of the wells in the new assay plate, 80 μ l of CatS, diluted in assay buffer and DTT (1 mM) to the concentration determined in the initial dilution experiment, was added. The plate was then read at excitation wavelengths of 360 – 390 nm and emission wavelengths of 450 – 470 nm every 30 seconds for 61 cycles. The rate is fitted by linear regression, plotted against substrate concentration and fitted to the Michaelis-Menten equation. The specific activity of CatS can be calculated using the formula $(V_{max} \times \text{assay dilution}) / (\text{enzyme concentration} \times 155 \times 25)$, where 155 is the fluorescence of 1 μ M AMC and 25 is the MW of CatS in kDa.

Inhibitor kinetics were determined as follows. The CatS substrate boc-val-leu-lys-AMC (Bachem, Switzerland) was diluted in assay buffer to 1 mM, of which 20 μ l was added to the first wells in two rows of a 96-well plate, while 10 μ l was added to the wells 2 – 8 in these two rows of the plate. The CatS inhibitor MVO78590 was diluted in DMSO to 10 μ M, and 2 μ l was added to the first well in the top row, while 2 μ l of DMSO only was added to the first well in the other row (as a control for the activity of uninhibited CatS). To each well in the assay plate, CatS, diluted in assay buffer and DTT (1 mM) to the concentration determined in the initial dilution experiment, was added. 190 μ l of diluted CatS was added to the first well in both rows, while 80 μ l was added to the remaining wells. A double dilution was then performed by transferring 100 μ l of the contents of the first wells to the next wells in that row of the plate, discarding the last 100 μ l. The plate was read in a spectrophotometer at excitation wavelengths of 360 – 390 nm and emission wavelengths of 450 – 470 nm every 30 seconds for 61 cycles. The rates were fitted by linear regression, plotted against $\log(\text{inhibitor concentration})$ and fitted to the competitive inhibition equation (IC_{50}).

3.2.2 Isolation and culture of mouse dorsal root ganglia

All experiments were performed in accordance with the United Kingdom Home Office Regulations (Scientific Procedures Act, 1986). Experiments were carried out on 6-18 weeks old adult male and female C57/BL6 mice obtained from Charles River. Animals were housed in the Biological Services Unit, King's College London in groups of 8 per cage, on a 12 hour day/night cycle with ad libitum access to water and food.

Mice were humanely killed either by terminal anaesthesia with an overdose of sodium pentobarbital (Euthanol, 200 mg/kg body weight) or by concussion of the brain by striking the cranium followed by decapitation. The spinal column from the base of the skull to the

level of the hips was removed and cut in half along the dorsal and ventral midpoints. Using forceps, the spinal cord was removed and discarded (Figure 3.2). By gently tugging on the axon bundles of the DRGs with the forceps, the DRGs could be removed from the crevices along the length of the spinal column. The roots were trimmed from the DRGs and the DRGs were placed in a dish containing 2 ml of Ham's DMEM F-12 (Sigma, UK). Up to 30 DRGs were removed per mouse.

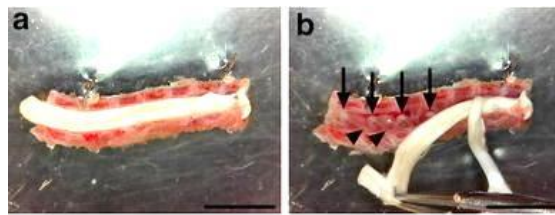


Figure 3.2: Dissection of DRGs from the spinal cord (adapted from Sleight et al., 2016)

The spinal column was removed from the mouse and cut in half along the dorsal and ventral midpoints to expose the spinal cord (A). The spinal cord was removed, revealing the DRGs which were located within crevices along the length of the spinal column (black arrows) (B). Axon bundles could also be observed (black arrowheads). Scale bar = 0.5 cm.

Isolation and culture of mouse DRGs was performed following a protocol adapted from Malin et al., (2007) and Simeoli et al. (2017). In brief, 5% w/v type-4 collagenase (Worthington, Lorne Laboratories, UK) was added to the culture dish containing the dissected DRGs (final collagenase concentration 0.125% w/v) and incubated at 37°C 5% CO₂ for 60 to 120 minutes. Following digestion, cells were triturated using either flame-polished glass Pasteur pipettes or P1000 pipette tips with 5 mm cut off from the tips. Ham's DMEM F-12 (Sigma, UK) containing 10% FBS (Sigma, UK) was then added to the cells to neutralise the collagenase. The cells were centrifuged at 600 rpm for 5 minutes and the media was aspirated from the pellet of cells. Cells were resuspended in Ham's DMEM F-12 supplemented with 10% FBS, 1% penicillin/streptomycin (Thermo Fisher Scientific, UK) and 10 ng/ml 7S murine NGF (Promega, UK). Cells were plated on glass coverslips (13 mm diameter) pre-coated with 100 µg/ml poly-L-ornithine (Sigma, UK) and 50 µg/ml collagen type-1 (Ibidi, Germany or Sigma, UK) at a volume of 5 – 20 µl/well, yielding about 1,500 – 6,000 cells per coverslip, and flooded with 500 µl of Ham's DMEM F-12 after at least 30 minutes of incubation. DRGs were cultured at 37°C 5% CO₂ until ready to use.

3.2.3 Patch clamping

Patch clamping experiments were performed on isolated mouse DRGs that had been in culture for 1 – 3 days, measuring changes in membrane current following application of various substances. All recordings were made at room temperature. Recordings were performed using an Axopatch 200B amplifier (Molecular Devices, USA) and command voltages were generated with a Digidata 1320A interface (Molecular Devices, USA). Neurons were held at -60 mV or -90 mV for KCl (Sigma, UK) application and -60 mV for all other applications. Data were digitised and analysed using Clampex 9.2 and Clampfit 9.2 (Molecular Devices, USA). Cells were viewed using a Nikon Diaphot 300 microscope at x200 magnification. During patch clamping, cells were maintained in a HEPES buffer (HEPES, 5 mM, Sigma, UK; NaCl, 130 mM, Sigma, UK; glucose, 5 mM, Sigma, UK; KCl, 3 mM, Sigma, UK; MgCl₂, 1 mM, G Biosciences, USA; CaCl₂, 1 mM, Fisher Scientific, UK; pH7.4 adjusted with NaOH), similar in composition to extracellular solution, with a flow rate of 2 ml/minute. Cells were patched using a microelectrode pipette made from a 1.5 mm outside diameter borosilicate glass capillary with filament (World Precision Instruments, UK) pulled using a Model P-97 Flaming/Brown Micropipette Puller (Sutter Instrument Company, USA). The microelectrode tip was heat polished and then backfilled with a HEPES buffer similar in composition to intracellular solution and passed through a 0.2 µM syringe filter (HEPES, 10 mM, Sigma, UK; KCl, 120 mM, Sigma, UK; MgCl₂, 1 mM, G Biosciences, USA; CaCl₂, 1 mM, Fisher Scientific, UK; EGTA, 10 mM, Sigma, UK; pH7.4 adjusted with NaOH). The filled microelectrode tip was placed on a thin silver chloride wire attached to an Axon Instruments CV 203BU Headstage. To patch the neurons, the tip of the microelectrode was placed over a cell and lowered until a small “bight dent” appeared on the surface of the cell. Recordings were made using whole cell parameters. The “VC Seal” protocol was run, which involved stepping the holding potential from -90 mV to 0 mV for 30 ms, and then back to -90 mV, during which gentle suction was applied to the micropipette in order to form a patch onto the cell. Once the cell had been patched, the “VC Seal” protocol showed a characteristic trace in which the step to and from 0 mV was characterised by upward and downward peaks in the trace (Figure 3.3 A). The pipette offset was adjusted until the trace was at 0 nA when the command potential was at 0 mV. To improve the quality of the clamp, the “VC Cap” protocol was run, during which the holding potential was stepped from -90 mV to -100 mV for 30 ms, and then back to -90 mV. Whole cell capacitance and series resistance parameters were adjusted until the peaks in the trace during the steps to and from -100 mV were as flat as possible (Figure 3.3 B). Cells that had a holding current of less than -0.3 nA were not used in experiments. Finally, to disrupt the patch and allow access of the

microelectrode in to the cell interior (i.e. to establish a “whole cell recording”), increased suction was applied to the microelectrode or a brief oscillation of the command potential was carried out. Changes in the membrane current of cells were recorded in response to substances applied using either the bath perfusion method or the pressure puffer method.

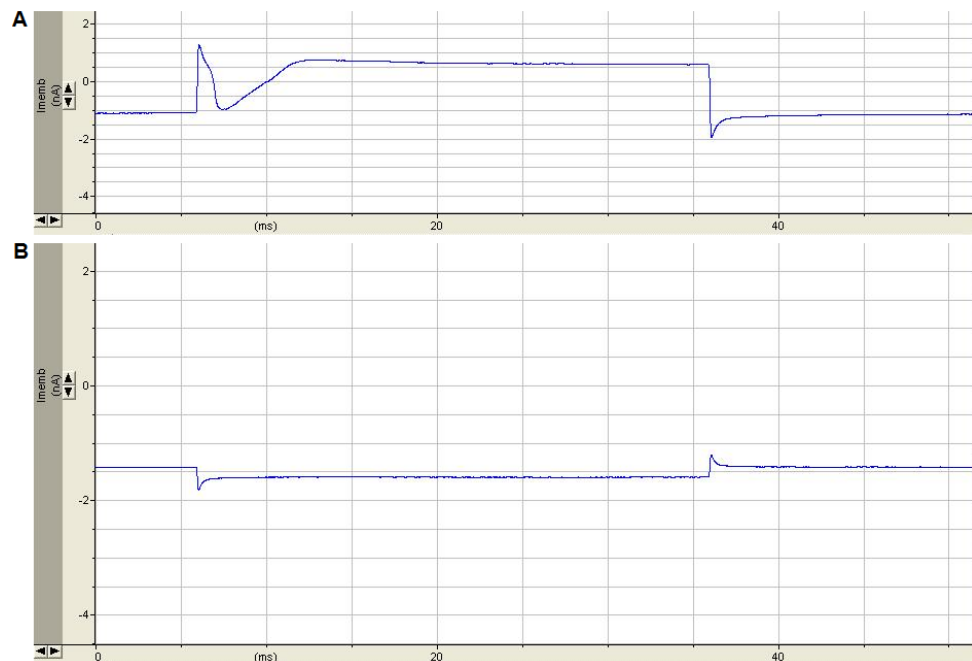


Figure 3.3: Example current traces during patching of the neurons

The “VC Seal” protocol involved stepping the holding potential from -90 mV to 0 mV for 30 ms and then back to -90 mV, characterised by upward and downward peaks during the steps (A). The “VC Cap” protocol involved stepping the holding protocol from -90 mV to -100 mV for 30 ms and then back to -90 mV (B).

HEPES buffer was applied to the cells using bath perfusion at a rate of about 2 ml/minute. Substances were applied directly onto the cells using a thin glass pipette attached to a PV830 Pneumatic PicoPump (World Precision Instruments, UK) located only a few micrometres away from the patched cell. This resulted in the application of the substance directly onto the cell over a period of 5 seconds at about 5 psi with 600 – 800 nl/puff. Patched cells were voltage clamped at -60 mV and substances were applied 3 times with a 50 second interval between applications. Because application of substances in this way was local and did not affect cells located further away in the chamber, this method could be used on several cells on the same coverslip. Furthermore, because the glass pipette held only a few microliters of solution, this method of application was suitable for applying CatS, which was available to us in only small volumes. KCl (12 mM), extracellular buffer (control

for KCl), capsaicin (1 μM) in 0.01% DMSO, 0.01% DMSO (control for capsaicin), and DPBS with 1 μM Ca^{2+} and Mg^{2+} (control for CatS) were also applied using the pressure puffer.

3.2.4 Calcium imaging

Calcium imaging experiments were performed on DRG cultures that had been plated on coverslips 24 hours beforehand. Experiments were carried out and analysed using either PTI Image Master software or PTI Easy Ratio Pro software (version 1.2.1.87). Cells were incubated in Fura-2-AM (2 μM ; Teflabs, Cambridge Bioscience, UK) for 1 hour prior to experiments being conducted. Coverslips were placed cell-side-down on a chamber and sealed in place with a ring of Vaseline to prevent leakage. The chambers were filled with 1 x HBSS (Gibco, UK) with 10 mM HEPES (Sigma, UK) at pH7.4) and secured onto the microscope stage. Recordings were made at room temperature. Fluorescence of calcium in cells was measured at 340 nm and 380 nm excitation and 510 nm emission wavelengths. Results are expressed as a 340/380 nm emission ratio. Substances were applied directly into the chambers using mostly bath perfusions, although attempts were made to apply directly to the chamber using a pipette or injected into the chamber using a syringe. Application of substances using bath perfusion involved setting up reservoirs above the chamber with tubing connecting to one side of the chamber on the microscope. The rate of perfusion was 4 ml/minute. For calcium imaging experiments, most substances were applied into the bathing solution surrounding the cells (the so-called bath perfusion). For this, the substances to be applied were contained in reservoirs located above the chamber, and connected into one end of the chamber via a tube, where they entered the chamber at a rate of 4 ml/minute. HEPES calcium buffer, capsaicin (10 nM – 1 μM ; Sigma, UK), mustard oil (1 μM – 100 μM ; Sigma, UK), CatS (400 nM; Medivir, Sweden), SLIGRL-NH₂ (1 μM – 50 μM ; Insight Biotechnology, UK), the CatS inhibitor MDV-590 (0.5 μM – 5 μM ; Medivir, Sweden), the PAR2 antagonist FSLLRY-NH₂ (1 μM – 10 μM ; Sigma, UK) (Al-Ani et al., 2002a), and KCl (50 mM, Sigma, UK) were all applied using this method. Substances were applied for 2 minutes, with responses observed 1-2 minutes after application. In the case of CatS application, CatS was applied to the cells for 2 minutes, after which the flow was switched off and the cells were left to incubate in CatS for 2, 10, or 20 minutes, before resuming the flow and application of other substances (Figure 3.4 A). In the case of the CatS inhibitor MDV-590 and the PAR2 antagonist FSLLRY-NH₂, cells were left to incubate in either of these substances for 10 minutes and then incubated in CatS in the presence of either of these substances for a further 20 minutes (Figure 3.4 B). At the end of each experiment, KCl (50 mM) was applied to identify all viable neurons.

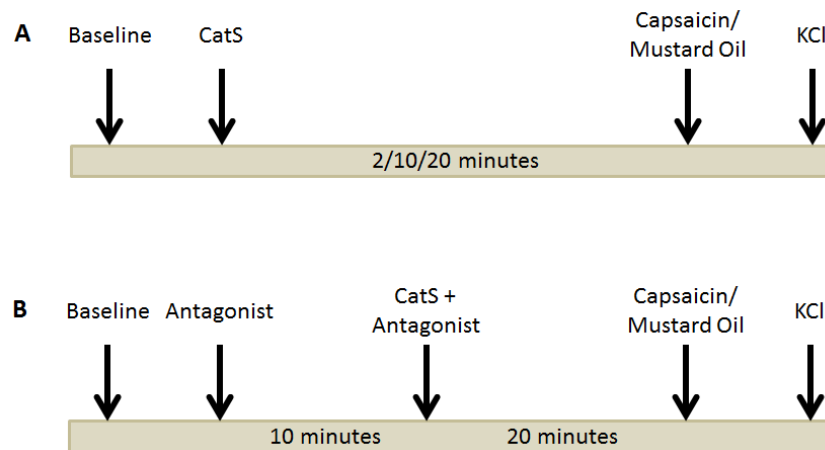


Figure 3.4: Schematic of drug application and incubation protocol for calcium imaging experiments

Isolated DRGs in culture were exposed to most substances for 2 minutes, except for CatS (A), the CatS inhibitor MDV-590, and the PAR2 antagonist FSLLRY-NH₂ (B), to which the cells were exposed to for up to 20 minutes.

The main drawback of applying CatS to the cells using the bath application was the volume of CatS that was required. Because CatS was provided to us in aliquots of 80 μ M in 50 μ l buffer, we were restricted in the concentration and volume that could be applied to our cells in our experiments. To apply CatS using the bath method of application, CatS was diluted to give the minimum volume required to be able to apply using this method, i.e. approximately 5 ml of 400 nM CatS. Additional methods of applying CatS to the cells were also tested, although each of these had their own limitations too and were ultimately not used in further experiments. In order to apply concentrated CatS to the cells, 50 μ l of CatS (40 μ M to 500 nM) was carefully pipetted directly into the chambers during calcium imaging experiments. However, it was not possible to accurately determine the volume of fluid in the chamber, and hence the final concentration of CatS in the chamber. In addition, it was not possible to determine whether the CatS applied in this way mixed with the solution in the chamber, and hence whether cells being imaged had been exposed to CatS. To ensure all cells in the chamber were exposed to CatS, CatS stocks were diluted to give 500 μ l of 1 μ M CatS. The diluted CatS was loaded into a 1 ml syringe and attached to a 23G needle and connected to an inlet into the chamber by a short length of 0.86 mm ID/1.27 mm OD tubing. To avoid bubbles in the tube, the tubing and syringe were backfilled with CatS. CatS was injected slowly and gently into the chamber, displacing the buffer already present in the chamber and replacing it with the CatS solution. Typically it took about 1 minute to empty the contents of the syringe into the chamber. However, this method of application caused

cells to move, creating artefact responses presumably as a result of mechanical stimulation of the cells due to fluid being forced into the chamber, and making it difficult to track cells during analysis of the experiment. Thus, bath perfusion for application of substances was used in all calcium imaging experiments.

3.2.5 Quantitative Polymerase Chain Reaction (qPCR)

Total RNA was extracted from mouse DRG cultures that had been plated on 13 mm diameter coverslips (4 coverslips per mouse) 48 hours beforehand using the PureLink RNA Mini Kit (Invitrogen, UK), according to the manufacturer's protocol. The total concentration of extracted RNA was measured using a NanoDrop spectrometer. Total RNA (1 µg) was used to synthesise first strand cDNA using the Superscript VILO cDNA Synthesis Kit (Invitrogen, UK) according to the manufacturer's protocol. Expression levels of protease activated receptor-2 (PAR2) were analysed, with 18S rRNA used as a reference transcript.

Amplification was performed with a LightCycler 480 (Roche, UK) using SYBR Green I Master (Roche, UK). The primers used are given in Table 3.1. The instrument was programmed as follows: 95°C for 5 minutes and 45 cycles of 3 steps of 10 seconds each, including denaturing at 95°C, annealing at 60°C, and primer extension at 72°C. All samples were run as duplicates, with 18S as the housekeeping gene. Samples in which the melting curve had more than one peak were excluded from analysis. Data was analysed using LightCycler 480 software (version 1.5.1). The relative gene expression level was calculated according to the 2- Δ Ct method, where Ct represents the threshold cycle.

Table 3.1: Primers used for PAR2 and 18S in qPCR

Genes	Forward Sequence	Reverse Sequence	Reference
PAR2	GGACCGAGAACCTTGAC	GAACCCCTTTCCAGTGATT	Touw et al., 2012; Li et al., 2016a
18S	GCTGGAATTACCGCGGCT	CGGCTACCACATCCAAGGAA	Denning et al., 2008

3.2.6 Data analysis and statistics

For patch clamping experiments, recordings were analysed using Clampfit 9.2 software. Data were lowpass filtered at 3 Hz (-3 dB, 8-pole Bessel filter) and sampled at 100 Hz. The baseline was adjusted by subtracting the slope between time-points at 0 seconds and at 10 or more seconds of the recording (which ever was more stable) prior to drug application. The peak polarity at the most negative-going points during drug application was then

obtained. A cell was considered to have responded to application of a substance if the holding was less than -0.3 nA and the magnitude of the response was greater than the control responses ± 2 standard deviations.

Once the recordings had been made for calcium imaging experiments, cells were circled using the PTI Image Master or PTI Easy Ratio Pro software and non-responders to KCl or other substances were removed. A cell was considered to have responded to application of a substance if the response to that substance was at least 20% of the size of the response of the same cell to application of KCl. Traces of responders were individually analysed for drifts in the baseline that might otherwise be considered to be responses, and such “responses” were subsequently classed as false positives and removed from analysis.

Data were analysed and graphs generated using GraphPad Prism 5 (Graphpad Software Inc., USA) using unpaired Student's t-tests when comparing just two groups (application of a substance compared with its control), or one-way ANOVA when comparing more than two groups. One-way ANOVA was followed by Dunnett's multiple comparison test when comparing multiple groups against one control group, while Bonferroni's multiple comparison tests were used when comparing multiple groups with each other. Two-way ANOVA was used when comparing the percentages of cells that responded to various concentrations of capsaicin or mustard oil following pre-incubation in buffer or CatS. Chi-squared tests (Fisher's exact tests) were used to compare the number of cells that responded to application of capsaicin or mustard oil following pre-incubation in buffer or CatS. The n numbers are displayed within the figure legends of the results section. Data are presented as mean \pm standard error of the mean (SEM). $P \leq 0.05$ was set as the level of statistical significance.

3.3 Results

To investigate whether sensory neurons could respond directly to application of CatS and characterise these neurons, isolated mouse DRGs were exposed to CatS and various other compounds in both patch clamping and calcium imaging experiments.

3.3.1 Cathepsin S induces inward current in dorsal root ganglia

74 out of 121 cells (61.2%) responded to application of one or more of the agonists applied to them using pressure puffer application method. It is proposed that itch-sensitive neurons comprise a subpopulation of the TRPV1-expressing nociceptors (Han et al., 2013; Imamachi

et al., 2009; Shim et al., 2007). We first wanted to determine whether the neurons in our culture were viable for patch clamping and whether they expressed TRPV1 cells by testing if they could respond to TRPV1 agonists such as capsaicin. Isolated mouse DRGs were voltage-clamped and exposed to capsaicin (1 μ M) or KCl (12 mM), or their respective controls, DMSO (0.01%) or HEPES buffer. Significant increases in membrane currents were observed when cells were exposed to capsaicin or KCl, but not to their respective controls (DMSO or buffer) (Figure 3.5). 56% of cells responded to capsaicin and 67% responses to KCl applied in this way. Our cells were therefore also able to respond to substances applied directly to them using this method.

CatS was supplied to us as 80 μ M buffer exchanged into Dulbecco's PBS without calcium or magnesium. Application of this concentration of CatS directly to the cells using a pressure puffer resulted in an initial large inward current response, followed by responses of much smaller magnitude upon subsequent application of CatS. However, because the buffer which the CatS was supplied contained no calcium or magnesium ions, and because low extracellular Ca^{2+} can cause hyperexcitability of the cell, we could not be sure that the response we were observing was due to application of CatS, and not due to low extracellular calcium (Hille, 2001). To overcome this, 80 μ M stocks of CatS were diluted in 1 x DPBS containing 2 mM Ca^{2+} and Mg^{2+} making a final concentration of 40 μ M CatS stock in buffer containing 1 mM Ca^{2+} and Mg^{2+} . Application of this Cathepsin S resulted in a large inward current, which was severely reduced in magnitude following subsequent applications of Cathepsin S to the same cell 50 seconds after the previous application (Figure 3.6), suggesting desensitisation of the cell to further applications of Cathepsin S. 13% of the cells that were patched responded to application of Cathepsin S.

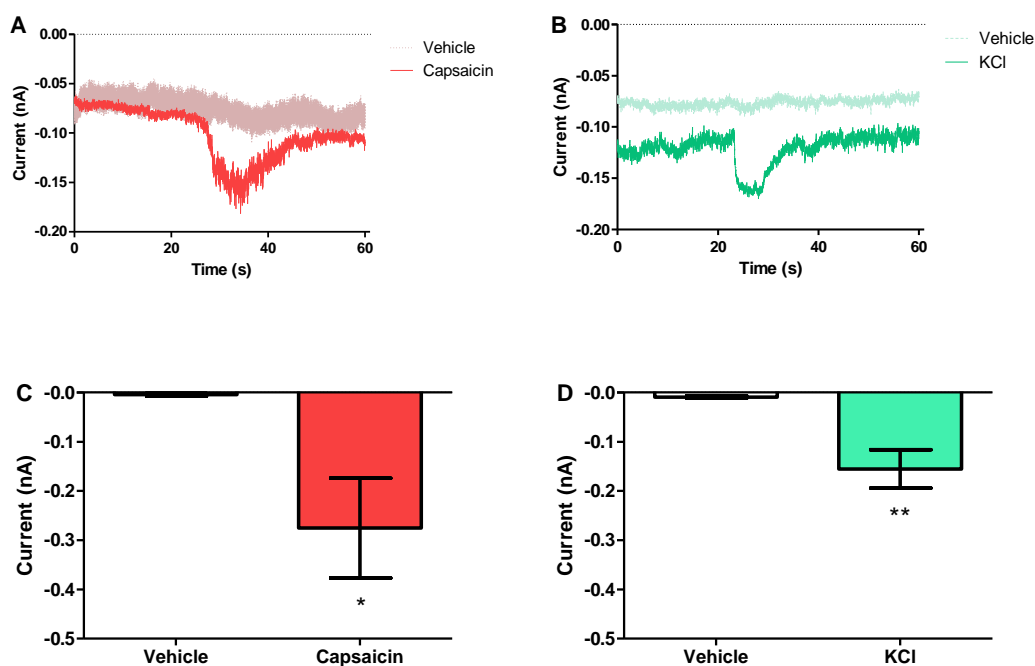


Figure 3.5: Inward currents in neurons following direct application of capsaicin or KCl
 Representative traces of changes in membrane current following puffer application of capsaicin and DMSO vehicle (A), or KCl and buffer vehicle (B). Quantification of changes in membrane current (C-D). $n = 9, 10$, data are mean \pm SEM. $*p \leq 0.05$, $**p \leq 0.01$, unpaired Student's *t*-test.

Table 3.2: Data for Figure 3.5

Data in nA.

DMSO	Capsaicin	Buffer	KCl
0.001288	-0.044903	-0.014726	-0.192489
-0.009065	-0.259192	-0.015522	-0.342306
-0.00149055	-0.059744	-0.007274	-0.387971
-0.00416846	-0.629548	-0.003006	-0.101497
-0.005175	-0.0683356	-0.006363	-0.057037
-0.023099	-0.776179	-0.000788	-0.0905533
-0.011752	-0.586358	-0.011477	-0.0424436
0.001425	-0.033194	-0.021058	-0.194678
-0.003576	-0.022551	-0.003769	-0.097612
0.010495	X	X	-0.048764

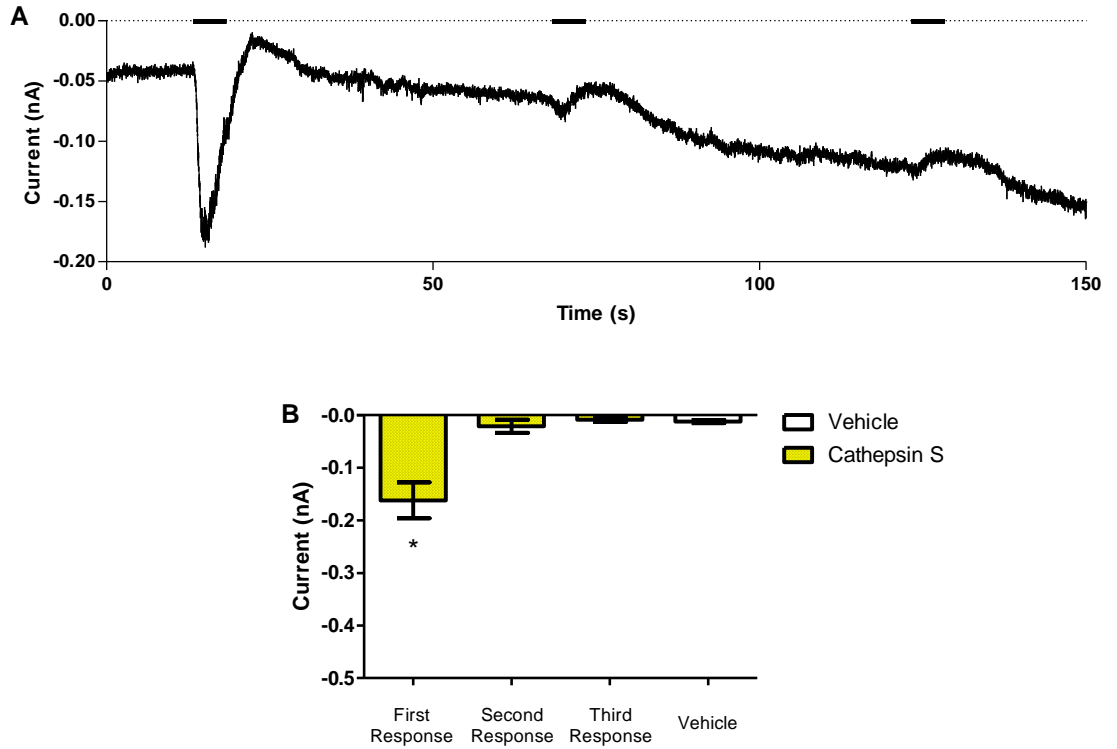


Figure 3.6: Inward currents in neurons following direct application of Cathepsin S

Representative trace of changes in membrane current following puffer application of hr-CatS (A). Solid lines at the top of the trace indicate duration of CatS application. Quantification of changes in membrane current (B). $n = 5 - 18$, data are mean \pm SEM. $*p \leq 0.05$, One-way ANOVA followed by Dunnett's multiple comparison test vs CatS first response.

Table 3.3: Data for Figure 3.6

Data in nA.

CatS First Response	CatS Second Response	CatS Third Response	DPBS
-0.143236	-0.005988	-0.021298	-0.005477
-0.060741	-0.070957	-0.013383	-0.004115
-0.214871	-0.011885	-0.001582	-0.008405
-0.134273	-0.012808	-0.001448	-0.009399
-0.257351	-0.005692	-0.007718	-0.003197

3.3.2 Cathepsin S-mediated calcium influx in dorsal root ganglia

Patch clamping experiments were initially performed with the intention of characterising the neurons that responded to CatS applied directly to the cells. However, we were unable to obtain robust responses following application of agonists to the bath, and hence were unable to characterise the cells that responded to CatS applied directly using the pressure puffer. We decided therefore to use calcium imaging to investigate CatS responses in sensory neurons and to further characterise cells that responded to CatS. For calcium imaging experiments, the ratiometric dye Fura-2-AM was used to measure the calcium responses of cells following application of various substances. Excitation of cells at 340 nm and 380 nm allowed for changes in calcium levels to be detected as changes in fluorescence and expressed as a ratio (i.e. the F340/F380 ratio). The use of a ratiometric dye over other types of calcium indicators was essential to reduce the effects of photobleaching and leakage during the long incubation times with CatS.

As with patch clamping, we first applied capsaicin to determine whether the neurons were viable for calcium imaging and whether any of them belonged to the TRPV1-expressing subpopulation. Isolated mouse DRGs were exposed to capsaicin (10 nM – 50 nM) for 2 minutes followed by 2-minute washes between applications. A delay of about 1 to 2 minutes was observed between application of substances and the cells responding, presumably reflecting the time taken for the substance solution to reach the cells and equilibrate in the bath as a result of the length of tubing used and/or the application system. 31% of cells responded to 10 nM capsaicin, 38% to 20 nM capsaicin, and 54% to 50 nM capsaicin (Figure 3.7 A, C). Similarly, DRGs were also exposed to mustard oil to test whether any belonged to the TRPA1-expressing subpopulation of neurons. Mustard oil (1 μ M – 100 μ M) was applied for 2 minutes, with a 2-minute wash between applications. 2.7% of cells responded to application of 1 μ M mustard oil and 5.8% responded to 10 μ M mustard oil. More than 50% responded to application of 100 μ M mustard oil (Figure 3.7 B, D).

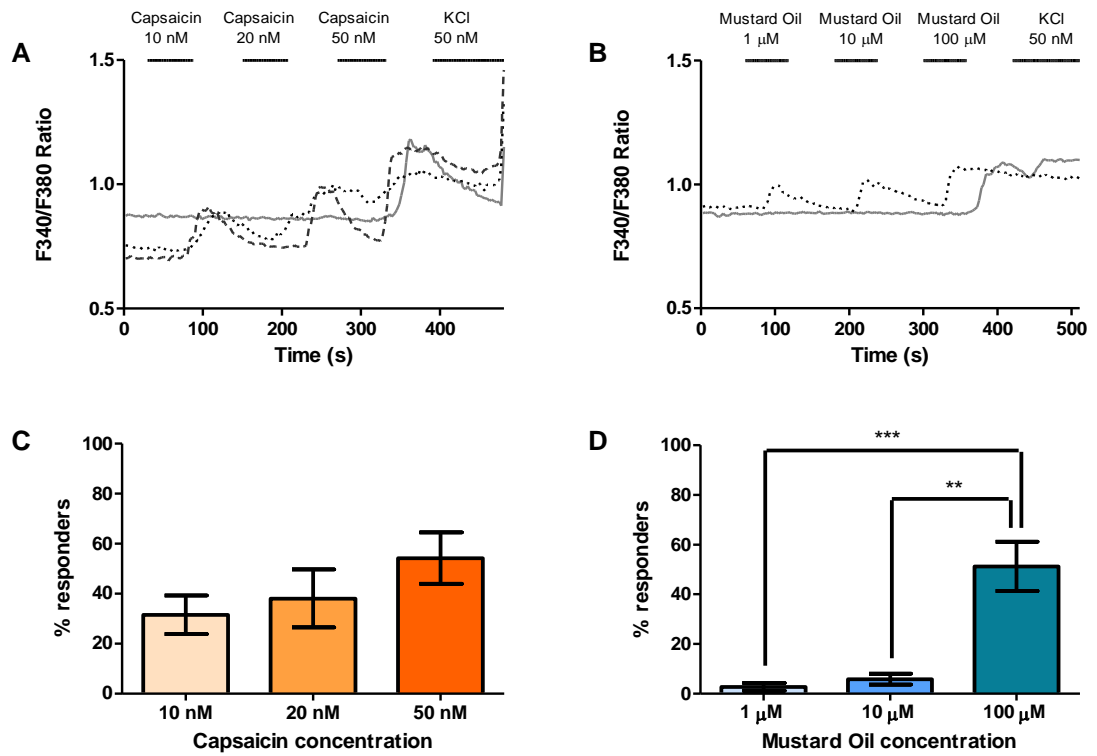


Figure 3.7: Calcium increase in neurons following bath application of capsaicin and mustard oil

Representative traces to application of capsaicin. The solid grey line shows the trace of a cell responding to application of 50 nM capsaicin only. The dotted and dashed black lines are Representative traces to application of capsaicin (A) or mustard oil (B). Solid lines at the top of the graph indicate application of agonists. Analysis showing the percentage of cells responding to application of capsaicin (C), from 144 cells, $n = 5$; 1 - 3 coverslips per mouse, data are mean \pm SEM. No significance, One-way ANOVA followed by Bonferroni's multiple comparison test. Analysis showing the percentage of cells responding to application of mustard oil (D), from 83 cells, $n = 4$; 1 coverslip per mouse, data are mean \pm SEM. $**p \leq 0.01$, $***p \leq 0.001$, One-way ANOVA followed by Bonferroni's multiple comparison test.

Table 3.4: Data for Figure 3.7

Data as the percentage of cells in each experiment that responded to application of agonist.

Capsaicin		
10 nM	20 nM	50 nM
56.590910	16.363640	28.409090
15.625000	25.000000	43.750000
14.714720	18.318320	44.894890
37.500000	75.000000	87.500000
33.333330	55.555560	66.666660
Mustard Oil		
1 μM	10 μM	100 μM
5.555555	0.000000	27.777780
0.000000	5.263158	42.105260
5.263158	10.526320	68.421050
0.000000	7.407407	66.666660

Because CatS was supplied to us in very small volumes (50 μ l), and because application of substances to the bath in this way requires millilitres of the substance, we were limited in the amount and concentration of CatS that could be applied using this method. The most concentrated CatS in the minimum volume required to apply to the bath using this method was 400 nM, which was the concentration subsequently used in all further calcium imaging experiments. CatS (400 nM) was applied to the cells for 2 minutes, until a stable CatS concentration was achieved, and the flow was stopped and the cells were left to incubate in CatS for up to 20 minutes. Some cells responded to application of CatS, with the number of responders increasing as the incubation time with CatS increased. The percentage of cells that responded to 20 minutes exposure to CatS (15.3 %) was significantly greater than the percentage that responded to 20 minutes exposure to buffer (5.9 %). In contrast, there was no significant difference in the percentage of cells that responded to 2 or 10 minutes exposure to CatS and 20 minutes exposure to buffer (Figure 3.8). Thus, cells can respond to CatS applied to the bath, although unlike the fast current changes observed following direct application of high concentration CatS to the cells in patch clamping, these calcium responses to lower concentration CatS take some time to occur. 20 minutes incubation in 400 nM CatS was used in all subsequent experiments involving application of CatS.

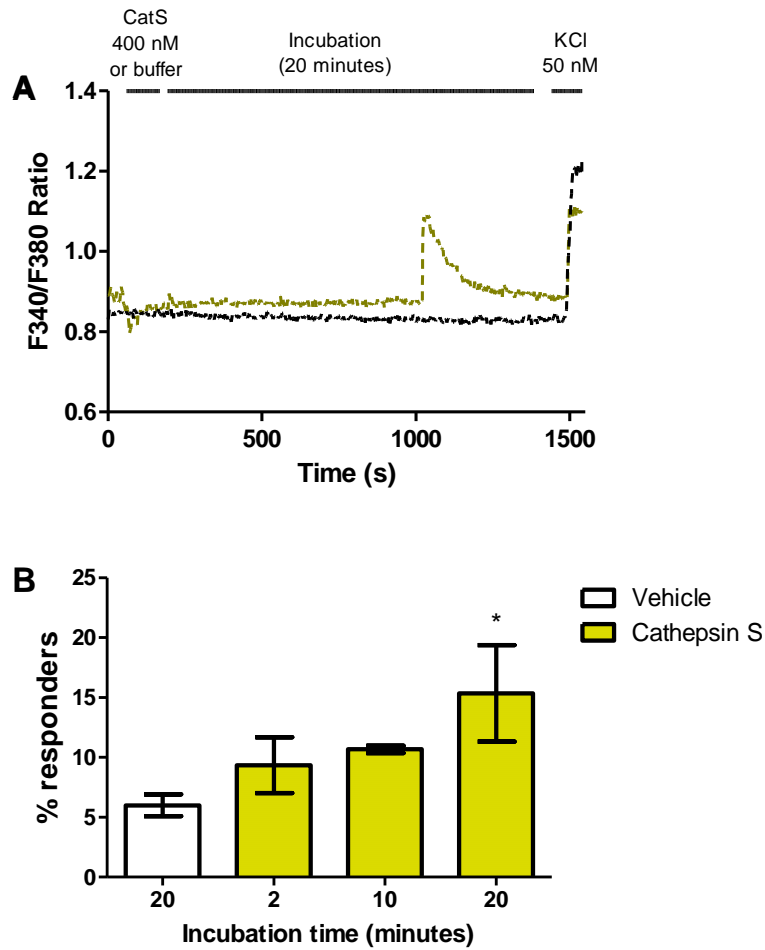


Figure 3.8: Calcium increase in neurons following bath application of Cathepsin S

Representative traces; the dashed gold line shows traces of a cell that responded to CatS, while the dotted black line shows the traces of a cell that did not respond to application of CatS, but did respond to KCl (50 nM) (A). Analysis of the percentage of cells that responded to application and incubation of CatS (B). From 461 cells, $n = 4 - 5$, 1 coverslip per mouse, data are mean \pm SEM. $*p \leq 0.05$, One-way ANOVA followed by Dunnett's multiple comparison test, vs 20 minutes buffer incubation.

Table 3.5: Data for Figure 3.8

Data as the percentage of cells in each experiment that responded to application of CatS.

Buffer (20 minutes)	CatS (2 minutes)	CatS (10 minutes)	CatS (20 minutes)
9.090909	7.692307	11.428570	26.666670
3.571429	14.285710	10.526320	7.692307
5.000000	3.636364	10.000000	14.545450
5.882353	11.764710	10.714290	12.500000
6.451613	X	X	X

Cathepsin S acts via PAR2 to cause calcium fluxes in dorsal root ganglia

To confirm that the observed calcium responses were due to CatS activity, cells were pre-incubated with the CatS inhibitor, MDV-590. Because MDV-590 was dissolved in DMSO, we tested for the optimal concentration to use that would not interfere with the calcium imaging assay. Incubation in MDV-590 (0.5 μ M) for 10 minutes resulted in calcium responses in 1.7% of cells, while incubating in 1 μ M MDV-590 resulted in calcium responses in 7.6% of cells (Figure 3.9 A). We therefore used MDV-590 at 0.5 μ M concentration for our experiments, as this was the concentration that appeared to interfere least with the assay. Pre-incubation of cells for 10 minutes in 0.5 μ M MDV-590 and application of 400 nM CatS for 20 minutes in the presence of MDV-590 resulted in a reduction of cells responding to CatS, with percent inhibition at 51%. Calcium responses were noted only in 8.9% of cells following 10 minutes pre-incubation with MDV-590 and 20 minutes application of buffer in the presence of MDV-590, and was comparable to that of the percentage of cells that responded to buffer alone (Figure 3.9 C). Therefore, MDV-590 reduces the percentage of cells responding to CatS, suggesting the calcium responses detected are due activity of CatS.

It has previously been suggested that CatS might exert its effects via activation of the PAR2 receptor (Reddy et al., 2010). We therefore tested the possibility that the calcium responses observed following application and incubation of cells in CatS were due to enzymatic activation at the PAR2 receptor by using the PAR2 antagonist, FSLLRY-NH₂. To test for the optimal concentration of FSLLRY-NH₂ that would not interfere with the assay, cells were exposed to 1 μ M, 5 μ M, and 10 μ M FSLLRY-NH₂ for 10 minutes. Incubation of cells in 1 μ M FSLLRY-NH₂ resulted in calcium responses in 1% of cells, while incubation in 5 μ M resulted in calcium responses in 4.6% of cells, and incubating in 10 μ M FSLLRY-NH₂ resulted in calcium responses in 11.7% of cells (Figure 3.9 B). We thus chose to use 5 μ M FSLLRY-NH₂ for our experiments as this concentration did not appear to interfere significantly with the assay, in that the percentage of cell that showed calcium responses was similar to that observed following incubation in buffer. Pre-incubation of cells for 10 minutes in 5 μ M FSLLRY-NH₂ followed by application of 400 nM CatS for 20 minutes in the presence of FSLLRY-NH₂ resulted in a reduction in the percentage of cells responding to CatS by 48.5%. Calcium responses were detected in only 8.4% of cells following 10 minutes pre-incubation with FSLLRY-NH₂ and 20 minutes application of buffer in the presence of FSLLRY-NH₂ (Figure 3.9 C). Because pre-incubating the cells with FSLLRY-NH₂ resulted in a significant decrease in the percentage of cells that responded to CatS, we propose that the CatS-induced calcium fluxes were mediated via PAR2.

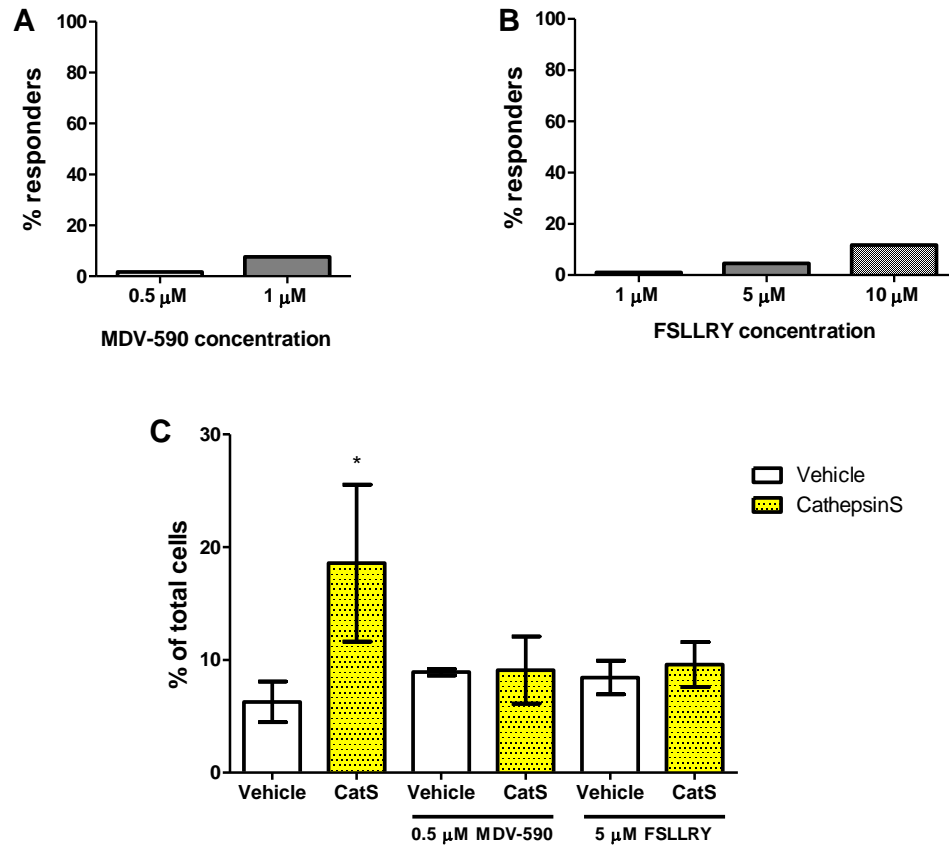


Figure 3.9: Calcium increase in neurons following application of Cathepsin S (400 nM) in the presence of the Cathepsin S inhibitor MDV-590 or the PAR2 antagonist FLLRY-NH₂ DRGs were incubated in different concentrations of MDV-590 (A) or FLLRY-NH₂ (B) for 10 minutes. From 82, 83 cells; n = 2, 1 coverslip per mouse, data are mean. Analysis of the percentage of cells that responded to application and incubation of CatS in the presence of the CatS inhibitor MDV-590 or the PAR2 antagonist FLLRY-NH₂ (C). From 663 cells, n = 3, 4 ; 1 coverslip per mouse, data are mean \pm SEM. *p \leq 0.05, One-way ANOVA followed by Dunnett's multiple comparison test, vs 20 minutes buffer incubation.

Table 3.6: Data for Figure 3.9 A and B

Data as the percentage of cells in each experiment that responded to application of the CatS inhibitor MDV-590 or the PAR2 antagonist FSLLRY-NH₂.

MDV-590		
0.5 μ M	1 μ M	
3.448276	4.761905	
0.000000	10.526320	
FSLLRY-NH ₂		
1 μ M	5 μ M	10 μ M
0.000000	2.857143	8.571428
2.127660	6.382979	14.893620

Table 3.7: Data for Figure 3.11 C

Data as the percentage of cells in each experiment that responded to application of the CatS in the presence or absence of MDV-590 or FSLLRY-NH₂.

Buffer		MDV-590		FSLLRY	
Vehicle	CatS	Vehicle	CatS	Vehicle	CatS
9.677420	10.344830	9.090909	5.681818	8.333333	8.333333
3.030303	32.432430	8.108109	8.108109	9.090909	13.636360
3.278688	12.962960	8.888889	17.777780	4.545455	4.545455
9.090909	X	9.523809	4.761905	11.764710	11.764710

Because the PAR2 antagonist FSLLRY-NH₂ significantly reduced the percentage of cells responding to CatS, we wondered whether activation of the PAR2 receptor directly would result in calcium responses in our cells. We first confirmed the expression of PAR2 mRNA in our cell cultures using qPCR (Table 3.8). Expression of PAR2 relative to 18S was 0.003.

Table 3.8: Ct values for PAR2 expression

Average Ct values of samples run as duplicates.

	18S	PAR2
Sample 1	14.905	26.64
Sample 2	18.84	30.66

After confirming expression of PAR2 in our cultures, we tested whether calcium responses could be detected in our cells following exposure to the PAR2 agonist, SLIGRL-NH₂. The percentage of cells that responded to buffer or any concentration of SLIGRL-NH₂ tested did not differ (Figure 3.10), suggesting that application of this PAR2 receptor agonist at these concentrations does not result in calcium increases in DRG cells.

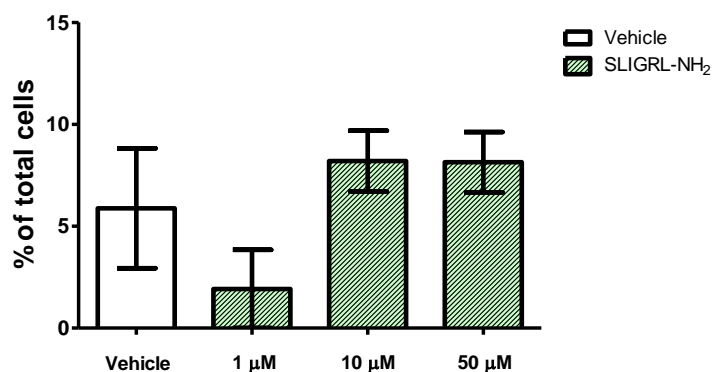


Figure 3.10: No calcium responses following application of the PAR2 agonist SLIGRL-NH₂
Application of SLIGRL-NH₂ for 10 minutes did not cause calcium responses in cells. From 213 cells, $n = 3 - 6$; 1 coverslip per mouse, data are mean \pm SE. No significance, One-way ANOVA followed by Dunnett's multiple comparison test, vs 20 minutes buffer incubation.

Table 3.9: Data for Figure 3.10

Data as the percentage of cells in each experiment that responded to application of SLIGRL-NH₂.

Buffer	1 mM SLIGRL-NH ₂	10 mM SLIGRL-NH ₂	50 mM SLIGRL-NH ₂
6.250000	0.000000	10.714290	7.692307
7.142857	0.000000	8.333333	4.000000
0.000000	0.000000	5.555555	9.090909
0.000000	0.000000	X	6.896552
16.000000	11.538460	X	13.043480
X	0.000000	X	X

Calcium influx following to application and incubation of Cathepsin S is decreased in cultures from TRPV1 knock-out mice and TRPA1 knock-out mice

Itch neurons are thought to belong to a subset of TRPV1 nociceptors (Han et al., 2013; Imamachi et al., 2009; Shim et al., 2007). Indeed, we previously observed that scratching behaviour in response to injection of CatS was significantly reduced in TRPV1 KO mice. Some

pruriceptors (mainly those responsible for non-histaminergic itch) are also proposed to express TRPA1 (Wilson et al., 2011). We therefore investigated whether calcium responses to application of CatS were altered in DRGs cultured from TRPV1 KO mice. In DRGs cultured from TRPV1 KO mice, the percentage of cells that showed calcium responses following application of CatS decreased from 15.7% to 7.5% (Figure 3.11). DRGs cultured from TRPA1 KO mice were also exposed to CatS, and it was found that the percentage of cells that responded decreased from 15.7% to 5.9% (Figure 3.11). As expected, DRGs cultured from TRPV1 KO mice and TRPA1 KO mice also showed a reduction in the percentage that responded to capsaicin or mustard oil, respectively.

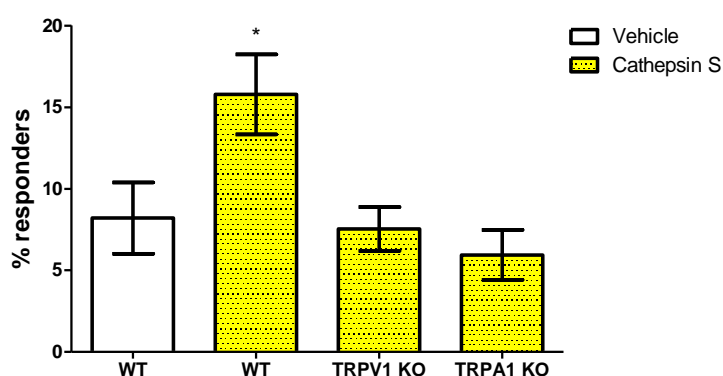


Figure 3.11: Reduction in response to Cathepsin S in TRPV1 KO and TRPA1 KO DRGs compared with WT controls

The percentage of responders to CatS in DRG cultures from TRPV1 or TRPA1 KO mice, from 373 cells, $n = 3 - 5$; 1 coverslip per mouse, data are mean \pm SEM. $*p \leq 0.05$, One-way ANOVA followed by Dunnett's multiple comparison test, vs 20 minutes buffer incubation.

Table 3.10: Data for Figure 3.11

Data as the percentage of cells in each experiment that responded to application of CatS.

Buffer	CatS		
	WT	TRPV1 KO	TRPA1 KO
2.222222	12.500000	10.526320	6.250000
7.692307	14.285710	5.555555	7.317073
11.764710	20.588240	5.000000	7.407407
11.111110	X	9.090909	0.000000
X	X	X	8.695652

Because the percentage of cells that responded to CatS was significantly reduced in DRG cultures from TRPV1 and TRPA1 KO mice, this suggests that the neurons which respond to CatS belong to the TRPV1 and TRPA1 subpopulation of nociceptors. Indeed, most of the cells that responded to CatS also responded to capsaicin (10 nM or greater) or mustard oil (10 μ M or greater) applied after CatS (Figure 3.12).

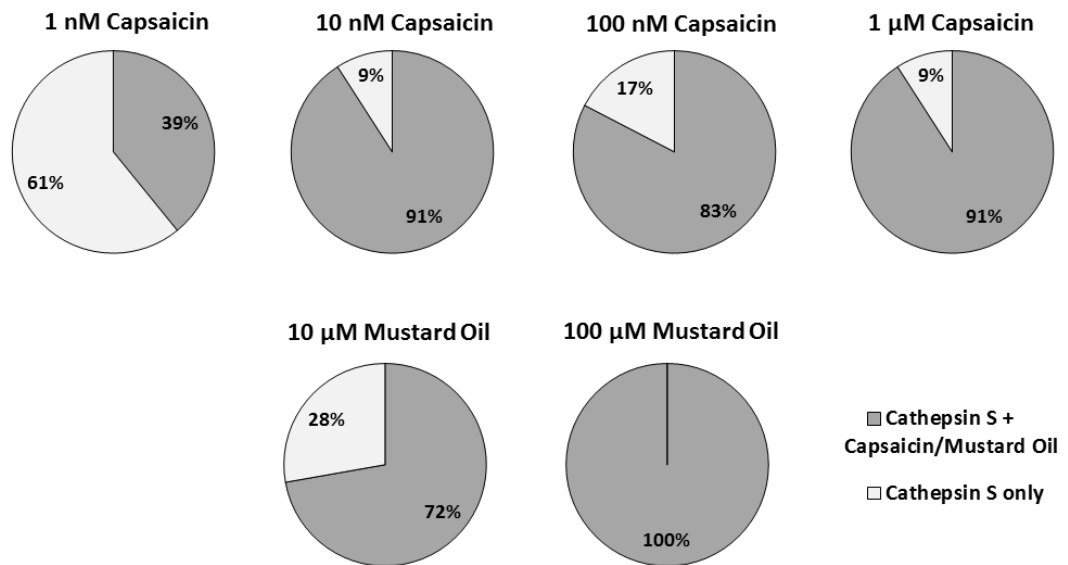


Figure 3.12: Most of the cells that responded to Cathepsin S also responded to capsaicin or mustard oil

Following application of CatS to DRG neurons in culture, cells were subsequently exposed to capsaicin (10 nM – 1 μ M) or mustard oil (10 μ M or 100 μ M). For capsaicin at 10 nM concentration or greater, more than 80% of the cells that responded to CatS also responded to capsaicin. More than 70% of the cells that responded to CatS also responded to mustard oil. $n = 3, 4$; 111 cells in total for 1 nM capsaicin; 63 cells in total for 10 nM capsaicin; 111 cells in total for 100 nM capsaicin; 63 cells in total for 1 μ M capsaicin; 108 cells in total for 10 μ M capsaicin; 108 cells in total for 100 μ M capsaicin.

Pre-application of Cathepsin S increases the number of cells that respond to capsaicin or mustard oil

One observation we made was that the percentage of cells responding to capsaicin and mustard oil following application of CatS was greater than the percentage of DRG cells that typically respond to application of these agonists in calcium imaging experiments. For example, Kwan et al. (2006) reported that approximately 31% of their DRGs from WT mice responded to application of 3 μ M capsaicin and that 23% responded to application of 10 μ M mustard oil. Wilson et al. (2011) observed that about 55% of cultured sensory neurons

responded to 1 μM capsaicin in calcium imaging experiments. We therefore wondered whether CatS could be sensitising cells to respond to agonists such as capsaicin and mustard oil. To test this, we applied capsaicin (10 nM – 1 μM) or mustard oil (10 μM or 100 μM) to cells following application of CatS or buffer. The number and percentage of cells that responded to capsaicin increased when cells were first exposed to CatS before application of capsaicin, compared with when they were first exposed to buffer before application of capsaicin (Table 3.11; Figure 3.13 A). Similarly, the number and percentage of cells that responded to mustard oil also increased when cells were first exposed to CatS (Table 3.11; Figure 3.13 B). This suggests that CatS could be sensitising the TRP channels on these cells, making them more likely to respond to application of their agonists. As activation of PAR2 has previously been reported to sensitise TRPV1 and TRPA1 channels, cleavage of PAR2 by CatS could be responsible for the sensitisation we observed (Amadesi et al., 2004; Amadesi et al., 2006; Dai et al., 2004; Dai et al., 2007).

Table 3.11: Increase in the number of cells that responded to capsaicin or mustard oil following pre-incubation with Cathepsin S

	Buffer	Cathepsin S	P value
Capsaicin (1 nM)	3 of 115	33 of 114	*** $P \leq 0.001$
Capsaicin (10 nM)	33 of 109	35 of 63	** $P \leq 0.01$
Capsaicin (100 nM)	51 of 115	74 of 114	** $P \leq 0.01$
Capsaicin (1 μM)	67 of 109	48 of 63	No significance
Mustard oil (10 μM)	11 of 132	41 of 108	*** $P \leq 0.001$
Mustard oil (100 μM)	83 of 132	88 of 108	** $P \leq 0.01$

n = 3 – 5, Chi-squared test (Fisher's exact test).

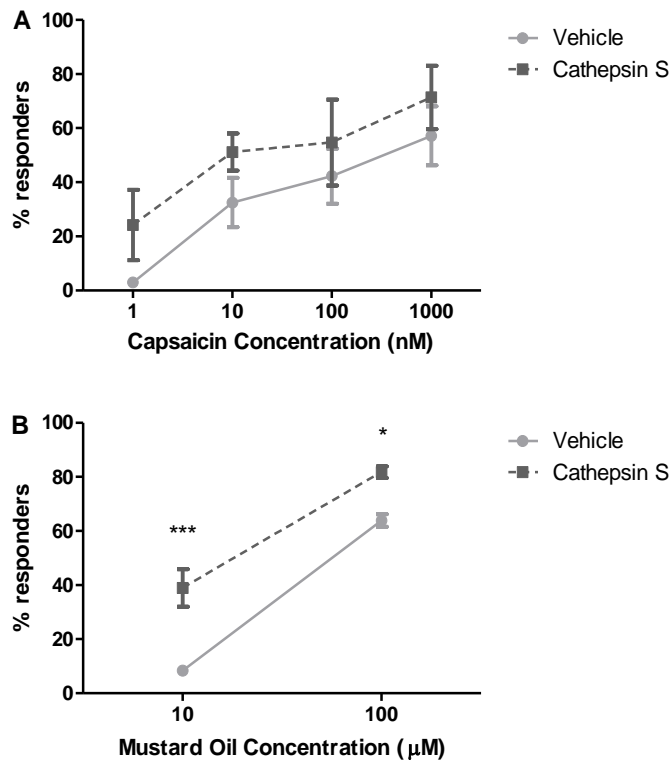


Figure 3.13: Pre-application of Cathepsin S resulted in an increase in the percentage of cells that responded to either capsaicin or mustard oil

The percentage of cells that responded to each concentration of capsaicin (A) or mustard oil (B) tested following application of CatS tended to be greater than the percentage that responded to capsaicin or mustard oil following application of buffer. Data are mean. $n = 3 - 5$, * $P \leq 0.01$; *** $P \leq 0.001$, Two-way ANOVA followed by Bonferroni post hoc test.

3.4 Discussion

The main finding of this chapter is that application of CatS to sensory neurons in culture resulted in both inward currents in the membrane and calcium increases in the cell, suggesting neurons can respond directly to CatS. 13% of patched cells responded to CatS applied directly to the cell, and in calcium imaging experiments 10-15% of cells responded following incubation in CatS for up to 20 minutes. The percentage of cells that responded with calcium fluxes to CatS is similar to what has previously been reported at 8-10% (Reddy et al., 2015). In calcium imaging experiments, the effect of CatS was prevented by the CatS inhibitor, MDV-590, confirming the calcium fluxes observed were due to the enzymatic activity of CatS. The effect of CatS was also prevented by the PAR2 antagonist FSLRY-NH₂, suggesting that PAR2 mediated the effects of CatS. However, the percentage of cells that responded to CatS is lower than the percentage of sensory neurons found to express PAR2,

reported by others to be around 60% in rat DRG sections, using both antibody staining and *in situ* hybridisation (Russell et al., 2012; Steinhoff et al., 2000). This suggests activation of additional receptors or channels could be involved in CatS-mediated responses.

Alternatively, species differences and differences in the tissue stained could also explain the difference in the percentage of DRGs reported to express PAR2 compared to the percentage of responders to application of CatS as a PAR2 agonist. Indeed, Vellani et al., (2010) reported that 21.5% of their mouse DRGs in culture were positive for PAR2 using in-situ hybridisation, which is closer in agreement with the percentage of cells we observed to respond to application of CatS.

Although CatS-mediated calcium fluxes could be reduced in the presence of the PAR2 antagonist, FSLLRY-NH₂, suggesting the involvement of PAR2 in these responses, we were unable to observe significant responses in our cells to application of the PAR2 agonist, SLIGRL-NH₂. This is unlikely to be due to lack of expression of PAR2 on the DRG neurons, as qPCR revealed the presence of PAR2 mRNA in our cells and expression of PAR2 on sensory neurons has previously been described by others. One possibility is that the concentration of SLIGRL-NH₂ used in our experiments was not sufficient to elicit a significant percentage of cells to respond compared with the percentage that responded following application of buffer. Indeed, Liu et al. (2011b) used 100 µM SLIGRL-NH₂ in their calcium imaging experiments and observed calcium fluxes in about 3% of their DRG cultures. Furthermore, the variance in the percentage of cells that responded was quite high, especially for the responders to buffer, which may have masked any potential increase in the percentages of cells responding to SLIGRL-NH₂, particularly if only a small percentage of cells would respond to application of SLIGRL-NH₂.

Previous studies in KNRK (Kirsten Murine Sarcoma Virus transformed rat kidney epithelial) cells expressing PAR2 reported that cleavage of PAR2 by CatS results in coupling to G α s and the activation of adenylyl cyclase, resulting in the formation of cAMP (Zhao et al., 2014a). Mobilisation of calcium was not reported, suggesting that cleavage of PAR2 by CatS is not coupled to G α q, at least in this cell line. How then, might the calcium fluxes observed following incubation with CatS be explained? Calcium fluxes following application of CatS have been observed in other cell lines and DRGs, suggesting, in line with our observations, that CatS can cause either influx of extracellular calcium or mobilisation of intracellular calcium in cells (Elmariah et al., 2014; Lieu et al., 2016; Reddy et al., 2010; Reddy et al., 2015; Zhao et al., 2014a). One possible explanation is that CatS can exert its effects not only

by acting on PAR2, but also by acting on other receptors. When Zhao et al. used HEK293 and KNRK cell lines transfected with PAR2 in their experiments, calcium responses to CatS were not observed. However, when they used mouse DRGs (which express a wide variety of different receptors in addition to PAR2), calcium transients occurred, suggesting the requirement of additional receptors or channels for CatS-mediated calcium fluxes. Similarly, our experiments were performed in mouse DRGs expressing many different types of receptors and channels. In addition to non-canonical cleavage of PAR2 and activation of the receptor by a tethered ligand, CatS has also been reported to activate PAR4 (Reddy et al., 2010), as well as Mrgprs by a change in conformation of the receptor (Reddy et al., 2015). Various agonists at PAR4 and MrgprC11 are reported to result in calcium fluxes, and so CatS activity at these receptors could also result in calcium fluxes (de la Fuente et al., 2012; Han et al., 2002; Megyeri et al., 2009; Wilson et al., 2011). Indeed, increasing evidence suggests CatS is likely to act at receptors other than or in addition to PAR2. For example, Reddy et al., (2015) reported that DRGs from PAR2 KO mice still showed calcium fluxes following treatment with CatS, while no calcium fluxes were observed in DRGs from Mrgpr KO mice. Future experiments in which PAR4 and MrgprC11 are blocked or inhibited are required to further elucidate the mechanisms by which CatS activates its receptors and results in calcium fluxes. However, if this is the case, then it does not explain the reduction in calcium responses we observed when CatS was applied in the presence of a PAR2 antagonist, unless the antagonist is capable of blocking activity at other receptors, including PAR4 and/or MrgprC11, which has not yet been reported.

Our finding that CatS-mediated calcium transients can be reduced in the presence of a PAR2 antagonist does not appear to be in agreement with the reports of Reddy et al., (2015) that CatS-mediated calcium fluxes are not abolished in DRG cultures from PAR2 KO mice. We found that the PAR2 antagonist could significantly reduce the percentage of cells responding to CatS to that of the control level (i.e. the percentage that responded to buffer), although it cannot be ruled out from our results that some DRGs can be additionally activated by CatS at receptors other than PAR2. Furthermore, in their calcium imaging experiments, Reddy et al. used CatS at 2 μ M concentration while we performed our calcium imaging experiments using CatS at a much lower concentration of 400 nM. It cannot be excluded that CatS when used at higher concentrations can activate additional receptors, such as Mrgprs, while lower concentrations of CatS mostly cleave PAR2. This could also explain some of the delay required for calcium responses to occur in our calcium imaging experiments, reflecting the time taken for an indirect effect of calcium entry into the cell following cleavage of PAR2 by

CatS, while activation of other receptors by higher concentration CatS could result in immediate entry of calcium into the cells, as observed by Reddy et al. **The observed calcium responses to CatS may also be explained by the existence of additional cleavage sites on PAR2 for CatS.** Elmariah et al. (2014) reported the existence a cleavage site for CatS on PAR2 different than the site reported by Zhao et al. (2014a), which, when cleaved, resulted in calcium fluxes. The synthetic peptide agonist for this cleavage site, KVDGTS, was also able to generate calcium responses (albeit with slightly different kinetics than when activated by CatS). Future experiments which prevent cleavage of PAR2 at this site will be required to address this issue. The factors that determine which of the sites on PAR2 is cleaved by CatS also remain to be investigated. Variations in pH, cell type, concentration of CatS, the number of PAR2 receptors, the presence of other receptors, and dimerisation of PAR2 with other receptors could all potentially affect the cleavage site for CatS.

Finally, there is the possibility that the calcium responses observed are not due to direct activation of the cell by CatS acting on PAR2, but instead are due to indirect effects of CatS acting on the cell. Activation of PAR2 sensitises TRPV1 and TRPA1, to the point where TRPV1 channels become activated at a temperature about 10°C lower than usual (Amadesi et al., 2004; Amadesi et al., 2006; Dai et al., 2004; Dai et al., 2007). Thus, rather than directly resulting in calcium fluxes in neurons, the calcium transients could be due to spontaneous activity more likely to occur as a result of sensitisation of channels such as TRP channels following activation of neuronal PAR2, resulting in increased opening of these channels and subsequent entry of cations into the cell. Alternatively, because mixed DRG cultures were used for our experiments, activation of PAR2 on other non-neuronal cells could result in the release of mediators that in turn activate neurons in close proximity, which could explain the delay observed between application of CatS and the time taken for calcium fluxes to occur. Cultured fibroblasts have been observed to express PAR2 (Gruber et al., 2004). Activation of PAR2 expressed on human lung fibroblasts by trypsin has been reported to result in the release of IL-6, IL-8, and prostaglandin E2 (PGE₂) (Asokanathan et al., 2015). Expression of the IL-6 receptor has been reported in rodent neuronal DRG cell bodies and can be upregulated following injury (Brazda et al., 2013; Gadiant and Otten, 1996; Thier et al., 1999). However, neuronal activation by IL-6 is unlikely to result in calcium transients, as this cytokine signals via JAK/STAT, ERK, and PI3 kinase (Erta et al., 2012; Rothaug et al., 2016). IL-8 is not expressed in rodents, so involvement of this cytokine can be excluded (Guenet, 2005). PGE₂ signalling through the EP1 receptor can cause calcium transients in cultured human myometrial cells and Chinese hamster ovary cells (Asbóth et al., 1996;

Watabe et al., 1993), and expression of EP1 on DRGs is reported to be increased following nerve injury (Durrenberger et al., 2006). However, whether EP1 is expressed on cultured DRGs and results in calcium transients has not been thoroughly investigated. Indeed, in sensory neurons EP1 has been reported to signal via PKC to cause sensitisation of TRPV1, although activation of TRPV1 could in turn cause neuronal calcium transients (Moriyama et al., 2005). However, whether cleavage of PAR2 expressed on murine fibroblasts by CatS would result in a similar release of cytokines and mediators and cause calcium transients in DRG cells is not clear. Nevertheless, activation of PAR2 or other receptors that can be cleaved by CatS on other cell types in close proximity to DRG neurons is a potential mechanism by which neurons might be caused to respond.

PAR2 has also been reported to sensitise TRPV4 (Grace et al., 2014; Grant et al., 2007; Poole et al., 2013; Zhao et al., 2014a). It has been proposed that CatS cleaves PAR2 on sensory neurons, which in turn sensitises neuronal TRPV4 via the adenylyl cyclase/cAMP/PKA pathway, resulting in an influx of calcium ions from the extracellular space, rather than mobilisation of calcium from internal stores, and that this is responsible for the calcium transients observed in DRGs during calcium imaging experiments with CatS (Zhao et al., 2014a). Importantly, this CatS-mediated influx of calcium ions was reported to be reduced in DRG cultures from PAR2 KO mice or in the presence of a TRPV4 antagonist, suggesting the requirement of both PAR2 and TRPV4 for CatS-mediated calcium responses in DRGs. This is one explanation for the calcium transients we observed in our DRGs following incubation with CatS. However, whether functional TRPV4 is expressed on sensory neurons remains controversial. Expression of TRPV4 in sensory neurons has been confirmed by reverse transcription PCR, immunohistochemistry, and Western blotting, although concerns about the specificity of antibodies available for TRPV4 have been raised (Alexander et al., 2013; Grant et al., 2007; Kim et al., 2016). Furthermore, even if TRPV4 is expressed in neurons, whether it is normally functional is also disputed. Alexander et al. (2013) failed to observe calcium fluxes in most DRGs cultured from wild-type or TRPV4 KO mice in response to application of the TRPV4 agonist GSK1016790A. It was reported that a small percentage of thoracic DRGs cultured from wild-type mice (but not TRPV4 KO mice) did respond to the agonist, although a similar percentage of TG neurons from both wild-type and TRPV4 KO mice also responded to GSK1016790A, suggesting these calcium fluxes could in fact be an artefact or off-target effects. Instead, it is suggested that the role of TRPV4 in hyperalgesia and inflammation is not due to the activity of neuronal TRPV4, but instead of non-neuronal TRPV4. In support of this, TRPV4 is also expressed in non-neuronal cells, including

endothelial cells, and indeed reports of expression of TRPV4 detected during reverse transcription PCR and Western blotting of DRGs could be of vascular rather than neuronal origin (Hartmannsgruber et al., 2007). An alternative explanation may be that TRPV4 expressed on neurons is not normally functional, but can become functional following sensitisation or under inflammatory conditions. In agreement with this, Poole et al. (2013) observed that approximately half of their DRGs that responded to application of trypsin also responded to application of GSK1016790A. Because they applied trypsin prior to application of GSK1016790A and did not stimulate neurons in the absence of trypsin or any other PAR2 agonists, it cannot be excluded that TRPV4 was sensitised or primed by activation of PAR2, resulting in calcium fluxes to TRPV4 agonists that otherwise would not have been observed. Furthermore, differences in basal somatic sensation between wild-type and TRPV4 KO mice have not been reported (Alexander et al., 2013; Grant et al., 2007). In contrast, increased sensitivity to noxious pressure is reported in wild-type mice treated with NGF, but not TRPV4 KO mice treated with NGF, suggesting activation of TRPV4 is more likely to be involved in enhanced excitability in inflammation and pathological conditions such as atopic dermatitis (Alexander et al., 2013).

The role of TRP channels in itch (and pain) sensations has been well documented, and these channels are reported to be expressed on sensory neurons (Caterina et al., 1997; Nagata et al., 2005; Tominaga et al., 1998). They can be activated by a number of different agonists and under various conditions. TRPV1 is known to be activated by capsaicin, noxious heat, and low pH (Caterina et al., 1997; Tominaga et al., 1998), while agonists of TRPA1 include mustard oil, cinnamon oil, cannabinoids, and bradykinin (Bandell et al., 2004; Jordt et al., 2004). Activation of these receptors results in the opening of the channels forming a pore that allows the passage of cations including calcium and sodium, making them suitable for investigating in calcium imaging and electrophysiology experiments (Caterina et al., 1997; Jordt et al., 2004). The calcium fluxes observed following activation and opening of these channels can be prevented by the removal of extracellular calcium from the medium, suggesting that most or all of the calcium is derived from the extracellular environment (Caterina et al., 1997; Jordt et al., 2004). However, calcium may also be released from intracellular stores. Canonical signalling of PAR2 is reported to result in release of calcium from intracellular stores via coupling to Gαq and subsequent activation of PLC and production of IP₃ (Wang et al., 2010; Zhao et al., 2014a), although the exact mechanism of calcium release from intracellular stores may vary depending on cell type as it is not reported to occur by this mechanism in all cells (Oikawa et al., 2013). In contrast to

canonical activation of PAR2, CatS-mediated activation of PAR2 does not mobilise intracellular calcium, resulting instead in generation of cAMP (Zhao et al., 2014a). Thus, it is likely that the calcium fluxes observed were due to the influx of extracellular calcium, likely through TRP channels which are permeable to cations. However, further experiments should be performed to investigate the role of both intracellular and extracellular calcium in CatS-mediated neuronal responses.

Calcium ions also play a role in the inactivation and desensitisation of TRP channels (Caterina et al., 1997; Nagata et al., 2005; Wang et al., 2008). However, the requirement of these channels in mediating itch signalling from pruritogens detected by nerve terminals in the skin has recently come under dispute. Using skin-nerve preparations, Ru et al., (2017) reported that blocking TRP channels with Ruthenium red or using preparations from TRPV1 or TRPA1 KO mice did not affect responses to various pruritogens applied at the nerve terminals, although responses could be reduced in the presence of a chloride channel inhibitor. It was proposed that activity of TRP channels in the cell body may be important for the behavioural responses to pruritogens, which explains why scratching behaviour in response to pruritogens is reduced in TRP KO mice. However, this does not explain why calcium transients are observed in DRGs following application of pruritogens, such as we observed with CatS, and others have observed with histamine, and how such responses can be reduced in cultures from TRP KO animals, unless differences in experimental techniques are considered. In the skin-nerve preparations used by Ru et al., (2017), the axons of the sensory neurons innervating the skin remain intact, whereas in calcium imaging experiments DRGs are cultured and are required to regrow their neurites. Thus, the expression and function of receptors and channels such as TRPs in cultured DRGs may not accurately reflect their expression and function in the terminals of unaxotomised neurons. Nevertheless, we were able to demonstrate the requirement of expression of TRPV1 and TRPA1 in sensory neurons for CatS-mediated calcium signals *in vitro*.

Of all the neurons that responded to CatS, most also responded to the TRPV1 agonist capsaicin or the TRPA1 agonist mustard oil. Furthermore, the percentage of cells that responded to CatS in calcium imaging experiments was reduced in cultures from TRPV1 KO and TRPA1 KO mice. We therefore conclude that cells that respond to CatS are likely to belong to the TRPV1 and TRPA1 expressing subpopulation of sensory neurons. This is in agreement with previous studies in which a high incidence of co-localisation of PAR2 and TRPV1 or TRPA1 in neurons has been reported (Dai et al., 2004; Dai et al., 2007).

Furthermore, because the neurons responsible for pruriception are likely to be a subset of nociceptors, we would expect neurons that respond to pruritogens such as CatS to express TRPV1 and respond to capsaicin (Imamachi et al., 2009). However, one of the limitations of our patch-clamping and calcium imaging assays is that it cannot distinguish pruriceptors from nociceptors, and whether the neurons are polymodal or specific for conveying itch or pain. Thus, although we can conclude that DRGs that respond to CatS are a subset of nociceptors, we cannot determine the sensation(s) they are responsible for conveying. In fact, because injections of CatS in mice cause both nocifensive wiping and scratching behaviours, it is likely that neurons that respond to CatS are involved in conveying both pain and itch sensations, as observed in our behavioural studies in mice. Whether the different sensations result by activation of different receptors by CatS or by different subsets of cells remains to be investigated.

In addition to the neurons that responded to CatS belonging to the TRPV1/TRPA1-expressing subpopulation, we also observed that a greater percentage of cells responded to the TRPV1 agonist capsaicin or the TRPA1 agonist mustard oil if the cells were exposed to CatS first, suggesting sensitisation of these channels. Since PAR2 can sensitise TRPV1 and TRPA1, one likely explanation is that CatS has cleaved and activated PAR2 in our neuronal cultures, which has resulted in sensitisation of TRPV1 and TRPA1, making the cells more likely to respond when exposed to capsaicin and mustard oil (Amadesi et al., 2004; Amadesi et al., 2006; Dai et al., 2004; Dai et al., 2007). Previous studies have investigated the role of PAR2 activated by trypsin or the synthetic peptide agonist that is produced following cleavage of PAR2 by trypsin. In the case of TRPV1, sensitisation was found to occur via PKC and PKA phosphorylation of TRPV1, while TRPA1 was found to be sensitised by hydrolysis of PIP₂ by PLC. However, whether CatS causes sensitisation of TRPV1 and TRPA1 by the same mechanisms is not yet known. Indeed, since the mechanisms of sensitisation of TRPV4 by PAR2 are different when PAR2 is cleaved by CatS compared with cleavage at the canonical site (Zhao et al., 2014a), it would not be surprising if the mechanisms by which TRPV1 and TRPA1 became sensitised by PAR2 were also different following cleavage of PAR2 by CatS compared with trypsin. Activation of PAR4 has also been reported to cause sensitisation of TRPV1 by PKC (Vellani et al., 2010), and because CatS has been reported to cleave PAR4 in addition to PAR2, the increase in the percentage of neurons responding to capsaicin following application of CatS might also be due to activity at PAR4 (Reddy et al., 2010).

In DRG neurons cultured from TRPV1 KO mice, a significant reduction in the percentage of cells that responded to CatS was observed. This is in agreement with what was observed in our behavioural studies, in which CatS-induced itching was significantly reduced in TRPV1 KO mice compared with wild-type mice. Thus, functional TRPV1 appears to be essential for both CatS-mediated calcium responses in neurons *in vitro* and scratching behaviour *in vivo*. One discrepancy we are unable to explain, however, is the reduction in calcium response of cultured DRGs from TRPA1 KO mice to CatS, while no significant reduction in scratching behaviour was observed when CatS was injected in TRPA1 KO mice. Although a slight reduction in scratching behaviour was noted following injection of CatS into TRPA1 KO mice compared with WT mice, this was not significant. In contrast, a significant decrease in the percentage of cells that responded to CatS was observed in cultures from TRPA1 KO mice compared with wild-type mice. One explanation for this is the difference between *in vivo* behavioural studies and *in vitro* assays looking at the responses of cells, which may not necessarily be the same; in this instance we are assuming that calcium fluxes and activation of the cell means transmission of itch signals and subsequent scratching behaviour. Compensatory mechanisms may exist in TRPA1 KO mice, such that no obvious defects in CatS-mediated scratching are observed. For instance, Petrus et al. (2007) found that CFA-induced hyperalgesia could be reduced in wild-type mice treated with a TRPA1 inhibitor, while mice lacking functional TRPA1 receptors still displayed considerable CFA-induced hyperalgesia. Changes in the expression of other TRP channels in DRGs and other cell types are thought to be responsible for this, although these have yet to be demonstrated. However, a similar compensatory mechanism may result in CatS-induced scratching behaviour in TRPA1 KO mice, even in the absence of calcium responses in these DRGs *in vitro*. Furthermore, because TRPV1 and TRPA1 are also reported to be expressed on skin keratinocytes and mast cells as well as sensory neurons, it is possible that in behavioural studies the presence or absence of these channels on non-neuronal cells could also be mediating an indirect effect on CatS-induced scratching in behavioural studies, which would not be detected in neuronal calcium imaging experiments (Atoyán et al., 2009; Biro et al., 1998; Inoue et al., 2002; Oh et al., 2013; Southall et al., 2003). Thus, although CatS did not cause calcium responses in neurons cultured from TRPA1 KO mice, itch sensations and scratching behaviour could still occur, for instance, via the release of histamine from mast cells and sensitisation or compensation of TRPV1 expressed on neurons and other cell types.

To conclude, CatS causes inward currents and increased calcium fluxes in a sub-population of murine DRGs. Most of these neurons responded to TRPV1 and TRPA1 agonists, and

responses to CatS were reduced in DRGs cultured from TRPV1 and TRPA1 KO mice, suggesting these neurons belong to a subset of nociceptors, as would be expected for pruriceptors. Furthermore, CatS was able to sensitise these receptors, increasing the percentage of neurons that responded to application of either capsaicin or mustard oil. CatS is likely to mediate at least some of its effects via PAR2, since calcium fluxes to CatS were reduced in the presence of a PAR2 antagonist. However, a number of questions remain unanswered, such as whether these responses reflect the signalling of itch or pain sensations (or both), the mechanism by which CatS sensitises TRPV1 and TRPA1, and whether sensitisation of TRPV4 is also involved.

Chapter 4

Activation of dorsal horn neurons and release of itch-related peptides by intraplantar Cathepsin S

4.1 Introduction

Activation of primary afferent neurons by pruritogens causes release of neurotransmitters and neuropeptides from their central terminals in the dorsal horn of the spinal cord, in turn activating interneurons and projection neurons to result in transmission of the itch signal to higher centres of the CNS. We have demonstrated that CatS could activate primary sensory neurons that are likely pruriceptors belonging to a subset of nociceptors, and that activation may occur via PAR2. Activation of PAR2 using trypsin and synthetic agonists has already been demonstrated to cause the release of the neuropeptides CGRP and substance P from C-fibre terminals (Steinhoff et al., 2000). However, whether CatS-mediated activation of primary afferents also causes neurons in the spinal cord itch circuitry to become activated had not yet been addressed.

Chapter Objectives

The aim of this chapter was to test the hypothesis that activation of pruriceptors by CatS in the periphery results in the release of NPPB by the central terminals of sensory neurons, in turn activating spinal cord dorsal horn neurons. To address this aim, we first examined whether intradermal injection of CatS resulted in neuronal activation in the dorsal horn of the spinal cord. We then confirmed expression of the itch-related neuropeptides NPPB and GRP in the mouse DRG and spinal cord. Next, we investigated whether CatS would cause the release of NPPB from primary sensory neurons in DRG culture as well as in the dorsal horn following intraplantar injection of the protease. We focused on expression and release of NPPB from DRG cells, as there is much evidence of the role of this neuropeptide in the itch circuitry and it is likely to be released from the afferents of primary sensory neurons following non-histaminergic pruritic stimuli where it would then result in activation of neurons in the dorsal horn of the spinal cord, providing a link between CatS-induced responses of primary afferent neurons and activation of dorsal horn neurons. As a positive control, the expression of CGRP was also investigated as a neuropeptide that is co-expressed with NPPB and released from these cells.

4.2 Methods

4.2.1 Quantitative polymerase chain reaction (qPCR)

Dissection of murine DRGs was performed as described in Chapter 3. 30 DRGs were removed from each mouse. Total RNA was extracted using Trizol reagent (Ambion, Life Technologies, UK) and the PureLink RNA Mini Kit (Ambion, Life Technologies, UK), according to the manufacturer's protocol. Total RNA concentration was measured using the NanoDrop spectrometer. 1000 ng RNA was used to synthesise first strand DNA using the Superscript VILO cDNA Synthesis Kit (Invitrogen, UK) according to the manufacturer's protocol. Expression levels of NPPB and GRP were analysed, using β -actin as a reference transcript. Amplification was performed with a LightCycler 480 (Roche) using SYBR Green I Master (Roche). The primers used are given in Table 4.1. The instrument was programmed as follows: 95°C for 5 minutes and 45 cycles of 3 steps of 10 seconds each, including denaturing at 95°C, annealing at 60°C, and primer extension at 72°C. Samples were run as duplicates, with 18S as the housekeeping gene. Samples in which the melting curve had more than one peak were excluded from analysis. Data was analysed using LightCycler 480 software (version 1.5.1). The relative gene expression level was calculated according to the $2^{-\Delta Ct}$ method, where Ct represents the threshold cycle.

Table 4.1: Primers used for NPPB, GRP, and β -actin in qPCR

Genes	Forward Sequence	Reverse Sequence	Reference
NPPB	GTTTGGGCTGTAACGCACTG	CAGAGCTGGGGAAAGAGACC	Solorzano et al., 2015
GRP	CCGGTGTGACAGGCGCAG	TCAGCCGCATACAGGGACGG	Solorzano et al., 2015
β-actin	GGCTGTATTCCCCTCCATCG	CCAGTTGGTAACAATGCCATGT	Jiang et al., 2017a; Veres-Szekely et al., 2017

4.2.2 Enzyme-linked immunosorbent assay (ELISA) for natriuretic polypeptide B

Culture of murine DRGs was performed as described in Chapter 3 with 5,000 – 6,000 cells per coverslip. DRGs were cultured overnight followed by stimulation with capsaicin (1 μ M, Sigma, UK) or DMSO (0.01%, Sigma, UK) in the presence of phosphoramidon (1 μ M, Sigma, UK), added to prevent potential digestion of NPPB by endogenous endopeptidases, in HEPES at pH7.4 (HEPES, 10 mM, Sigma, UK; NaCl, 150 mM, Sigma, UK; KCl, 5 mM, Sigma, UK; MgCl₂,

1 mM, G Biosciences, USA; CaCl₂, 1 mM, Fisher Scientific, UK; glucose, 5.55 mM, Sigma, UK). NPPB content in cell media was measured using an ELISA for murine NPPB (Cloud-Clone Corp., USA), according to the manufacturer's protocol. All samples were run in duplicate. The optical density of each well was determined at 450 nm wavelength using a FLUOstar Omega Spectrophotometer (BMG Labtech, UK). A standard curve of 1.37 pg/ml to 1,000 pg/ml was generated using a serial dilution of the stock standard provided by the manufacturer, and the concentration of NPPB released from the samples into the supernatants was determined from the standard curve.

4.2.3 Immunohistochemical staining

Following completion of behavioural experiments, mice were anaesthetised with sodium pentobarbital (Euthanol, 100 mg/kg body weight) and transcardially perfused with 0.9% saline followed by 4% paraformaldehyde in 0.1 M phosphate buffer. Tissues were removed and post-fixed for 2 hours in 4% paraformaldehyde at 4°C and cryoprotected in 20% sucrose in 0.1 M phosphate buffer for 24 hours at 4°C. Tissues were then frozen in OCT embedding medium (VWR, UK) and stored at -80°C. Using a cryostat (Bright Instruments, UK), DRG and TG sections (7 µm thick) were cut, while lumbar spinal cord tissues were transversely sectioned at 20 µm, and mounted onto 25 mm x 75 mm x 1 mm microscopic glass slides (VWR, UK). Slides were stored at -20°C.

Tissue sections were rehydrated in PBS for 10 minutes prior to staining. For staining with NPPB, β-III-tubulin, and IB4, antigen retrieval was performed using citrate antigen unmasking solution (Vector Laboratories, USA) diluted 1:100 in H₂O for 30 minutes at 80°C, followed by blocking in 2% milk for 30 minutes at room temperature. Unless being used for co-staining with NPPB, tissues were blocked in 1% BSA + 0.1% NaN₃ + 0.2% Triton X blocking buffer at room temperature for 1 hour for staining with CGRP. A similar blocking buffer comprising 1% BSA + 0.1% Triton X was used to block tissues stained with pERK. Tissues were then incubated overnight at room temperature in primary antibody diluted in the appropriate blocking buffer, followed by washes and incubation for 2 hours at room temperature in secondary antibody diluted in the appropriate blocking buffer (Table 4.2). A minimum of three washes in PBST was performed after each antibody incubation. Sections were mounted in Vectashield mounting medium with DAPI (Vector Laboratories, USA). A 22 x 55 mm coverslip (Academy Science, UK) was placed over the slide and sealed with nail varnish. Images were taken using a Zeiss Axioplan 2 fluorescent microscope and Axiovision

version 4.8.2 software (Zeiss, UK) or a Zeiss LSM 710 confocal microscope (Zeiss, UK). A minimum of three tissue sections per animal were acquired.

Table 4.2: Table of primary and secondary antibodies used for immunocytochemistry

Primary	Concentration	Secondary	Concentration
Goat anti-NPPB, V-17 (Santa Cruz Biotechnology Inc, UK)	1:500	Donkey-anti-goat IgG- conjugated AlexaFluor 488 (Molecular Probes, USA)	1:500
Sheep-anti-CGRP, CA1137 (Enzo Life Sciences, USA)	1:1000	Donkey-anti-sheep IgG- conjugated AlexaFluor 546 (Molecular Probes, USA)	1:500
Rabbit-anti- β -III-tubulin, ab18207 (Abcam, UK)	1:2000	Donkey-anti-rabbit IgG- conjugated AlexaFluor 546 (Molecular Probes, USA)	1:500
IB4, L2140 (Sigma, UK)	1:100	Extra-avidin TRITC (Sigma, UK)	1:400
Rabbit-anti-pERK, 4370 ICII Signaling Technology, USA)	1:400	Goat-anti-rabbit IgG- conjugated AlexaFluor 488 (Molecular Probes, USA)	1:1000

4.2.4 In-situ hybridisation

NPPB mRNA in DRG sections was labelled using fluorescent in-situ hybridisation. Various oligonucleotide sequences were designed from mouse NPPB cDNA (GenBank accession number NM_008726) as well as scramble sequences. Sequences were 33 nucleotides in length and BLAST searches were performed check whether they could potentially anneal to similar sequences. Sequences that did not form dimers and had weak or no secondary structures were selected for use. The oligonucleotides in table 4.3 were selected for testing and were ordered from Sigma (UK) and diluted to 1 μ M before use. Oligonucleotides were labelled with biotin-11-dUTP using the biotin 3' end DNA labelling kit (Thermo Scientific, UK) according to the manufacturer's protocol.

Table 4.3: Oligonucleotide probes used for in-situ hybridisation

<i>NPPB Primers</i>			
Primer Number	Sequence	T _m	CG%
190	CCTACAACAACCTTCAGTGC GTTACAGCCCAAAC	76.1	48.5
263	GCTTGAGATATGTGT CACCTTGG AATTTGAGG	74.2	42.4
377	GAGCTGTCTCTGGGCCATTTCTCCGACTTTTC	79.9	54.5
380	CTGTCTCTGGGCCATTTCTCCGACTTTTCTCT	78.3	51.5
<i>Scramble Primers</i>			
Primer Number	Sequence	T _m	CG%
15	CCCAAACCTTCACTCAACATTGTTACCATGTAG	73.1	42.5
16	ACAAAGAGACTTTAGTCTCCCATTCCTCTGGA	74.6	45.5

To investigate whether oligoprobes would hybridise to RNA present in tissues, the probes were tested on sections that had been treated with RNase (1x, Sigma, UK) at 37°C for 30 minutes or left untreated. Sections were then dehydrated in 70%, 95%, and 100% ethanol and left to dry. Meanwhile, oligoprobes were diluted 1:40 in hybridisation buffer (formamide 50%, Sigma, UK; dextran sulfate 10%, Sigma, UK; 0.1% SDS, Sigma, UK; salmon sperm DNA, 300 ng/ml, Sigma, UK; saline-sodium citrate (SSC) buffer, 2x, Sigma, UK). The final concentration of labelled oligoprobe was 2.5 nM. Oligoprobes were placed on a heat block at 65°C for 15 minutes and kept on ice before use. The prepared oligoprobe was added to the tissue sections on the slides and an ethanol-treated glass coverslip was lowered over each slide to prevent evaporation and loss of the oligoprobe. Slides were then incubated overnight at 50°C. The following day, slides were washed in SSC buffer and PBS (according to the schematic in Figure 4.1). Avidin-Biotin Complex (ABC) (Vector Laboratories, USA) was prepared by diluting according to the manufacturer's protocol, and sections were incubated in ABC for 30 minutes at room temperature. Biotinyl tyramide (NEN Life Science, UK) was prepared and diluted according to the manufacturer's protocol, with which sections were incubated for 10 minutes. Sections were then incubated in Extra-avidin FITC (1:400 dilution, Sigma, UK) diluted in 0.1% PBS-T for to 2 hours at room temperature. After a final set of washes, sections were either mounted in Vectashield mounting medium with DAPI and covered with a 22 x 55 mm coverslip, or underwent antibody staining as for above. Sections were imaged using a Zeiss Axioplan 2 fluorescent microscope and Axiovision version 4.8.2 software. A minimum of three tissue sections per animal were acquired.

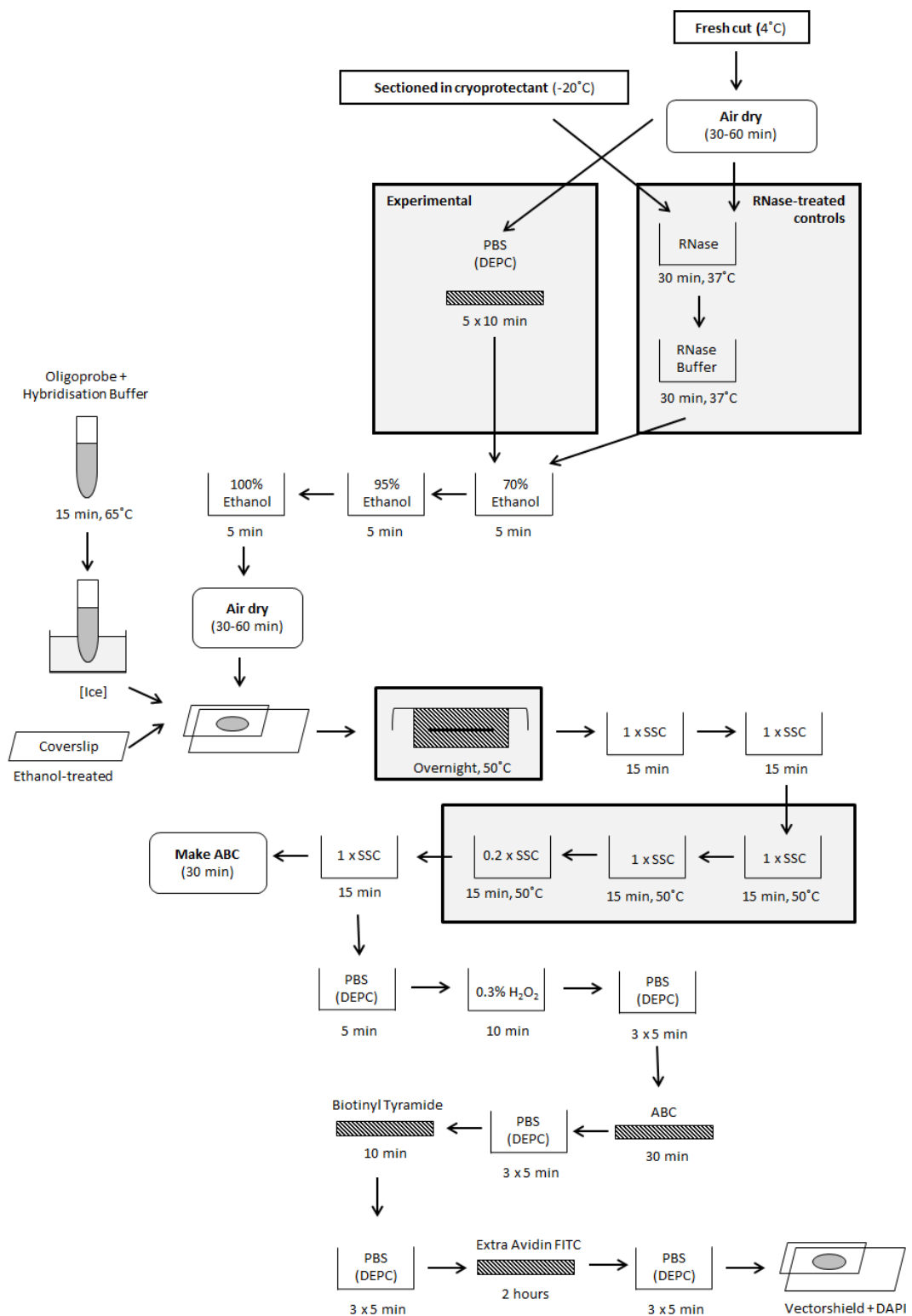


Figure 4.1: Schematic of fluorescent in-situ hybridisation staining protocol

Mouse DRG tissue sections underwent in-situ hybridisation for NPPB using biotin-labelled oligoprobes. All solutions, including RNase buffer, phosphate buffered saline (PBS), saline-sodium citrate (SSC), Avidin-Biotin Complex (ABC), and biotinyl tyramide were prepared using diethyl pyrocarbonate (DEPC) treated water.

4.2.5 Quantification of staining

Sensory ganglia

For quantifying staining of neurons in sensory ganglia sections, the total number of neurons was first obtained by identifying based on their shape and size or β -III-tubulin staining. Individual neurons were labelled and a threshold was established for determining whether cells were positively stained. The threshold was based on the intensity of staining of the cell and a cell was classified as positively stained if the intensity was at least 40 % and 50 % greater than the average intensity of negatively-stained cells, for NPPB and CGRP, respectively. Intensity was measured using Image J software. Because of high background staining in some images, a manual count was also performed for some images with the experimental group blinded, in addition to the threshold count. An average value for the percentage of positively-stained cells for each animal was calculated.

Spinal cord

Release of neurotransmitters from the central terminals of primary afferent neurons was measured by quantification of staining for neurotransmitters in the spinal cord dorsal horn, following a method modified from Lever et al. (2001). Quantitative assessment of immunoreactivity (IR) in the spinal cord was performed by determining the intensity of fluorescence in laminae I and II of the dorsal horn with the experimental group blinded. Three boxes measuring 100 x 100 pixels were spaced equally across the superficial laminae of the dorsal horn. Using Axiovision SE64 4.9.1 software (Zeiss, UK), the mean intensity of each of the boxes was determined. The background intensity for each image was determined using a 100 x 100 pixel box and was subtracted from the intensity values obtained. An average value for fluorescence intensity for the superficial dorsal horn was then calculated.

Quantitative assessment of immunoreactivity in the spinal cord was also performed by determining area of fluorescence in laminae I and II of the dorsal horn with the experimental group blinded. This method was performed in two different ways. The first involved placing three boxes measuring 100 x 100 pixels equally across the superficial laminae of the dorsal horn. Using Image J software, a threshold intensity was set such that the immunoreactivity areas were highlighted, while areas that were free from staining were not highlighted. This threshold was kept the same for all images analysed for each experiment. The percentage of area occupied for in each 100 x 100 pixel box was

determined and an average value for fluorescence area for the superficial dorsal horn was then calculated. The second method was similar to this but involved outlining the entire area of laminae I and II of the dorsal horn to which a threshold was set to determine areas of immunoreactivity.

4.2.6 Behavioural testing

Thermal hyperalgesia

Thermal withdrawal thresholds were assessed using the radiant heat (Hargreaves) test. Mice were acclimatised in 8 x 5 x 10 cm Perspex cubicles over a glass surface for 60 minutes prior to testing. Infrared radiation of 80-100 mWatts/cm² was applied to the plantar surface of the right hindpaw only. Intensity was calibrated to give an average withdrawal response after 10 seconds, while a cut-off time of 20 seconds was used to avoid tissue damage. The averages of three applications to each paw were recorded, with at least 5 minutes between recordings.

Mechanical hyperalgesia

Mechanical withdrawal thresholds were assessed using von Frey filaments (Linton Instruments, UK) applied to the plantar surface of the hind paw. Mice were acclimatised in 8 x 5 x 10 cm cubicles over a wire mesh for 60 minutes before testing. Von Frey filaments ranging between 0.008 g and 1 g were applied to the plantar surface of each hind paw until the filament bent, and was then held in place for 3 seconds or until the paw was withdrawn. Reflexes associated with movement or grooming were excluded. The “up-down” method was used to calculate the 50% paw withdrawal threshold (Chaplan et al., 1994). Assessments started with the 0.07 g filament. Upon observing a positive withdrawal response to application of the filament, the next lower force filament was then applied. In contrast, an absence of withdrawal response to application of the filament resulted in application of the next higher force filament, up to 1 g. Responses to four subsequent filaments were assessed in this way according to the up-down sequence.

Drug administration

2.5 S murine NGF (Alomone, Isreal) was dissolved in sterile 0.9% saline and 20 µg/100 µl was injected subcutaneously into the nape of the neck using a 25 G needle every second day for up to 12 days. Thermal hyperalgesia was assessed one hour after injection of NGF or saline vehicle. hr-CatS (Medivir, Sweden) was diluted in sterile 0.9% saline and 1 µg/10 µl was

injected intraplantar into the right hind paw using a 25 G needle. Mechanical hyperalgesia was assessed 30 minutes or 3 hours after injection of CatS or saline vehicle. Capsaicin (Sigma, UK) was dissolved in ethanol and Tween-80 and diluted in sterile 0.9% saline. Capsaicin (1 µg/10 µl) was injected intraplantar into the right hind paw using a 25 G needle. Mechanical hyperalgesia was assessed 30 minutes or 3 hours after injection of capsaicin or saline vehicle.

4.2.7 Statistical analysis

All data were analysed and graphs were generated using GraphPad Prism 5 (Graphpad Software Inc., USA) and are shown as mean ± standard error of the mean (SEM). $P \leq 0.05$ was set as the level of statistical significance for all experiments.

qPCR results were analysed using a Student's t-test to compare expression of NPPB with that of GRP.

For immunohistochemical and in-situ hybridisation data, statistics was performed on raw data. For cell number counts, fluorescence intensity, and fluorescence area measurements, average values were obtained for each animal. A mean value for each experimental group was obtained and groups were compared with one another using Student's t-test or one-way ANOVA followed by Bonferroni post-tests to measure differences between two or more groups, respectively.

For the assessment of thermal sensitivity, data was calculated from the averages of three readings per mouse and expressed as the average time for paw withdrawal for each group. Data were analysed using two-way ANOVA with Bonferroni post-hoc test to compare between groups at different time points.

For assessment of mechanical hyperalgesia, data are expressed as the average 50% paw withdrawal thresholds (PWT) for both hind paws, calculated using the method as described by Dixon, 1980. Data were analysed using one-way ANOVA with Bonferroni post-hoc test to compare between groups at each time points.

4.3 Results

4.3.1 Intraplantar injection of Cathepsin S activates cells in the dorsal horn

Peripheral injection of pruritogens, including histamine and SLIGRL-NH₂, has previously been demonstrated to activate cells in the dorsal horn (Akiyama et al., 2009b; Akiyama et al., 2016a; Bell et al., 2016; Jinks et al., 2002; Kiguchi et al., 2016; Nakano et al., 2008; Nojima et al., 2003; Zhang et al., 2014). Activation of primary afferent fibres by pruritogens results in release of neurotransmitters and neuropeptides from their central terminals, which in turn activating cells in the dorsal horn. Activation of these neurons has also been demonstrated to be required for scratching behaviours in mice, as preventing activation of these cells inhibits transmission of itch signals. For instance, Zhang et al. (2014) reported that intrathecal injection of the U0126 (which inhibits phosphorylation of ERK) reduces histamine-induced scratching behaviour, suggesting activation of neurons in the dorsal horn is required for transmission of itch signals and/or the behavioural scratching responses that occur as a consequence of activation of pruriceptors. We therefore performed a preliminary study to investigate whether neurons in the dorsal horn responded to intraplantar injection of hr-Cathepsin S or capsaicin by expressing pERK. Whilst capsaicin did not result in changes in pERK expression, intraplantar CatS was associated with a significant increase in the number of cells positive for pERK compared with saline or capsaicin (Figure 4.2). The lack of effect of capsaicin is likely because we stained for pERK 30 minutes after injection of capsaicin, while peak activation of pERK in the dorsal horn is reported to occur at 2-10 minutes after injection of capsaicin (Ji et al., 1999).

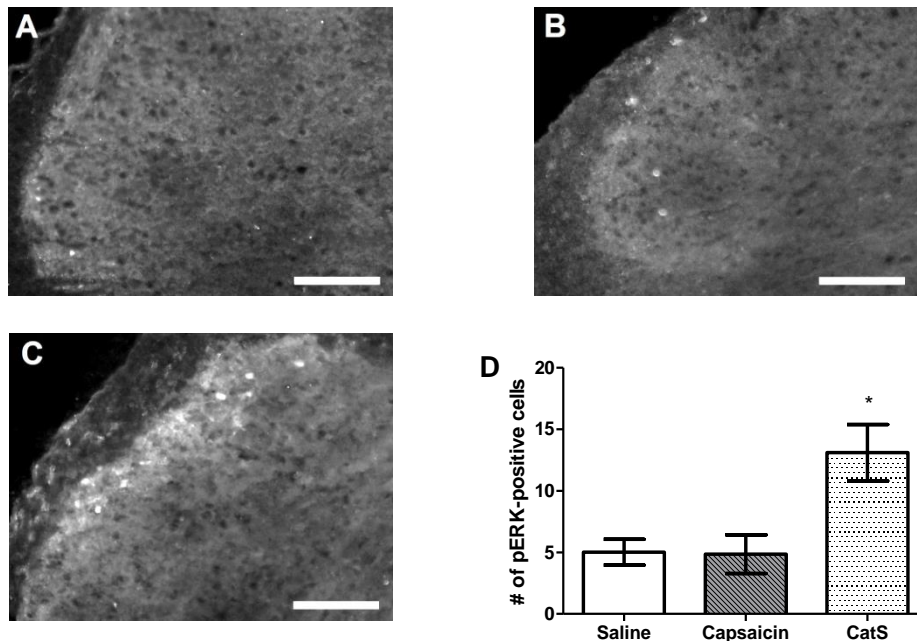


Figure 4.2: Injection of Cathepsin S into the hindpaw resulted in an increase in the number of pERK positive cells in the ipsilateral side of the dorsal horn of the spinal cord

Representative image of dorsal horn stained for pERK following injection of saline (A), capsaicin (1 µg/10 µl) (B), or CatS (1 µg/10 µl) (C) Scalebar = 100 µm. Quantified data of number of pERK-positive cells in the dorsal horn 30 minutes after intraplantar injection of the substances indicated (D). $n = 3, 4$ per group, data are mean \pm SEM. * $p \leq 0.05$, One-way ANOVA followed by Bonferroni post-hoc test.

4.3.2 Itch-related peptides are expressed in dorsal root ganglia and spinal cord

To investigate whether activation of dorsal horn neurons following injection of CatS was associated with neuropeptides released from primary afferent fibres acting on these neurons, we had to confirm expression of these neuropeptides in sensory neurons. GRP and NPPB are two neuropeptides that are proposed to be involved in itch. Both have been reported to be expressed in DRGs and released from the terminals of primary sensory neurons, where they bind to their respective receptors on interneurons located within the dorsal horn of the spinal cord (Abdelalim et al., 2016; Goswami et al., 2014; Kiguchi et al., 2016; Liu et al., 2014b; Mishra and Hoon, 2013; Pitake et al., 2017; Solorzano et al., 2015; Sun and Chen, 2007). Using qPCR, we therefore investigated whether mRNAs of these neuropeptides were expressed in mouse DRGs. We observed that both NPPB and GRP were expressed in DRG tissues (Figure 4.3, Table 4.4). Expression of NPPB was greater than that of GRP, although this difference in expression was not significant.

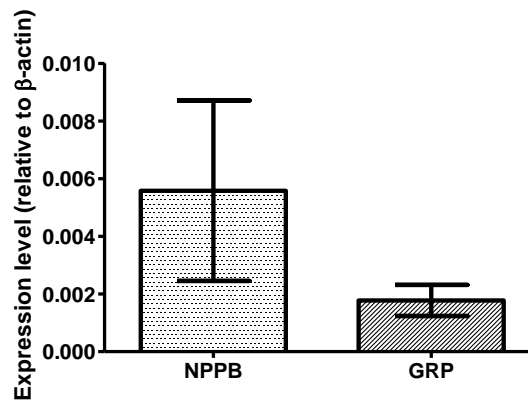


Figure 4.3: Expression of NPPB and GRP mRNA in mouse DRG tissues

Expression of NPPB and GRP mRNA extracted from mouse DRG relative to that of β -actin. $n = 4$; 2 replicates per sample, data are mean \pm SEM. No significance, unpaired Student's t -test.

Table 4.4: Ct values for NPPB and GRP expression

Average Ct values of samples run as duplicates.

	β -actin	NPPB	GRP
Sample 1	18.305	30.595	27.7
Sample 2	18.01	30.065	28.89
Sample 3	18.5	25.16	27.49
Sample 4	20.055	26.435	28.375

Expression of NPPB mRNA was also confirmed in mouse TG and DRG using in-situ hybridisation. We first tested different oligoprobes for NPPB in the presence and absence of RNase. Of the different oligoprobes tested, probe N263 gave the best results, with approximately 11% of cells staining positive for NPPB mRNA and significantly reduced in the presence of RNase (Figure 4.4 A – C). The number of cells positive for NPPB mRNA was similar to that previously reported in sensory ganglia (Huang et al., 2018; Mishra and Hoon, 2013). This probe was thus used for all further in-situ hybridisation experiments. Probe N380 did stain some cells, but a lower percentage than that stained by the N263 probe (Figure 4.4 D – F). The remaining probes did not give reliable staining. The scramble probe did not stain many cells (Figure 4.4 G – I).

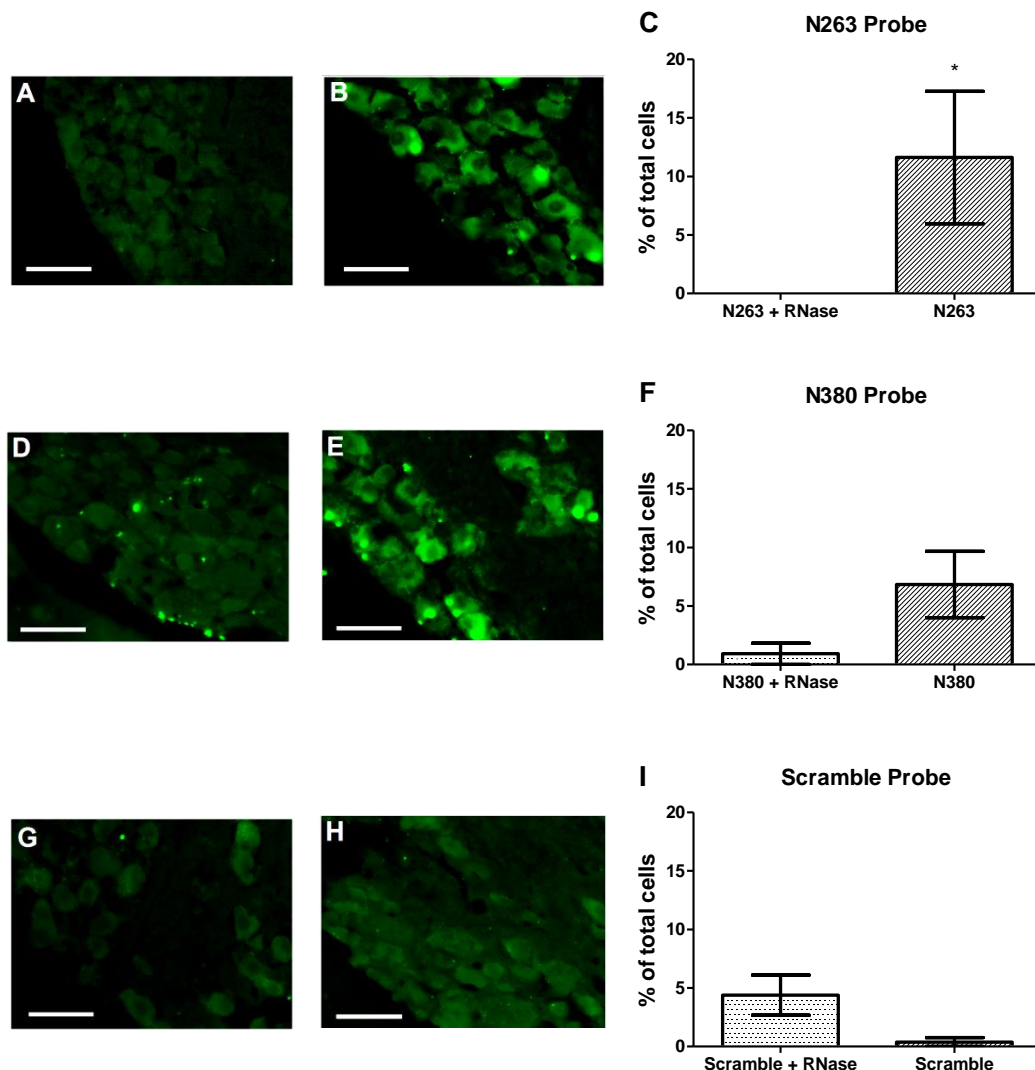


Figure 4.4: Expression and quantification of NPPB mRNA in mouse TG

Representative image of staining obtained in mouse TG tissue with the N263 probe in the presence (A) or absence (B) of RNase, the N380 probe in the presence (D) or absence (E) of RNase, or the scramble probe in the presence (G) or absence (H) of RNase. Quantified data of the percentage of cells in the TG stained for NPPB mRNA using the N263 (C), N380 probe (F), or scramble probe (I) in the presence or absence of RNase, $n = 6 - 8$, from 4 animals, data are mean \pm SEM. * $p \leq 0.05$, unpaired Student's t -test. Scalebar = 50 μ m.

Although we confirmed expression of NPPB mRNA in murine tissues, we also wanted to be able to confirm expression of NPPB peptide. This was achieved using antibody staining. In mouse TG, 7.5% of cells stained positive for NPPB peptide (Figure 4.5 A and B). Expression of NPPB peptide was also observed in the DRG (Figure 4.5 C) and in laminae I and II of the dorsal horn of the spinal cord (Figure 4.5 D). Attempts were made to stain for NPPB in the trigeminal nuclei of the brain stem, where the endings of the TGs are located, but this was

unsuccessful due to difficulties in locating the nuclei for processing and staining. We therefore proceeded with investigating expression of NPPN peptide in the dorsal horn only.

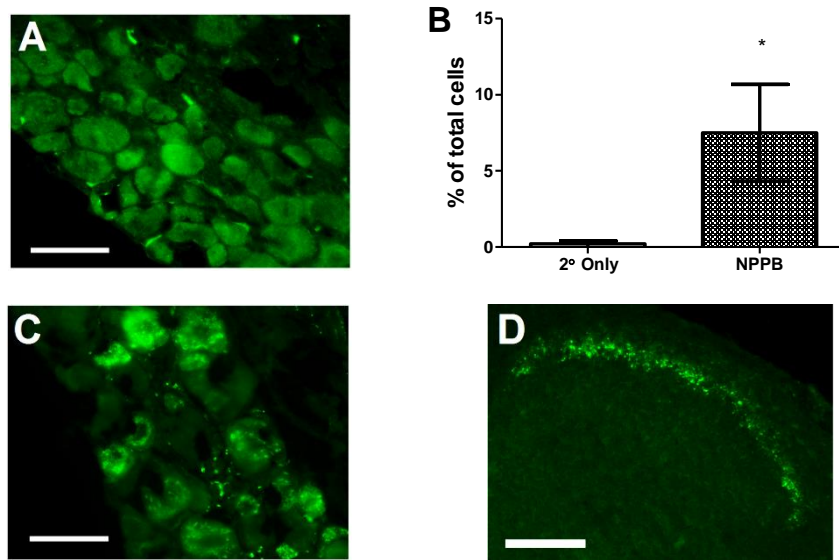


Figure 4.5: Expression of NPPB peptide in mouse TG, DRG, and spinal cord

Representative image of staining for NPPB peptide in mouse TG (A), DRG (C) and spinal cord (D) tissues. Scalebar = 50 μm in B and D, 100 μm in D. Quantified data (B) of the percentage of cells in the TG stained for NPPB peptide at 1:500 dilution. $n = 8$, from 4 animals, data are mean \pm SEM. * $p \leq 0.05$, unpaired Student's t -test.

To compare expression of NPPB mRNA with NPPB peptide, DRGs underwent staining using both in-situ hybridisation probes and antibodies. 13% of cells were positive for NPPB mRNA and less than 4% were positive for the scramble probe (Figure 4.6 D). 12% of cells were positive for NPPB peptide, which was not affected by the presence of the probe used for in-situ hybridisation (Figure 4.6 E). Of the cells that were positive for NPPB mRNA, about 71% were also positive for the NPPB peptide (Figure 4.6 F). More than 86% of the cells that were positive for both NPPB mRNA and peptide were small diameter cells with an area of less than 300 μm^2 (Figure 4.6 G).

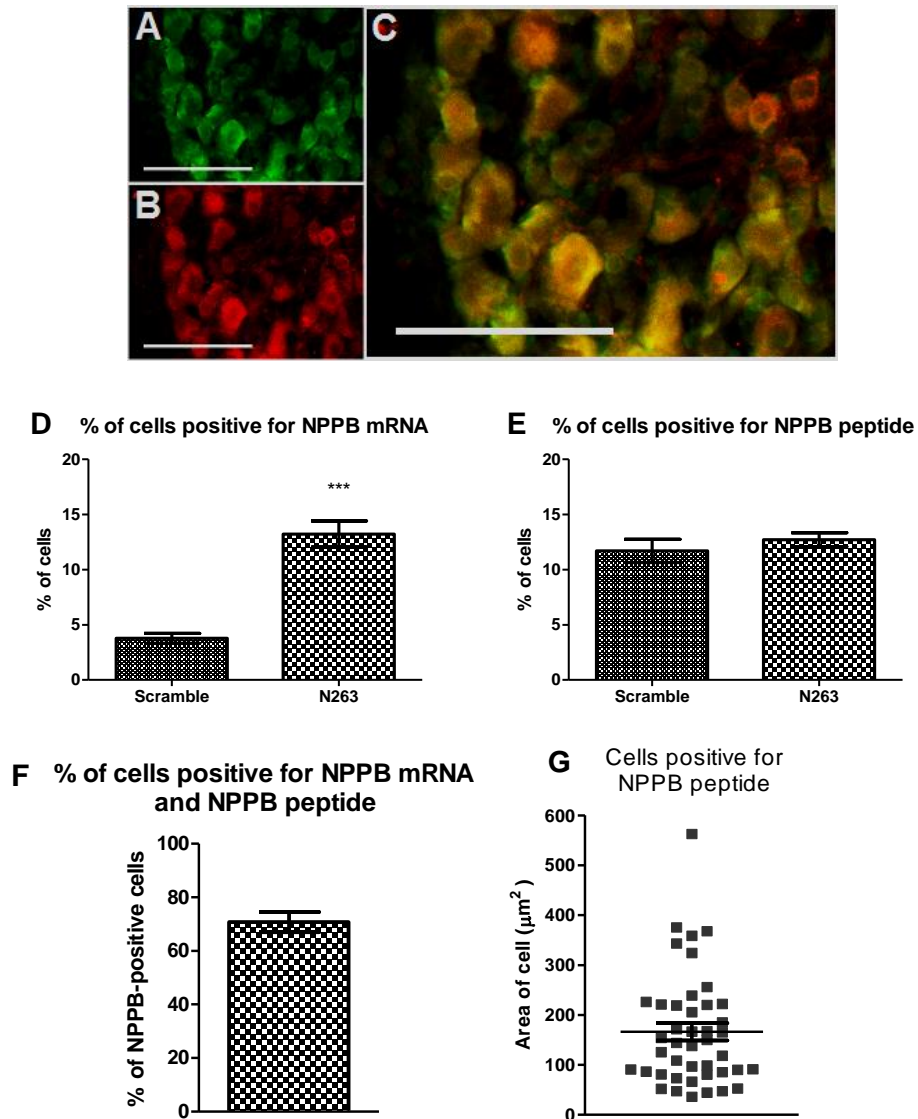


Figure 4.6: Quantification of NPPB mRNA and NPPB peptide in mouse DRG

A-C. Representative image of staining for NPPB mRNA using the N263 probe (green) and NPPB peptide (red) in DRG tissue. Scalebar = 100 μm. Quantified data of the percentage of cells in the DRG stained for NPPB mRNA (D), peptide (E), or both NPPB mRNA and peptide (F). Area of DRG cells positive for both NPPB mRNA and peptide (G). $n = 3$, from 3, 4 sections per animal, data are mean \pm SEM. *** $p \leq 0.001$, unpaired Student's t -test.

To investigate whether neurons that expressed NPPB belonged to the peptidergic population of sensory neurons, DRGs were co-stained for NPPB mRNA and CGRP peptide. 15% of cells were positive for NPPB mRNA and only 5.4% of cells were positive for the scramble sequence (Figure 4.7 D). 31-32% of cells were positive for the CGRP peptide, and the percentage of cells positive for CGRP peptide was not affected by the in-situ probe used (Figure 4.7 E). Of the cells that were positive for NPPB mRNA, 73% were also positive for

CGRP peptide (Figure 4.7 F). Almost 90% of the cells that were positive for NPPB mRNA and CGRP peptide were small diameter cells with an area of less than 300 μm^2 (Figure 4.7 G).

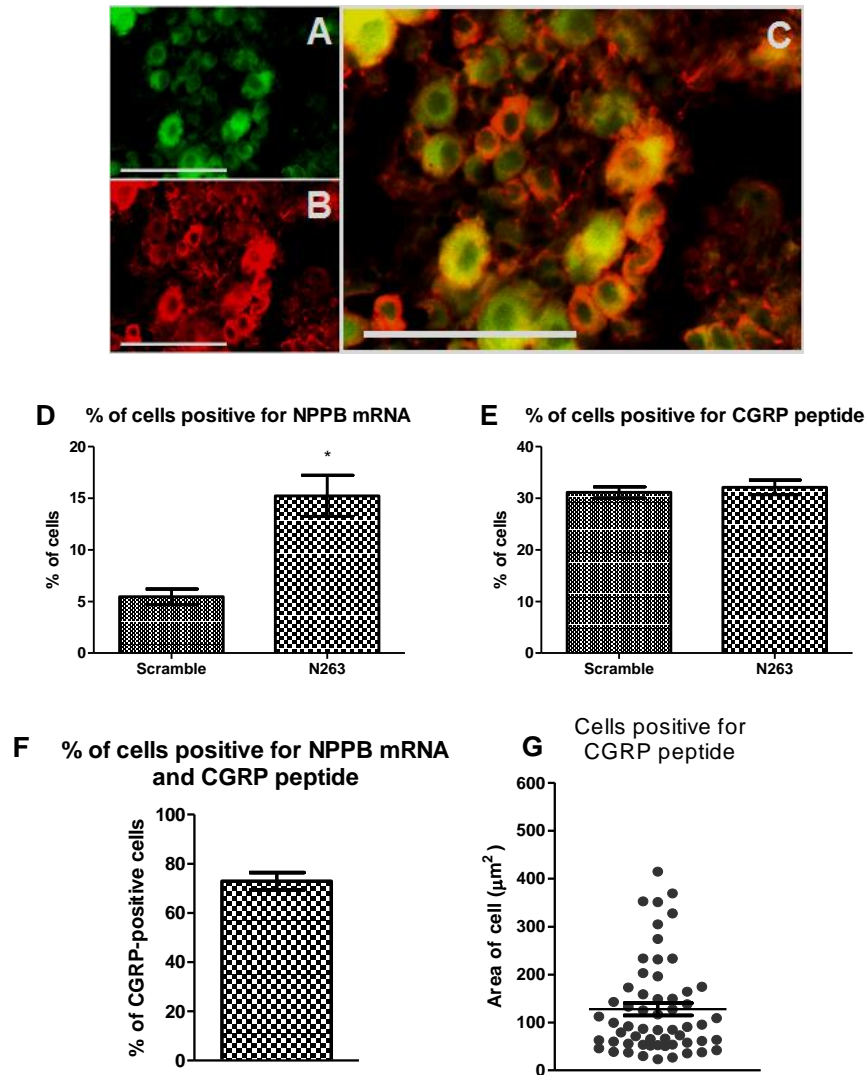


Figure 4.7: Quantification of NPPB mRNA and CGRP peptide in mouse DRG

A-C. Representative image of staining for NPPB mRNA using the N263 probe (green) and CGRP peptide (red) in DRG tissue. Scalebar = 100 μm . Quantified data of the percentage of cells in the DRG stained for NPPB mRNA (D), CGRP peptide (E), or both NPPB mRNA and CGRP peptide (F). Area of DRG cells positive for both NPPB mRNA and CGRP peptide (G). $n = 3$, from 3, 4 sections per animal, data are mean \pm SEM. * $p \leq 0.05$, unpaired Student's *t*-test.

We also investigated whether NPPB is expressed in the terminals of sensory neurons in the dorsal horn of the spinal cord, and evaluated whether expression could be up-regulated and release of neuropeptide could be determined by a reduction of expression using immunohistochemistry. NPPB peptide was detected in the outer laminae of the dorsal horn. However, co-staining of NPPB and CGRP peptides proved problematic, with complete co-

staining observed (Figure 4.8 C), suggesting cross reaction of the antibodies. Staining overall appeared to be more widespread than that observed with NPPB alone, and more similar to that obtained with CGRP. In contrast, co-staining of NPPB and IB4 revealed hardly any overlap of staining (Figure 4.8 F), suggesting that NPPB-positive nerve terminals likely comprise a different population of cells to the mainly non-peptidergic IB4-positive terminals.

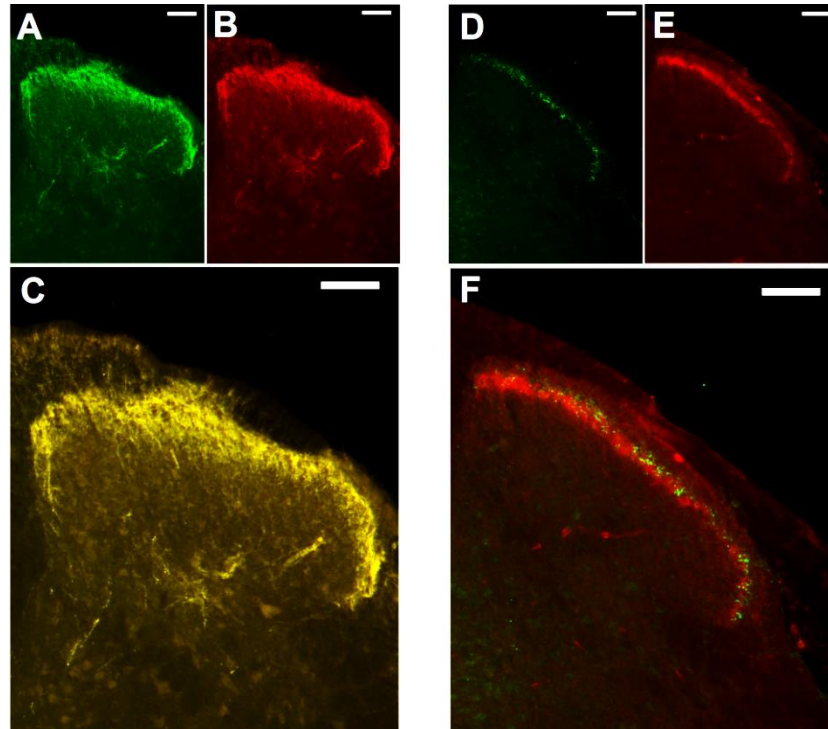


Figure 4.8: Expression of NPPB, CGRP, and IB4 peptides in the spinal cord dorsal horn

A-C. Representative images of dorsal spinal cord sections stained for NPPB (green) and CGRP (red), with co-staining for NPPB and CGRP (yellow). Scalebar = 100 μ m.

D-F. Representative images of dorsal spinal cord sections stained for NPPB (green) and IB4 (red), with co-staining for NPPB and IB4 (yellow). Scalebar = 100 μ m.

Upregulation of NPPB expression

After confirming expression of NPPB in murine tissues, we examined whether expression of NPPB could be increased following treatment with NGF. Previous work has shown that systemic injection of NGF results in increased sensitisation to thermal and mechanical stimuli (Alexander et al., 2013). In rodent DRG, NGF also causes increased expression of neuropeptides such as CGRP and substance P (Verge et al., 1995). We thus sought to investigate whether treatment with NGF would result in upregulation of NPPB in mouse DRGs, and therefore provide more peptide for our release experiments. As expected, mice injected with NGF (2.5S, mouse) exhibited a significant decrease in the response time to noxious thermal stimuli compared to those injected with saline, as early as one hour after

the first injection. This increased sensitivity to thermal stimuli was maintained for the duration of the experiment (Figure 4.9). Treatment with NGF resulted in a significant increase in the percentage of DRGs cells positive for NPPB from 9% to nearly 20% (Figure 4.10), suggesting up-regulation of peptide expression in neurons.

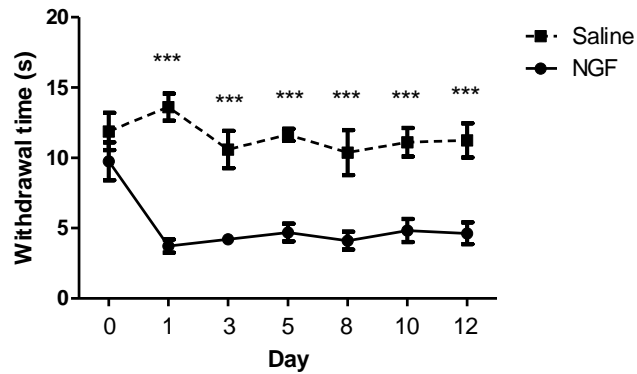


Figure 4.9: NGF-induced thermal hyperalgesia

The effect of NGF injected subcutaneously into nape of neck of mice 1 hour before testing of thermal sensitivity using the Hargreaves tests. $n = 4$ for both groups, averages of 3 readings from each animal, data are mean \pm SEM. *** $p \leq 0.001$, Two-way ANOVA followed by Bonferroni post-hoc test.

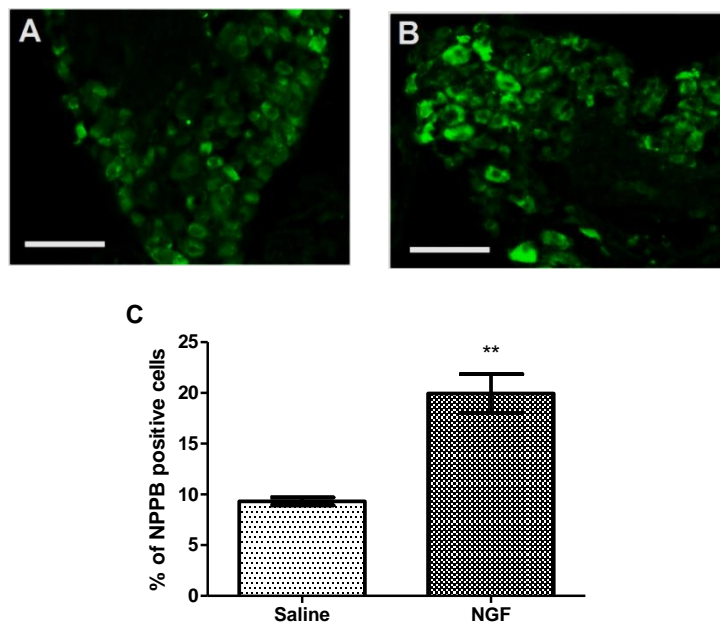


Figure 4.10: The effect of NGF on the expression of NPPB in DRGs

Representative image of staining for NPPB peptide in DRG of mouse injected with saline (A) or NGF (B). Scalebar = 100 μ m. NGF treatment for 2 weeks significantly increased expression of NPPB peptide in the DRGs (C). $n = 4$ for both groups, averages of 3, 4 sections from each animal, data are mean \pm SEM. ** $p \leq 0.01$, unpaired Student's t -test.

NPPB expression was observed in the outer laminae of the dorsal horn of the spinal cord. However, no differences in either intensity of staining or percentage of area stained were observed in spinal cords from mice injected with either NGF or saline (Figure 4.11). Spinal cords were also stained for CGRP peptide as a positive control. No differences in staining intensity were observed in spinal cords from mice injected with either NGF or saline (Figure 4.12).

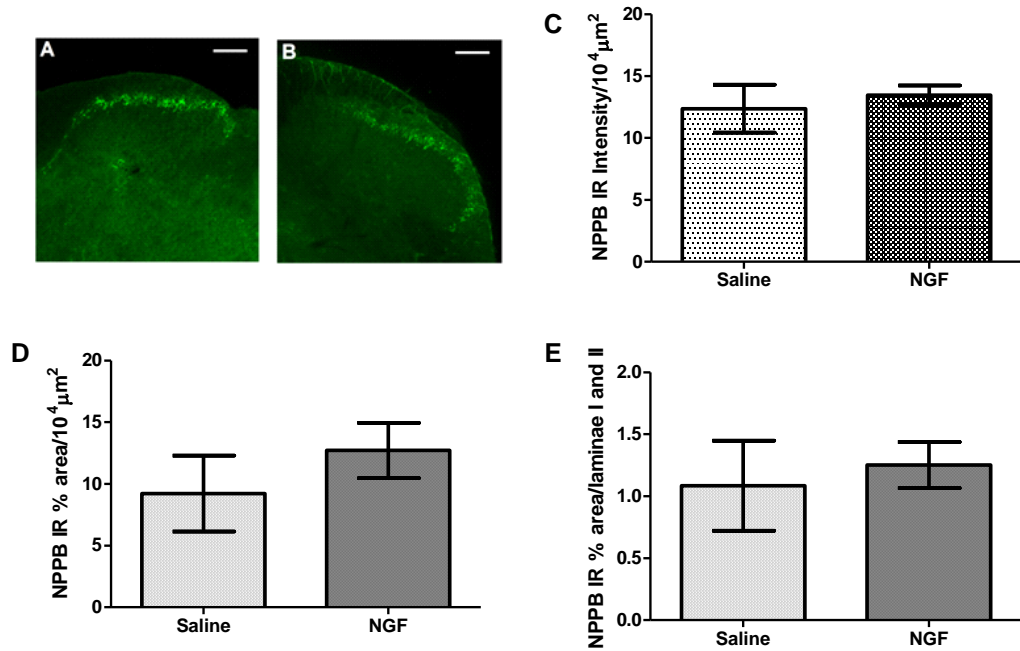


Figure 4.11: The effect of NGF on the expression of NPPB in the spinal cord

Representative image of mouse spinal cord dorsal horn stained for NPPB from mouse injected with saline (A) or NGF (B). Scalebar = 100 μm . NGF did not alter the expression of NPPB protein in the dorsal horn of the spinal cord, as measured by intensity (C) or area (D) using 100 x 100 pixel boxes, or the area of laminae I and II that were positively stained for NPPB (E). $n = 4$ for both groups, averages of 3, 4 sections from each animal, data are mean \pm SEM. No significance, unpaired Student's t-test.

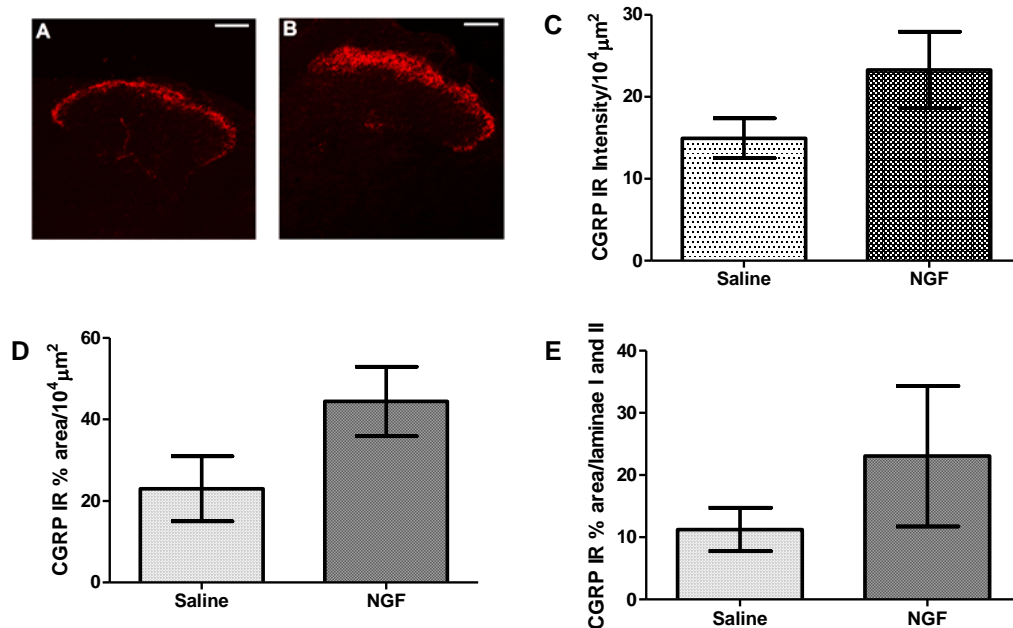


Figure 4.12: The effect of NGF on the expression of CGRP in the spinal cord

Representative image of mouse spinal cord dorsal horn stained for CGRP from mouse injected with saline (A) or NGF (B). Scalebar = 100 μm. NGF did not alter the expression of NPPB protein in the dorsal horn of the spinal cord, as measured by intensity (C) or area (D) using 100 x 100 pixel boxes, or the area of laminae I and II that were positively stained for CGRP (E). $n = 4$ for both groups, averages of 3, 4 sections from each animal, data are mean \pm SEM. * $p \leq 0.05$, unpaired Student's t -test.

4.3.3 Release of natriuretic polypeptide B from sensory neurons

After confirming the expression of NPPB mRNA and peptide in the DRG, we investigated whether release of this peptide from DRGs could be detected. A preliminary study was performed by measuring the concentration of NPPB released from cultured murine DRGs using an ELISA. Cells were incubated for 10 minutes before collection of the supernatant and measuring the concentration of NPPB in the supernatant. Cells were incubated twice in buffer (baseline 1 and 2), followed by a third incubation period in either DMSO (0.01%) or capsaicin (1 μM), followed by two more incubations in buffer (recovery 1 and 2). However, no NPPB was detected in the supernatant at any time point (Figure 4.13), suggesting the cells did not release NPPB under our stimulating conditions, or the concentration of the peptide was below the sensitivity of the assay. However, 1 μM capsaicin has previously been found to be a poor stimulator of CGRP release from cultured DRG neurons as measured using ELISA, while 100 - 250 nM capsaicin resulted in more robust release of CGRP (Calcott et al., 2011; Lu et al., 2017). We therefore cannot exclude the possibility that release of

NPPB from our DRG neurons was suboptimal and may have been increased using a different concentration of capsaicin.

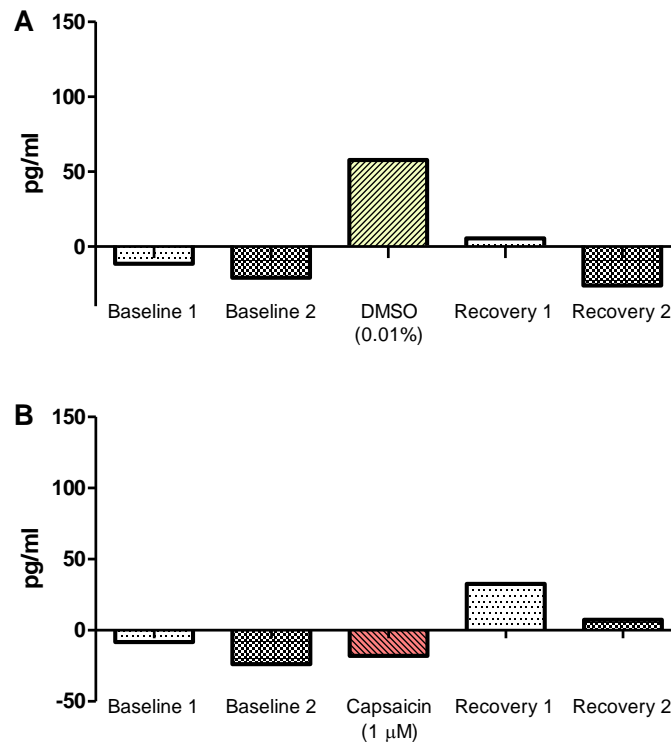


Figure 4.13: The release of NPPB was not detected from cultured DRGs

Preliminary study investigating NPPB release from DRGs measured by ELISA following stimulation with DMSO (A) or capsaicin (B). n=2; 2 wells per condition per mouse, samples run in duplicate, data are mean. No statistics performed.

Intraplantar injection of Cathepsin S and release NPPB in the spinal cord

Once we ascertained that NGF upregulated the expression of NPPB in the DRGs as well as CGRP in the spinal cord, we continued to investigate whether CatS could induce release of NPPB (and CGRP) by primary afferent fibres in the dorsal horn of the spinal cord. This was achieved by injection of human recombinant CatS (1 μg/10 μl) intraplantar into the hindpaw of mice and assessment of peptide expression in the dorsal horn by immunohistochemistry. To confirm the effect of CatS, mechanical hyperalgesia was tested at 30 minutes and 3 hours after injection using von Frey testing. As expected, mechanical hyperalgesia was detected in the ipsilateral paw of mice injected with CatS 30 minutes, but not 3 hours after injection (Barclay et al., 2007) (Figure 4.14). Mice injected with saline did not show any mechanical hyperalgesia at any of the time points (Figure 4.14).

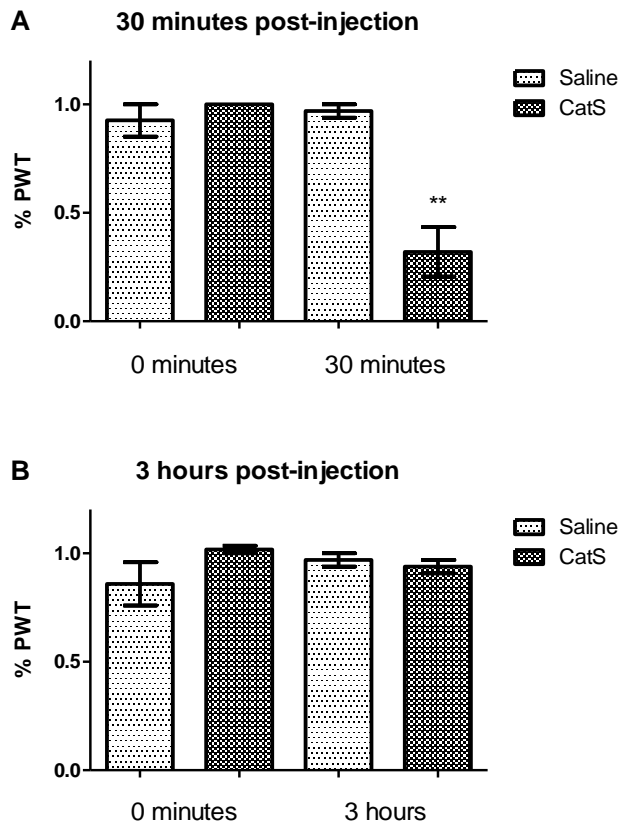


Figure 4.14: Cathepsin S induced mechanical hyperalgesia

Injection of CatS results in a decrease in paw withdrawal threshold (PWT) 30 minutes after injection (A). No changes in PWT are observed 3 hours after injection of CatS (B). n = 3 per group, data are mean ± SEM. No significance, One-way ANOVA followed by Bonferroni post-hoc test.

No changes in staining for NPPB were observed in either the ipsilateral or contralateral sides of mice injected with saline or CatS from tissues collected 30 minutes or 3 hours after injection (Figure 4.15). Similarly, no changes in staining for CGRP as a positive control were observed in either the ipsilateral or contralateral sides of mice injected with saline or CatS from tissues collected 30 minutes or 3 hours after injection (Figure 4.16), suggesting that our approach will need to be refined.

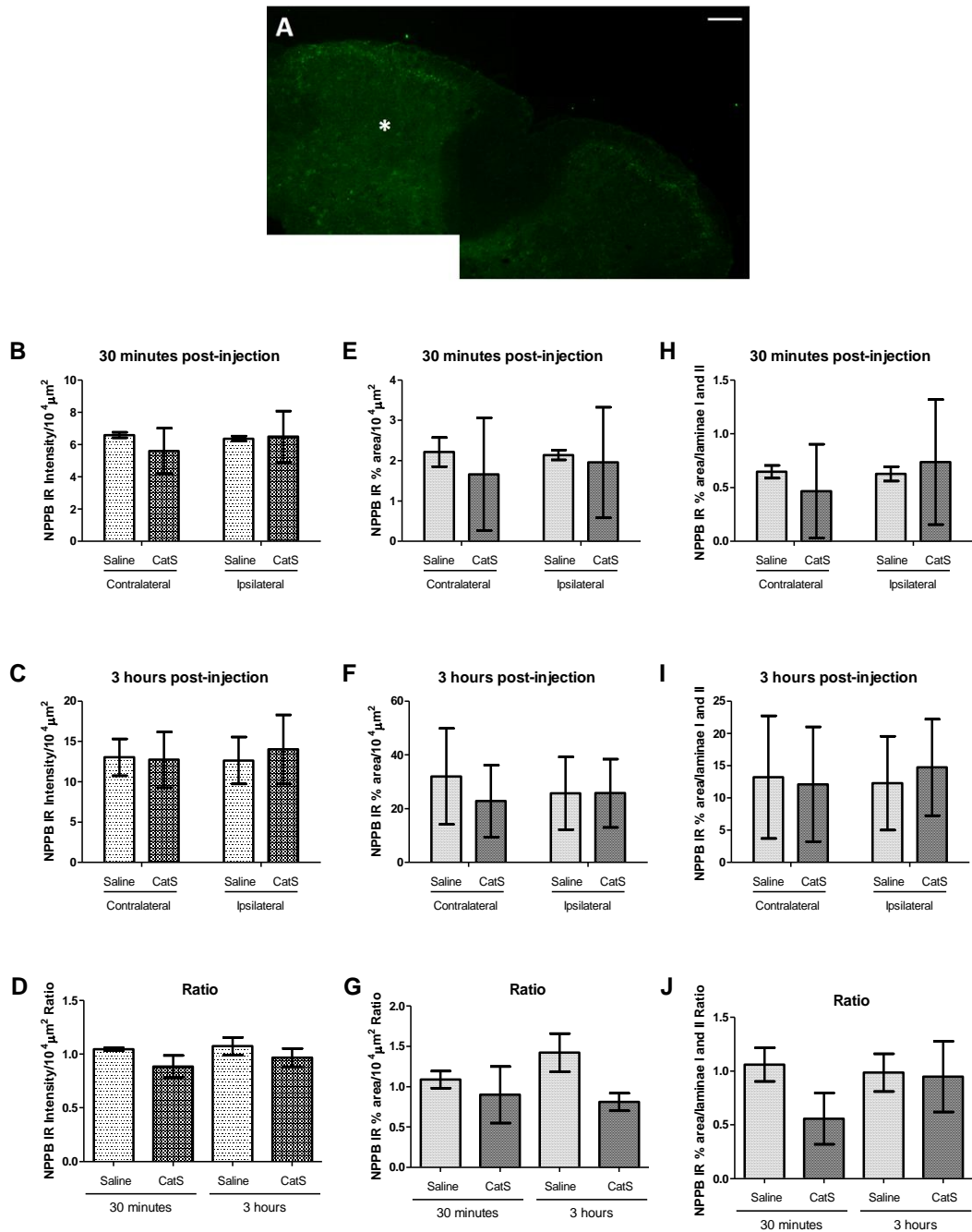


Figure 4.15: No effect of Cathepsin S on staining for NPPB in the spinal cord

Typical image of mouse spinal cord dorsal horn stained for NPPB, ipsilateral (injected) side indicated by asterisk. Scalebar = 100 μm . Injection of CatS 30 minutes (B, E, H) or 3 hours (C, F, I) before taking tissues did not alter the expression of NPPB protein in the dorsal horn of the spinal cord, as measured by pixel area or intensity using 100 x 100 pixel boxes, or the percentage of laminae I and II that were positively stained. No differences in the ratio of contralateral:ipsilateral NPPB staining using any of the quantification methods (D, G, J). $n = 3$ for all groups, averages of 3, 4 sections from each animal, data are mean \pm SEM. No significance, Two-way ANOVA followed by Bonferroni post-hoc test.

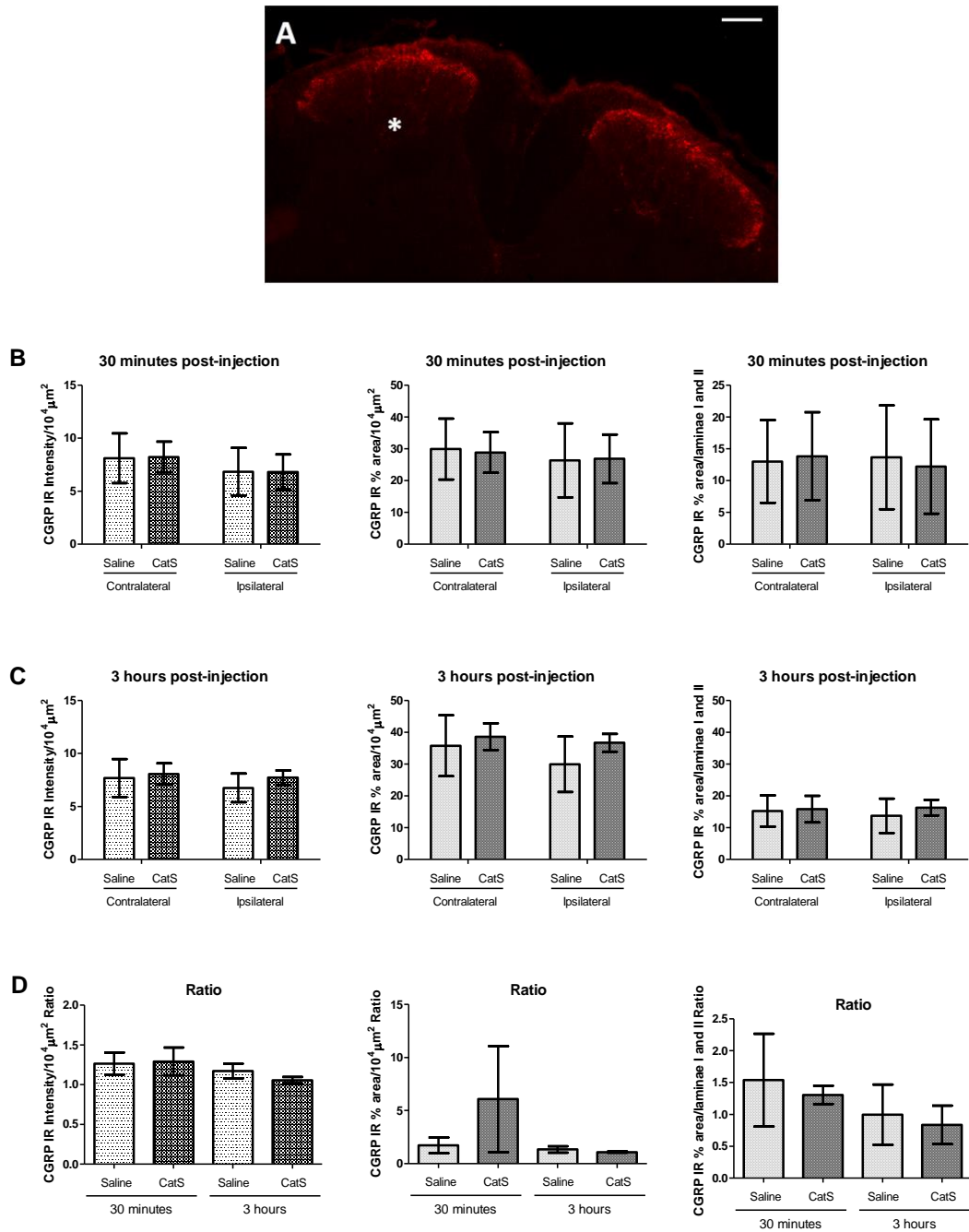


Figure 4.16: No effect of Cathepsin S on staining for CGRP in the spinal cord

Typical image of mouse spinal cord dorsal horn stained for CGRP, ipsilateral (injected) side indicated by asterisk. Scalebar = 100 μm . Injection of CatS 30 minutes (B, E, H) or 3 hours (C, F, I) before taking tissues did not affect the expression of CGRP protein in the spinal cord dorsal horn, measured by pixel area or intensity using 100 x 100 pixel boxes, or the percentage of laminae I and II that were positively stained. No differences in the ratio of contralateral:ipsilateral CGRP staining using any of the quantification methods (D, G, J). $n = 3$ for all groups, averages of 3, 4 sections from each animal, data are mean \pm SEM. No significance, Two-way ANOVA followed by Bonferroni post-hoc test.

4.4 Discussion

Intraplantar CatS induces mechanical hypersensitivity that is associated with increased expression of pERK in dorsal horn neurons. Thus, sensory neurons activated by CatS can cause neurons in the dorsal horn to respond, likely due to release of neurotransmitters and/or neuropeptides from the central terminals of these primary afferent fibres. We also detected expression of both NPPB and GRP in the cell bodies of sensory neurons in the DRG. In addition to being detected in the DRG, NPPB peptide was found in the dorsal horn of the spinal cord, where it appeared to be restricted to fibres in the outer laminae. Furthermore, we found that expression of NPPB in DRG could be upregulated following treatment with NGF, whilst no changes in the dorsal horn of the spinal cord were observed. While intraplantar CatS increases expression of pERK in dorsal horn neurons, we did not find evidence of changes in NPPB expression in the dorsal horn.

Peripheral administration of CatS causes activation of cells in the dorsal horn of the spinal cord, as measured by an increase in the number of pERK-positive cells. Induction of c-Fos and phosphorylation of ERK have both been used as markers for activation of cells following noxious stimulation (Gao and Ji, 2009). Expression of c-Fos is increased in the dorsal horn in a rat model of chemotherapy-induced neuropathic pain and surgical pain (Kalynovska et al., 2017; Uchytlova et al., 2015), while phosphorylation of ERK is increased in the lumbar spinal cord in an intensity-dependent manner following immersion of the hindpaw in hot water and in a mouse model of arthritic pain (Chen et al., 2009; Ji et al., 1999). Injection of capsaicin results in an increase in c-Fos activity and phosphorylation of ERK in dorsal horn neurons (Akiyama et al., 2016a; Ji et al., 1999; Jinks et al., 2002; Nojima et al., 2003; White et al., 2010). We did not find an increase in the number of pERK-positive cells in mice injected with capsaicin compared with those injected with saline; however, we collected tissues 30 minutes after injection of capsaicin, while peak phosphorylation of ERK in the dorsal horn is reported to occur 2 – 10 minutes after injection of capsaicin (Ji et al., 1999; White et al., 2010). Thus, it is likely we missed the optimum time for measuring phosphorylation of ERK after injection of capsaicin. Staining for c-Fos, which is downstream of pERK, may have enabled us to observe activation of dorsal horn neurons by capsaicin at this later timepoint.

TRPV1 is required for induction of c-Fos and phosphorylation of ERK, as TRPV1 antagonists or desensitisation of TRPV1-expressing peripheral nerves reduces the number of c-Fos positive cells (Kalynovska et al., 2017; Uchytlova et al., 2015), while the number of pERK-

positive cells is reduced in TRPV1 KO mice with arthritic pain (Chen et al., 2009). This suggests that activation of dorsal horn neurons, as evidenced by c-Fos and pERK, is required for transmission of pain signals.

In addition to activation after peripheral noxious stimulation, activation of cells in the dorsal horn is also likely to occur following stimulation of peripheral neurons by pruritogens. Intradermal injection of pruritogens including histamine, chloroquine, the PAR2 agonist SLIGRL-NH₂, and serotonin results in an increase in c-Fos immunoreactivity mainly in dorsal horn interneurons (Akiyama et al., 2009b; Akiyama et al., 2016a; Bell et al., 2016; Jinks et al., 2002; Kiguchi et al., 2016; Nakano et al., 2008; Nojima et al., 2003; Zhang et al., 2014). Meanwhile, injection of histamine or a mast cell degranulator is associated with neuronal activation in the dorsal horn, with the number of pERK-positive neurons reaching peak at 3 minutes after injection of histamine (Jiang et al., 2015; Zhang et al., 2014). Most neurons positive for pERK, and hence activated following intradermal injection of histamine, are excitatory interneurons, with some inhibitory interneurons and projection neurons also showing activation following injection of histamine (Jiang et al., 2015). Furthermore, preventing activation of cells in the dorsal horn prevents histamine-mediated scratching behaviour in mice (Zhang et al., 2014). However, in contrast to histamine, Zhang et al. (2014) reported that injection of chloroquine and SLIGRL-NH₂ did not result in phosphorylation of ERK in the spinal cord, although Bell et al. (2016) reported a significant increase in the number of pERK-positive cells in the spinal cords of their mice after injection of chloroquine. Whether or not the animals are allowed to scratch at the injected site might explain these different observations, as Zhang et al. (2014) allowed their mice to scratch to confirm the pruritic effects of their agents, while Bell et al. (2016) prevented their mice from scratching through the use of collars. Another reason for this could be that chloroquine and SLIGRL-NH₂ are not always strong enough to activate pERK but are sufficient for activation of c-Fos. It is unlikely that pruritogens activating PAR2 or MrgprC11-expressing neurons does not result in phosphorylation of ERK, as injection of SLIGRL-NH₂ has already been demonstrated to activate cells in the dorsal horn (Nakano et al., 2008) and we observed an increase in the number of pERK-positive cells in the dorsal horn of mice 30 minutes after injection of CatS, which is reported to activate both receptors. Because the intensity of the stimulus affects phosphorylation of ERK (Gao and Ji, 2009; Ji et al., 1999), it is possible that CatS is a more potent activator of neurons than chloroquine or SLIGRL-NH₂ and thus more reliably causes activation of cells in the spinal cord.

The observation that intraplantar injection of CatS activates cells in the dorsal horn suggests activation of sensory neurons. We presume intradermal injection of CatS into the skin would likewise result in activation of neurons in the dorsal horn following activation of sensory neurons and release of itch-related peptides from the endings of primary afferent fibres. However, intradermal injection of CatS would also result in scratching behaviour, which would complicate interpretation of the results as activation of dorsal horn neurons could be due to either the release of neurotransmitters and neuropeptides from activated primary sensory neurons by the pruritogen, or as a result of scratching at the injected site. In rats and mice, intraplantar injection of the PAR2 agonists SLIGRL-NH₂ or tryptase results in thermal and mechanical hyperalgesia and activation of neurons in the spinal cord as indicated by c-Fos (Vergnolle et al., 2001). Because CatS also acts via PAR2 receptors, activation of PAR2 expressed on sensory neurons by CatS may also result in similar activation of neurons in the dorsal horn. We initially hypothesised that activation of primary afferent neurons by CatS would result in the release of NPPB, which in turn may directly activate dorsal horn neurons or result in the activation of dorsal horn neurons via the release of other neurotransmitters and/or neuropeptides released from interneurons. Although these activated dorsal horn neurons are likely to be interneurons (Akiyama et al., 2016a), it is unlikely they are GRP-expressing interneurons, which tend not to show activation indicated by phosphorylation of ERK following injection of pruritogens (Bell et al., 2016). Thus, it is probable these neurons express the GRP receptor, as these are the other main class of interneurons in the spinal itch circuitry that may be activated by pruritogens, although interneurons of other itch circuits, such as NMB receptor-expressing interneurons, may also be activated. Future experiments characterising these neurons and investigating the time-course and dose-dependence of CatS-induced phosphorylation of ERK and c-Fos would be of interest to find the optimal conditions for activation of dorsal horn neurons and determining which part of the spinal cord itch circuitry they belong to.

When this project was first undertaken, the role of NPPB and GRP in the itch circuitry in the spinal cord was only beginning to be elucidated, with some groups arguing the release of GRP from the central terminals of primary afferent fibres was responsible for mediating itch signals while other groups stressed the importance of NPPB. Hence at the time it was necessary for us to confirm for ourselves which of these neuropeptides was likely released from primary afferent fibres in response to pruritogens. Several studies have previously reported the expression of both NPPB and GRP in the DRG, although expression of GRP is usually very low and difficult to detect (Barry et al., 2016; Fleming et al., 2012; Liu et al.,

2014b; Mishra and Hoon, 2013; Solorzano et al., 2015). However, we observed almost equal expression of both NPPB and GRP mRNA in our tissues. Similar to Barry et al. (2016), we found that a large cycle number was required for detection of GRP mRNA, with an average of 28 or more cycles required before GRP mRNA could be detected. Although this is slightly fewer than the number of cycles Barry et al. (2016) reported was required for detection of GRP mRNA in their mouse DRG samples, it is still near the limits of accurate detection of mRNA using this technique. However, we found that a similar number of cycles was required to detect expression of NPPB mRNA, suggesting that expression of NPPB mRNA is also low in our tissues. Although we report similar expression of NPPB mRNA relative to β -actin mRNA as Solorzano et al. (2015), our level of GRP mRNA is much higher than theirs and is similar to that for NPPB mRNA. The reason for this discrepancy is unclear, although we may have used different primers for β -actin than Solorzano et al. (2015), who did not provide the primer sequence they used for β -actin in their paper. Thus, it cannot be ruled out that differences in the efficiency of detection of β -actin mRNA contributed to this discrepancy. Expression of GRP in the DRG is reported to be increased by 20-fold after peripheral nerve injury (Solorzano et al., 2015), where its expression level would then be closer to that observed for NPPB. Likewise, an increase in the expression of GRP mRNA in the DRG is reported in a mouse model of dry skin itch (Barry et al., 2016). However, we used wild-type untreated mice in our experiments, and so expression of GRP would not be expected to be increased. Variances in normal the expression of GRP and NPPB mRNA in the DRG may exist between individual mice, however, which may explain some of the differences observed between our results and others, and indeed between different groups. In support of this, Fleming et al. (2012) reported that GRP cDNA could sometimes, but not always, be amplified from isolated mouse DRG transcripts. Furthermore, large variances in the difference in expression of GRP in the mouse dorsal horn and DRG were observed, ranging from a 63 to a 1155 fold-difference. This suggests that, at least for GRP mRNA, the expression level varies between individual mice, being at or above the threshold level of detection for some mice and being below the threshold level of detection for others.

Expression of NPPB mRNA in the DRG and in the TG was further confirmed using in-situ hybridisation, where it was expressed in about 10% of cells, similar to that previously reported (Huang et al., 2018; Mishra and Hoon, 2013). To confirm the specificity of our in-situ hybridisation, DRG sections were co-stained for NPPB mRNA and NPPB peptide using in-situ hybridisation probes and antibodies, respectively. Around 12% of DRG cells expressed NPPB peptide. Moreover, most of the cells that expressed NPPB mRNA were also positive

for the peptide. However, there remained a sub-population of neurons that were positive for NPPB mRNA but not the peptide. It is possible that not all neurons were detected during staining or that some neurons were non-specifically stained. Indeed, it is likely that a few cells were non-specifically stained for NPPB peptide, as around 4% of cells were stained with the scramble probe during the in-situ hybridisation procedure. Furthermore, not all neurons that express the mRNA transcripts necessarily translate them to proteins, thus some cells that were positive for the mRNA might not express the protein.

To characterise NPPB-expressing neurons in the DRG, they were co-stained for CGRP peptide. Around one third of the cells were positive for CGRP peptide, similar to previous reports in rat (Fernihough et al., 2005; McCarthy and Lawson, 1990; Staton et al., 2007), guinea pig (Lawson et al., 2002), and mouse (Chen et al., 2008; McCoy et al., 2013). 73% of cells that were positive for NPPB mRNA were also positive for CGRP peptide, suggesting that most NPPB-expressing neurons in the DRG belong to the peptidergic subpopulation. This is further supported by the finding that almost 90% of the cells that were positive for NPPB mRNA and CGRP peptide were small to medium-sized cells, in agreement with previous observations (Staton et al., 2007). Ideally we would have also investigated co-expression of both NPPB and CGRP peptides in the DRG, however, this was not possible due to cross-reactivity of the antibodies being used. Thus, while we are unable to confirm co-expression of NPPB and CGRP peptides in the DRG, it is likely that cells expressing NPPB mRNA make up a subpopulation of CGRP-positive cells. There are, however, some cells that express NPPB mRNA but not CGRP peptide. Although these cells did not differ in size from those that expressed NPPB mRNA and CGRP peptide, they could belong to a different subpopulation of neurons in the DRG. For example, using in-situ hybridisation in mouse DRGs, Mishra and Hoon (2013) reported that half of their NPPB-expressing cells also expressed NMB, suggesting the existence of more than one population of NPPB-expressing neurons in the DRG. However, in contrast to our observations, Mishra and Hoon (2013) also found that only one quarter of their NPPB-expressing cells expressed CGRP. In contrast, Zhang et al. (2010) claimed that in rat 95% of NPPB-positive neurons were positive for CGRP, while nearly 90% were also positive for IB4. Li et al. (2016) also found co-expression of NPPB and IB4 in rat DRG cells. Furthermore, Zhang et al. (2010) also reported expression of NPPB in half of their DRG neurons. Thus, large variations in the number of cells expressing NPPB and the subpopulation of neurons in which NPPB-expressing cells are found exists, although species differences may contribute to this. We propose that the majority of NPPB-expressing neurons in the DRG belong to the peptidergic CGRP-positive population, with around a

quarter of NPPB-expressing cells belonging to other subpopulations of small diameter neurons. This other population of NPPB-expressing neurons is unlikely to belong to the non-peptidergic IB4-positive population of neurons however, as hardly any overlap in the expression of NPPB peptide and IB4 was observed in our spinal cord sections.

NPPB-expressing sensory neurons have previously been reported to co-express TRPV1, suggesting they do belong to the subset of nociceptors potentially involved in pruritus, as well as MrgprA and MrgprC11, suggesting they may belong to non-histaminergic itch circuitry (Mishra and Hoon, 2013). In addition to establishing whether our mouse sensory neurons also co-express NPPB with TRPV1 and Mrgprs, future experiments should be performed to determine whether NPPB-expressing neurons also express PAR2, thereby providing additional evidence for a mechanism by which activation of PAR2 by CatS could result in release of this neuropeptide.

In addition to being detected in the DRG, NPPB peptide was also found in the dorsal horn of the spinal cord, where it appeared restricted to fibres in the outer laminae, similar to previous reports (Kiguchi et al., 2016). As mentioned previously, cross-reactivity of the antibodies for NPPB and CGRP prevented us from co-staining for NPPB and CGRP peptides, and because others have been unable to find expression of NPPB mRNA in the spinal cord it was not feasible to attempt in-situ hybridisation for NPPB mRNA in the spinal cord (Mishra and Hoon, 2013; Pitake et al., 2017). Previous studies have suggested that NPPB-positive fibres in the dorsal horn are likely to be positive for CGRP (Abdelalim et al., 2016). However, we note that the staining for NPPB and CGRP obtained by Abdelalim et al. shows an almost complete overlap, similar to the staining we obtained when we attempted to co-stain for NPPB and CGRP peptides. In particular, we found that when tissues were stained for NPPB peptide alone, staining appeared as a thin band mostly restricted to the outer part of lamina II, as reported by Kiguchi et al. In contrast, co-staining for NPPB and CGRP peptides revealed a complete overlap over a wider area comprising much of lamina I and II. Because they did not show any staining of dorsal horn tissues for NBBP alone, we cannot know whether the findings of Abdelalim et al. are due to cross-reactivity of the antibodies or whether expression of NPPB peptide in the dorsal horn can extend out further than what we have observed. Experiments which utilise amplification systems (such as tyramide amplification of one of the antibodies) to reduce cross-reactivity or different primary antibodies should be performed to address the issue. We can, however, report that staining for NPPB peptide and

IB4 does not overlap in the spinal cord, with most of the staining for IB4 occurring somewhat deeper in the dorsal horn than that for NPPB.

We also found that expression of NPPB could be upregulated following treatment with NGF, as has previously been reported for other neuropeptides. NGF increases the expression of neuropeptides such as CGRP and substance P in DRGs in culture compared with neurons cultured in the absence of NGF or with other growth factors such as brain-derived neurotrophic factor and neurotrophin-3 (Nicol and Vasko, 2007). As well as increasing the expression of CGRP in cultured DRG neurons, NGF increases release of CGRP from these cells when stimulated with high extracellular potassium or capsaicin (Hingtgen et al., 2006; Park et al., 2010). Subcutaneous injection of NGF increases expression of substance P in rat DRG, while rats treated with anti-NGF antibodies have decreased NGF content in the DRG and spinal cord (Otten et al., 1980). Moreover, in rats subcutaneously injected with NGF, the basal and electrically evoked release of substance P and CGRP from the spinal cord is increased (Malcangio et al., 1997; Malcangio et al., 2000). Expression of the NGF receptor tropomyosin receptor kinase A (TrkA) on small diameter neurons that also express neuropeptides suggests that it is the activity of NGF on this receptor that is responsible for mediating the effects of NGF. Electrically-evoked release of substance P from spinal cord slices is reduced in rats treated systemically with a TrkA antibody (Malcangio et al., 2000), supporting a role for TrkA in NGF-mediated increase of neuropeptides from primary afferent fibres. However, most sensory neurons that express TrkA also co-express the p75 receptor (Nicol and Vasko, 2007). Although the affinity of NGF for p75 is lower than for TrkA, increased NGF, as for example is observed during inflammation, could also signal via p75 to exert its effects. p75 might also increase the sensitivity of TrkA for NGF, as activation of TrkA by NGF is reduced in the presence of a p75 blocking antibody (Barker and Shooter, 1994). We found that systemic treatment of NGF for two weeks resulted in a doubling of the number of cells in the DRG that were positive for the NPPB peptide, suggesting NGF upregulates the expression of NPPB in sensory neurons.

A role for NGF in chronic itch conditions has previously been proposed, with increased expression of NGF reported in atopic dermatitis, contact dermatitis, and psoriasis conditions (Ikoma et al., 2006). NGF levels are increased in the skin of a mouse model of atopic dermatitis characterised by excessive scratching behaviour and development of skin lesions (Tanaka and Matsuda, 2005). Skin keratinocytes and dermal fibroblasts were found to express NGF, making these cells a likely source of NGF in chronic itch conditions (Tanaka and

Matsuda, 2005). NGF affects growth of nerve fibres in the skin, with keratinocytes from atopic dermatitis patients capable of increasing neurite outgrowth, especially of CGRP-positive fibres (Roggenkamp et al., 2012). Moreover, NGF increases expression of CGRP and substance P in rat DRGs following injury (Verge et al., 1995). This suggests NGF is involved in chronic itch conditions and may exert its effects by altering the growth and expression of neuropeptides in sensory neurons innervating the skin. Our finding that expression of NPPB in sensory ganglia is increased following NGF treatment is thus not surprising given the role of NPPB in pruritus, and is a potential mechanism whereby increased expression of NGF in the skin could lead to exacerbation of pruritus. However, future experiments further confirming increased expression of NPPB in sensory neurons (for example using qPCR), should be performed, and these neurons characterised to investigate whether *de novo* expression of NPPB occurs and whether they belong to the same class of neurons that express NPPB under normal conditions. Interestingly, NGF treatment has been found to decrease expression of NPPB mRNA in myocardial tissue in a rat model of heart failure (He et al., 2012), however, regulation in the expression of NPPB by NGF may be different in different tissues.

Although expression of NPPB peptide was increased in sensory ganglia following NGF treatment, we were unable to detect changes in the expression of NPPB in the dorsal horn of the spinal cord using antibody staining, suggesting an increase in the local synthesis of NPPB in the cell body but not its transport or release from primary afferents in the spinal cord. Alternatively, upregulation of NPPB does occur from primary afferents in the spinal cord but cannot be detected using this method. In contrast, the area of staining for CGRP peptide in the dorsal horn is increased following NGF treatment, confirming an increase in the expression of this neuropeptide in the spinal cord. However, no differences were observed in the intensity of staining for CGRP peptide following NGF treatment. Because NGF has previously been shown to increase expression of CGRP and other neuropeptides in the DRG (Nicol and Vasko, 2007), it is likely our technique is not sensitive enough to detect small changes in expression of peptides in the dorsal horn, which could explain why no changes in intensity of staining for CGRP or in the area or intensity for NPPB peptide were observed. Thus, while we were unable to demonstrate changes in the expression of NPPB peptide in the dorsal horn in response to NGF treatment, we cannot conclude that no such changes in expression and release of peptides do occur.

Injection of NGF increased sensitivity to thermal stimuli, as previously reported in rodents (Alexander et al., 2013; Eskander et al., 2015). This behaviour was apparent as early as one hour after the first dose of NGF, as has also been previously reported, and was observed after each subsequent injection of NGF (Alexander et al., 2013). NGF has been shown to increase expression of TRPV1 proteins in DRG neurons and to sensitise TRPV1 by phosphorylation of the Y200 residue on the TRPV1 channel following an increase in intracellular calcium, resulting in rapid insertion of TRPV1 into the cell membrane (Ji et al., 2002; Zhang et al., 2005). This provides a potential explanation for the increased sensitivity to thermal stimuli observed in NGF-treated mice. We therefore conclude that our NGF treatment was successful in our mice, and that systemic NGF for two weeks increases the expression of NPPB peptide in the sensory ganglia, and possibly also CGRP, in the dorsal horn. Blocking MAPK activity reduces NGF-mediated increase in CGRP expression in neuronal cell cultures, supporting the involvement of MAPK in upregulation of CGRP by NGF, likely via regulation of the CGRP promoter (Durham and Russo, 2003; Park et al., 2010; Xu and Hall, 2007). NGF-mediated increase in CGRP content is also reduced following over-expression of a dominant negative Ras in sensory neurons or exposure of neurons to a farnesyltransferase inhibitor to reduce Ras activity, while over-expressing a constitutively active Ras in sensory neurons increases NGF-mediated increase in CGRP content in these cells (Park et al., 2010). This suggests activation of the MAPK and Ras pathways are involved in increasing the expression of neuropeptides such as CGRP in response to NGF, and similar pathways may also be responsible for NFG-induced upregulation of NPPB in DRG neurons.

Injection of CatS into the hindpaw was not associated with changes in expression of NPPB or CGRP in the dorsal horn. This suggests that CatS activation of sensory neurons in the periphery is not associated with significant release of these neuropeptides from the central terminals of such neurons, as might be interpreted from a decrease in expression in the spinal cord. However, we cannot rule out that the techniques and analysis methods used were insufficient for detecting these changes, particularly if the changes were small. A more sensitive method of measuring the release of neuropeptides from sensory neurons, such as ELISA, may have provided more information. However, we were unable to detect the presence of NPPB in the supernatant of DRG cells even after stimulation with capsaicin, and so did not proceed with using this method to further investigate release of NPPB from cells. We therefore are unable to conclude whether CatS affects the expression or release of NPPB and other neuropeptides from sensory neurons.

In mice, we confirmed that CatS locally injected in the hindpaw resulted in acute mechanical hyperalgesia that resolved by 3 hours. Similar results have previously been reported following injection of rat recombinant CatS in rats (Barclay et al., 2007; Clark et al., 2007). Lieu et al. (2016) also reported an increase in mechanical sensitivity in mice injected with hr-CatS. However, in their mice, increased sensitivity to mechanical stimuli persisted for at least 4 hours after injection of CatS. The source of CatS used is unlikely to explain the differences in duration of mechanical hyperalgesia compared with our observations, as hr-CatS manufactured at Medivir was the source of CatS for both experiments. However, Lieu et al. (2016) injected 14 μg of CatS into the hindpaws of their mice, whereas we injected only 1 μg of CatS. Thus, the higher dose of CatS injected into their mice could explain the persistent hyperalgesia observed by Lieu et al. (2016). In addition to increased sensitivity to mechanical stimuli, thermal hyperalgesia and increased paw thickness were also reported by Lieu et al. (2016), although the onset of thermal hyperalgesia was slower than that for mechanical hyperalgesia, requiring at least 2 hours before the effects could be observed. We did not measure paw thickness in our mice following injection of CatS, although no obvious changes were noted. CatS-mediated hyperalgesia was reduced when mice were pre-treated with the PAR2 antagonist GB88 and in PAR2 KO mice (Lieu et al., 2016), suggesting CatS acting on PAR2 is responsible for the increased sensitivity to mechanical stimuli that was observed. Interestingly, Lieu et al. (2016) found that GB88 also reduced hyperalgesia following injection of trypsin or elastase, suggesting that both canonical and non-canonical cleavage of PAR2 can result in hyperalgesia.

Chapter 5

General discussion

The main findings of this work are:

1. Skin keratinocytes express CatS mRNA and the peptide can be released from these cells following TRPV4 activation.
2. Sensory neurons respond to direct application of CatS with inward currents and increased intracellular calcium.
3. CatS-responding neurons are a subset of TRPV1 and TRPA1-expressing neurons and expression of these channels is required for CatS-mediated calcium responses.
4. CatS causes sensitisation of TRPV1 and TRPA1-mediated responses in neurons.
5. CatS acts via PAR2 to cause calcium responses in sensory neurons.
6. Peripheral application of CatS activates cells in the dorsal horn.
7. DRG cells express NPPB, where it is mostly co-expressed with CGRP; however, we failed to observe release of peptides after CatS treatment.

Keratinocytes as a potential source of Cathepsin S in pruritus

Skin keratinocytes are a potential source of several pruritogens that may be involved in acute itch as well as chronic itch conditions such as atopic dermatitis. We have demonstrated expression of CatS mRNA and release of the protease from cells of the HaCaT human keratinocyte cell line, which we propose acts as a pruritogen and is responsible for itch sensations. Whether CatS released from keratinocytes could act as a pruritogen had not been addressed previously. In mice, over-expression of CatS in several tissues, including the skin, results in atopic dermatitis-like conditions (Kim et al., 2012), however whether CatS was released from keratinocytes and was directly responsible for activation of sensory neurons to transmit itch signals was not known, although our above observations combined with our finding that CatS activates sensory neurons *in vitro* supports this concept. Additional experiments in which CatS released from cultured keratinocytes is used to activate sensory neurons would further support this hypothesis, although other pruritogens and sensitising agents may additionally be released from keratinocytes and may also be involved.

Our findings and that of others suggest keratinocytes do not normally express CatS protein, which suggests CatS is not likely to be involved in acute itch (Kim et al., 2012; Schonefuss et

al., 2010). However, expression can be increased under certain conditions. In support of this, we observed an increase in Cathepsin mRNA in HaCaTs following incubation with LPS or the Th2 cytokines IL-4 and IL-13, while others have reported an increase of the protein in HaCaTs following incubation with IFN γ and TNF α , as well as in psoriatic keratinocytes (Ainscough et al., 2017; Schonefuss et al., 2010). This suggests expression of CatS could be increased in several chronic itch conditions, where it may be responsible for itch in these conditions, although the mechanism of increased expression of CatS is likely to differ in different conditions. In addition, the mechanisms by which different mediators result in an increase in the expression of CatS in keratinocytes has not been explored. IL-4 and IL-13 have previously been demonstrated to alter expression of several genes in human keratinocytes, including increased expression of chemokines such as CCL3, CCL4, CCL26 and cytokines including IL-6 and IL-8, and decreased expression of genes involved in cell adhesion and barrier function such as fibronectin, filaggrin, loricrin, involucrin, and several keratins (Omori-Miyake et al., 2014; Serezani et al., 2017). IL-4 and IL-13 induce activation of STAT-6, which translocates to the nucleus where it affects transcription of several genes (Goenka and Kaplan, 2011; Serezani et al., 2017). Moreover, STAT-6 promotes the production of IgE in B cells and the differentiation of Th2 cells, contributing to the phenotype of atopic dermatitis and resulting in a positive feedback cycle with the release of more Th2 cytokines (Goenka and Kaplan, 2011). Activation of STAT-6 by IL-4 and IL-13 may also affect transcription of CatS in keratinocytes, and future experiments in which keratinocytes incubated in IL-4 and IL-13 in the presence of a STAT-6 inhibitor would confirm this. IL-13 has previously been reported to induce expression of CatS in lung tissues via STAT-6 (Lee et al., 2006; Zheng et al., 2000), and may similarly do so in skin keratinocytes, along with IL-4.

Although CatS mRNA was increased following incubation of HaCaTs in IL-4 and IL-13, neither intracellular CatS activity nor activity of CatS in the supernatant was found to be increased, suggesting there was no increase in protein following these treatments. However, due to time constraints, neither Western blotting nor immunostaining for CatS peptide had been performed to check whether protein levels could be increased following treatment with these cytokines, which would have enabled us to determine whether IL-4 and IL-13 are capable of increasing protein as well as mRNA levels. In contrast, IL-4 and IL-13 have previously been shown to increase both expression and release of CatS and other cathepsins from bone marrow-derived macrophages (Yan et al., 2016). It is possible additional mediators are required for increased production and release of CatS protein from

keratinocytes. Furthermore, despite expressing the P2X₇ and TLR4 receptors for high concentration ATP and LPS, respectively, we could not detect release of CatS from HaCaTs following incubation with LPS and ATP, even though this has been reported to cause release of from other cell types such as microglia (Clark et al., 2010). This suggests the mechanism of CatS release is different in keratinocytes than for microglia. Moreover, release of CatS and other pruritogens from keratinocytes may be different under inflammatory conditions than in normal healthy skin. To test this possibility, we also measured release of CatS following incubation in Th2 cytokines as well as LPS and ATP, although no CatS activity was detected. However, because we were also unable to detect an increase in the transcription of genes used as markers for atopic dermatitis following incubation in IL-4 and IL-13, we cannot rule out that our cells were not optimally stimulated to release CatS. Further experiments in which the concentration and duration of incubation in these cytokines is required to determine the optimal conditions for modelling atopic dermatitis and release of CatS from these cells.

In addition to expression receptors for LPS and ATP, we also noted that HaCaTs express TRPV4. TRPV4 is activated by osmotic pressure, innocuous heat, and ultraviolet B radiation (Moore et al., 2013; Nilius et al., 2003; White et al., 2016). Activation of this channel has also been shown to result in scratching behaviour in mice (Chen et al., 2016). In light of this, we investigated whether stimulation of this receptor would result in the release of CatS from HaCaTs. Indeed, incubation of HaCaTs in the TRPV4 agonist GSK1016790A was sufficient to cause release of CatS, although specificity of the agonist for TRPV4 still needs to be confirmed using a TRPV4-specific antagonist. Nevertheless, this suggests CatS could be the pruritogen responsible for the TRPV4-induced acute scratching behaviour recently reported in mice (Chen et al., 2016). However, activation of TRPV4 in keratinocytes increases expression of endothelin-1, which has also been shown to be a pruritogen (McQueen et al., 2007; Moore et al., 2013; Trentin et al., 2006). Thus, activation of TRPV4 may result in the release of several pruritogens, including CatS, that activate pruriceptors in the skin, which must be taken into consideration when investigating TRPV4-mediated pruritus. Because we did not measure release of endothelin-1 or other substances following activation of keratinocyte TRPV4 channels, we cannot exclude the release and involvement of other pruritogens.

In the context of chronic itch, one possible scenario is that keratinocytes continually release CatS, which may then act as a pruritogen to result in constant transmission of itch signals.

This continual release of CatS may or may not be due to continued activation of TRPV4 on keratinocytes. In atopic dermatitis, enhanced activity of TRPV4 may occur as a result of increased water loss and the development of dry skin resulting in changes in osmolarity. Changes in skin pH may also result in activation of TRPV4. The pH of the corneal layer of the epidermis is increased in atopic dermatitis and acidic pH has been reported to inhibit TRPV4-mediated calcium responses in mouse esophageal epithelial cells (Rippke et al., 2004; Shikano et al., 2011), suggesting reduced inhibition of TRPV4 on keratinocytes may be responsible for increased release of CatS and other pruritogens in atopic dermatitis. However, other groups have reported that TRPV4 channels expressed in Chinese hamster ovary cells are opened by a decrease in pH (Suzuki et al., 2003). Although we performed the CatS activity assays from the HaCaT cell lysates at both pH7 and pH5 to investigate the possibility that other proteases may have been cleaving the substrate used in the assay, the release assays were performed only at pH7 to ensure specific activity of CatS on the substrate. Performing the release assay at pH5 might allow us to determine if TRPV4 opens in response to a decrease in pH and hence if there is an increase in CatS release, or if low pH reduces opening of the channel and reduces release of CatS. However, any increases in activity observed at low pH may also be due to increased activity of CatS at this pH or the activity of other proteases on the substrate; therefore other methods of measuring activity of TRPV4 and release of CatS from keratinocytes at various pH levels would need to be utilised. In any event, because CatS retains activity at neutral pH, it is a good candidate pruritogen for the increased skin pH in atopic dermatitis, where other proteases may lose activity.

Increased release of other pruritogens such as the kallikreins and TSLP from keratinocytes, IL-31 from mast cells and T cells, and histamine and tryptase from mast cells may also contribute to enhanced transmission of itch in chronic itch conditions (Andoh et al., 2015; Che et al., 2018; Dillon et al., 2004; Kawakami et al., 2009; Niyonsaba et al., 2010; Wilson et al., 2013). An alternative possibility is that release of pruritogens from keratinocytes and other cells is not increased in chronic itch conditions, but instead neurons become sensitised due to release of prostaglandins, bradykinin, and other mediators (Stander et al., 2003). As well as being a pruritogen, CatS increases sensitivity of neurons by sensitisation of TRP channels (Amadesi et al., 2004; Amadesi et al., 2006; Dai et al., 2004; Dai et al., 2007), thereby providing an additional mechanism by which CatS released from skin keratinocytes could result in enhanced transmission of itch signals. Finally, increased sprouting of nerve fibres in the skin has been reported in chronic itch conditions (Tobin et al., 1992; Tominaga

et al., 2009; Urashima and Mihara, 1998), and this may result in increased ability to detect and respond to pruritogens, regardless of whether there is an increase in the release of pruritogens and mediators that cause sensitisation of neurons.

Activation of sensory neurons by Cathepsin S occurs via PAR2 and requires TRPV1 and TRPA1

CatS, released from keratinocytes, may directly activate the endings of sensory neurons in the skin to result in transmission of itch signals. Using patch clamping and calcium imaging techniques, we have shown that sensory neurons *in vitro* can respond to application of CatS. The PAR2 antagonist FSLRY-NH₂ reduced CatS-induced calcium responses in neurons, supporting the notion that CatS cleaving PAR2 activates the cells, in agreement with previous observations (Lieu et al., 2016; Zhao et al., 2014a). It has also been reported that CatS cleaves PAR4 and MrgprC11 (Reddy et al., 2010; Reddy and Lerner 2010; Reddy et al., 2015). Although we found that inhibiting activation of PAR2 alone was sufficient to prevent CatS-induced calcium responses, activation of PAR4 and/or MrgprC11 may also contribute to these responses in neurons. Indeed, preventing activation of any of these receptors may be sufficient to prevent CatS-induced activation of the cell and/or scratching behaviour. However, in a recent study by Reddy et al. (2015), calcium responses to CatS were observed in DRG cells cultured from PAR2 KO mice, although it should be noted they used a much greater concentration of CatS in their assays than we used, which may result in non-specific cleavage of receptors and non-physiologically relevant responses. It would therefore be of interest to determine the most physiologically relevant concentration of CatS to use and to examine whether CatS-mediated calcium responses in DRGs are still reduced in the presence of this concentration of CatS and the PAR2 antagonist or in DRG cultures from PAR2 KO mice. Furthermore, it remains to be explored whether sensory neurons *in vivo* respond directly to peripheral application of CatS and to link this to itch sensations in humans and scratching behaviour in mice.

We noted that sensory neurons that responded with calcium fluxes following application of CatS were also likely to respond to agonists of TRPV1 or TRPA1, suggesting CatS-responding neurons belong to a subpopulation of TRPV1 and/or TRPA1-expressing cells. This is in agreement with what has been reported for other non-histaminergic pruritogens such as chloroquine and in particular members of the papain superfamily of cysteine proteases such as mucunain (Bautista et al., 2014; Ross, 2011; Wilson et al., 2011), and supports the role of CatS as a pruritogen of non-histaminergic itch. If CatS is the pruritogen or one of the

pruritogens responsible for increased transmission of itch signals in conditions such as atopic dermatitis, then this could explain why anti-histamines are ineffective in treating the disease. Moreover, not only do CatS-responding cells belong to a subpopulation of TRPV1 and/or TRPA1-expressing neurons, but expression of both receptors is required for CatS-induced calcium responses, as demonstrated by the finding that when CatS was applied to DRG cells cultured from TRPV1 KO or TRPA1 KO mice, the percentage of cells responding to CatS was reduced to baseline. Preliminary behavioural experiments performed by our group found that CatS-mediated scratching behaviour was significantly reduced in TRPV1 KO mice compared with wild-type mice, and our calcium imaging experiments in DRGs from TRPV1 KO mice support the role of TRPV1 in CatS-mediated responses. In contrast, the observation that CatS-mediated scratching behaviour was only slightly reduced in TRPA1 KO mice and that this reduction was not significant compared with scratching behaviour in wild-type mice is at odds with our finding that CatS-mediated calcium responses were prevented in DRG cultures from TRPA1 KO mice. If, however, CatS cleaves other receptors such as MrgprC11 (Reddy et al., 2015), then it would be expected that expression of functional TRPA1 would be required for CatS-mediated signalling and scratching behaviour, as MrgprC11 signals through this channel (Wilson et al., 2011). Thus, the involvement of TRPA1 in CatS-induced calcium responses in neurons also agrees with the notion that CatS signals via MrgprC11.

Similarly, the proposed cleavage of PAR4 by CatS is also likely to require signalling via both TRPV1 and TRPA1 channels, as PAR4-induced scratching behaviour is reduced when mice are pre-treated with TRPV1 or TRPA1 antagonists (Patricio et al., 2015). However, as with our observations in mice, Patricio et al. reported that PAR4-induced scratching behaviour was reduced in TRPV1 KO mice but not in TRPA1 KO mice, which the authors suggested was due to compensatory mechanisms in TRPA1 mice such as increased expression of other TRP channels, which could also explain our observation that CatS-induced scratching behaviour was not reduced in TRPA1 KO mice. As with PAR2, PAR4 has also been shown to sensitise TRPV1 channels in neurons (Vellani et al., 2010). Thus, one possible scenario is that CatS cleaves multiple receptors to signal via both TRPV1 and TRPA1, with TRPV1 being crucial for scratching behaviours and hence presumably itch sensations, while activation of TRPA1 may contribute additionally but is dispensable for scratching behaviour and can be compensated for by activation of other TRP channels expressed on neurons, such as TRPV1 (Figure 5.1).

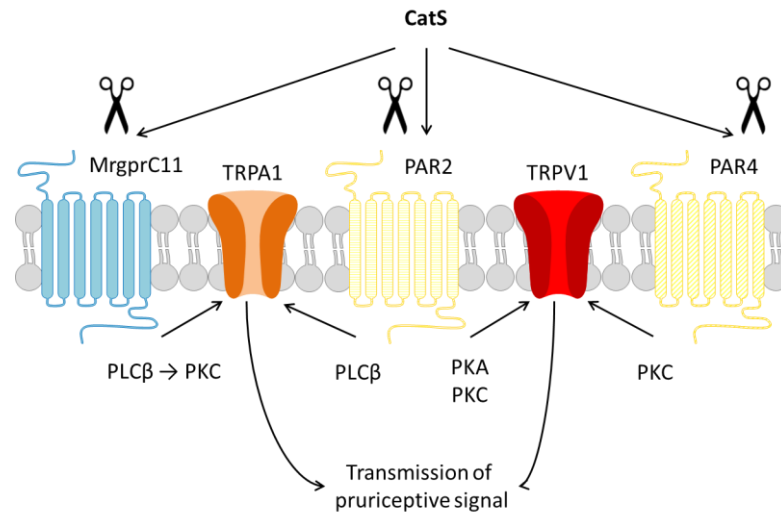


Figure 5.1: Activation of receptors and sensitisation of TRP channels by Cathepsin S

As well as responding to application of CatS, we found an increase in the number of sensory neurons that responded to TRPV1 and TRPA1 agonists when the cells were exposed to CatS before exposure to these agonists, suggestive of sensitisation of these TRP channels by CatS. This observation is not surprising given that activation of PAR2 has previously been shown to sensitise TRPV1 and TRPA1 channels (Amadesi et al., 2004; Amadesi et al., 2006; Dai et al., 2004; Dai et al., 2007), and the ability of CatS to cleave and activate PAR2 (Elmariah et al., 2014; Reddy et al., 2010; Zhao et al., 2014a). Sensitisation of neurons to TRPV1 and TRPA1 agonists increases the likelihood that these cells will respond and could be an additional mechanism by which CatS causes calcium responses in neurons. As far as we are aware, this is the first time it has been demonstrated that CatS sensitises neuronally-expressed TRPV1 and TRPA1 channels *in vitro*. We hypothesise that CatS cleaves neuronal PAR2 to sensitise TRPV1 and TRPA1 channels similar to that previously reported for PAR2-mediated sensitisation of TRPV1 and TRPA1 (Figure 5.1).

Activation of dorsal horn neurons by Cathepsin S

Once activated by pruritogens, sensory neurons release neurotransmitters and neuropeptides from their terminals in the dorsal horn of the spinal cord, in turn activating cells involved in the spinal cord itch circuitry. We proposed that activation of sensory neurons by CatS would result in the release of NPPB from their central terminals, although, in preliminary experiments using an ELISA, we were unable to detect NPPB released into the supernatant of DRG cell cultures following incubation with capsaicin. However, NPPB has recently been demonstrated to be released from DRG cells in culture following incubation

with the pruritogen IL-31 using an ELISA, confirming the ability of these cells to release NPPB and detect it using this technique (Meng et al., 2018; Pitake et al., 2018). We therefore cannot rule out that DRG neurons do not release NPPB following incubation with capsaicin or pruritogens such as CatS. We could, however, confirm expression of both NPPB mRNA and peptide in DRG neurons using qPCR, in-situ hybridisation, and immunostaining techniques, as has previously been reported (Li et al., 2016a; Mishra and Hoon, 2013; Pitake et al., 2017; Pitake et al., 2018; Solorzano et al., 2015; Zhang et al., 2010).

We also detected expression of NPPB in the outer laminae of the dorsal horn of the spinal cord, supporting the notion that this neuropeptide may be released from the endings of sensory neurons. This prompted us to measure release of NPPB in the spinal cord. Using a similar technique previously employed by Lever et al. (2001) to measure release of BDNF from the terminals of sensory neurons in the dorsal horn, we performed immunostaining of dorsal horn sections to measure release of NPPB following intraplantar injection of CatS into the hindpaw. Although intraplantar injection of CatS resulted in mechanical hyperalgesia, confirming successful injection of the protease, no changes in staining for NPPB were observed between the ipsilateral and contralateral sides of animals injected with CatS or saline. Because NPPB is co-expressed with and likely to be released with other peptides such as CGRP (Meng et al., 2018; Mishra and Hoon, 2013), we also stained for CGRP to measure its release as a control, but likewise found no differences in staining between the ipsilateral and contralateral sides of CatS or saline-injected animals. Although this suggests NPPB and CGRP are not released from the terminals of sensory neurons following their activation by CatS, more probable is that our technique was not sensitive enough to be able to detect small differences in the release of these neuropeptides. Alternatively, neuropeptides other than NPPB might be released from primary afferent fibres in response to activation by CatS. For example, some DRG neurons have been reported to express GRP (Barry et al., 2016). We also found some expression of GRP mRNA in our DRG tissues, and this might be the neuropeptide that is released by neurons when they are activated by CatS. NMB is another neuropeptide proposed to be involved in itch and is expressed by DRGs, and along with CatS is reported to be upregulated in a canine model of atopic dermatitis (Olivry et al., 2016). The release of other neuropeptides such as GRP and NMB from the terminals of primary afferents following activation by CatS remains to be investigated.

While we did not find evidence of release of neuropeptides, we did find an increase in the number of cells in the dorsal horn that were activated following intraplantar injection of

CatS compared with injection of saline. This suggests neuropeptides and/or neurotransmitters are released from primary afferent terminals in response to CatS, which in turn activate cells in the dorsal horn. Whether these cells are interneurons of the itch pathway or projection neurons has not yet been explored, although might be confirmed by co-staining, for instance for the NPPB receptor NPRA. Because we only stained for phosphoERK at one time point after injection of CatS, it is possible that even greater activation of neurons in the dorsal horn may be observed at different timepoints, as has been observed with capsaicin (Ji et al., 1999), although the number of activated cells we observed was considerably greater than that for saline-injected animals. As already mentioned, we likely missed the optimum timepoint for measuring activation of cells in the spinal cord following injection of capsaicin and we did not perform staining for downstream activation of c-Fos. However, it would be interesting to compare optimum activation of dorsal horn neurons in the spinal cord following peripheral injection of CatS and capsaicin, as well as other pruritogens, and determine if the same neurons are activated. It was recently reported that release of NPPB from the peripheral endings of sensory neurons resulted in activation of cultured human keratinocytes and the release of cytokines such as IL-17A from these cells (Meng et al., 2018). NPPB released from the central terminals of primary afferents could also result in similar activation of cells in the dorsal horn of the spinal cord. It is therefore possible that activation of sensory neurons by CatS has caused the release of NPPB from their central terminals resulting in activation of neurons in the dorsal horn.

The main drawback with our observations in the dorsal horn of the spinal cord is that they relate to the activities of CatS as an algogen rather than a pruritogen. Previous work in our lab has demonstrated CatS acts as both an algogen and a pruritogen when injected into mice, suggesting it activates both nociceptors and pruriceptors, or neurons that transmit both nociceptive and pruriceptive signals. Whether CatS injected intradermally into the hairy skin of the cheek results in activation of the same populations of neurons as CatS injected intraplantar into the glabrous skin of the hindpaw remains to be investigated. Different types of skin are innervated by different types of neurons and to different extents. For example, Cain et al. (2001) reported that neurons innervating the glabrous skin of mice had a greater threshold to mechanical stimuli and a lower threshold to noxious heat compared with neurons innervating hairy skin, while Boada et al. (2010) found that neurons innervating the glabrous skin of rats comprised a higher proportion of high-threshold mechanosensitive nociceptors and a faster conduction velocity of fast-conducting

nociceptors compared with those innervating hairy skin. Nevertheless, we have demonstrated that CatS can both activate sensory neurons and cells in the spinal cord dorsal horn, making it a candidate pruritogen for the release of neuropeptides involved in itch signalling in the dorsal horn.

Conclusion

To conclude, we propose the following pathway of CatS -induced itch (Figure 5.2), in which CatS released from skin keratinocytes, for example following activation of TRPV4 and subsequent influx of calcium, cleaves receptors such as PAR2 expressed on the endings of sensory neurons in the skin. This results in sensitisation of TRPV1 and TRPA1 channels, causing an influx of sodium and calcium ions into the cells and the opening of voltage-gated channels to result in propagation of action potentials. The terminals of these primary afferents likely release neuropeptides such as NPPB, which then binds to its receptor on interneurons in the dorsal horn that in turn release GRP. The itch signal then continues along the spinothalamic tract to the thalamus where it is relayed to other brain centres such as the somatosensory cortex where the itch sensation is perceived.

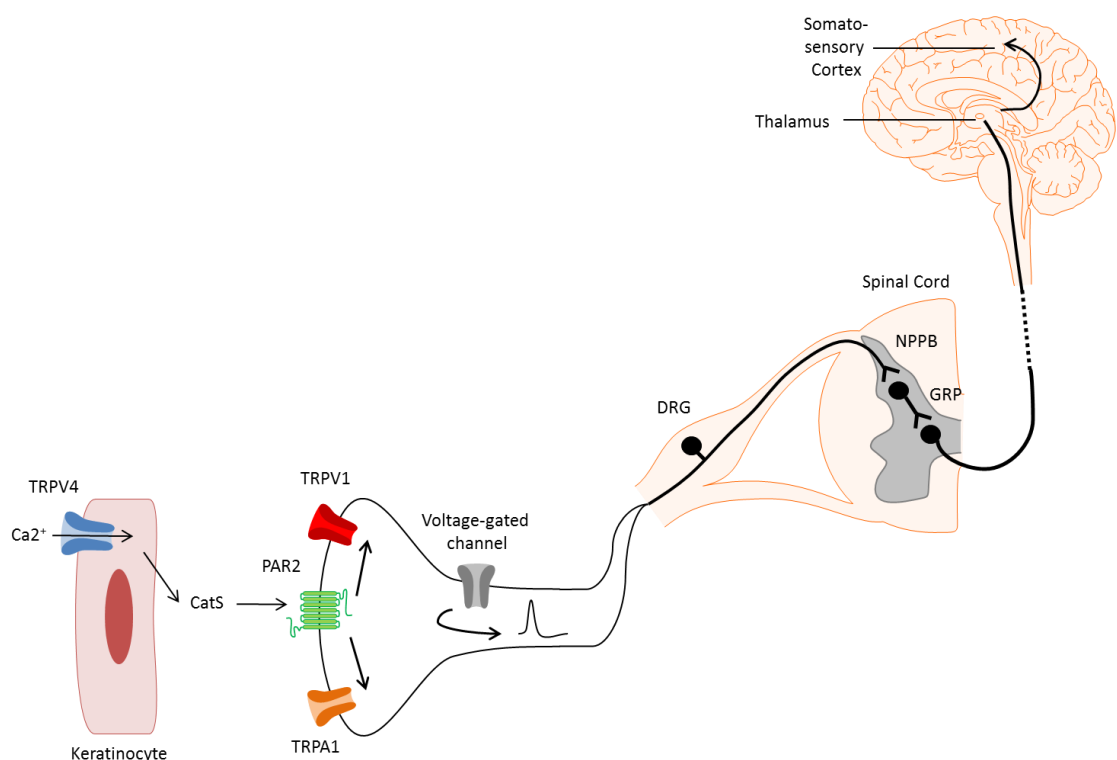


Figure 5.2: Proposed pathway of Cathepsin S-induced itch from the periphery to the brain

References

- Abey H T, Fairlie D P, Moffatt J D, Balzary R W, Cocks T M (2006). Protease-activated receptor-2 peptides activate neurokinin-1 receptors in the mouse isolated trachea. *Journal of Pharmacology and Experimental Therapeutics*, 317(2):598-605.
- Abdelalim E M, Bellier J P, Tooyama I (2016). Localization of Brain Natriuretic Peptide Immunoreactivity in Rat Spinal Cord. *Frontiers in Neuroanatomy*, 10:116.
- Abtin A, Jain R, Mitchell A J, Roediger B, Brzoska A J, Tikoo S, Cheng Q, Ng L G, Cavanagh L L, von Andrian U H, Hickey M J, Firth N, Weninger W (2014). Perivascular macrophages mediate neutrophil recruitment during bacterial skin infection. *Nature Immunology*, 15(1):45-53.
- Aihara K, Kuroda S, Kanayama N, Matsuyama S, Tanizawa K, Horie M (2003). A neuron-specific EGF family protein, NELL2, promotes survival of neurons through mitogen-activated protein kinases. *Molecular Brain Research*, 116(1-2):86-93.
- Ainscough J S, Macleod T, McGonagle D, Brakefield R, Baron J M, Alase A, Wittmann M, Stacey M (2017). Cathepsin S is the major activator of the psoriasis-associated proinflammatory cytokine IL-36 gamma. *Proceedings of the National Academy of Sciences of the United States of America*, 114(13):E2748-E2757.
- Aioi A, Tonogaito H, Suto H, Hamada K, Ra C, Ogawa H, Maibach H, Matsuda H (2001). Impairment of skin barrier function in NC/Nga Tnd mice as a possible model for atopic dermatitis. *British Journal of Dermatology*, 144(1):12-18.
- Akiyama T, Carstens E (2013). Neural Processing of Itch. *Neuroscience*, 20:697-714.
- Akiyama T, Carstens M I, Carstens E (2010a). Differential Itch- and Pain-related Behavioral Responses and mu-opioid Modulation in Mice. *Acta Dermato-Venereologica*, 90(6):575-581.
- Akiyama T, Carstens M I, Carstens E (2010b). Facial Injections of Pruritogens and Algogens Excite Partly Overlapping Populations of Primary and Second-Order Trigeminal Neurons in Mice. *Journal of Neurophysiology*, 104(5):2442-2450.
- Akiyama T, Carstens M I, Carstens E (2011). Transmitters and Pathways Mediating Inhibition of Spinal Itch-Signaling Neurons by Scratching and Other Counterstimuli. *PLoS ONE*, 6(7):e22665.
- Akiyama T, Curtis E, Nguyen T, Carstens M I, Carstens E (2016a). Anatomical evidence of pruriceptive trigeminothalamic and trigeminoparabrachial projection neurons in mice. *Journal of Comparative Biology*, 524(2):244-256.
- Akiyama T, Ivanov M, Nagamine M, Davoodi A, Carstens M I, Ikoma A, Cevikbas F, Kempkes C, Buddenkotte J, Steinhoff M, Carstens E (2016b). Involvement of TRPV4 in Serotonin-Evoked Scratching. *Journal of Investigative Dermatology*, 136(1):154-160.
- Akiyama T, Merrill A W, Carstens M I, Carstens E (2009a). Activation of Superficial Dorsal Horn Neurons in the Mouse by a PAR-2 Agonist and 5-HT: Potential Role in Itch. *Journal of Neuroscience*, 29(20):6691-6699.

Akiyama T, Merrill A W, Zanotto K, Carstens M I, Carstens E (2009b). Scratching Behavior and Fos Expression in Superficial Dorsal Horn Elicited by Protease-Activated Receptor Agonists and Other Itch Mediators in Mice. *Journal of Pharmacology and Experimental Therapeutics*, 329(3):945-951.

Akiyama T, Nguyen T, Curtis E, Nishida K, Devireddy J, Delahanty J, Carstens M I, Carstens E (2015). A central role for spinal dorsal horn neurons that express neurokinin-1 receptors in chronic itch. *Pain*, 156(7):1240-1246.

Akiyama T, Tominaga M, Davoodi A, Nagamine M, Blansit K, Horwitz A, Carstens M I, Carstens E (2012). Cross-sensitization of histamine-independent itch in mouse primary sensory neurons. *Neuroscience*, 226:305-312.

Akiyama T, Tominaga M, Takamori K, Carstens M I, Carstens E (2014). Roles of glutamate, substance P, and gastrin-releasing peptide as spinal neurotransmitters of histaminergic and nonhistaminergic itch. *Pain*, 155(1):80-92.

Al-Ani B, Hollenberg M D (2003). Selective tryptic cleavage at the tethered ligand site of the amino terminal domain of proteinase-activated receptor-2 in intact cells. *Journal of Pharmacology and Experimental Therapeutics*, 304(3):1120-1128.

Al-Ani B, Saifeddine M, Kawabata A, Hollenberg M D (1999). Proteinase activated receptor 2: role of extracellular loop 2 for ligand-mediated activation. *British Journal of Pharmacology*, 128(5):1105-1113.

Al-Ani B, Saifeddine M, Wijesuriya S J, Hollenberg M D (2002a). Modified proteinase-activated receptor-1 and-2 derived peptides inhibit proteinase-activated receptor-2 activation by trypsin. *Journal of Pharmacology and Experimental Therapeutics*, 300(2):702-708.

Al-Ani B, Wijesuriya S J, Hollenberg M D (2002b). Proteinase-activated receptor 2: Differential activation of the receptor by tethered ligand and soluble peptide analogs. *Journal of Pharmacology and Experimental Therapeutics*, 302(3):1046-1054.

Alexander R, Kerby A, Aubdool A A, Power A R, Grover S, Gentry C, Grant A D (2013). 4 alpha-phorbol 12,13-didecanoate activates cultured mouse dorsal root ganglia neurons independently of TRPV4. *British Journal of Pharmacology*, 168(3):761-772.

Amadesi S, Bunnett N (2004). Protease-activated receptors: protease signaling in the gastrointestinal tract. *Current Opinion in Pharmacology*, 4(6):551-556.

Amadesi S, Cottrell G S, Divino L, Chapman K, Grady E F, Bautista F, Karanjia R, Barajas-Lopez C, Vanner S, Vergnolle N, Bunnett N W (2006). Protease-activated receptor 2 sensitizes TRPV1 by protein kinase C epsilon- and A-dependent mechanisms in rats and mice. *Journal of Physiology*, 575(2):555-571.

Amadesi S, Nie J, Vergnolle N, Cottrell G S, Grady E F, Trevisani M, Manni C, Geppetti P, McRoberts J A, Ennes H, Davis J B, Mayer E A, Bunnett N W (2004). Protease-activated receptor 2 sensitizes the capsaicin receptor transient receptor potential vanilloid receptor 1 to induce hyperalgesia. *Journal of Neuroscience*, 24(18):4300-4312.

- Andersen H H, Elberling J, Solvsten H, Yosipovitch G, Arendt-Nielsen L (2017). Nonhistaminergic and mechanical itch sensitization in atopic dermatitis. *Pain*, 158(9):1780-1791.
- Andersen H, Greenberg D L, Fujikawa K, Xu W F, Chung D W, Davie E W (1999). Protease-activated receptor 1 is the primary mediator of thrombin-stimulated platelet procoagulant activity. *Proceedings of the National Academy of Sciences of the United States of America*, 96(20):11189-11193.
- Andoh T, Asakawa Y, Kuraishi Y (2018). Non-myelinated C-fibers, but not myelinated A-fibers, elongate into the epidermis in dry skin with itch. *Neuroscience Letters*, 672:84-89.
- Andoh T, Harada A, Inagaki Y (2017). Involvement of Leukotriene B-4 Released from Keratinocytes in Itch-associated Response to Intradermal Interleukin-31 in Mice. *Acta Dermato-Venereologica*, 97(8):922-927.
- Andoh T, Katsube N, Maruyama M, Kuraishi Y (2001). Involvement of leukotriene B-4 in substance P-induced itch-associated response in mice. *Journal of Investigative Dermatology*, 117(6):1621-1626.
- Andoh T, Kuraishi Y (1998). Intradermal leukotriene B-4, but not prostaglandin E-2, induces itch-associated responses in mice. *European Journal of Pharmacology*, 353(1):93-96.
- Andoh T, Tsujii K, Kuraishi Y (2015). Increase in pruritogenic kallikrein 5 in the skin of NC mice with chronic dermatitis. *Experimental Dermatology*, 24(12):978-980.
- Andrei C, Margiocco P, Poggi A, Lotti L V, Torrisi M R, Rubartelli A (2004). Phospholipases C and A(2) control lysosome-mediated IL-1 beta secretion: Implications for inflammatory processes. *Proceedings of the National Academy of Sciences of the United States of America*, 101(26):9745-9750.
- Andrews N W (2002). Lysosomes and the plasma membrane: trypanosomes reveal a secret relationship. *Journal of Cell Biology*, 158(3):389-394.
- Arachiche A, Mumaw M M, de la Fuente M, Nieman M T (2013). Protease-activated Receptor 1 (PAR1) and PAR4 Heterodimers Are Required for PAR1-enhanced Cleavage of PAR4 by alpha-Thrombin. *Journal of Biological Chemistry*, 288(45):32553-32562.
- Arai I, Tsuji M, Miyagawa K, Takeda H, Akiyama N, Saito S (2015). Repeated administration of IL-31 upregulates IL-31 receptor A (IL-31RA) in dorsal root ganglia and causes severe itch-associated scratching behaviour in mice. *Experimental Dermatology*, 24(1):75-78.
- Aral M, Arican O, Gul M, Sasmaz S, Kocturk S A, Kastal U, Ekerbicer H C (2006). The relationship between serum levels of total IgE, IL-18, IL-12, IFN-gamma and disease severity in children with atopic dermatitis. *Mediators of Inflammation*, 73098.
- Aresh B, Freitag F B, Perry S, Blumel E, Lau J, Franck M C M, Lagerstrom MC (2017). Spinal cord interneurons expressing the gastrin-releasing peptide receptor convey itch through VGLUT2-mediated signaling. *Pain*, 158(5):945-961.
- Arthur R P, Shelley W B (1955). The role of proteolytic enzymes in the production of pruritus in man. *Journal of Investigative Dermatology*, 25(5):341-346.

Asbóth G, Phaneuf S, Europe-Finner G N, Tóth M, Bernal A L (1996). Prostaglandin E2 activates phospholipase C and elevates intracellular calcium in cultured myometrial cells: involvement of EP1 and EP3 receptor subtypes. *Endocrinology*, 137(6):2572-2579.

Asokanathan N, Lan R S, Graham P T, Bakker A J (2015). Activation of protease-activated receptors (PARs)-1 and -2 promotes alpha-smooth muscle actin expression and release of cytokines from human lung fibroblasts. *Physiological Reports*, 3(2):e12295.

Atoyan R, Shander D, Botchkareva N V (2009). Non-Neuronal Expression of Transient Receptor Potential Type A1 (TRPA1) in Human Skin. *Journal of Investigative Dermatology*, 129(9):2312-2315.

Bandell M, Story G M, Hwang S W, Viswanath V, Eid S R, Petrus M J, Earley, T, Patapoutian A (2004). Noxious cold ion channel TRPA1 is activated by pungent compounds and bradykinin. *Neuron*, 41(6):849-857.

Banwell M E, Tolley N S, Williams T J, Mitchell T J (2002). Regulation of human eotaxin-3/CCL26 expression: Modulation by cytokines and glucocorticoids. *Cytokine*, 17(6):317-323.

Bao L, Shi V Y, Chan L S (2012). IL-4 regulates chemokine CCL26 in keratinocytes through the Jak1, 2/Stat6 signal transduction pathway: Implication for atopic dermatitis. *Molecular Immunology*, 50(1-2):91-97.

Bao Y J, Gao Y B, Yang L P, Kong X Y, Zheng H G, Hou W, Hua B J (2015). New insights into protease-activated receptor 4 signaling pathways in the pathogenesis of inflammation and neuropathic pain: a literature review. *Channels*, 9(1):5-13.

Bao L, Shi V Y, Chan L S (2013). IL-4 up-regulates epidermal chemotactic, angiogenic, and pro-inflammatory genes and down-regulates antimicrobial genes *in vivo* and *in vitro*: Relevant in the pathogenesis of atopic dermatitis. *Cytokine*, 61(2):419-425.

Barclay J, Clark A K, Ganp P, Gentry C, Patel S, Wotherspoon G, Buxton F, Song C Z, Ullah J, Winter J, Fox A, Bevan S, Malcangio M (2007). Role of the cysteine protease cathepsin S in neuropathic hyperalgesia. *Pain*, 130(3):225-234.

Bardoni R (2013). Role of Presynaptic Glutamate Receptors in Pain Transmission at the Spinal Cord Level. *Current Neuropharmacology*, 11(5):477-483.

Barker J N W N, Karabin G D, Stoof T J, Sarma V J, Dixit V M, Nickoloff B J (1991). Detection of interferon-gamma mRNA in psoriatic epidermis by polymerase chain reaction. *Journal of Dermatological Science*, 2(2):106-111.

Barker P A, Shooter E M (1994). Disruption of NGF binding to the low affinity neurotrophin receptor p75LNTR reduces NGF binding to TrkA on PC12 cells. *Neuron*, 13(1):203-215.

Baron R, Schwarz K, Kleinert A, Schattschneider J, Wasner G (2001). Histamine-induced itch converts into pain in neuropathic hyperalgesia. *Neuroreport*, 12(16):3475-3478.

Baroni A, Buommino E, De Gregorio V, Ruocco E, Ruocco V, Wolf R (2012). Structure and function of the epidermis related to barrier properties. *Clinics in Dermatology*, 30(3):257-262.

Barr A J, Brass L F, Manning D R (1997). Reconstitution of receptors and GTP-binding regulatory proteins (G proteins) in Sf9 cells - A direct evaluation of selectivity in receptor center dot G protein coupling. *Journal of Biological Chemistry*, 272(4):2223-2229.

Barry D M, Li H, Liu X Y, Shen K F, Liu X T, Wu Z Y, Munanairi A, Chen X J, Yin J, Sun, Y G, Li Y Q, Chen Z F (2016). Critical evaluation of the expression of gastrin-releasing peptide in dorsal root ganglia and spinal cord. *Molecular Pain*, 12:1744806916643724.

Bäumer W, Stahl J, Sander K, Petersen L J, Paps J, Stark H, Kietzmann M, Olivry T (2011). Lack of preventing effect of systemically and topically administered histamine H-1 or H-4 receptor antagonists in a dog model of acute atopic dermatitis. *Experimental Dermatology*, 20(7):577-581.

Bautista D M, Wilson S R, Hoon M A (2014). Why we scratch an itch: the molecules, cells and circuits of itch. *Nature Neuroscience*, 17(2):175-182.

Baxter R M, Brissette J L (2002). Role of the nude gene in epithelial terminal differentiation. *Journal of Investigative Dermatology*, 118(2):303-309.

Becker D, Blase C, Bereiter-Hahn J, Jendrach M (2005). TRPV4 exhibits a functional role in cell-volume regulation. *Journal of Cell Science*, 118(11):2435-2440.

Beers C, Burich A, Kleijmeer M J, Griffith J M, Wong P, Rudensky A Y (2005). Cathepsin S controls MHC class II-mediated antigen presentation by epithelial cells *in vivo*. *Journal of Immunology*, 174(3):1205-1212.

Belghiti M, Estevez-Herrera J, Gimenez-Garzo C, Gonzalez-Usano A, Montoliu C, Ferrer-Montiel A, Felipe V, Planells-Cases R (2013). Potentiation of the Transient Receptor Potential Vanilloid 1 Channel Contributes to Pruritogenesis in a Rat Model of Liver Disease. *Journal of Biological Chemistry*, 288(14):9675-9685.

Bell A M, Gutierrez-Mecinas M, Polgar E, Todd A J (2016). Spinal neurons that contain gastrin-releasing peptide seldom express Fos or phosphorylate extracellular signal-regulated kinases in response to intradermal chloroquine. *Molecular Pain*, 12:1744806916649602.

Bell J K, McQueen D S, Rees J L (2004). Involvement of histamine H-4 and H-1 receptors in scratching induced by histamine receptor agonists in BalbC mice. *British Journal of Pharmacology*, 142(2):374-380.

Bender K O, Ofori L, van der Linden W A, Mock E D, Datta G K, Chowdhury S, Li, H, Segal E, Lopez M S, Ellman J A, Figdor CG, Bogyo M, Verdoes M (2015). Design of a Highly Selective Quenched Activity-Based Probe and Its Application in Dual Color Imaging Studies of Cathepsin S Activity Localization. *Journal of the American Chemical Society*, 137(14):4771-4777.

Bernard D, Mehul B, Thomas-Collignon A, Simonetti L, Remy V, Bernard M A, Schmidt R (2003). Analysis of proteins with caseinolytic activity in a human stratum corneum extract revealed a yet unidentified cysteine protease and identified the so-called "stratum corneum thiol protease" as cathepsin L2. *Journal of Investigative Dermatology*, 120(4):592-600.

Bernink J H, Peters C P, Munneke M, te Velde A A, Meijer S L, Weijer K, Hreggvidsdottir H S, Heinsbroek S E, Legrand N, Buskens C J, Bemelman W A, Mjosberg J M, Spits H (2013).

Human type 1 innate lymphoid cells accumulate in inflamed mucosal tissues. *Nature Immunology*, 14(3):221-229.

Bettelli E, Korn T, Kuchroo V K (2007). Th17: the third member of the effector T cell trilogy. *Current Opinion in Immunology*, 19(6):652-657.

Bieber T (2010). Atopic Dermatitis. *Annals of Dermatology*, 22(2): 125–137.

Bien K, Zmigrodzka M, Orłowski P, Fruba A, Szymanski A, Stankiewicz W, Nowak Z, Malewski T, Krzyzowska M (2017). Involvement of Fas/FasL pathway in the murine model of atopic dermatitis. *Inflammation Research*, 66(8):679-690.

Bikle D D (2004). Vitamin D regulated keratinocyte differentiation. *Journal of Cellular Biochemistry*, 92(3):436-444.

Biro T, Maurer M, Modarres S, Lewin N E, Brodie C, Acs G, Acs P, Paus R, Blumberg P M (1998). Characterization of functional vanilloid receptors expressed by mast cells. *Blood*, 91(4):1332-1340.

Bjerke J R, Livden J K, Degre M, Matre R (1983). Interferon in suction blister fluid from psoriatic lesions. *British Journal of Dermatology*, 108(3):295-299.

Blott E J, Griffiths G M (2002). Secretory lysosomes. *Nature Reviews Molecular Cell Biology*, 3(2):122-131.

Boada M D, Houle T T, Eisenach J C, Ririe D G (2010). Differing Neurophysiologic Mechanosensory Input from Glabrous and Hairy Skin in Juvenile Rats. *Journal of Neurophysiology*, 104(6):3568-3575.

Bockelmann R, Horn T, Gollnick H, Bonnekoh B (2005). Interferon-gamma-dependent *in vitro* model for the putative keratin 17 autoimmune loop in psoriasis: Exploration of pharmacologic and gene-therapeutic effects. *Skin Pharmacology and Physiology*, 18(1):42-54.

Boelsma E, Verhoeven M C H, Ponc M (1999). Reconstruction of a human skin equivalent using a spontaneously transformed keratinocyte cell line (HaCaT). *Journal of Investigative Dermatology*, 112(4):489-498.

Böhm S K, Khitin L M, Grady E F, Aponte G, Payan D G, Bunnett N W (1996a). Mechanisms of desensitization and resensitization of proteinase-activated receptor-2. *Journal of Biological Chemistry*, 271(36):22003-22016.

Böhm S K, Kong W Y, Bromme D, Smeekens S P, Anderson D C, Connolly A, Kahn M, Nelken N A, Coughlin S R, Payan D G, Bunnett, N W (1996b). Molecular cloning, expression and potential functions of the human proteinase-activated receptor-2. *Biochemical Journal*, 314:1009-1016.

Bonanno J A, Srinivas S P, Brown M (1995). Effect of acetazolamide on intracellular pH and bicarbonate transport in bovine corneal endothelium. *Experimental Eye Research*, 60(4):425-434.

Bos J D, Hagenaars C, Das P K, Krieg S R, Voorn W J, Kapsenberg M L (1989). Predominance of “memory” T cells (CD4+, CDw29+) over “naive” T cells (CD4+, CD45R+) in both normal and diseased human skin. *Archives of Dermatological Research*. 281(1):24-30.

Boukamp P, Petrussevska R T, Breitkreutz D, Hornung J, Markham A, Fusenig N E (1988). Normal keratinization in a spontaneously immortalized aneuploid human keratinocyte cell-line. *Journal of Cell Biology*, 106(3):761-771.

Bovenschen H J, van Vlijmen-Willems I M J J, van de Kerkhof P C M, van Erp P E J (2006). Identification of lesional CD4+ CD25+ Foxp3+ regulatory T cells in psoriasis. *Dermatology*, 213(2):111-117.

Boyce ST, Ham R G (1983). Calcium-regulated differentiation of normal human epidermal keratinocytes in chemically defined clonal culture and serum-free serial culture. *Journal of Investigative Dermatology*, 81(1):33-40.

Boyman O, Hefti H P, Conrad C, Nickoloff B J, Suter M, Nestle F O (2004). Spontaneous development of psoriasis in a new animal model shows an essential role for resident T cells and tumor necrosis factor-alpha. *Journal of Experimental Medicine*, 199(5):731-736.

Braz J M, Juarez-Salinas D, Ross S E, Basbaum A I (2014a). Transplant restoration of spinal cord inhibitory controls ameliorates neuropathic itch. *Journal of Clinical Investigation*, 124(8):3612-3616.

Braz J, Solorzano C, Wang X D, Basbaum A I (2014b). Transmitting Pain and Itch Messages: A Contemporary View of the Spinal Cord Circuits that Generate Gate Control. *Neuron*, 82(3):522-536.

Brazda V, Klusakova I, Svizenska I H, Dubovy P (2013). Dynamic response to peripheral nerve injury detected by in situ hybridization of IL-6 and its receptor mRNAs in the dorsal root ganglia is not strictly correlated with signs of neuropathic pain. *Molecular Pain*, 9:42.

Briot A, Deraison C, Lacroix M, Bonnart C, Robin A, Besson C, Dubus P, Hovnanian A (2009). Kallikrein 5 induces atopic dermatitis-like lesions through PAR2-mediated thymic stromal lymphopoietin expression in Netherton syndrome. *Journal of Experimental Medicine*, 206(5):1135-1147.

Bromme D, Bonneau P R, Lachance P, Wiederanders B, Kirschke H, Peters C, Thomas D Y, Storer A C, Vernet T (1993). Functional expression of human cathepsin-S in *saccharomyces-cerevisiae* - purification and characterization of the recombinant enzyme. *Journal of Biological Chemistry*, 268(7):4832-4838.

Bromme D, Rinne R, Kirschke H (1991). Tight-binding inhibition of cathepsin S by cystatins. *Biomedica Biochimica Acta*, 50(4-6):631-635.

Burnier L, Mosnier L O (2013). Novel mechanisms for activated protein C cytoprotective activities involving noncanonical activation of protease-activated receptor 3. *Blood*, 122(5):807-816.

Buth H, Wolters B, Hartwig B, Meier-Bornheim R, Veith H, Hansen M, Sommerhoff C P, Schaschke N, Machleidt N, Fusenig N E, Boukamp P, Brix K (2004). HaCaT keratinocytes secrete lysosomal cysteine proteinases during migration. *European Journal of Cell Biology*, 83(11):781-795.

Cain D M, Khasabov S G, Simone D A (2001). Response properties of mechanoreceptors and nociceptors in mouse glabrous skin: an *in vivo* study. *Journal of Neurophysiology*, 85(4):1561-1574.

Calcott G, White J P M, Nagy I (2011). Xenon fails to inhibit capsaicin-evoked CGRP release by nociceptors in culture. *Neuroscience Letters*, 499(2):124-126.

Cannon K E, Chazot P L, Hann V, Shenton F, Hough L B, Rice F L (2007). Immunohistochemical localization of histamine H-3 receptors in rodent skin, dorsal root ganglia, superior cervical ganglia, and spinal cord: Potential antinociceptive targets. *Pain*, 129(1-2):76-92.

Carroll J M, Romero M R, Watt F M (1995). Suprabasal integrin expression in the epidermis of transgenic mice results in developmental defects and a phenotype resembling psoriasis. *Cell*, 83(6):957-968.

Carstens E E, Carstens M I, Simons C T, Jinks S L (2010). Dorsal horn neurons expressing NK-1 receptors mediate scratching in rats. *Neuroreport*, 21(4):303-308.

Casaca V I, Illi S, Klucker E, Ballenberger N, Schedel M, von Mutius E, Kabesch M, Schaub B (2013). STAT6 polymorphisms are associated with neonatal regulatory T cells and cytokines and atopic diseases at 3 years. *Allergy*, 68(10):1249-1258.

Castellani M L, Felaco P, Galzio R J, Tripodi D, Toniato E, De Lutiis M A, Fulcheri M, Caraffa A, Antinolfi P, Tete S, Felaco M, Conti F, Pandolfi F, Theoharides T C, Shaik-Dasthagirisahab Y B (2010). IL-31 a Th2 cytokine involved in immunity and inflammation. *International Journal of Immunopathology and Pharmacology*, 23(3):709-713.

Caterina M J, Schumacher M A, Tominaga M, Rosen T A, Levine J D, Julius D (1997). The capsaicin receptor: a heat-activated ion channel in the pain pathway. *Nature*, 389(6653):816-824.

Caubet C, Jonca N, Brattsand M, Guerrin M, Bernard D, Schmidt R, Egelrud T, Simon M, Serre G (2004). Degradation of corneodesmosome proteins by two serine proteases of the kallikrein family, SCTE/KLK5/hK5 and SCCE/KLK7/hK7. *Journal of Investigative Dermatology*, 122(5):1235-1244.

Cevikbas F, Wang X D, Akiyama T, Kempkes C, Savinko T, Antal A, Kukova G, Buhl T, Ikoma A, Buddenkotte J, Soumelis V, Feld M, Alenius H, Dillon S R, Carstens E, Homey B, Basbaum A, Steinhoff M (2014). A sensory neuron-expressed IL-31 receptor mediates T helper cell-dependent itch: Involvement of TRPV1 and TRPA1. *Journal of Allergy and Immunology*, 133(2):448+.

Chambers L S, Black J L, Poronnik P, Johnson P R A (2001). Functional effects of protease-activated receptor-2 stimulation on human airway smooth muscle. *American Journal of Physiology - Lung Cellular and Molecular Biology*, 281(6):L1369-L1378.

Chan L S, Robinson N, Xu L T (2001). Expression of interleukin-4 in the epidermis of transgenic mice results in a pruritic inflammatory skin disease: An experimental animal model to study atopic dermatitis. *Journal of Investigative Dermatology*, 117(4):977-983.

Chaplan S R, Bach F W, Pogrel J W, Chung J M, Yaksh T L (1994). Quantitative Assessment of Tactile Allodynia in the Rat Paw. *Journal of Neuroscience Methods*, 53(1):55-63.

Chapman H A (2006). Endosomal proteases in antigen presentation. *Current Opinion in Immunology*, 18(1):78-84.

Chapman H A, Riese R J, Shi G P (1997). Emerging roles for cysteine proteases in human biology. *Annual Review of Physiology*, 59:63-88.

Che D N, Cho B O, Shin J Y, Kang H J, Kim Y S, Jang S I (2018). Fisetin inhibits IL-31 production in stimulated human mast cells: Possibilities of fisetin being exploited to treat histamine-independent pruritus. *Life Sciences*, 201:121-129.

Chen Y, Yang C, Wang Z J (2011). Proteinase-activated receptor 2 sensitizes transient receptor potential vanilloid 1, transient receptor potential vanilloid 4, and transient receptor potential ankyrin 1 in paclitaxel-induced neuropathic pain. *Neuroscience*, 193:440-451.

Chen Y, Fang Q, Wang Z, Zhang J Y, MacLeod A S, Hall R P, Liedtke W B, Wolfgang B (2016). Transient Receptor Potential Vanilloid 4 Ion Channel Functions as a Pruriceptor in Epidermal Keratinocytes to Evoke Histaminergic Itch. *Journal of Biological Chemistry*, 291(19):10252-10262.

Chen Y, Willcockson H H, Valtschanoff J G (2008). Increased expression of CGRP in sensory afferents of arthritic mice – effect of genetic deletion of the vanilloid receptor TRPV1. *Neuropeptides*, 42(5-6):551-556.

Chen Y, Willcockson H H, Valtschanoff J G (2009). Vanilloid receptor TRPV1-mediated phosphorylation of ERK in murine adjuvant arthritis. *Osteoarthritis and Cartilage*. 17(2):244-251.

Chen K, Zhang Z F, Liao M F, Yao W L, Wang J, Wang X R (2015). Blocking PAR2 attenuates oxaliplatin-induced neuropathic pain via TRPV1 and releases of substance P and CGRP in superficial dorsal horn of spinal cord. *Journal of the Neurological Sciences*, 352(1-2):62-67.

Choi M, Lee C (2015). Immortalization of Primary Keratinocytes and Its Application to Skin Research. *Biomolecules & Therapeutics*. 23(5):391–399.

Chuang H H, Prescott E D, Kong H, Shields S, Jordt S E, Basbaum A I, Chao M V, Julius D (2001). Bradykinin and nerve growth factor release the capsaicin receptor from PtdIns(4,5)P₂-mediated inhibition. *Nature*, 411(6840):957-62.

Cicala C, Pinto A, Bucci M, Sorrentino R, Walker B, Harriot P, Cruchley A (1999). Protease-activated receptor-2 involvement in hypotension in normal and endotoxemic rats *in vivo*. *Circulation*, 99(19):2590-2597.

Clark R A, Chong B, Mirchandani N, Brinster N K, Yamanaka K, Dowgiert R K, Kupper T S (2006). The vast majority of CLA(+) T cells are resident in normal skin. *Journal of Immunology*, 176(7):4431-4439.

Clark R A, Schlapbach C (2017). T(H)9 cells in skin disorders. *Seminars in Immunology*, 39(1):47-54.

Clark A K, Wodarski R, Guida F, Sasso O, Malcangio M (2010). Cathepsin S Release from Primary Cultured Microglia Is Regulated by the P2X₇ Receptor. *Glia*, 58(14):1710-1726.

Clark A K, Yip P K, Grist J, Gentry C, Staniland A A, Marchand F, Dehvari M, Wotherspoon G, Winter J, Ullah J, Bevan S, Malcangio M (2007). Inhibition of spinal microglial cathepsin S for the reversal of neuropathic pain. *Proceedings of the National Academy of Sciences of the United States of America*, 104(25):10655-10660.

Colombo I, Sangiovanni E, Maggio R, Mattozzi C, Zava S, Corbett Y, Fumagalli M, Carlino C, Corsetto P, Scaccabarozzi D, Calvieri S, Gismondi A, Taramelli D, Dell'Agli M (2017). HaCaT Cells as a Reliable *In Vitro* Differentiation Model to Dissect the Inflammatory/Repair Response of Human Keratinocytes. *Mediators of inflammation*, 7435621.

Compton S J (2003). Glycosylation and proteinase-activated receptor function. *Drug Development Research*, 59(4):350-354.

Compton S J, Renaux B, Wijesuriya S J, Hollenberg M D (2001). Glycosylation and the activation of proteinase-activated receptor 2 (PAR(2)) by human mast cell tryptase. *British Journal of Pharmacology*, 134(4):705-718.

Costa R, Marotta D M, Manjavachi M N, Fernandes E S, Lima-Garcia J F, Paszcuk A F, Quintao N L M, Juliano L, Brain S D, Calixto J B (2008). Evidence for the role of neurogenic inflammation components in trypsin-elicited scratching behaviour in mice. *British Journal of Pharmacology*, 154(5):1094-1103.

Cook P W, Piepkorn M, Clegg C H, Plowman G D, DeMay J M, Brown R, Pittelkow M R (1997). Transgenic expression of the human amphiregulin gene induces a psoriasis-like phenotype. *Journal of Clinical Investigation*, 100(9):2286-2294.

Coughlin S R (2005). Protease-activated receptors in hemostasis, thrombosis and vascular biology. *Journal of Thrombosis and Haemostasis*, 3(8):1800-1814.

Covic L, Gresser A L, Talavera J, Swift S, Kuliopulos A (2002). Activation and inhibition of G protein-coupled receptors by cell-penetrating membrane-tethered peptides. *Proceedings of the National Academy of Sciences of the United States of America*, 99(2):643-648.

Cowen T, Trigg P, Eady R A J (1979). Distribution of mast cells in human dermis: development of a mapping technique. *British Journal of Dermatology*, 100(6):635-640.

Daehn I S, Varelias A, Rayner T E (2010). T-lymphocyte-induced, fas-mediated apoptosis is associated with early keratinocyte differentiation. *Experimental Dermatology*, 19(4):372-380.

Dahl S W, Halkier T, Lauritzen C, Dolenc I, Pedersen J, Turk V, Turk B (2001). Human recombinant pro-dipeptidyl peptidase I (cathepsin C) can be activated by cathepsins L and S but not by autocatalytic processing. *Biochemistry*, 40(6):1671-1678.

Dai Y, Moriyama T, Higashi T, Togashi K, Kobayashi K, Yamanaka H, Tominaga M, Noguchi K (2004). Proteinase-activated receptor 2-mediated potentiation of transient receptor potential vanilloid subfamily 1 activity reveals a mechanism for proteinase-induced inflammatory pain. *Journal of Neuroscience*, 24(18):4293-4299.

Dai Y, Wang S, Tominaga M, Yamamoto S, Fukuoka T, Higashi T, Kobayashi K, Obata K, Yamanaka H, Noguchi K (2007). Sensitization of TRPA1 by PAR2 contributes to the sensation of inflammatory pain. *Journal of Clinical Investigation*, 117(10):1979-1987.

Dai X, Segre J A (2004). Transcriptional control of epidermal specification and differentiation. *Current Opinion in Genetics & Development*, 14(5):485-491.

Dixon W J (1980). Efficient analysis of experimental observations. *Annual Review of Pharmacology and Toxicology*, 20:441-462.

Dam T N, Kang S, Nickoloff B J, Voorhees J J (1999). 1 alpha,25-Dihydroxycholecalciferol and cyclosporine suppress induction and promote resolution of psoriasis in human skin grafts transplanted on to SCID mice. *Journal of Investigative Dermatology*, 113(6):1082-1089.

Danso M O, van Drongelen V, Mulder A, van Esch J, Scott H, van Smeden J, El Ghalbzouri A, Bouwstra J A (2014). TNF-alpha and Th2 Cytokines Induce Atopic Dermatitis-Like Features on Epidermal Differentiation Proteins and Stratum Corneum Lipids in Human Skin Equivalents. *Journal of Investigative Dermatology*, 134(7):1941-1950.

Darsow U, Drzezga A, Frisch M, Munz F, Weilke F, Bartenstein P, Schwaiger M, Ring J (2000). Processing of histamine-induced itch in the human cerebral cortex: A correlation analysis with dermal reactions. *Journal of Investigative Dermatology*, 115(6):1029-1033.

Dascal N (2001). Ion-channel regulation by G proteins. *Trends in Endocrinology and Metabolism*, 12(9):391-398.

Davidson S, Giesler G J (2010). The multiple pathways for itch and their interactions with pain. *Trends in Neurosciences*, 33(12):550-558.

Davidson S, Zhang X J, Khasabov S G, Moser H R, Honda C N, Simone D A, Giesler G J (2012). Pruriceptive spinothalamic tract neurons: physiological properties and projection targets in the primate. *Journal of Neurophysiology*, 108(6):1711-1723.

Davidson S, Zhang X, Khasabov S G, Simone D A, Giesler G J (2009). Relief of itch by scratching: state-dependent inhibition of primate spinothalamic tract neurons. *Nature neuroscience*, 12(5):544-546.

Davidson S, Zhang X J, Yoon C H, Khasabov S G, Simone D A, Giesler G J (2007). The itch-producing agents histamine and cowhage activate separate populations of primate spinothalamic tract neurons. *Journal of Neuroscience*, 27(37):10007-10014.

Décombaz J, Beaumont M, Vuichoud J, Bouisset F, Stellingwerff T (2012). Effect of slow-release β -alanine tablets on absorption kinetics and paresthesia. *Amino Acids*, 43(1):67-76.

DeFea K A, Zalevsky J, Thoma M S, Dery O, Mullins R D, Bunnett N W (2000). Beta-Arrestin-dependent endocytosis of proteinase-activated receptor 2 is required for intracellular targeting of activated ERK1/2. *Journal of Cell Biology*, 148(6):1267-1281.

de Garavilla L, Vergnolle N, Young S H, Ennes H, Steinhoff M, Ossovskaya V S, D'Andrea M R, Mayer E A, Wallace J L, Hollenberg M D, Andrade-Gordon P, Bunnett N W (2001). Agonists of proteinase-activated receptor 1 induce plasma extravasation by a neurogenic mechanism. *British Journal of Pharmacology*, 133(7):975-987.

de la Fuente M, Noble D N, Verma S, Nieman M T (2012). Mapping Human Protease-activated Receptor 4 (PAR4) Homodimer Interface to Transmembrane Helix 4. *Journal of Biological Chemistry*, 287(13):10414-10423.

Denda M, Sokabe T, Fukumi-Tominaga T, Tominaga M (2007). Effects of skin surface temperature on epidermal permeability barrier homeostasis. *Journal of Investigative Dermatology*, 127(3):654-659.

Dery O, Thoma M S, Wong H, Grady E F, Bunnett N W (1999). Trafficking of proteinase-activated receptor-2 and beta-arrestin-1 tagged with green fluorescent protein - beta-arrestin-dependent endocytosis of a proteinase receptor. *Journal of Biological Chemistry*, 274(26):18524-18535.

Dhand A, Aminoff M J (2014). The neurology of itch. *Brain*, 137:313-322.

Denning G M, Ackermann L W, Barna T J, Armstrong J G, Stoll L L, Weintraub N L, Dickson E W (2008). Proenkephalin expression and enkephalin release are widely observed in non-neuronal tissues. *Peptides*, 29(1):83-92.

D'Erme A M, Wilsmann-Theis D, Wagenpfeil J, Holzel M, Ferring-Schmitt S, Sternberg S, Wittmann M, Peters B, Bosio A, Bieber T, Wenzel J (2015). IL-36 gamma (IL-1F9) Is a Biomarker for Psoriasis Skin Lesions. *Journal of Investigative Dermatology*, 135(4):1025-1032.

Deyrieux A F, Wilson V G (2007). *In vitro* culture conditions to study keratinocyte differentiation using the HaCaT cell line. *Cytotechnology*, 54(2):77-83.

Dillon S R, Sprecher C, Hammond A, Bilsborough J, Rosenfeld-Franklin M, Presnell S R, Haugen H S, Maurer M, Harder B, Johnston J, Bort S, Mudri S, Kuijper J L, Bukowski T, Shea P, Dong D L, Dasovich M, Grant F J, Lockwood L, Levin S D, LeCiel C, Waggle K, Day H, Topouzis S, Kramer J, Kuestner R, Chen Z, Foster D, Parrish-Novak J, Gross J A (2004). Interleukin 31, a cytokine produced by activated T cells, induces dermatitis in mice. *Nature Immunology*, 5(7):752-760.

Diogenes A, Akopian A N, Hargreaves K M (2007). NGF up-regulates TRPA1: implications for orofacial pain. *Journal of Dental Research*, 86(6):550 – 555.

Di Virgilio F, Chiozzi P, Ferrari D, Falzoni S, Sanz J M, Morelli A, Torboli M, Bolognesi G, Baricordi O R (2001). Nucleotide receptors: an emerging family of regulatory molecules in blood cells. *Blood*, 97(3):587-600.

Doering T, Holleran W M, Potratz A, Vielhaber G, Elias P M, Suzuki K, Sandhoff K (1999). Sphingolipid activator proteins are required for epidermal permeability barrier formation. *Journal of Biological Chemistry*, 274(16):11038-11045.

Dong X T, Dong X Z (2018). Peripheral and Central Mechanisms of Itch. *Neuron*, 98(3):482-494.

Drzezga A, Darsow U, Treede R D, Siebner H, Frisch M, Munz F, Weilke F, Ring J, Schwaiger M, Bartenstein P (2001). Central activation by histamine-induced itch: analogies to pain processing: a correlational analysis of O-15H(2)O positron emission tomography studies. *Pain*, 92(1-2):295-305.

Duesberg P, Stindl R, Li R H, Hehlmann R, Rasnick D (2001). Aneuploidy versus gene mutation as cause of cancer. *Current Science*, 81(5):490-500.

Dulon S, Candé C, Bunnett N W, Hollenberg M D, Chignard M, Pidard D (2003). Proteinase-activated receptor-2 and human lung epithelial cells: disarming by neutrophil serine proteinases. *American Journal of Respiratory Cell and Molecular Biology*, 28(3):339-346.

- Dunford P J, Williams K N, Desai P J, Karlsson L, McQueen D, Thurmond R L (2007). Histamine H-4 receptor antagonists are superior to traditional antihistamines in the attenuation of experimental pruritus. *Journal of Allergy and Clinical Immunology*, 119(1):176-183.
- Durham P L, Russo A F (2003). Stimulation of the calcitonin gene-related peptide enhancer by mitogen-activated protein kinases and repression by an antimigraine drug in trigeminal ganglia neurons. *Journal of Neuroscience*, 23(3):807-815.
- Eberlein-Konig B, Schafer T, Huss-Marp J, Darsow U, Mohrenschlager M, Herbert O, Abeck D, Kramer U, Behrendt H, Ring J (2000). Skin Surface pH, Stratum Corneum Hydration, Trans-epidermal Water Loss and Skin Roughness Related to Atopic Eczema and Skin Dryness in a Population of Primary School Children. *Acta Dermato-Venereologica*, 80(3):188-191.
- Ebrahimi S, Rahmani F, Behnam-Rassouli R, Hoseinkhani F, Parizadeh M R, Keramati M R, Khazaie M, Avan A, Hassanian S M (2017). Proinflammatory signaling functions of thrombin in cancer. *Journal of Cellular Physiology*, 232(9):2323-2329.
- Egberts F, Heinrich M, Jensen J M, Winoto-Morbach S, Pfeiffer S, Wickel M, Schunck M, Steude J, Saftig P, Proksch E, Schutze S (2004). Cathepsin D is involved in the regulation of transglutaminase 1 and epidermal differentiation. *Journal of Cell Science*, 117(11):2295-2307.
- Elmariah S B, Reddy V B, Lerner E A (2014). Cathepsin S Signals via PAR2 and Generates a Novel Tethered Ligand Receptor Agonist. *PLoS ONE*, 9(6):e99702.
- Erta M, Quintana A, Hidalgo J (2012). Interleukin-6, a Major Cytokine in the Central Nervous System. *International Journal of Biological Sciences*, 8(9):1254-1266.
- Erturk I E, Arican O, Omurlu I K, Sut N (2012). Effect of the Pruritus on the Quality of Life: A Preliminary Study. *Annals of Dermatology*, 24(4):406-412.
- Eskander M A, Ruparel S, Green D P, Chen P B, Por E D, Jeske N A, Gao X L, Flores E R, Hargreaves K M (2015). Persistent Nociception Triggered by Nerve Growth Factor (NGF) Is Mediated by TRPV1 and Oxidative Mechanisms. *Journal of Neuroscience*, 35(22):8593-8603.
- Exton J H (1996). Regulation of phosphoinositide phospholipases by hormones, neurotransmitters, and other agonists linked to G proteins. *Annual Review of Pharmacology and Toxicology*, 36:481-509.
- Fan F K, Nie S, Dammer E B, Duong D M, Pan D, Ping L Y, Zhai L H, Wu J Z, Hong X C, Qin L S, Xu P, Zhang Y H (2012). Protein Profiling of Active Cysteine Cathepsins in Living Cells Using an Activity-Based Probe Containing a Cell-Penetrating Peptide. *Journal of Proteome Research*, 11(12):5763-5772.
- Fang Y, Liu G X, Xie C Z, Qian K, Lei X H, Liu Q, Liu G, Cao Z Y, Fu J, Du H H, Liu S S, Huang S F, Hu J X, Xu X D (2018). Pharmacological inhibition of TRPV4 channel suppresses malignant biological behavior of hepatocellular carcinoma via modulation of ERK signaling pathway. *Biomedicine and Pharmacotherapy*, 101:910-919.
- Featherstone D E (2010). Intercellular Glutamate Signaling in the Nervous System and Beyond. *ACS Chemical Neuroscience*, 1(1):4-12.

- Feingold K R, Elias P M (2014). Role of lipids in the formation and maintenance of the cutaneous permeability barrier. *Biochimica et Biophysica Acta (BBA) - Molecular and Cell Biology of Lipids*, 1841(3):280-294.
- Feld M, Garcia R, Buddenkotte J, Katayama S, Lewis K, Muirhead G, Hevezi P, Plessner K, Schrupf H, Krjutskov K, Sergeeva O, Muller H W, Tsoka S, Kere J, Dillon S R, Steinhoff M, Homey B (2016). The pruritus- and T(H)2-associated cytokine IL-31 promotes growth of sensory nerves. *Journal of Allergy and Clinical Immunology*, 138(2):500+.
- Fenner J, Clark R A F (2016). Chapter 1 – Anatomy, Physiology, Histology, and Immunohistochemistry of Human Skin. In *Skin Tissue Engineering and Regenerative Medicine*. Academic Press.
- Fernihough J, Gentry C, Bevan S, Winter J (2005). Regulation of calcitonin gene-related peptide and TRPV1 in a rat model of osteoarthritis. *Neuroscience Letters*, 388(2):75-80.
- Fields R D, Burnstock G (2006). Purinergic signalling in neuron-glia interactions. *Nature Reviews Neuroscience*, 7(6):423-436.
- Fleming M S, Ramos D, Han S B, Zhao J Y, Son Y J, Luo W Q (2012). The majority of dorsal spinal cord gastrin releasing peptide is synthesized locally whereas neuromedin B is highly expressed in pain- and itch-sensing somatosensory neurons. *Molecular Pain*, 8:52.
- Fonovic U P, Jevnikar Z, Kos J (2013). Cathepsin S generates soluble CX3CL1 (fractalkine) in vascular smooth muscle cells. *Biological Chemistry*, 394(10):1349-1352.
- Fortunel N O, Martin M T (2012). Cellular organization of the human epidermal basal layer: Clues sustaining a hierarchical model. *International Journal of Radiation Biology*, 88(10):677-681.
- Foster E, Wildner H, Tudeau L, Haueter S, Ralvenius W T, Jeggen M, Johannssen H, Hosli L, Haenraets K, Ghanem A, Conzelmann K K, Bosl M, Zeilhofer H U (2015). Targeted Ablation, Silencing, and Activation Establish Glycinergic Dorsal Horn Neurons as Key Components of a Spinal Gate for Pain and Itch. *Neuron*, 85(6):1289-1304.
- Foster C A, Yokozeki H, Rappersberger K, Koning F, Volcplutzer B, Rieger A, Coligan J E, Wolff K, Stingl G (1990). Human epidermal T-cells predominantly belong to the lineage expressing alpha-beta-T cell receptor. *Journal of Experimental Medicine*, 171(4):997-1013.
- Fujita H (2013). The role of IL-22 and Th22 cells in human skin diseases. *Journal of Dermatological Science*, 72(1):3-8.
- Fukuoka M, Miyachi Y, Ikoma A (2003). Mechanically evoked itch in humans. *Pain*, 154(6):897-904.
- Fusi C, Materazzi S, Minocci D, Maio V, Oranges T, Massi D, Nassini R (2014). Transient Receptor Potential Vanilloid 4 (TRPV4) Is Downregulated in Keratinocytes in Human Non-Melanoma Skin Cancer. *Journal of Investigative Dermatology*, 134(9):2408-2417.
- Gadient R A, Otten U (1996). Postnatal expression of interleukin-6 (IL-6) and IL-6 receptor (IL-6R) mRNAs in rat sympathetic and sensory ganglia. *Brain Research*, 724(1):41-46.

- Gao Y J, Ji R R (2009). c-Fos and pERK, which is a better marker for neuronal activation and central sensitization after noxious stimulation and tissue injury? *Open Pain Journal*, 1(2):11-17.
- Ge L, Ly Y, Hollenberg M, DeFea K (2003). A beta-arrestin-dependent scaffold is associated with prolonged MAPK activation in pseudopodia during protease-activated receptor-2-induced chemotaxis. *Journal of Biological Chemistry*, 278(36):34418-34426.
- Ge L, Shenoy S K, Lefkowitz R J, DeFea K (2004). Constitutive protease-activated receptor-2-mediated migration of MDA MB-231 breast cancer cells requires both beta-arrestin-1 and -2. *Journal of Biological Chemistry*, 279(53):55419-55424.
- Gebhardt T, Wakim L M, Eidsmo L, Reading P C, Heath W R, Carbone F R (2009). Memory T cells in nonlymphoid tissue that provide enhanced local immunity during infection with herpes simplex virus. *Nature Immunology*, 10(5):524-530.
- Gebhardt T, Whitney P G, Zaid A, Mackay L K, Brooks A G, Heath W R, Carbone F R, Mueller S N (2011). Different patterns of peripheral migration by memory CD4(+) and CD8(+) T cells. *Nature*, 477(7363):216-U119.
- Geppetti P, Veldhuis N A, Lieu T, Bunnett N W (2015). G Protein-Coupled Receptors: Dynamic Machines for Signaling Pain and Itch. *Neuron*, 88(4):635-649.
- Gibbins I L, Wattchow D, Coventry B (1987). Two immunohistochemically identified populations of calcitonin gene-related peptide (CGRP)-immunoreactive axons in human skin. *Brain Research*, 414(1):143-148.
- Goenka S, Kaplan M H (2011). Transcriptional regulation by STAT6. *Immunologic Research*, 50(1):87-96.
- Gomides L F, Duarte I D, Ferreira R G, Perez A C, Francischi J N, Klein A (2012). Proteinase-Activated Receptor-4 Plays a Major Role in the Recruitment of Neutrophils Induced by Trypsin or Carrageenan during Pleurisy in Mice. *Pharmacology*, 89(5-6):275-282.
- Gordins P, Clough G F, Church M K, Friedmann P S, McEuen A R, Walls A F (2004). Itch and biphasic flare response following injection of chymase into the skin of human subjects. *Clinical and Experimental Allergy*, 34(11):1806-1806.
- Goswami S C, Thierry-Mieg D, Thierry-Mieg J, Mishra S, Hoon M A, Mannes A J, Iadarola M J (2014). Itch-associated peptides: RNA-Seq and bioinformatic analysis of natriuretic precursor peptide B and gastrin releasing peptide in dorsal root and trigeminal ganglia, and the spinal cord. *Molecular Pain*, 10:44.
- Grace M S, Lieu T, Darby B, Abogadie F C, Veldhuis N, Bunnett N W, McIntyre P (2014). The tyrosine kinase inhibitor bafetinib inhibits PAR2-induced activation of TRPV4 channels *in vitro* and pain *in vivo*. *British Journal of Pharmacology*, 171(16):3881-3894.
- Grant A D, Cottrell G S, Amadesi S, Trevisani M, Nicoletti P, Materazzi S, Altier C, Cenac N, Zamponi G, Bautista-Cruz F, Lopez C B, Joseph E K, Levine J D, Liedtke W, Vanner S, Vergnolle N, Geppetti P, Bunnett N W (2007). Protease-activated receptor 2 sensitizes the transient receptor potential vanilloid 4 ion channel to cause mechanical hyperalgesia in mice. *Journal of Physiology*, 578(3):715-733.

Green D, Dong X Z (2016). The cell biology of acute itch. *Journal of Cell Biology*, 213(2):155-161.

Grewe M, Bruijnzeel-Koomen C A F M, Schopf E, Thepen T, Langeveld-Wildschut A G, Ruzicka T, Krutmann J (1998). A role for Th1 and Th2 cells in the immunopathogenesis of atopic dermatitis. *Immunology Today*, 19(8):359-361.

Grewe M, Gyufko K, Schöpf E, Krutmann J (1994). Lesional expression of interferon- γ in atopic eczema. *Lancet*, 343(8888):25-26.

Grewe M, Walther S, Gyufko K, Czech W, Schopf E, Krutmann J (1995). Analysis of the cytokine pattern expressed in situ in inhalant allergen patch test reactions of atopic dermatitis patients. *Journal of Investigative Dermatology*, 105(3):407-410.

Griffiths-Johnson D A, Collins P D, Rossi A G, Jose P J, Williams T J (1993). The chemokine, eotaxin, activates guinea-pig eosinophils in-vitro and causes their accumulation into the lung in-vivo. *Biochemical and Biophysical Research Communications*. 197(3):1167-1172.

Grimsey N, Soto A G, Trejo J A (2011). Regulation of Protease-activated Receptor Signaling by Posttranslational Modifications. *IUBMB Life*, 3(6):403-411.

Gruber B L, Marchese M J, Santiago-Schwarz F, Martin C A, Zhang J H, Kew, RR (2004). Protease-activated receptor-2 (PAR-2) expression in human fibroblasts is regulated by growth factors and extracellular matrix. *Journal of Investigative Dermatology*, 123(5):832-839.

Guenet J L (2005). The mouse genome. *Genome Research*, 15(12):1729-1740.

Guo A, Jahoda C A (2009). An improved method of human keratinocyte culture from skin explants: cell expansion is linked to markers of activated progenitor cells. *Experimental Dermatology*, 18(8):720-726.

Gutierrez-Mecinas M, Furuta T, Watanabe M, Todd A J (2016). A quantitative study of neurochemically defined excitatory interneuron populations in laminae I-III of the mouse spinal cord. *Molecular Pain*, 12:1744806916629065.

Gutierrez-Mecinas M, Watanabe M, Todd A J (2014). Expression of gastrin-releasing peptide by excitatory interneurons in the mouse superficial dorsal horn. *Molecular Pain*, 10:79.

Guttman-Yassky E, Lowes M A, Fuentes-Duculan J, Zaba L C, Cardinale I, Nogales K E, Khatcherian A, Novitskaya I, Carucci J A, Bergman R, Krueger J G (2008). Low Expression of the IL-23/Th17 Pathway in Atopic Dermatitis Compared to Psoriasis. *Journal of Immunology*, 181(10):7420-7427.

Gutowski S, Smrcka A, Nowak L, Wu D G, Simon M, Sternweis P C (1991). Antibodies to the alpha q subfamily of guanine nucleotide-binding regulatory protein alpha subunits attenuate activation of phosphatidylinositol 4,5-bisphosphate hydrolysis by hormones. *Journal of Biological Chemistry*, 266(30):20519-20524.

Gutzmer R, Mommert S, Gschwandtner M, Zwingmann K, Stark H, Werfel T (2009). The histamine H4 receptor is functionally expressed on T(H)2 cells. *Journal of Allergy and Clinical Immunology*, 123(3):619-625.

- Hachisuka J, Chiang M C, Ross S E (2018). Itch and neuropathic itch. *Pain*, 159(3):603-609.
- Hall C (2004). Essential biochemistry and physiology of (NT-pro)BNP. *European Journal of Heart Failure*, 6(3):257-260.
- Hamilton J R, Frauman A G, Cocks T M (2001). Increased expression of protease-activated receptor-2 (PAR2) and PAR4 in human coronary artery by inflammatory stimuli unveils endothelium-dependent relaxations to PAR2 and PAR4 agonists. *Circulation Research*. 89(1):92-98.
- Hamilton J R, Nguyen P B, Cocks T M (1998). Atypical protease-activated receptor mediates endothelium-dependent relaxation of human coronary arteries. *Circulation Research*, 82(12):1306-1311.
- Hammond G R, Dove S K, Nicol A, Pinxteren J A, Zicha D, Schiavo G (2006). Elimination of plasma membrane phosphatidylinositol (4,5)-bisphosphate is required for exocytosis from mast cells. *Journal of Cell Science*, 15(119):2084-2094.
- Han S K, Dong X Z, Hwang J I, Zylka M J, Anderson D J, Simon M I (2002). Orphan G protein-coupled receptors MrgA1 and MrgC11 are distinctively activated by RF-amide-related peptides through the G alpha(q/11) pathway. *Proceedings of the National Academy of Sciences of the United States of America*, 99(23):14740-14745.
- Han L, Ma C, Liu Q, Weng H J, Cui Y Y, Tang Z X, Kim Y S, Nie H, Qu L T, Patel K N, Li Z, McNeil B, He S Q, Guan Y, Xiao B, LaMotte R H, Dong X Z (2013). A subpopulation of nociceptors specifically linked to itch. *Nature Neuroscience*, 16(2):174-182.
- Han SK, Mancino V, Simon MI (2006). Phospholipase C beta 3 mediates the scratching response activated by the histamine H1 receptor on C-fiber nociceptive neurons. *Neuron*, 52(4):691-703.
- Han W, Wang Z, Lu X, Guo C (2012). Protease activated receptor 4 status of mast cells in post infectious irritable bowel syndrome. *Neurogastroenterology and Motility*, 24(2):113-E82.
- Hansen K K, Saifeddine M, Hollenberg M D (2004). Tethered ligand-derived peptides of proteinase-activated receptor 3 (PAR(3)) activate PAR(1) and PAR(2) in Jurkat T cells. *Immunology*, 112(2):183-190.
- Hao F, Tan M Q, Xu X M, Cui M Z (2008). Histamine induces Egr-1 expression in human aortic endothelial cells via the H1 receptor-mediated protein kinase C delta-dependent ERK activation pathway. *Journal of Biological Chemistry*, 283(40):26928-26936.
- Harder J, Bartels J, Christophers E, Schroder J M (1997). A peptide antibiotic from human skin. *Nature*, 387(6636):861-861.
- Hartmannsgruber V, Heyken W T, Kacik M, Kaistha A, Grgic I, Harteneck C, Liedtke W, Hoyer J, Kohler R (2007). Arterial Response to Shear Stress Critically Depends on Endothelial TRPV4 Expression. *PLoS ONE*, 2(9):e827.
- Hasdemir B, Murphy J E, Cottrell G S, Bunnett N W (2009). Endosomal Deubiquitinating Enzymes Control Ubiquitination and Down-regulation of Protease-activated Receptor 2. *Journal of Biological Chemistry*, 284(41):28453-28466.

- He B, Ye F, Zhou X, Li H, Xun X Q, Ma X Q, Liu X D, Wang Z H, Xu P X, Li Y M (2012). Exogenous nerve growth factor supplementation elevates myocardial immunoreactivity and attenuates cardiac remodeling in pressure-overload rats. *Acta Biochimica Et Biophysica Sinica*, 44(11):931-938.
- Kunisada T (2001). Skin antigens in the steady state are trafficked to regional lymph nodes by transforming growth factor-beta 1-dependent cells. *International Immunology*, 13(5):695-704.
- Hennings H, Michael D, Cheng C, Steinert P, Holbrook K, Yuspa S H (1980). Calcium regulation of growth and differentiation of mouse epidermal-cells in culture. *Cell*, 19(1):245-254.
- Henseler T, Christophers E (1995). Disease concomitance in psoriasis. *Journal of the American Academy of Dermatology*, 32(6):982-986.
- Herde L, Forster C, Strupf M, Handwerker HO (2007). Itch induced by a novel method leads to limbic deactivations - A functional MRI study. *Journal of neurophysiology*, 98(4):2347-2356.
- Heron A, Rouleau A, Cochois V, Pillot C, Schwartz J C, Arrang J M (2001). Expression analysis of the histamine H-3 receptor in developing rat tissues. *Mechanisms of Development*, 105(1-2):167-173.
- Herzog J L, Solomon J A, Draelos Z, Fleischer A, Stough D, Wolf D I, Abramovits W, Werschler W, Green E, Duffy M, Rothaul A, Tansley R (2011). A Randomized, Double-Blind, Vehicle-Controlled Crossover Study to Determine the Anti-Pruritic Efficacy, Safety and Local Dermal Tolerability of a Topical Formulation (SRD174 Cream) of the Long-Acting Opioid Antagonist Nalmefene in Subjects With Atopic Dermatitis. *Journal of Drugs in Dermatology*, 10(8):853-860.
- Heyer G, Groene D, Martus P (2002). Efficacy of naltrexone on acetylcholine-induced alloeknesis in atopic eczema. *Experimental Dermatology*, 11(5):448-455.
- Hikita I, Yoshioka T, Mizoguchi T, Tsukahara K, Tsuru K, Nagai H, Hirasawa T, Tsuruta Y, Suzuki R, Ichihashi M, Horikawa T (2002). Characterization of dermatitis arising spontaneously in DS-Nh mice maintained under conventional conditions: another possible model for atopic dermatitis. *Journal of Dermatological Science*, 30(2):142-153.
- Hille B (2001). *Ion Channels of Excitable Membranes (Third Edition)*, Sinauer, Sunderland.
- Hingtgen C M, Roy S L, Clapp D W (2006). Stimulus-evoked release of neuropeptides is enhanced in sensory neurons from mice with a heterozygous mutation of the Nf1 gene. *Neuroscience*, 137(2):637-645.
- Hoeck E A, Marker J B, Gazerani P, Andersen H H, Arendt-Nielsen L (2016). Preclinical and human surrogate models of itch. *Experimental Dermatology*, 25(10):750-757.
- Hollenberg M D, Saifeddine M (2001). Proteinase-activated receptor 4 (PAR4): activation and inhibition of rat platelet aggregation by PAR4-derived peptides. *Canadian Journal of Physiology and Pharmacology*, 79(5):439-442.

Homma T, Kageyama S, Nishikawa A, Nagata K (2018). Melanosome degradation in epidermal keratinocytes related to lysosomal protease cathepsin V. *Biochemical and Biophysical Research Communications*, 500(2):339-343.

Honey K, Rudensky A Y (2003). Lysosomal cysteine proteases regulate antigen presentation. *Nature Reviews Immunology*, 3(6):472-482.

Hong J, Buddenkotte J, Berger T G, Steinhoff M (2011). Management of Itch in Atopic Dermatitis. *Seminars in Cutaneous Medicine and Surgery*, 30(2):71-86.

Hoon M A (2015). Molecular dissection of itch. *Current Opinion in Neurobiology*, 34:61-66.

Horikoshi T, Igarashi S, Uchiwa H, Brysk H, Brysk M M (1999). Role of endogenous cathepsin D-like and chymotrypsin-like proteolysis in human epidermal desquamation. *British Journal of Dermatology*, 141(3):453-459.

Horiuchi Y, Bae S J, Katayama I (2005). Nerve growth factor (NGF) and epidermal nerve fibers in atopic dermatitis model NC/Nga mice. *Journal of Dermatological Science*, 39(1):56-58.

Hosogi M, Schmelz M, Miyachi Y, Ikoma A (2006). Bradykinin is a potent pruritogen in atopic dermatitis: a switch from pain to itch. *Pain*, 126(1-3):16-23.

Howell M D, Kim B E, Gao P, Grant A V, Boguniewicz M, Schneider L, Beck L A, Barnes K, Leung D Y M (2007). Cytokine modulation of atopic dermatitis filaggrin skin expression. *Journal of Allergy and Clinical Immunology*, 120(1):150-155.

Hsing L C, Rudensky A Y (2005). The lysosomal cysteine proteases in MHC class II antigen presentation. *Immunological Reviews*, 207:229-241.

Huang C H, Kuo I C, Xu H, Lee Y S, Chua K Y (2003). Mite allergen induces allergic dermatitis with concomitant neurogenic inflammation in mouse. *Journal of Investigative Dermatology*, 121(2):289-293.

Huang J, Polgar E, Solinski H J, Mishra S K, Tseng P Y, Iwagaki N, Boyle K A, Dickie A C, Kriegbaum M C, Wildner H, Zeilhofer H U, Watanabe M, Riddell J S, Todd A J, Hoon M A (2018). Circuit dissection of the role of somatostatin in itch and pain. *Nature Neuroscience*, 21(5)707+.

Hung D T, Vu T H, Nelken N A, Coughlin SR (1992). Thrombin-induced events in non-platelet cells are mediated by the unique proteolytic mechanism established for the cloned platelet thrombin receptor. *Journal of Cell Biology*, 116(3):827-832.

Hwang S J, Burette A, Rustioni A, Valtschanoff J G (2004). Vanilloid receptor VR1-positive primary afferents are glutamatergic and contact spinal neurons that co-express neurokinin receptor NK1 and glutamate receptors. *Journal of Neurocytology*, 33(3):321-329.

Hwang S W, Cho H, Kwak J, Lee S Y, Kang C J, Jung J, Cho S, Min K H, Suh Y G, Kim D, Oh U (2000). Direct activation of capsaicin receptors by products of lipoxygenases: Endogenous capsaicin-like substances. *Proceedings of the National Academy of Sciences of the United States of America*, 97(11):6155-6160.

Hwang C, Jang S, Choi D K, Kim S, Lee J H, Lee Y, Kim C D, Lee J H (2009). The Role of Nkx2.5 in Keratinocyte Differentiation. *Annals of Dermatology*, 21(4):376-381.

Igarashi S, Takizawa T, Takizawa T, Yasuda Y, Uchiwa H, Hayashi S, Brysk H, Robinson J M, Yamamoto K, Brysk M M, Horikoshi T (2004). Cathepsin D, but not cathepsin E, degrades desmosomes during epidermal desquamation. *British Journal of Dermatology*, 151(2):355-361.

Igawa K, Satoh T, Yokozeki H (2009). A therapeutic effect of STAT6 decoy oligodeoxynucleotide ointment in atopic dermatitis: a pilot study in adults. *British Journal of Dermatology*, 160(5):1124-1126.

Ikoma A, Fartasch M, Heyer G, Miyachi Y, Handwerker H, Schmelz M (2004). Painful stimuli evoke itch in patients with chronic pruritus - Central sensitization for itch. *Neurology*, 62(2):212-217.

Ikoma A, Handwerker H, Miyachi Y, Schmelz M (2005). Electrically evoked itch in humans. *Pain*, 113(1-2):148-154.

Ikoma A, Rukwied R, Stander S, Steinhoff M, Miyachi Y, Schmelz M (2003). Neuronal sensitization for histamine-induced itch in lesional skin of patients with atopic dermatitis. *Archives of Dermatology*, 139(11):1455-1458.

Ikoma A, Steinhoff M, Stander S, Yosipovitch G, Schmelz M (2006). The neurobiology of itch. *Nature Reviews Neuroscience*, 7(7):535-547.

Imamachi N, Park G H, Lee H, Anderson D J, Simon M I, Basbaum A I, Han S K (2009). TRPV1-expressing primary afferents generate behavioral responses to pruritogens via multiple mechanisms. *Proceedings of the National Academy of Sciences of the United States of America*, 106(27):11330-11335.

Inoue K, Koizumi S, Fuziwara S, Denda S, Inoue K, Denda M (2002). Functional vanilloid receptors in cultured normal human epidermal keratinocytes. *Biochemical and Biophysical Research Communications*, 291(1):124-129.

Inoue A, Uchida H, Nakazawa T, Yamamoto T, Ito S (2016). Phosphorylation of NMDA receptor GluN2B subunit at Tyr1472 is important for trigeminal processing of itch. *European Journal of Neuroscience*, 44(7):2474 – 2482.

Ishihara H, Connolly A J, Zeng D W, Kahn M L, Zheng Y W, Timmons C, Tram T, Coughlin S R (1997). Protease-activated receptor 3 is a second thrombin receptor in humans. *Nature*, 386(6624):502-506.

Ishii K, Chen J, Ishii M, Koch W J, Freedman N J, Lefkowitz R J, Coughlin S R (1994). Inhibition of thrombin receptor signaling by a G-protein coupled receptor kinase. Functional specificity among G-protein coupled receptor kinases. *Journal of Biological Chemistry*, 269(2):1125-1130.

Iotzova-Weiss G, Freiberger S N, Johansen P, Kamarachev J, Guenova E, Dziunycz P J, Roux G A, Neu J, Hofbauer G F L (2017). TLR4 as a negative regulator of keratinocyte proliferation. *PLoS ONE*, 12(10):e0185668.

Ishida-Yamamoto A, Kishibe M (2011). Involvement of corneodesmosome degradation and lamellar granule transportation in the desquamation process. *Medical Molecular Morphology*, 44(1):1-6.

Ishiuji Y, Coghill R C, Patel T S, Oshiro Y, Kraft R A, Yosipovitch G (2009). Distinct patterns of brain activity evoked by histamine-induced itch reveal an association with itch intensity and disease severity in atopic dermatitis. *British Journal of Dermatology*, 161(5):1072-1080.

Ito Y, Satoh T, Takayama K, Miyagishi C, Walls A F, Yokozeki H (2011). Basophil recruitment and activation in inflammatory skin diseases. *Allergy*, 66(8):1107-1113.

Iyengar S, Ossipov M H, Johnson K W (2017). The role of calcitonin gene-related peptide in peripheral and central pain mechanisms including migraine. *Pain*, 158(4):543-559.

Jacob C, Cottrell G S, Gehring D, Schmidlin F, Grady E F, Bunnett N W (2005). c-Cbl mediates ubiquitination, degradation, and down-regulation of human protease-activated receptor 2. *Journal of Biological Chemistry*, 280(16):16076-16087.

Jans R, Sartor M, Jadot M, Poumay (2004). Calcium entry into keratinocytes induces exocytosis of lysosomes. *Archives of Dermatological Research*, 296(1):30-41.

Jaubert J, Cheng J, Segre JA (2003). Ectopic expression of Kruppel like factor 4 (Klf4) accelerates formation of the epidermal permeability barrier. *Development*, 130(12):2767-2777.

Ji R R (2015). Neuroimmune interactions in itch: Do chronic itch, chronic pain, and chronic cough share similar mechanisms? *Pulmonary pharmacology & therapeutics*, 35:81 – 86.

Ji R R, Baba H, Brenner G J, Woolf C J (1999). Nociceptive-specific activation of ERK in spinal neurons contributes to pain hypersensitivity. *Nature Neuroscience*, 2(12):1114-1119.

Ji Y, Jang Y, Lee W J, Yang Y D, Shim W S (2018). Different perception levels of histamine-induced itch sensation in young adult mice. *Physiology and Behaviour*, 188:188-193.

Ji R R, Samad T A, Jin S X, Schmoll R, Woolf C J (2002). p38 MAPK activation by NGF in primary sensory neurons after inflammation increases TRPV1 levels and maintains heat hyperalgesia. *Neuron*, 36(1):57-68.

Jian T Y, Yang N N, Yang Y, Zhu C, Yuan X L, Yu G, Wang C M, Wang Z L, Shi H, Tang M, He Q, Lan L, Wu G Y, Tang Z X (2016). TRPV1 and PLC Participate in Histamine H4 Receptor-Induced Itch. *Neural Plasticity*, 1682972.

Jiang G Y, Dai M H, Huang K, Chai G D, Chen J Y, Chen L, Lang B, Wang Q X, St Clair D, McCaig C, Ding Y Q, Zhang L (2015). Neurochemical characterization of pERK-expressing spinal neurons in histamine-induced itch. *Scientific Reports*, 5:12787.

Jiang C, Diao F, Sang Y J, Xu N, Zhu R L, Wang X X, Chen Z, Tao W W, Yao B, Sun H X, Huang X X, Xue B, Li C J (2017a). GGPP-Mediated Protein Geranylgeranylation in Oocyte Is Essential for the Establishment of Oocyte-Granulosa Cell Communication and Primary-Secondary Follicle Transition in Mouse Ovary. *PLoS Genetics*, 13(1):e1006535.

Jiang Y H, Yau M K, Kok R M, Lim J X, Wu K C, Liu L G, Hill T A, Suen J Y, Fairlie D P (2017b). Biased Signaling by Agonists of Protease Activated Receptor 2. *ACS Chemical Biology*, 12(5):1217-1226.

Jiao Y, Sun Z, Lee T, Fusco F R, Kimble T D, Meade C A, Cuthbertson S, Reiner A (1999). A simple and sensitive antigen retrieval method for free-floating and slide-mounted tissue sections. *Journal of Neuroscience Methods*, 93:149-162.

Jinks S L, Carstens E (2002). Responses of superficial dorsal horn neurons to intradermal serotonin and other irritants: comparison with scratching behavior. *Journal of Neurophysiology*, 87(3):1280-1289.

Jinks S L, Simons C T, Dessirier J M, Carstens M I, Antognini J F, Carstens E (2002). C-fos induction in rat superficial dorsal horn following cutaneous application of noxious chemical or mechanical stimuli. *Experimental Brain Research*, 145(2):261-269.

Johanek LM, Meyer RA, Friedman RM, Greenquist KW, Shim B, Borzan J, Hartke T, LaMotte RH, Ringkamp M (2008). A role for polymodal C-fiber afferents in nonhistaminergic itch. *Journal of Neuroscience*, 28(30):7659-7669.

Johanson C E, Parandoosh Z, Dyas M L (1992). Maturation differences in acetazolamide-altered pH and HCO₃ of choroid-plexus, cerebrospinal-fluid, and brain. *American Journal of Physiology*, 262(5):R909-R914.

Kagami S, Kakinuma T, Saeki H, Tsunemi Y, Fujita H, Nakamura K, Takekoshi T, Kishimoto M, Mitsui H, Torii H, Komine M, Asahina A, Tamaki K (2003). Significant elevation of serum levels of eotaxin-3/CCL26, but not of eotaxin-2/CCL24, in patients with atopic dermatitis: serum eotaxin-3/CCL26 levels reflect the disease activity of atopic dermatitis. *Clinical and Experimental Immunology*, 134(2):309-313.

Kagami S, Rizzo H L, Lee J J, Koguchi Y, Blauvelt A (2010). Circulating Th17, Th22, and Th1 Cells Are Increased in Psoriasis. *Journal of Investigative Dermatology*, 130(5):1373-1383.

Kagami S, Saeki H, Komine M, Kakinuma T, Tsunemi Y, Nakamura K, Sasaki K, Asahina A, Tamaki K (2005). Interleukin-4 and interleukin-13 enhance CCL26 production in a human keratinocyte cell line, HaCaT cells. *Clinical and Experimental Immunology*, 141(3):459-466.

Kagami S, Sugaya M, Suga H, Morimura S, Kai H, Ohmatsu H, Fujita H, Tsunemi Y, Sato S (2013). Serum Gastrin-Releasing Peptide Levels Correlate with Pruritus in Patients with Atopic Dermatitis. *Journal of Investigative Dermatology*, 133(6):1673-1675.

Kajihara Y, Murakami M, Imagawa T, Otsuguro K, Ito S, Ohta T (2010). Histamine potentiates acid-induced responses mediating transient receptor potential V1 in mouse primary sensory neurons. *Neuroscience*, 166(1):292-304.

Kalynovska N, Adamek P, Palecek J (2017). TRPV1 Receptors Contribute to Paclitaxel-Induced c-Fos Expression in Spinal Cord Dorsal Horn Neurons. *Physiological Research*, 66(3):549-552.

Kam P C, Tan K H (1996). Pruritus - itching for a cause and relief? *Anaesthesia*, 51(12):1133-1138.

- Kamo A, Negi O, Tengara S, Kamata Y, Noguchi A, Ogawa H, Tominaga M, Takamori K (2014). Histamine H-4 Receptor Antagonists Ineffective against Itch and Skin Inflammation in Atopic Dermatitis Mouse Model. *Journal of Investigative Dermatology*, 134(2):546-548.
- Kamsteeg M, Bergers M, de Boer R, Zeeuwen P L J M, Hato S V, Schalkwijk J, Tjabringa G S (2011). Type 2 Helper T-Cell Cytokines Induce Morphologic and Molecular Characteristics of Atopic Dermatitis in Human Skin Equivalent. *American Journal of Pathology*, 178(5):2091-2099.
- Kamsteeg M, Jansen P A M, van Vlijmen-Willems I M J J, van Erp P E J,; Rodijk-Olthuis D, van der Valk P G, Feuth T, Zeeuwen P L J M, Schalkwijk J (2010). Molecular diagnostics of psoriasis, atopic dermatitis, allergic contact dermatitis and irritant contact dermatitis. *British Journal of Dermatology*, 162(3):568-578.
- Kamsteeg M, Zeeuwen P L J M, de Jongh G J, Rodijk-Olthuis D, Zeeuwen-Franssen M E J, van Erp P E J, Schalkwijk J (2007). Increased expression of carbonic anhydrase II (CA II) in lesional skin of atopic dermatitis: Regulation by Th2 cytokines. *Journal of Investigative Dermatology*, 127(7):1786-1789.
- Kaplan A P (2002). Chronic urticaria and angioedema. *New England Journal of Medicine*, 346(3):175-179.
- Kardon A P, Polgar E, Hachisuka J, Snyder L M, Cameron D, Savage S, Cai X Y, Karnup S, Fan C R, Hemenway G M, Bernard C S, Schwartz E S, Nagase H, Schwarzer C, Watanabe M, Furuta T, Kaneko T, Koerber H R, Todd A J, Ross S E (2014). Dynorphin Acts as a Neuromodulator to Inhibit Itch in the Dorsal Horn of the Spinal Cord. *Neuron*, 82(3):573-586.
- Karli U O, Schäfer T, Burger M M (1990). Fusion of neurotransmitter vesicles with target membrane is calcium independent in a cell-free system. *Proceedings of the National Academy of Sciences of the United States of America*, 87(15):5912-5915.
- Kato A, Fujii E, Watanabe T, Takashima Y, Matsushita H, Furuhashi T, Morita A (2014). Distribution of IL-31 and its receptor expressing cells in skin of atopic dermatitis. *Journal of Dermatological Science*, 74(3):229-235.
- Kawabata A, Kawao N (2005). Physiology and pathophysiology of proteinase-activated receptors (PARs): PARs in the respiratory system: Cellular signaling and physiological/pathological roles. *Journal of Pharmacological Sciences*, 97(1):20-24.
- Kawabata A, Nakaya Y, Ishiki T, Kubo S, Kuroda R, Sekiguchi F, Kawao N, Nishikawa H, Kawai K (2004). Receptor-activating peptides for PAR-1 and PAR-2 relax rat gastric artery via multiple mechanisms. *Life Sciences*, 75(22):2689-2702.
- Kawakami T, Ando T, Kimura M, Wilson B S, Kawakami Y (2009). Mast cells in atopic dermatitis. *Current Opinion in Immunology*, 21(6):666-678.
- Kawamura M, Kuraishi Y, Minami M, Satoh M (1989). Antinociceptive effect of intrathecally administered antiserum against calcitonin gene-related peptide on thermal and mechanical noxious stimuli in experimental hyperalgesic rats. *Brain Research*, 497(1):199-203.

- Kida N, Sokabe T, Kashio M, Haruna K, Mizuno Y, Suga Y, Nishikawa K, Kanamaru A, Hongo M, Oba A, Tominaga M (2012). Importance of transient receptor potential vanilloid 4 (TRPV4) in epidermal barrier function in human skin keratinocytes. *Pflügers Archiv-European Journal of Physiology*, 463(5):715-725.
- Kiguchi N, Sukhtankar D D, Ding H P, Tanaka K, Kishioka S, Peters C M, Ko M C (2016). Spinal Functions of B-Type Natriuretic Peptide, Gastrin-Releasing Peptide, and Their Cognate Receptors for Regulating Itch in Mice. *Journal of Pharmacology and Experimental Therapeutics*, 356(3):596-603.
- Kim N, Bae K B, Kim M O, Yi D H, Kim H J, Yuh H S, Ji Y R, Park S J, Kim S, Son K H, Park S J, Yoon D, Lee D S, Lee S, Lee H S, Kim T Y, Ryoo Z Y (2012). Overexpression of cathepsin S induces chronic atopic dermatitis in mice. *Journal of Investigative Dermatology*, 132(4):1169-1176.
- Kim S, Barry D M, Liu X Y, Yin S J, Munanairi A, Meng Q T, Cheng W, Mo P, Wan L, Liu S B, Ratnayake K, Zhao Z Q, Gautam N, Zheng J, Karunarathne W K A, Chen Z F (2016). Facilitation of TRPV4 by TRPV1 is required for itch transmission in some sensory neuron populations. *Science Signaling*, 9(437):ra71.
- Kim D K, Kim H J, Sung K S, Kim H, Cho S A, Kim K M, Lee C H, Kim J J (2007). 12(S)-HPETE induces itch-associated scratchings in mice. *European Journal of Pharmacology*, 554(1):30-33.
- Kim B M, Lee S H, Shim W S, Oh U (2004). Histamine-induced Ca²⁺ influx via the PLA(2)/lipoxygenase/TRPV1 pathway in rat sensory neurons. *Neuroscience Letter*, 361(1-3):159-162.
- Kim B E, Leung D Y M, Boguniewicz M, Howell M D (2008). Loricrin and involucrin expression is down-regulated by Th2 cytokines through STAT-6. *Clinical Immunology*, 126(3):332-337.
- Kini S P, DeLong L K, Veledar E, McKenzie-Brown A M, Schaufele M, Chen S C (2011). The Impact of Pruritus on Quality of Life: The Skin Equivalent of Pain. *Archives of Dermatology*, 147(10):1153-1156.
- Kirschke H, Wiederanders B (1994). Cathepsin-S and related lysosomal endopeptidases. *Methods in Enzymology*, 244:500-511.
- Klein A, Carstens M I, Carstens E (2011). Facial injections of pruritogens or algogens elicit distinct behavior responses in rats and excite overlapping populations of primary sensory and trigeminal subnucleus caudalis neurons. *Journal of Neurophysiology*, 106(3):1078-1088.
- Klein P A, Clark R A F (1999). An evidence-based review of the efficacy of antihistamines in relieving pruritus in atopic dermatitis. *Archives of Dermatology*, 135(12):1522-1525.
- Kniep E M, Roehlecke C, Ozkucur N, Steinberg A, Reber F, Knels L, Funk R H W (2006). Inhibition of apoptosis and reduction of intracellular pH decrease in retinal neural cell cultures by a blocker of carbonic anhydrase. *Investigative Ophthalmology and Visual Science*, 47(3):1185-1192.

Knight D A, Lim S, Scaffidi A K, Roche N, Chung K F, Stewart GA, Thompson P J (2001). Protease-activated receptors in human airways: Upregulation of PAR-2 in respiratory epithelium from patients with asthma. *Journal of Allergy and Clinical Immunology*, 108(5):797-803.

Kollisch G, Kalali B N, Voelcker V, Wallich R, Behrendt H, Ring J, Bauer S, Jakob T, Mempel M, Ollert M (2005). Various members of the Toll-like receptor family contribute to the innate immune response of human epidermal keratinocytes. *Immunology*, 114(4):531-541.

Kollmeier A, Francke K, Chen B, Dunford P J, Greenspan A J, Xia Y C, Xu X L, Zhou B, Thurmond R L (2014). The Histamine H-4 Receptor Antagonist, JNJ 39758979, Is Effective in Reducing Histamine-Induced Pruritus in a Randomized Clinical Study in Healthy Subjects. *Journal of Pharmacology and Experimental Therapeutics*, 350(1):181-187.

Komatsu N, Saijoh K, Toyama T, Ohka R, Otsuki N, Hussack G, Takehara K, Diamandis E P (2005). Multiple tissue kallikrein mRNA and protein expression in normal skin and skin diseases. *British Journal of Dermatology*, 153(2):274-281.

Komatsu N, Takata M, Otsuki N, Toyama T, Ohka R, Takehara K, Saijoh K (2003). Expression and localization of tissue kallikrein mRNAs in human epidermis and appendages. *Journal of Investigative Dermatology*, 121(3):542-549.

Komuves L, Oda Y, Tu C L, Chang W H, Ho-Pao C L, Mauro T, Bikle D D (2002). Epidermal expression of the full-length extracellular calcium-sensing receptor is required for normal keratinocyte differentiation. *Journal of Cellular Physiology*, 192(1):45-54.

Konishi H, Tsutsui H, Murakami T, Yumikura-Futatsugi S, Yamanaka K, Tanaka M, Iwakura Y, Suzuki N, Takeda K, Akira S, Nakanishi K, Mizutani H (2002). IL-18 contributes to the spontaneous development of atopic dermatitis-like inflammatory skin lesion independently of IgE/stat6 under specific pathogen-free conditions. *Proceedings of the National Academy of Sciences of the United States of America*, 99(17):11340-11345.

Kopitar G, Dolinar M, Strukelj B, Pungercar J, Turk V (1996). Folding and activation of human procathepsin S from inclusion bodies produced in *Escherichia coli*. *European Journal of Biochemistry*, 236(2):558-562.

Koshimizu T A, Van Goor F, Tomić M, Wong A O, Tanoue A, Tsujimoto G, Stojilkovic S S (2000). Characterization of calcium signaling by purinergic receptor-channels expressed in excitable cells. *Molecular Pharmacology*, 58(5):936-945.

Kouzaki H, O'Grady S M, Lawrence C B, Kita H (2009). Proteases Induce Production of Thymic Stromal Lymphopoietin by Airway Epithelial Cells through Protease-Activated Receptor-2. *Journal of Immunology*, 183(2):1427-1434.

Krueger G G, Chambers D A, Shelby J (1981). Involved and uninvolved skin from psoriatic subjects - are they equally diseased - assessment by skin transplanted to congenitally athymic (nude) mice. *Journal of Clinical Investigation*, 68(6):1548-1557.

Kularathna P K, Pagel C N, Mackie E J (2014). Tumour progression and cancer-induced pain: A role for protease-activated receptor-2? *International Journal of Biochemistry & Cell Biology*, 57:149-156.

- Kumar P, Lau C S, Mathur M, Wang P, DeFea K A (2007). Differential effects of beta-arrestins on the internalization, desensitization and ERK1/2 activation downstream of protease activated receptor-2. *American Journal of Physiology - Cell Physiology*, 293(1):C346-C357.
- Kuraishi Y, Nagasawa T, Hayashi K, Satoh M (1995). Scratching behavior induced by pruritogenic but not algesciogenic agents in mice. *European Journal of Pharmacology*, 275(3):229-233.
- Kwan K Y, Allchorne A J, Vollrath M A, Christensen A P, Zhang D S, Woolf C J, Corey D P (2006). TRPA1 contributes to cold, mechanical, and chemical nociception but is not essential for hair-cell transduction. *Neuron*, 50(2): 277-289.
- Lagerstrom M C, Rogoz K, Abrahamsen B, Persson E, Reinius B, Nordenankar K, Olund C, Smith C, Mendez J A, Chen Z F, Wood J N, Wallen-Mackenzie A, Kullander K (2010). VGLUT2-Dependent Sensory Neurons in the TRPV1 Population Regulate Pain and Itch. *Neuron*, 68(3):529-542.
- LaMotte R H, Dong X Z, Ringkamp M (2014). Sensory neurons and circuits mediating itch. *Nature Reviews Neuroscience*, 15(1):19-31.
- LaMotte R H, Shimada S G, Sikand P (2011). Mouse models of acute, chemical itch and pain in humans. *Experimental Dermatology*, 20(10):778-782.
- Landmann L (1986). Epidermal permeability barrier: transformation of lamellar granule-disks into intercellular sheets by a membrane-fusion process, a freeze-fracture study. *Journal of Investigative Dermatology*, 87(2):202-209.
- Laniyonu A A, Hollenberg M D (1995). Vascular actions of thrombin receptor-derived polypeptides: structure-activity profiles for contractile and relaxant effects in rat aorta. *British Journal of Pharmacology*, 114(8):1680-1686.
- Lauerma A I, Fenn B, Maibach H I (1997). Trimellitic anhydride-sensitive mouse as an animal model for contact urticaria. *Journal of Applied Toxicology*, 17(6):357-360.
- Lawson S N, Crepps B, Perl E R (2002). Calcitonin gene-related peptide immunoreactivity and afferent receptive properties of dorsal root ganglion neurones in guinea-pigs. *Journal of Physiology*, 540(3):989-1002.
- Lee H, Ko M C (2015). Distinct functions of opioid-related peptides and gastrin-releasing peptide in regulating itch and pain in the spinal cord of primates. *Scientific Reports*, 5:11676.
- Lee Y L, Yen J J Y, Hsu L C, Kuo N W, Su M W, Yang M F, Hsiao Y P, Wang I J, Liu F T (2015). Association of STAT6 genetic variants with childhood atopic dermatitis in Taiwanese population. *Journal of Dermatological Science*, 79(3):222-228.
- Lee Y S, Yuspa S H, Dlugosz A A (1998). Differentiation of cultured human epidermal keratinocytes at high cell densities is mediated by endogenous activation of the protein kinase C signaling pathway. *Journal of Investigative Dermatology*, 111(5):762-766.
- Lee P J, Zhang X C, Shan P Y, Mail B, Lee C G, Homer R J, Zhu Z, Rincon M, Mossman B T, Elias J A (2006). ERK1/2 mitogen-activated protein kinase selectively mediates IL-13-induced lung inflammation and remodeling *in vivo*. *Journal of Clinical Investigation*, 116(1):163-173.

Leger A J, Jacques S L, Badar J, Kaneider N C, Derian C K, Andrade-Gordon P, Covic L, Kuliopulos A (2006). Blocking the protease-activated receptor 1-4 heterodimer in platelet-mediated thrombosis. *Circulation*, 113(9):1244-1254.

Leknes S G, Bantick S, Willis C M, Wilkinson J D, Wise R G, Tracey I (2007). Itch and motivation to scratch: An investigation of the central and peripheral correlates of allergen- and histamine-induced itch in humans. *Journal of Neurophysiology*, 97(1):415-422.

Leung D Y M, Soter N A (2001). Cellular and immunologic mechanisms in atopic dermatitis. *Journal of the American Academy of Dermatology*, 44(1):S1-S12.

Leurs R, Traiffort E, Arrang J M, Tardivel-Lacombe J, Ruat M, Schwartz J C (1994). Guinea pig histamine H1 receptor. II. Stable expression in Chinese hamster ovary cells reveals the interaction with three major signal transduction pathways. *Journal of Neurochemistry*, 62(2):519–527.

Lever I J, Bradbury E J, Cunningham J R, Adelson D W, Jones M G, McMahon S B, Marvizon J C G, Malcangio M (2001). Brain-derived neurotrophic factor is released in the dorsal horn by distinctive patterns of afferent fiber stimulation. *Journal of Neuroscience*, 21(12):4469-4477.

Levi K, Baxter J, Meldrum H, Misra M, Pashkovski E, Dauskardt R H (2008). Effect of corneodesmosome degradation on the intercellular delamination of human stratum corneum. *Journal of Investigative Dermatology*, 128(9):2345-2347.

Li F W, Adase C A, Zhang L J (2017). Isolation and Culture of Primary Mouse Keratinocytes from Neonatal and Adult Mouse Skin. *Journal of Visualized Experiments*, 125:e56027.

Li X R, Garrity A G, Xu H X (2013). Regulation of membrane trafficking by signalling on endosomal and lysosomal membranes. *Journal of Physiology*, 591(18):4389-4401.

Li J G, Leyva-Castillo J M, Hener P, Eisenmann A, Zaafour S, Jonca N, Serre G, Birling M C, Li M (2016a). Counterregulation between thymic stromal lymphopoietin- and IL-23-driven immune axes shapes skin inflammation in mice with epidermal barrier defects. *Journal of Allergy and Clinical Immunology*, 138(1):150+.

Li C L, Li K C, Wu D, Chen Y, Luo H, Zhao J R, Wang S S, Sun M M, Lu Y J, Zhong Y Q, Hu X Y, Hou R, Zhou B B, Bao L, Xiao H S, Zhang X (2016b). Somatosensory neuron types identified by high-coverage single-cell RNA-sequencing and functional heterogeneity. *Cell Research*, 26(1):83-102.

Li A G, Wang D, Feng X H, Wang X J (2004). Latent TGF beta 1 overexpression in keratinocytes results in a severe psoriasis-like skin disorder. *EMBO Journal*, 23(8):1770-1781.

Li Z W, Wu B, Ye P, Tan Z Y, Ji Y H (2016c). Brain natriuretic peptide suppresses pain induced by BmK I, a sodium channel-specific modulator, in rats. *Journal of Headache and Pain*, 17:90.

Lichti U, Anders J, Yuspa S H (2008). Isolation and short term culture of primary keratinocytes, hair follicle populations, and dermal cells from newborn mice and keratinocytes from adult mice, for in vitro analysis and for grafting to immunodeficient mice. *Nature Protocols*, 3(5):799–810.

Liebig T, Erasmus J, Kalaji R, Davies D, Loirand G, Ridley A, Braga V M M (2009). RhoE Is Required for Keratinocyte Differentiation and Stratification. *Molecular Biology of the Cell*, 20(1):452-463.

Lieu T, Savage E, Zhao P, Edgington-Mitchell L, Barlow N, Bron R, Poole D P, McLean P, Lohman R J, Fairlie D P, Bunnett N W (2016). Antagonism of the proinflammatory and pronociceptive actions of canonical and biased agonists of protease-activated receptor-2. *British Journal of Pharmacology*, 173(18):2752-2765.

Lieu T, Jayaweera G, Zhao P S, Poole D P, Jensen D, Grace M, McIntyre P, Bron R, Wilson Y M, Krappitz M, Haerteis S, Korbmacher C, Steinhoff M S, Nassini R, Materazzi S, Geppetti P, Corvera C U, Bunnett N W (2014). The Bile Acid Receptor TGR5 Activates the TRPA1 Channel to Induce Itch in Mice. *Gastroenterology*, 147(6):1417-1428.

Lieu T, Savage E, Zhao P, Edgington-Mitchell L, Barlow N, Bron R, Poole D P, McLean P, Lohman R J, Fairlie D P, Bunnett N W (2016). Antagonism of the proinflammatory and pronociceptive actions of canonical and biased agonists of protease-activated receptor-2. *British Journal of Pharmacology*, 173(18):2752-2765.

Lipshetz B, Khasabov S G, Truong H, Netoff T I, Simone D A, Giesler G J (2018). Responses of thalamic neurons to itch- and pain-producing stimuli in rats, *Journal of Neurophysiology*, 120(3):1119-1134.

Liu F T, Goodarzi H, Chen H Y (2011a). IgE, Mast Cells, and Eosinophils in Atopic Dermatitis. *Clinical Reviews in Allergy and Immunology*, 41(3):298-310.

Liu T, Ji R R (2013). New insights into the mechanisms of itch: are pain and itch controlled by distinct mechanisms? *Pflügers Archiv-European Journal of Physiology*, 465(12):1671-1685.

Liu S, Liu Y P, Yue D M, Liu G J (2014a). Protease-activated receptor 2 in dorsal root ganglion contributes to peripheral sensitization of bone cancer pain. *European Journal of Pain*, 18(3):326-337.

Liu Y, Samad O A, Zhang L, Duan B, Tong Q C, Lopes C, Ji R R, Lowell B B, Ma Q F (2010). VGLUT2-Dependent Glutamate Release from Nociceptors Is Required to Sense Pain and Suppress Itch. *Neuron*, 68(3):543-556.

Liu Q, Sikand P, Ma C, Tang Z X, Han L, Li Z, Sun S H, LaMotte R H, Dong X Z (2012). Mechanisms of Itch Evoked by beta-Alanine. *Journal of Neuroscience*, 32(42):14532-14537.

Liu Q, Tang Z X, Surdenikova L, Kim S, Patel K N, Kim A, Ru F, Guan Y, Weng H J, Geng Y X, Udem B J, Kollarik M, Chen Z F, Anderson D J, Dong X Z (2009). Sensory neuron-specific GPCR Mrgprs are itch receptors mediating chloroquine-induced pruritus. *Cell*, 139(7):1353-1365.

Liu X Y, Wan L, Huo F Q, Barry D M, Li H, Zhao Z Q, Chen Z F (2014b). B-type natriuretic peptide is neither itch-specific nor functions upstream of the GRP-GRPR signaling pathway. *Molecular Pain*, 10:4.

Liu Q, Weng H J, Patel K N, Tang Z, Bai H, Steinhoff M, Dong X (2011b). The distinct role of two GPCRs, MrgprC11 and PAR2, in itch and hyperalgesia. *Science Signaling*, 4(181):ra45.

Liuzzo J P, Petanceska S S, Moscatelli D, Devi L A (1999). Inflammatory mediators regulate cathepsin S in macrophages and microglia: A role in attenuating heparan sulfate interactions. *Molecular Medicine*, 5(5):320-333.

Llewellyn-Smith I J, Basbaum A I, Braz J M (2018). Long-term, dynamic synaptic reorganization after GABAergic precursor cell transplantation into adult mouse spinal cord. *Journal of Comparative Neurology*, 526(3):480-495.

Lopez R G, Garcia-Silva S, Moore S J, Bereshchenko O, Martinez-Cruz, A B, Ermakova O, Kurz E, Paramio J M, Nerlov C (2009). C/EBP alpha and beta couple interfollicular keratinocyte proliferation arrest to commitment and terminal differentiation. *Nature Cell Biology*, 11(10):1181-U40.

Lowes M A, Kikuchi T, Fuentes-Duculan J, Cardinale I, Zaba L C, Haider A S, Bowman E P, Krueger J G (2008). Psoriasis vulgaris lesions contain discrete populations of Th1 and Th17 T cells. *Journal of Investigative Dermatology*, 128(5):1207-1211.

Lu C R, Willcockson H H, Phend K D, Lucifora S, Darstein M, Valtschanoff J G, Rustioni A (2005). Ionotropic glutamate receptors are expressed in GABAergic terminals in the rat superficial dorsal horn. *Journal of Comparative Neurology*, 486(2):169-178.

Lu R R, Flauaus C, Kennel L, Petersen J, Drees O, Kallenborn-Gerhardt W, Ruth P, Lukowski R, Schmidtko A (2017). K_(Ca)3.1 channels modulate the processing of noxious chemical stimuli in mice. *Neuropharmacology*, 125:386-395.

Luo J L, Feng J, Liu S B,; Walters E T, Hu H Z (2015). Molecular and cellular mechanisms that initiate pain and itch. *Cellular and Molecular Life Sciences*, 72(17):3201-3223.

Luo J L, Feng J, Yu G, Yang P, Mack M R, Du J H, Yu W H, Qian A H, Zhang Y J, Liu S B, Yin S J, Xu A, Cheng J Z, Liu Q Y, O'Neil R G, Xia Y, Ma L, Carlton S M, Kim B S, Renner K, Liu Q, Hu H Z (2018). Transient receptor potential vanilloid 4-expressing macrophages and keratinocytes contribute differentially to allergic and nonallergic chronic itch. *Journal of Allergy and Clinical Immunology*, 141(2):608+.

Luo W, Wang Y F, Reiser G (2007). Protease-activated receptors in the brain: Receptor expression, activation, and functions in neurodegeneration and neuroprotection. *Brain Research Reviews*, 56(2):331-345.

Ma H L, Liang S, Li J, Napierata L, Brown T, Benoit S, Senices M, Gill D, Dunussi-Joannopoulos K, Collins M, Nickerson-Nutter C, Fouser L A, Young D A (2008). IL-22 is required for Th17 cell-mediated pathology in a mouse model of psoriasis-like skin inflammation. *Journal of Clinical Investigation*, 118(2):597-607.

Macfarlane S R, Seatter M J, Kanke T, Hunter G D, Plevin R (2001). Proteinase-activated receptors. *Pharmacological Reviews*, 53(2):245-282.

Mackay L K, Rahimpour A, Ma J Z, Collins N, Stock A T, Hafon M L, Vega-Ramos J, Lauzurica P, Mueller S N, Stefanovic T, Tschärke D C, Heath W R, Inouye M, Carbone F R, Gebhardt T (2013). The developmental pathway for CD103(+)CD8(+) tissue-resident memory T cells of skin. *Nature Immunology*, 14(12):1294+.

Mackay L K, Wynne-Jones E, Freestone D, Pellicci D G, Mielke L A, Newman D M, Braun A, Masson F, Kallies A, Belz G T, Carbone F R (2015). T-box Transcription Factors Combine with the Cytokines TGF-beta and IL-15 to Control Tissue-Resident Memory T Cell Fate. *Immunity*, 43(6):1101-1111.

Madhusudhan T, Wang H J, Straub B K, Grone E, Zhou Q X, Shahzad K, Muller-Krebs S, Schwenger V, Gerlitz B, Grinnell BW, Griffin J H, Reiser J, Grone H J, Esmon C T, Nawroth P P, Isermann B (2012). Cytoprotective signaling by activated protein C requires protease-activated receptor-3 in podocytes. *Blood*, 119(3):874-883.

Malcangio M, Garrett N E, Tomlinson D R (1997). Nerve Growth Factor Treatment Increases Stimulus-evoked Release of Sensory Neuropeptides in the Rat Spinal Cord. *European Journal of Neuroscience*, 9:1101-1104.

Malcangio M, Ramer M S, Boucher T J, McMahon S B (2000). Intrathecally injected neurotrophins and the release of substance P from the rat isolated spinal cord. *European Journal of Neuroscience*, 12:139-144.

Malekzad F, Arbabi M, Mohtasham N, Toosi P, Jaberian M, Mohajer M, Mohammadi M R, Roodsari M R, Nasiri S (2009). Efficacy of oral naltrexone on pruritus in atopic eczema: a double-blind, placebo-controlled study. *Journal of the European Academy of Dermatology and Venerology*, 23(8):948-950.

Malin S A, Davis B M, Molliver D C (2007). Production of dissociated sensory neuron cultures and considerations for their use in studying neuronal function and plasticity. *Nature Protocols*, 2(1): 152-160.

Man M Q, Hatano Y, Lee S H, Man M, Chang S, Feingold K R, Leung D Y M, Holleran W, Uchida Y, Elias P M (2008). Characterization of a hapten-induced, murine model with multiple features of atopic dermatitis: Structural, immunologic, and biochemical changes following single versus multiple oxazolone challenges. *Journal of Investigative Dermatology*, 128(1):79-86.

Masuda T, Ozono Y, Mikuriya S, Kohro Y, Tozaki-Saitoh H, Iwatsuki K, Uneyama H, Ichikawa R, Salter M W, Tsuda M, Inoue K (2016). Dorsal horn neurons release extracellular ATP in a VNUT-dependent manner that underlies neuropathic pain, *Nature Communications*, 7:12529.

Matsuda H, Watanabe N, Geba G P, Sperl J, Tsudzuki M, Hiroi J, Matsumoto M, Ushio H, Saito S, Askenase P W, Ra C (1997). Development of atopic dermatitis-like skin lesion with IgE hyperproduction in NC/Nga mice. *International Immunology*, 9(3):461-466.

Matsumoto M, Ra C, Kawamoto K, Sato H, Itakura A, Sawada J, Ushio H, Suto H, Mitsuishi K, Hikasa Y, Matsuda H (1999). IgE hyperproduction through enhanced tyrosine phosphorylation of Janus kinase 3 in NC/Nga mice, a model for human atopic dermatitis. *Journal of Immunology*, 162(2):1056-1063.

Maubach G, Schilling K, Rommerskirch W, Wenz I, Schultz J E, Weber E, Wiederanders B (1997). The inhibition of cathepsin S by its propeptide. Specificity and mechanism of action. *European Journal of Biochemistry*, 250(3):745-750.

McCarthy P W, Lawson S N (1990). Cell type and conduction velocity of rat primary sensory neurons with calcitonin gene-related peptide-like immunoreactivity. *Neuroscience*, 34(3):623-632.

McCoy E S, Taylor-Blake B, Street S E, Pribisko A L, Zheng J H, Zylka M J (2013). Peptidergic CGRP alpha Primary Sensory Neurons Encode Heat and Itch and Tonicly Suppress Sensitivity to Cold. *Neuron*, 78(1):138-151.

McCoy E S, Taylor-Blake B, Zylka M J (2012). CGRP alpha-Expressing Sensory Neurons Respond to Stimuli that Evoke Sensations of Pain and Itch. *PLoS ONE*, 7(5):e36355.

McGeachy M J (2013). Th17 memory cells: live long and proliferate. *Journal of Leukocyte Biology*, 94(5):921-926.

McGrath M E (1999). The lysosomal cysteine proteases. *Annual Review of Biophysics and Biomolecular Structure*, 28:181-204.

McGrath J A, Eady R A, Pope F M (2004). *Rook's Textbook of Dermatology* (7th ed.). Blackwell Publishing, pp 3.1–3.6.

McGuire J J, Dai J Z, Andrade-Gordon P, Triggler C R, Hollenberg M D (2002). Proteinase-activated receptor-2 (PAR2) Vascular effects of a PAR2-derived activating peptide via a receptor different than PAR2. *Journal of Pharmacology and Experimental Therapeutics*, 303(3):985-992.

McLaughlin J N, Patterson M M, Malik A B (2007). Protease-activated receptor-3 (PAR3) regulates PAR1 signaling by receptor dimerization. *Proceedings of the National Academy of Sciences of the United States of America*, 104(13):5662-5667.

McLaughlin J N, Shen L X, Holinstat M, Brooks J D, DiBenedetto E, Hamm H E (2005). Functional selectivity of G protein signaling by agonist peptides and thrombin for the protease-activated receptor-1. *Journal of Biological Chemistry*, 280(26):25048-25059.

McMahon S B, Koltzenburg M (1992). Itching for an Explanation. *Trends in Neurosciences*, 15(12):497-501.

McQueen D S, Noble M A H, Bond S M (2007). Endothelin-1 activates ETA receptors to cause reflex scratching in BALB/c mice. *British Journal of Pharmacology*, 151(2):278-284.

Mease P J, Goffe B S, Metz J, VanderStoep A, Finck B, Burge D J (2000). Etanercept in the treatment of psoriatic arthritis and psoriasis: a randomised trial. *Lancet*, 356(9227):385-390.

Megyeri M, Mako V, Beinrohr L, Doleschall Z, Prohaszka Z, Cervenak L, Zavodszky P, Gal P (2009). Complement Protease MASP-1 Activates Human Endothelial Cells: PAR4 Activation Is a Link between Complement and Endothelial Function. *Journal of Immunology*, 183(5):3409-3416.

Meng J H, Moriyama M, Feld M, Buddenkotte J, Buhl T, Szollosi A, Zhang J M, Miller P, Ghetti A, Fischer M, Reeh P W, Shan C X, Wang J F, Steinhoff M (2018). New mechanism underlying IL-31-induced atopic dermatitis. *Journal of Allergy and Clinical Immunology*, 141(5):1677+.

Menon G K, Cleary G W, Lane M E (2012). The structure and function of the stratum corneum. *International Journal of Pharmaceutics*, 435(1):3-9.

Menon G K, Grayson S, Elias P M (1985). Ionic calcium reservoirs in mammalian epidermis - Ultrastructural-localization by ion-capture cyto-chemistry. *Journal of Investigative Dermatology*, 84(6):508-512.

Meyer-Hoffert U, Rogalski C, Seifert S, Schmeling G, Wingerts Zahn J, Proksch E, Wiedow O (2004). Trypsin induces epidermal proliferation and inflammation in murine skin. *Experimental Dermatology*, 13(4):234-241.

Mihara K, Ramachandran R, Renaux B, Saifeddine M, Hollenberg MD (2013). Neutrophil Elastase and Proteinase-3 Trigger G Protein-biased Signaling through Proteinase-activated Receptor-1 (PAR1). *Journal of Biological Chemistry*, 288(46):32979-32990.

Min H, Lee H, Lim H, Jang Y H, Chung S J, Lee C J, Lee S J (2014). TLR4 enhances histamine-mediated pruritus by potentiating TRPV1 activity. *Molecular Brain*, 7:59.

Minutti C M, Drube S, Blair N, Schwartz C, McCrae J C, McKenzie A N, Kamradt T, Mokry M, Coffey PJ, Sibilina M, Sijts A J, Fallon P G, Maizels R M, Zaiss D M (2017). Epidermal Growth Factor Receptor Expression Licenses Type-2 Helper T Cells to Function in a T Cell Receptor-Independent Fashion. *Immunity*, 47(4):710+.

Miotto D, Hollenberg M D, Bunnett N W, Papi A, Braccioni F, Boschetto P, Rea F, Zuin A, Geppetti P, Saetta M, Maestrelli P, Fabbri L M, Mapp C E (2002). Expression of protease activated receptor-2 (PAR-2) in central airways of smokers and non-smokers. *Thorax*, 57(2):146-151.

Mishra S K, Hoon M (2013). The cells and circuitry for itch responses in mice. *Science* 340(6135):968-971.

Mishra S K, Holzman S, Hoon M A (2012). A Nociceptive Signaling Role for Neuromedin B. *Journal of Neuroscience*, 32(25):8686-8695.

Miyai M, Tsunekage Y, Saito M, Kohno K, Takahashi K, Kataoka K (2017). Ectopic expression of the transcription factor MafB in basal keratinocytes induces hyperproliferation and perturbs epidermal homeostasis. *Experimental Dermatology*, 26(11):1039-1045.

Miyamoto T, Nojima H, Shinkado T, Nakahashi T, Kuraishi Y (2002). Itch-associated response induced by experimental dry skin in mice. *Japanese Journal of Pharmacology*, 88(3):285-292.

Mizuguchi H, Terao T, Kitai M, Ikeda M, Yoshimura Y, Das A K, Kitamura Y, Takeda N, Fukui H (2011). Involvement of Protein Kinase C delta/Extracellular Signal-regulated Kinase/Poly(ADP-ribose) Polymerase-1 (PARP-1) Signaling Pathway in Histamine-induced Up-regulation of Histamine H-1 Receptor Gene Expression in HeLa Cells. *Journal of Biological Chemistry*, 286(35):30542-30551.

Mizumoto N, Mummert M E, Shalhevet D, Takashima A (2003). Keratinocyte ATP release assay for testing skin-irritating potentials of structurally diverse chemicals. *Journal of Investigative Dermatology*, 121(5):1066-1072.

Mochizuki H, Inui K, Tanabe H C, Akiyama LF, Otsuru N, Yamashiro K, Sasaki A, Nakata H, Sadato N, Kakigi R (2009). Time Course of Activity in Itch-Related Brain Regions: A Combined MEG-fMRI Study. *Journal of Neurophysiology*, 102(5):2657-2666.

Mochizuki H, Tashiro M, Kano M, Sakurada Y, Itoh M, Yanai K (2003). Imaging of central itch modulation in the human brain using positron emission tomography. *Pain*, 105(1-2):339-346.

Moffatt J D, Cocks T M (1998). Endothelium-dependent and -independent responses to protease-activated receptor-2 (PAR-2) activation in mouse isolated renal arteries. *British Journal of Pharmacology*, 125(4):591-594.

Molino M, Barnathan E S, Numerof R, Clark J, Dreyer M, Cumashi A, Hoxie J A, Schechter N, Woolkalis M, Brass L F (1997). Interactions of mast cell tryptase with thrombin receptors and PAR-2. *Journal of Biological Chemistry*, 272(7):4043-4049.

Moore C, Cevikbas F, Pasolli H A, Chen Y, Kong W, Kempkes C, Parekh P, Lee S H, Kontchou N A, Ye I, Jorke N M, Fuchs E, Steinhoff M, Liedtke W B (2013). UVB radiation generates sunburn pain and affects skin by activating epidermal TRPV4 ion channels and triggering endothelin-1 signaling. *Proceedings of the National Academy of Sciences of the United States of America*, 110(34):E3225-E3234.

Moormann C, Artuc M, Pohl E, Varga G, Buddenkotte J, Vergnolle N, Brehler R, Henz B M, Schneider S W, Luger T A, Steinhoff M (2006). Functional characterization and expression analysis of the proteinase-activated receptor-2 in human cutaneous mast cells. *Journal of Investigative Dermatology*, 126(4):746-755.

Morasso M I, Markova N G, Sargent T D (1996). Regulation of epidermal differentiation by a Distal-less homeodomain gene. *Journal of Cell Biology*, 135(6):1879-1887.

Morita T, McClain S P, Batia L M, Pellegrino M, Wilson S R, Kienzler M A, Lyman K, Olsen A S B, Wong J F, Stucky C L, Brem R B, Bautista D M (2015). HTR7 Mediates Serotonergic Acute and Chronic Itch. *Neuron*, 87(1):124-138.

Moriyama T, Higashi T, Togashi K, Iida T, Segi E, Sugimoto Y, Tominaga T, Narumiya S, Tominaga M (2005). Sensitization of TRPV1 by EP1 and IP reveals peripheral nociceptive mechanism of prostaglandins. *Molecular Pain*, 1:3.

Moser H R, Giesler G J (2014). Characterization of pruriceptive trigeminothalamic tract neurons in rats. *Journal of Neurophysiology*, 111(8):1574-1589.

Mrozkova P, Palecek J, Spicarova D (2016a). The Role of Protease-Activated Receptor Type 2 in Nociceptive Signaling and Pain. *Physiological Research*, 65(3):357-367.

Mrozkova P, Spicarova D, Palecek J (2016b). Hypersensitivity Induced by Activation of Spinal Cord PAR2 Receptors Is Partially Mediated by TRPV1 Receptors. *PLoS ONE*, 11(10):e0163991.

Mudde G C, van Reijssen F C, Bruijnzeel-Koomen C A (1992). IgE-positive Langerhans cells and Th2 allergen-specific T cells in atopic dermatitis. *Journal of Investigative Dermatology*, 99(5):S103-S103.

Mueller S N, Zaid A, Carbone F R (2014). Tissue-resident T cells: dynamic players in skin immunity. *Frontiers in Immunology*, 5:332.

Murata Y, Song M, Kikuchi H, Hisamichi K, Xu X L, Greenspan A, Kato M, Chiou C F, Kato T, Guzzo C, Thurmond R L, Ohtsuki M, Furue M (2015). Phase 2a, randomized, double-blind, placebo-controlled, multicenter, parallel-group study of a H4R-antagonist (JNJ-39758979) in Japanese adults with moderate atopic dermatitis. *Journal of Dermatology*, 42(2):129-139.

Murota H, Izumi M, Abd El-Latif M I, Nishioka M, Terao M, Tani M, Matsui S, Sano S, Katayama I (2012). Artemin causes hypersensitivity to warm sensation, mimicking warmth-provoked pruritus in atopic dermatitis. *Journal of Allergy and Clinical Immunology*, 130(3):671 – 682.

Nagata K, Duggan A, Kumar G, Garcia-Anoveros J (2005). Nociceptor and hair cell transducer properties of TRPA1, a channel for pain and hearing. *Journal of Neuroscience*, 25(16):4052-4061.

Nakagawa N, Sakai S, Matsumoto M, Yamada K, Nagano M, Yuki T, Sumida Y, Uchiwa H (2004). Relationship between NMF (lactate and potassium) content and the physical properties of the stratum corneum in healthy subjects. *Journal of Investigative Dermatology*, 122(3):755-763.

Nakajima K, Terao M, Takaishi M, Kataoka S, Goto-Inoue N, Setou M, Horie K, Sakamoto F, Ito M, Azukizawa H, Kitaba S, Murota H, Itami S, Katayama I, Takeda J, Sano S (2013). Barrier Abnormality Due to Ceramide Deficiency Leads to Psoriasiform Inflammation in a Mouse Model *Journal of Investigative Dermatology*, 133(11):2555-2565.

Nakanishi-Matsui M, Zheng Y W, Sulciner D J, Weiss E J, Ludeman M J, Coughlin S R (2000). PAR3 is a cofactor for PAR4 activation by thrombin. *Nature*, 404(6778):609+.

Nakano T, Andoh T, Lee J B, Kuraishi Y (2008). Different dorsal horn neurons responding to histamine and allergic itch stimuli. *Neuroreport*, 19(7):723-726.

Nakayama T, Yamashita M (2008). Initiation and maintenance of Th2 cell identity. *Current Opinion in Immunology*, 20(3):265-271.

Nattkemper L A, Tey H L, Valdes-Rodriguez R, Lee H, Mollanazar N K, Albornoz C, Sanders K M, Yosipovitch G (2018). The Genetics of Chronic Itch: Gene Expression in the Skin of Patients with Atopic Dermatitis and Psoriasis with Severe Itch. *Journal of Investigative Dermatology*, 138(6):1311-1317.

Nattkemper L A, Zhao Z Q, Nichols A J, Papoiu A D P, Shively C A, Chen Z F, Yosipovitch G (2013). Overexpression of the Gastrin-Releasing Peptide in Cutaneous Nerve Fibers and Its Receptor in the Spinal Cord in Primates with Chronic Itch. *Journal of Investigative Dermatology*, 133(10):2489-2492.

Neis M M, Peters B, Dreuw A, Wenzel J, Bieber T, Mauch C, Krieg T, Stanzel S, Heinrich P C, Merk H F, Bosio A, Baron J M, Hermanns H M (2006). Enhanced expression levels of IL-31 correlate with IL-4 and IL-13 in atopic and allergic contact dermatitis. *Journal of Allergy and Clinical Immunology*, 118(4):930-937.

Nemes Z, Steinert P M (1999). Bricks and mortar of the epidermal barrier, *Experimental and Molecular Medicine*, 31(1):5-19.

- Nestle F O, Zheng X G, Thompson C B, Turka L A, Nickoloff B J. Characterization of dermal dendritic cells obtained from normal human skin reveals phenotypic and functionally distinctive subsets. *Journal of Immunology*, 151(11):6535-6545.
- Ng M F Y (2010). The role of mast cells in wound healing. *International Wound Journal*, 7(1):55-61.
- Nicol G D, Vasko M R (2007). Unraveling the story of NGF-mediated sensitization of nociceptive sensory neurons: On or off the Trks? *Molecular Interventions*, 7(1):26-41.
- Nilius B, Watanabe H, Vriens J (2003). The TRPV4 channel: structure-function relationship and promiscuous gating behaviour. *Pflugers Archiv-European Journal of Physiology*, 446(3):298-303.
- Nishi N, Yamamoto S, Ou W, Muro E, Inada Y, Hamasaki Y (2008). Enhanced CCL26 production by IL-4 through IFN-gamma-induced upregulation of type 1 IL-4 receptor in keratinocytes. *Biochemical and Biophysical Research Communications*, 376(1):234-240.
- Niyonsaba F, Ushio H, Hara M, Yokoi H, Tominaga M, Takamori K, Kajiwarra, N, Saito H, Nagaoka I, Ogawa H, Okumura K (2010). Antimicrobial Peptides Human beta-Defensins and Cathelicidin LL-37 Induce the Secretion of a Pruritogenic Cytokine IL-31 by Human Mast Cells. *Journal of Immunology*, 184(7):3526-3534.
- Nojima H, Carstens E (2003). 5-Hydroxytryptamine (5-HT)₂ receptor involvement in acute 5-HT-evoked scratching but not in allergic pruritus induced by dinitrofluorobenzene in rats. *Journal of Pharmacology and Experimental Therapeutics*, 306(1):245-252.
- Nojima H, Simons C T, Cuellar J M, Carstens M I, Moore J A, Carstens E (2003). Opioid modulation of scratching and spinal c-fos expression evoked by intradermal serotonin. *Journal of Neuroscience*, 23(34):10784-10790.
- Nomura L, Gao B, Boguniewicz M, Darst M A, Travers J B, Leung D Y M (2003). Distinct patterns of gene expression in the skin lesions of atopic dermatitis and psoriasis: A gene microarray analysis. *Journal of Allergy and Clinical Immunology*, 112(6):1195-1202.
- Novak N, Bieber T (2003). Allergic and nonallergic forms of atopic diseases. *Journal of Allergy and Clinical Immunology*, 112(2):252-262.
- Nystedt S, Emilsson I E, Wahlestedt C, Sundelin J (1994). Molecular-Cloning of a Potential Proteinase Activated Receptor. *Proceedings of the National Academy of Sciences of the United States of America*, 91(20):9208-9212.
- Ochiai S, Jagot F, Kyle R L, Hyde E, White R F, Prout M, Schmidt A J, Yamane H, Lamiabile O, Le Gros G, Ronchese F (2018). Thymic stromal lymphopoietin drives the development of IL-13(+) Th2 cells. *Proceedings of the National Academy of Sciences of the United States of America*, 115(5):1033-1038.
- Oh M H, Oh S Y, Lu J N, Lou H F, Myers A C, Zhu Z, Zheng T (2013). TRPA1-Dependent Pruritus in IL-13-Induced Chronic Atopic Dermatitis. *Journal of Immunology*, 191(11):5371-5382.

Oikawa M, Saino T, Kimura K, Kamada Y, Tamagawa Y, Kurosaka D, Satoh Y (2013). Effects of protease-activated receptors (PARs) on intracellular calcium dynamics of acinar cells in rat lacrimal glands. *Histochemistry and Cell Biology*, 140(4):463-476.

Oikonomopoulou K, Hansen K K, Saifeddine M, Vergnolle N, Tea I, Blaber M, Blaber S I, Scarisbrick I, Diamandis EP, Hollenberg MD (2006). Kallikrein-mediated cell signalling: targeting proteinase-activated receptors (PARs). *Biological Chemistry*, 387(6):817-824.

Olivan-Viguera A, Garcia-Otin A L, Lozano-Gerona J, Abarca-Lachen E, Garcia-Malinis A J, Hamilton K L, Gilaberte Y, Pueyo E, Kohler R (2018). Pharmacological activation of TRPV4 produces immediate cell damage and induction of apoptosis in human melanoma cells and HaCaT keratinocytes. *PLoS ONE*, 13(1):e0190307.

Olivry T, Mayhew D, Paps J S, Linder K E, Peredo C, Rajpal D, Hofland H, Cote-Sierra J (2016). Early Activation of Th2/Th22 Inflammatory and Pruritogenic Pathways in Acute Canine Atopic Dermatitis Skin Lesions. *Journal of Investigative Dermatology*, 136(10):1961-1969.

Ossovskaya V S, Bunnett N W (2004). Protease-activated receptors: Contribution to physiology and disease. *Physiological Reviews*, 84(2):579-621.

Ostadhadi S, Kordjazy N, Haj-Mirzaian A, Mansouri P, Dehpour A R (2015). 5-HT₃ receptors antagonists reduce serotonin-induced scratching in mice. *Fundamental and Clinical Pharmacology*, 29(3):310-315.

Ostertag D, Annahazi A, Krueger D, Michel K, Demir I E, Ceyhan G O, Zeller F, Schemann M (2017). Tryptase potentiates enteric nerve activation by histamine and serotonin: Relevance for the effects of mucosal biopsy supernatants from irritable bowel syndrome patients. *Neurogastroenterology and Motility*, 29(9):e13070.

Ostrowska E, Reiser G (2008). The protease-activated receptor-3 (PAR-3) can signal autonomously to induce interleukin-8 release. *Cellular and Molecular Life Sciences*, 65(6):970-981.

Otten U, Goedert M, Mayer N, Lembeck F (1980). Requirement of nerve growth factor for development of substance P-containing sensory neurones. *Nature*, 287(5778):158-159.

Oyoshi M K, Murphy G F, Geha R S (2009). Filaggrin-deficient mice exhibit T(H)17-dominated skin inflammation and permissiveness to epicutaneous sensitization with protein antigen. *Journal of Allergy and Clinical Immunology*, 124(3):485-U145.

Paing M M, Stutts A B, Kohout T A, Lefkowitz R J, Trejo J (2002). Beta-arrestins regulate protease-activated receptor-1 desensitization but not internalization or down-regulation. *Journal of Biological Chemistry*, 277(2):1292-1300.

Paing M M, Temple B R S, Trejo J (2004). A tyrosine-based sorting signal regulates intracellular trafficking of protease-activated receptor-1 - Multiple regulatory mechanisms for agonist-induced G protein-coupled receptor internalization. *Journal of Biological Chemistry*, 279(21):21938-21947.

Palmer C N A, Irvine A D, Terron-Kwiatkowski A, Zhao Y W, Liao H H, Lee S P, Goudie D R, Sandilands A, Campbell L E, Smith F J D, O'Regan G M, Watson R M, Cecil J E, Bale S J, Compton J G, DiGiovanna J J, Fleckman P, Lewis-Jones S, Arseculeratne G, Sergeant A, Munro C S, El Houate B, McElreavey K, Halkjaer L B, Bisgaard H, Mukhopadhyay S, McLean

- W H I (2006). Common loss-of-function variants of the epidermal barrier protein filaggrin are a major predisposing factor for atopic dermatitis. *Nature Genetics*, 38(4):441-446.
- Papoiu A D P, Coghill R C, Kraft R A, Wang H, Yosipovitch G (2012). A tale of two itches. Common features and notable differences in brain activation evoked by cowhage and histamine induced itch. *Neuroimage*, 59(4):3611-3623.
- Papoiu A D P, Tey H L, Coghill R C, Wang H, Yosipovitch G (2011). Cowhage-Induced Itch as an Experimental Model for Pruritus: A Comparative Study with Histamine-Induced Itch. *PLoS ONE*, 6(3):e17786.
- Papp H, Czifra G, Lazar J, Gonczi M, Csernoch L, Kovacs L, Biro T (2003). Protein kinase C isozymes regulate proliferation and high cell density-mediated differentiation in HaCaT keratinocytes. *Experimental Dermatology*, 12(6):811-824.
- Park K A, Fehrenbacher J C, Thompson E L, Duarte D B, Hingtgen C M, Vasko M R (2010). Signaling pathways that mediate nerve growth factor-induced increase in expression and release of calcitonin gene-related peptide from sensory neurons. *Neuroscience*, 171(3):910-923.
- Patricio E S, Costa R, Figueiredo C P, Gers-Barlag K, Bicca M A, Manjavachi M N, Segat G C, Gentry C, Luiz A P, Fernandes E S, Cunha T M, Bevan S, Calixto J B (2015). Mechanisms Underlying the Scratching Behavior Induced by the Activation of Proteinase-Activated Receptor-4 in Mice. *Journal of Investigative Dermatology*, 135(10):2484-2491.
- Pawar K, Sharbati J, Einspanier R, Sharbati S (2016). Mycobacterium bovis BCG Interferes with miR-3619-5p Control of Cathepsin S in the Process of Autophagy, *Frontiers in Cellular and Infection Biology*, 6:27.
- Pedrosa T D, De Vuyst E, Mound A, de Rouvroit C L, Maria-Engler S S, Poumay Y (2017). Methyl-beta-cyclodextrin treatment combined to incubation with interleukin-4 reproduces major features of atopic dermatitis in a 3D-culture model. *Archives of Dermatological Research*, 309(1):63-69.
- Pereira P J S, Lazarotto L F, Leal P C, Lopes T G, Morrone F B, Campos M M (2011). Inhibition of phosphatidylinositol-3 kinase gamma reduces pruriceptive, inflammatory, and nociceptive responses induced by trypsin in mice. *Pain*, 152(12):2861-2869.
- Petanceska S, Canoll P, Devi L A (1996). Expression of rat cathepsin S in phagocytic cells. *Journal of Biological Chemistry*, 271(8):4403-4409.
- Petrus M, Peier A M, Bandell M, Hwang S W, Huynh T, Olney N, Jegla T, Patapoutian A (2007). A role of TRPA1 in mechanical hyperalgesia is revealed by pharmacological inhibition. *Molecular Pain*, 3:40.
- Pierre P, Mellman I (1998). Developmental regulation of invariant chain proteolysis controls MHC class II trafficking in mouse dendritic cells. *Cell*, 93(7):1135-1145.
- Pitake S, DeBrecht J, Mishra S K (2017). Brain natriuretic peptide (BNP) expressing sensory neurons are not involved in acute, inflammatory or neuropathic pain. *Molecular Pain*, 13.

- Pitake S, Ralph P C, Debrecht J, Mishra S K (2018). Atopic Dermatitis Linked Cytokine Interleukin-31 Induced Itch Mediated via a Neuropeptide Natriuretic Polypeptide B. *Acto Dermato-Venereologica*. 98(8):795-796.
- Pitcher T, Baraznenok V, Henderson I, Lindstrom E, Malcangio M (2014). Role of Cathepsin S and PAR-2 receptors in the sensation of itch. Poster presented at the 15th World Congress on Pain, Buenos Aires, Argentina.
- Pivarcsi A, Bodai L, Rethi B, Kenderessy-Szabo A, Koreck A, Szell M, Beer Z, Bata-Csorgo Z, Magocsi M, Rajnavolgyi E, Dobozy A, Kemeny L (2003). Expression and function of Toll-like receptors 2 and 4 in human keratinocytes, *International Immunology*, 15(6):721-730.
- Pivarcsi A, Koreck A, Bodai L, Szell, Szeg C, Belso N, Kenderessy-Szabo A, Bata-Csorgo Z, Dobozy A, Kemeny L (2004). Differentiation-regulated expression of Toll-like receptors 2 and 4 in HaCaT keratinocytes, *Archives of Dermatological Research*, 296(3):120-124.
- Plank M W, Kaiko G E, Maltby S, Weaver J, Tay H L, Shen W, Wilson M S, Durum S K, Foster P S (2017). Th22 Cells Form a Distinct Th Lineage from Th17 Cells *In Vitro* with Unique Transcriptional Properties and Tbet-Dependent Th1 Plasticity. *Journal of Immunology*, 198(5):2182-2190.
- Ponath P D, Qin S X, Ringler D J, ClarkLewis I, Wang J, Kassam N, Smith H, Shi X J, Gonzalo J A, Newman W, GutierrezRamos J C, Mackay C R (1996). Cloning of the human eosinophil chemoattractant, eotaxin - Expression, receptor binding, and functional properties suggest a mechanism for the selective recruitment of eosinophils. *Journal of Clinical Investigation*, 97(3):604-612.
- Ponec M, Gibbs S, Weerheim A, Kempenaar J, Mulder A, Mommaas AM (1997). Epidermal growth factor and temperature regulate keratinocyte differentiation. *Archives of Dermatological Research*, 289(6):317-326.
- Poole D P, Amadesi S, Veldhuis N A, Abogadie F C, Lieu T, Darby W, Liedtke W, Lew M J, McIntyre P, Bunnett N W (2013). Protease-activated Receptor 2 (PAR(2)) Protein and Transient Receptor Potential Vanilloid 4 (TRPV4) Protein Coupling Is Required for Sustained Inflammatory Signaling. *Journal of Biological Chemistry*, 288(8):5790-5802.
- Portugal-Cohen M, Horev L, Ruffer C, Schlippe G, Voss W, Ma'or Z, Oron M, Soroka Y, Frusic-Zlotkin M, Milner Y, Kohen R (2012). Non-invasive skin biomarkers quantification of psoriasis and atopic dermatitis: Cytokines, antioxidants and psoriatic skin auto-fluorescence. *Biomedicine and Pharmacotherapy*, 66(4):293-299.
- Potter L R, Abbey-Hosch S, Dickey D M (2006). Natriuretic peptides, their receptors, and cyclic guanosine monophosphate-dependent signaling functions. *Endocrine Reviews*, 27(1):47-72.
- Poumay Y, Pittelkow M R (1995). Cell Density and Culture Factors Regulate Keratinocyte Commitment to Differentiation and Expression of Suprabasal K1/K10 Keratins. *Journal of Investigative Dermatology*, 104(2):271-276.
- Poumay Y, Roland IH, Leclercq-Smekens M, Leloup R (1994). Basal detachment of the epidermis using dispase: tissue spatial organization and fate of integrin alpha 6 beta 4 and hemidesmosomes. *Journal of Investigative Dermatology*, 102(1):111-117.

- Premkumar L S, Ahern G P (2000). Induction of vanilloid receptor channel activity by protein kinase C. *Nature*, 408(6815):985-990.
- Prescott E D, Julius D (2003). A modular PIP₂ binding site as a determinant of capsaicin receptor sensitivity. *Science*, 300(5623):1284-1288.
- Prout M S, Kyle R L, Ronchese F, Le Gros G (2018). IL-4 Is a Key Requirement for IL-4-and IL-4/IL-13-Expressing CD4 Th2 Subsets in Lung and Skin. *Frontiers in Immunology*, 9:1211.
- Qu L T, Fan N, Ma C, Wang T, Han L, Fu K, Wang Y D, Shimada S G, Dong X Z, LaMotte R H (2014). Enhanced excitability of MRGPRA3- and MRGPRD-positive nociceptors in a model of inflammatory itch and pain. *Brain*, 137:1039-1050.
- Quinton T M, Kim S, Derian C K, Jin J G, Kunapuli S P (2004). Plasmin-mediated activation of platelets occurs by cleavage of protease-activated receptor 4. *Journal of Biological Chemistry*, 279(18):18434-18439.
- Raap U, Weissmantel S, Gehring M, Eisenberg A M, Kapp A, Folster-Holst R (2012). IL-31 significantly correlates with disease activity and Th2 cytokine levels in children with atopic dermatitis. *Pediatric Allergy and Immunology*, 23(3):285-288.
- Raap U, Wichmann K, Bruder M, Stander S, Wedi B, Kapp A, Werfel T (2008). Correlation of IL-31 serum levels with severity of atopic dermatitis. *Journal of Allergy and Clinical Immunology*, 122(2):421-423.
- Raderer M, Müller C, Scheithauer W (1994). Ondansetron for pruritus due to cholestasis. *New England Journal of Medicine*, 330(21):1540.
- Ramachandran R, Hollenberg M D (2008). Proteinases and signalling: pathophysiological and therapeutic implications via PARs and more. *British Journal of Pharmacology*, 153:S263-S282.
- Ramachandran R, Mihara K, Chung H, Renaux B, Lau C S, Muruve D A, DeFea K A, Bouvier M, Hollenberg M D (2011). Neutrophil Elastase Acts as a Biased Agonist for Proteinase-activated Receptor-2 (PAR(2)). *Journal of Biological Chemistry*, 286(28):24638-24648.
- Ramachandran R, Mihara K, Mathur M, Rochdi M D, Bouvier M, DeFea K, Hollenberg M D (2009). Agonist-Biased Signaling via Proteinase Activated Receptor-2: Differential Activation of Calcium and Mitogen-Activated Protein Kinase Pathways. *Molecular Pharmacology*, 76(4):791-801.
- Ramachandran R, Noorbakhsh F, DeFea K, Hollenberg MD (2012). Targeting proteinase-activated receptors: therapeutic potential and challenges. *Nature Reviews Drug Discovery*, 11(1):69-86.
- Raphael I, Nalawade S, Eagar T N, Forsthuber T G (2015). T cell subsets and their signature cytokines in autoimmune and inflammatory diseases. *Cytokine*, 74(1):5-17.
- Rawlings A V, Matts P J (2005). Stratum corneum moisturization at the molecular level: An update in relation to the dry skin cycle. *Journal of Investigative Dermatology*, 124(6):1099-1110.

Rawlings A V, Scott I R, Harding C R, Bowser P A (1994). Stratum Corneum Moisturization at the Molecular Level. *Journal of Investigative Dermatology*, 103(5):731-740.

Reber F, Gersch U, Funk R H W (2003). Blockers of carbonic anhydrase can cause increase of retinal capillary diameter, decrease of extracellular and increase of intracellular pH in rat retinal organ culture. *Graefes Archive for Clinical and Experimental Ophthalmology*, 241(2):140-148.

Reddy V B, Azimi E, Chu L, Lerner E A (2018). Mas-Related G-Protein Coupled Receptors and Cowhage-Induced Itch. *Journal of Investigative Dermatology*, 138(2):461-464.

Reddy V B, Iuga A O, Shimada S G, LaMotte R H, Lerner E A (2008). Cowhage-evoked itch is mediated by a novel cysteine protease: A ligand of protease-activated receptors. *Journal of Neuroscience*, 28(17):4331-4335.

Reddy V B, Lerner E A (2010). Plant cysteine proteases that evoke itch activate protease-activated receptors. *British Journal of Dermatology*, 163(3):532-535.

Reddy V B, Shimada S G, Sikand P, LaMotte R H, Lerner A (2010). Cathepsin S elicits itch and signals via protease-activated receptors. *Journal of Investigative Dermatology*, 130(5):1468-1470

Reddy V B, Sun S H, Azimi E, Elmariah S B, Dong X Z, Lerner E A (2015). Redefining the concept of protease-activated receptors: cathepsin S evokes itch via activation of Mrgprs. *Nature Communications*, 6:7864.

Redrup A C, Howard B P, MacGlashan D W, Kagey-Sobotka A, Lichtenstein L M, Schroeder J T (1998). Differential regulation of IL-4 and IL-13 secretion by human basophils: Their relationship to histamine release in mixed leukocyte cultures. *Journal of Immunology*, 160(4):1957-1964.

Reinisch C M, Tschachler E (2012). The dimensions and characteristics of the subepidermal nerve plexus in human skin - Terminal Schwann cells constitute a substantial cell population within the superficial dermis. *Journal of Dermatological Science*, 65(3):162-169.

Ricks T K, Trejo J A (2009). Phosphorylation of Protease-activated Receptor-2 Differentially Regulates Desensitization and Internalization. *Journal of Biological Chemistry*, 284(49):34444-34457.

Ringkamp M, Schepers R J, Shimada S G, Johanek L M, Hartke T V, Borzan J, Shim B, LaMotte R H, Meyer R A (2011). A Role for Nociceptive, Myelinated Nerve Fibers in Itch Sensation. *Journal of Neuroscience*, 31(42):14841-14849.

Rippke F, Schreiner V, Doering T, Maibach H I (2004). Stratum corneum pH in atopic dermatitis. *American Journal of Clinical Dermatology*, 5(4):217-223.

Rippke F, Schreiner V, Schwanitz H J (2002). The acidic milieu of the horny layer: new findings on the physiology and pathophysiology of the skin pH. *American Journal of Clinical Dermatology*, 3(4):261-272.

Robas N, Mead E, Fidock M (2003). MrgX2 is a high potency cortistatin receptor expressed in dorsal root ganglion. *Journal of Biological Chemistry*, 278(45):44400-44404.

Roberson DP, Gudes S, Sprague J, Patoski HAW, Robson VK, Blas F, Duan B, Oh SB, Bean BP, Ma F, Binshtok AM, Woolf CJ (2013). Activity-dependent silencing reveals functionally distinct itch-generating sensory neurons. *Nature Neuroscience*, 16(7):910-919.

Rodriguez A, Webster P, Ortego J, Andrews NW (1997). Lysosomes behave as Ca²⁺-regulated exocytic vesicles in fibroblasts and epithelial cells. *Journal of Cell Biology*, 137(1):93-104.

Roediger B, Kyle R, Yip K H, Sumaria N, Guy T V, Kim B S, Mitchell A J, Tay S S, Jain R, Forbes-Blom E, Chen X, Tong P L, Bolton H A, Artis D, Paul W E, Fazekas de St Groth B, Grimbaldeston M A, Le Gros G, Weninger W (2013). Cutaneous immunosurveillance and regulation of inflammation by group 2 innate lymphoid cells. *Nature Immunology*, 14(6):564+.

Roggenkamp D, Falkner S, Stab F, Petersen M, Schmelz M, Neufang G (2012). Atopic Keratinocytes Induce Increased Neurite Outgrowth in a Coculture Model of Porcine Dorsal Root Ganglia Neurons and Human Skin Cells. *Journal of Investigative Dermatology*, 132(7):1892-1900.

Rogoz K, Lagerstrom M C, Dufour S, Kullander K (2012). VGLUT2-dependent glutamatergic transmission in primary afferents is required for intact nociception in both acute and persistent pain modalities. *Pain*, 153(7):1525-1536.

Ross SE (2011). Pain and Itch: insights into the neural circuits of aversive somatosensation in health and disease. *Current Opinion in Neurobiology*, 21(6):880-887.

Ross S E, Mardinly A R, McCord A E, Zurawski J, Cohen S, Jung C, Hu L D, Mok S I, Shah A, Savner E M, Tolia C, Corfas R, Chen S Z, Inquimbert P, Xu Y, McInnes R R, Rice F L, Corfas G, Ma Q F, Woolf C J, Greenberg M E (2010). Loss of Inhibitory Interneurons in the Dorsal Spinal Cord and Elevated Itch in Bhlhb5 Mutant Mice. *Neuron*, 65(6):886-898.

Rossbach K, Nassenstein C, Gschwandtner M, Schnell D, Sander K, Seifert R, Stark H, Kietzmann M, Bäumer W (2011). Histamine H-1, H-3 and H-4 Receptors are Involved in Pruritus. *Neuroscience*, 190:89-102.

Rothaug M, Becker-Pauly C, Rose-John S (2016). The role of interleukin-6 signaling in nervous tissue. *Biochimica et Biophysica Acta - Molecular Cell Research*, 1863(6):1218-1227.

Roy S S, Saifeddine M, Loutzenhiser R, Triggler C R, Hollenberg M D (1998). Dual endothelium-dependent vascular activities of proteinase-activated receptor-2-activating peptides: evidence for receptor heterogeneity. *British Journal of Pharmacology*, 123(7):1434-1440.

Ru F, Sun H, Jurcakova D, Herbstsomer R A, Meixong J, Dong X, Udem B J (2017). Mechanisms of pruritogen-induced activation of itch nerves in isolated mouse skin. *Journal of Physiology*, 595(11):3651-3666.

Rukwied R, Lischetzki G, McGlone F, Heyer G, Schmelz M (2000). Mast cell mediators other than histamine induce pruritus in atopic dermatitis patients: a dermal microdialysis study. *British Journal of Dermatology*, 142(6):1114-1120.

Russell F A, Schuelert N, Veldhoen V E, Hollenberg M D, McDougall J J (2012). Activation of PAR2 receptors sensitizes primary afferents and causes leukocyte rolling and adherence in the rat knee joint. *British Journal of Pharmacology*, 167(8):1665-1678.

Russell F A, Zhan S, Dumas A, Lagarde S, Pouliot M, McDougall J J (2011). The pronociceptive effect of proteinase-activated receptor-4 stimulation in rat knee joints is dependent on mast cell activation. *Pain*, 152(2):354-360.

Russo A, Soh U J K, Trejo J (2009). Proteases Display Biased Agonism at Protease-Activated Receptors: Location Matters! *Molecular Interventions*, 9(2):87-96.

Sakaguchi M, Miyazaki M, Takaishi M, Sakaguchi Y, Makino E, Kataoka N, Yamada H, Namba M, Huh N H (2003). S100C/A11 is a key mediator of Ca²⁺-induced growth inhibition of human epidermal keratinocytes. *Journal of Cell Biology*, 163(4):825-835.

Sakai T, Hatano Y, Matsuda-Hirose H, Zhang W, Takahashi D, Jeong S K, Elias P M, Fujiwara S (2016). Combined Benefits of a PAR2 Inhibitor and Stratum Corneum Acidification for Murine Atopic Dermatitis. *Journal of Investigative Dermatology*, 136(2):538-541.

Saleem M D, Oussedik E, D'Amber V, Feldman S R (2017). Interleukin-31 pathway and its role in atopic dermatitis: a systematic review. *Journal of Dermatological Treatment*, 28(7):591-599.

Sambrano G R, Huang W, Faruqi T, Mahrus S, Craik C, Coughlin S R (2000). Cathepsin G activates protease-activated receptor-4 in human platelets. *Journal of Biological Chemistry*, 275(10):6819-6823.

Sano S, Chan K S, Carbajal S, Clifford J, Peavey M, Kiguchi K, Itami S, Nickoloff B J, DiGiovanni J (2005). Stat3 links activated keratinocytes and immunocytes required for development of psoriasis in a novel transgenic mouse model. *Nature Medicine*, 11(1):43-49.

Sarafian V, Jans R, Poumay Y (2006). Expression of lysosome-associated membrane protein 1 (Lamp-1) and galectins in human keratinocytes is regulated by differentiation. *Archives of Dermatological Research*, 298(2):73-81.

Sardella T C P, Polgar E, Garzillo F, Furuta T, Kaneko T, Watanabe M, Todd A J (2011). Dynorphin is expressed primarily by GABAergic neurons that contain galanin in the rat dorsal horn. *Molecular Pain*, 7:76.

Schalkwijk J, van Vlijmen I M J J, Alkemade J A C, de Jongh G J (1993). Immunohistochemical localization of SKALP/elafin in psoriatic epidermis. *Journal of Investigative Dermatology*, 100(4):390-393.

Schauer U, Trube M, Jager R, Gieler U, Rieger C H L (1995). Blood eosinophils, eosinophil-derived proteins, and leukotriene C4 generation in relation to bronchial hyperreactivity in children with atopic dermatitis. *Allergy*, 50(2):126-132.

Scherrer G, Low S A, Wang X D, Zhang J, Yamanaka H, Urban R, Solorzano C, Harper B, Hnasko T S, Edwards R H, Basbaum A I (2010). VGLUT2 expression in primary afferent neurons is essential for normal acute pain and injury-induced heat hypersensitivity. *Proceedings of the National Academy of Sciences of the United States of America*, 107(51):22296-22301.

Schlaak J F, Buslau M, Jochum W, Hermann E, Girndt M, Gallati H, Zumbuschfeld K H M, Fleischer B (1994). T cells involved in psoriasis vulgaris belong to the Th1 subset. *Clinical and Experimental Immunology*, 135(1):1-8.

- Smchelz M (2010). Itch and pain. *Neuroscience and Behavioural Reviews*, 34:171 – 176.
- Schmelz M, Schmidt R, Bickel A, Handwerker HO, Torebjork HE (1997). Specific C-receptors for itch in human skin. *Journal of Neuroscience*, 17(20):8003-8008.
- Schmelz M, Schmidt R, Weidner C, Hilliges M, Torebjork H E, Handwerker H O (2003). Chemical response pattern of different classes of C-nociceptors to pruritogens and algogens. *Journal of Neurophysiology*, 89(5):2441-2448.
- Schneider E H, Seifert R (2016). The histamine H₄-receptor and the central and peripheral nervous system: A critical analysis of the literature. *Neuropharmacology*, 106:116-128.
- Schneider G, Stander S, Burgmer M, Driesch G, Heuft G, Weckesser M (2008). Significant differences in central imaging of histamine-induced itch between atopic dermatitis and healthy subjects. *European Journal of Pain*, 12(7):834-841.
- Schon M P, Detmar M, Parker C M (1997). Murine psoriasis-like disorder induced by naive CD4(+) T cells. *Nature Medicine*, 3(2):183-188.
- Schonefuss A, Wendt W, Schattling B, Schulten R, Hoffmann K, Stuecker M, Tigges C, Lubbert H, Stichel C (2010). Upregulation of cathepsin S in psoriatic keratinocytes. *Experimental Dermatology*, 19(8):E80-E88.
- Schoop V M, Mirancea N, Fusenig N E (1999). Epidermal organization and differentiation of HaCaT keratinocytes in organotypic coculture with human dermal fibroblasts. *Journal of Investigative Dermatology*, 112(3):343-353.
- Schuttenhelm B N, Duraku L S, Dijkstra J F, Walbeehm E T, Holstege J C (2015). Differential Changes in the Peptidergic and the Non-Peptidergic Skin Innervation in Rat Models for Inflammation, Dry Skin Itch, and Dermatitis. *Journal of Investigative Dermatology*, 135(8):2049-2057.
- Schwartz L B (1991). Mast cells and their role in urticaria. *Journal of the American Academy of Dermatology*, 25(1):190-204.
- Schwarz G, Boehncke W H, Braun M, Schröter C J, Burster T, Flad T, Dressel D, Weber E, Schmid H, Kalbacher H (2002). Cathepsin S activity is detectable in human keratinocytes and is selectively upregulated upon stimulation with interferon- γ . *Journal of Investigative Dermatology*, 119(1):44-49.
- Schwörer H, Ramadori G (1993). Improvement of cholestatic pruritus by ondansetron. *The Lancet*, 241(8855):1277.
- Scott I R, Harding C R (1986). Filaggrin breakdown to water binding compounds during development of the rat stratum corneum is controlled by the water activity of the environment. *Developmental Biology*, 115(1):84-92.
- Scott G, Leopardi S, Parker L, Babiarz L, Seiber, M, Han R J (2003). The proteinase-activated receptor-2 mediates phagocytosis in a Rho-dependent manner in human keratinocytes. *Journal of Investigative Dermatology*, 121(3):529-541.
- Segre J A, Bauer C, Fuchs E (1999). Klf4 is a transcription factor required for establishing the barrier function of the skin. *Nature Genetics*, 22(4):356-360.

Seo M D, Kang T J, Lee C H, Lee A Y, Noh M (2012). HaCaT Keratinocytes and Primary Epidermal Keratinocytes Have Different Transcriptional Profiles of Cornified Envelope-Associated Genes to T Helper Cell Cytokines. *Biomolecules and Therapeutics*, 20(2):171-176.

Serezani A P M, Bozdogan G, Sehra S, Walsh D, Krishnamurthy P, Potchanant E A S, Nalepa G, Goenka S, Turner M J, Spandau D F, Kaplan M H (2017). IL-4 impairs wound healing potential in the skin by repressing fibronectin expression. *Journal of Allergy and Clinical Immunology*, 139(1):142+.

Shepherd J, Little M C, Nicklin M J H (2004). Psoriasis-like cutaneous inflammation in mice lacking interleukin-1 receptor antagonist. *Journal of Investigative Dermatology*, 122(3):665-669.

Shi G P, Munger J S, Meara J P, Rich D H, Capman HA (1992). Molecular cloning and expression of human alveolar macrophage cathepsin S, an elastinolytic cysteine protease. *Journal of Biological Chemistry*, 267(11):7258-7262.

Shi G P, Sukhova G K, Kuzuya M, Ye Q, Du J, Zhang Y, Pan J H, Lu M L, Cheng X W, Iguchi A, Perrey S, Lee A M E, Chapman H A, Libby P (2003). Deficiency of the cysteine protease cathepsin S impairs microvessel growth. *Circulation Research*, 92(5):493-500.

Shikano M, Ueda T, Kamiya T, Ishida Y, Yamada T, Mizushima T, Shimura T, Mizoshita T, Tanida S, Kataoka H, Shimada S, Ugawa S, Joh T (2011). Acid inhibits TRPV4-mediated Ca(2+) influx in mouse esophageal epithelial cells. *Neurogastroenterology and Motility*, 23(11):1020-E497.

Shim W, Tak M, Lee M, Kim M, Kim M, Koo J, Lee C, Kim M, Oh U (2007). TRPV1 mediates histamine-induced itching via the activation of phospholipase A(2) and 12-lipoxygenase. *Journal of Neuroscience*, 27(9):2331-2337.

Shimada S G, LaMotte R H (2008). Behavioral differentiation between itch and pain in mouse. *Pain*, 139(3):681-687.

Shimada S G, Shimada K A, Collins J G (2006). Scratching behavior in mice induced by the proteinase-activated receptor-2 agonist, SLIGRL-NH₂. *European Journal of Pharmacology*, 530(3):281-283.

Shimizu K, Andoh T, Yoshihisa Y, Shimizu T (2015). Histamine Released from Epidermal Keratinocytes Plays a Role in alpha-Melanocyte-Stimulating Hormone-Induced Itching in Mice. *American Journal of Pathology*, 185(11):3003-3010.

Sikand P, Dong X Z, LaMotte R H (2011a). BAM8-22 Peptide Produces Itch and Nociceptive Sensations in Humans Independent of Histamine Release. *Journal of Neuroscience*, 31(20):7563-7567.

Sikand P, Shimada S G, Green B G, LaMotte R H (2009). Similar itch and nociceptive sensations evoked by punctate cutaneous application of capsaicin, histamine and cowhage. *Pain*, 144(1-2):66-75.

Sikand P, Shimada S G, Green B G, LaMotte R H (2011b). Sensory responses to injection and punctate application of capsaicin and histamine to the skin. *Pain*, 152(11):2485-2494.

- Simeoli R, Montague K, Jones H R, Castaldi L, Chambers D, Kelleher J H, Vacca V, Pitcher T, Grist J, Al-Ahdal H, Wong L F, Perretti M, Lai J, Mouritzen P, Heppenstall P, Malcangio M (2017). Exosomal cargo including microRNA regulates sensory neuron to macrophage communication after nerve trauma. *Nature Communications*, 8:1778.
- Simon D, Braathen L R, Simon H U (2004). Eosinophils and atopic dermatitis. *Allergy*, 59(6):561-570.
- Simone D A, Alreja M, LaMotte R H (1991). Psychophysical studies of the itch sensation and itchy skin (alloknesis) produced by intracutaneous injection of histamine. *Somatosensory and Motor Research*. 8(3):271-279.
- Simons F E R (2004). Drug therapy - Advances in H-1-antihistamines. *New England Journal of Medicine*, 351(21):2203-2217.
- Sinke J D, Thepen T, Bihari I C, Rutten V P M G, Willemsse T (1997). Immunophenotyping of skin-infiltrating T-cell subsets in dogs with atopic dermatitis. *Veterinary Immunology and Pathology*, 57(1-2):13-23.
- Sleigh J N, Weir G A, Schiavo G (2016). A simple, step-by-step dissection protocol for the rapid isolation of mouse dorsal root ganglia. *BMC Research Notes*, 9:82.
- Smith T H, Coronel L J, Li J G, Dores M R, Nieman M T, Trejo J (2016). Protease-activated Receptor-4 Signaling and Trafficking Is Regulated by the Clathrin Adaptor Protein Complex-2 Independent of β -Arrestins. *Journal of Biological Chemistry*, 291(35):18453–18464.
- Smith R, Jenkins A, Loubakos A, Thompson P, Ramakrishnan V, Tomlinson J, Deshpande U, Johnson D A, Jones R, Mackie E J, Pike R N (2000). Evidence for the activation of PAR-2 by the sperm protease, acrosin: expression of the receptor on oocytes. *FEBS Letters*, 484(3):285-290.
- Smits J P H, Niehues H, Rikken G, van Vlijmen-Willems I M J J, van de Zande G W H J F, Zeeuwen P L J M, Schalkwijk J, van den Bogaard E H (2017). Immortalized N/TERT keratinocytes as an alternative cell source in 3D human epidermal models. *Scientific Reports*, 7:11838.
- Soh U J K, Trejo J (2011). Activated protein C promotes protease-activated receptor-1 cytoprotective signaling through beta-arrestin and dishevelled-2 scaffolds. *Proceedings of the National Academy of Sciences of the United States of America*, 108(50):E1372-E1380.
- Solorzano C, Villafuerte D, Meda K, Cevikbas F, Braz J, Sharif-Naeini R, Juarez-Salinas D, Llewellyn-Smith IJ, Guan Z, Basbaum AI, (2015). Primary Afferent and Spinal Cord Expression of Gastrin-Releasing Peptide: Message, Protein, and Antibody Concerns. *Journal of Neuroscience*, 35(2), 648-657.
- Song P I, Park Y M, Abraham T, Harten B, Zivony A, Neparidze N, Armstrong C A, Ansel J C (2002). Human keratinocytes express functional CD14 and toll-like receptor 4, *Journal of Investigative Dermatology*, 119(2):424-432.
- Sonkoly E, Muller A, Lauerma A I, Pivarcsi A, Soto H, Kemeny L, Alenius H, Dieu-Nosjean M C, Meller S, Rieker J, Steinhoff M, Hoffmann T K, Ruzicka T, Zlotnik A, Homey B (2006). IL-31: a new link between T cells and pruritus in atopic skin inflammation. *The Journal of Allergy and Clinical Immunology* 117(2):411-417.

- Soto A G, Trejo J A (2010). N-linked glycosylation of protease-activated receptor-1 second extracellular loop: a critical determinant for ligand-induced receptor activation and internalization. *Journal of Biological Chemistry*, 285(24):18781-18793.
- Southall M D, Li T, Gharibova L S, Pei Y, Nicol G D, Travers J B (2003). Activation of epidermal vanilloid receptor-1 induces release of proinflammatory mediators in human keratinocytes. *Journal of Pharmacology and Experimental Therapeutics*, 304(1):217-222.
- Sparavigna A, Setaro M, Gualandri V (1999). Cutaneous pH in children affected by atopic dermatitis and in healthy children: a multicenter study. *Skin Research and Technology*, 5(4):221-227.
- Spergel J M, Mizoguchi E, Brewer J P, Martin T R, Bhan A K, Geha R S (1998). Epicutaneous sensitization with protein antigen induces localized allergic dermatitis and hyperresponsiveness to methacholine after single exposure to aerosolized antigen in mice. *Journal of Clinical Investigation*, 101(8):1614-1622.
- Spetz A L, Strominger J, GrohSpies V (1996). T cell subsets in normal human epidermis. *American Journal of Pathology*, 149(2):665-674.
- Spinsanti G, Zannolli R, Panti C, Ceccarelli I, Marsili L, Bachiocco V, Frati F, Aloisi A M (2008). Quantitative Real-Time PCR detection of TRPV1-4 gene expression in human leukocytes from healthy and hyposensitive subjects. *Molecular Pain*, 4:51.
- Sriwai W, Mahavadi S, Al-Shboul O, Grider J R, Murthy K S (2013). Distinctive G Protein-Dependent Signaling by Protease-Activated Receptor 2 (PAR2) in Smooth Muscle: Feedback Inhibition of RhoA by cAMP-Independent PKA. *PLoS ONE*, 8(6):e66743.
- Stalheim L, Ding Y, Gullapalli A, Paing M M, Wolfe B L, Morris D R, Trejo J (2005). Multiple independent functions of arrestins in the regulation of protease-activated receptor-2 signaling and trafficking. *Molecular Pharmacology*, 67(1):78-87.
- Stander S, Gunzer M, Metz D, Luger T, Steinhoff M (2002). Localization of mu-opioid receptor 1A on sensory nerve fibers in human skin. *Regulatory Peptides*, 110(1):75-83.
- Stander S, Steinhoff M, Schmelz M, Weisshaar E, Metz D, Luger T (2003). Neurophysiology of pruritus - Cutaneous elicitation of itch. *Archives of Dermatology*, 139(11):1463-1470.
- Ständer S, Weisshaar E, Mettang T, Szepietowski JC, Carstens E, Ikoma A, Bergasa NV, Gieler U, Misery L, Wallengren J, Darsow U, Streit M, Metz D, Luger T, Greaves MW, Schmelz M, Yosipovitch G, Bernhard JD (2007). Clinical classification of itch: a position paper of the International Forum for the Study of Itch. *Acta Dermato-Venereologica*, 87(4):291-294.
- Stefansson K, Brattsand M, Roosterman D, Kempkes C, Bocheva G, Steinhoff M, Egelrud T (2008). Activation of proteinase-activated receptor-2 by human kallikrein-related peptidases. *Journal of Investigative Dermatology*, 128(1):18-25.
- Staton P C, Wilson A W, Bountra C, Chessell I P, Day N C (2007). Changes in dorsal root ganglion CGRP expression in a chronic inflammatory model of the rat knee joint: differential modulation by rofecoxib and paracetamol. *European Journal of Pain*, 11(3):283-289.

Steinert P M, Marekov LN (1997). Direct evidence that involucrin is a major early isopeptide crosslinked component of the keratinocyte cornified cell envelope. *Journal of Biological Chemistry*, 272(3):2021-2030.

Steinhoff M, Bienenstock J, Schmelz M, Maurer M, Wei E, Bíró T (2006). Neurophysiological, neuroimmunological, and neuroendocrine basis of pruritus. *Journal of Investigative Dermatology*, 126(8):1705-1718.

Steinhoff M, Buddenkotte J, Lerner E A (2018). Role of mast cells and basophils in pruritus. *Immunological Reviews*, 282(1):248-264.

Steinhoff M, Buddenkotte J, Shpacovitch V, Rattenholl A, Moormann C, Vergnolle N, Luger T A, Hollenberg M D (2005). Proteinase-activated receptors: Transducers of proteinase-mediated signaling in inflammation and immune response. *Endocrine Reviews*, 26(1):1-43.

Steinhoff M, Corvera C U, Thoma M S, Kong, W McAlpine B E, Caughey G H, Ansel J C, Bunnett N W (1999). Proteinase-activated receptor-2 in human skin: tissue distribution and activation of keratinocytes by mast cell tryptase. *Experimental Dermatology*, 8(4):282-294.

Steinhoff M, Neisius U, Ikoma A, Fartasch M, Heyer G, Skov P S, Luger T A, Schmelz M (2003). Proteinase-activated receptor-2 mediates itch: A novel pathway for pruritus in human skin. *Journal of Neuroscience*, 23(15):6176-6180.

Steinhoff M, Vergnolle N, Young S H, Tognetto M, Amadesi S, Ennes HS, Trevisani M, Hollenberg M D, Wallace JL, Caughey G H, Mitchell S E, Williams L M, Geppetti P, Mayer E A, Bunnett N W (2000). Agonists of proteinase-activated receptor 2 induce inflammation by a neurogenic mechanism. *Nature Medicine*, 6(2):151-158.

Steinhoff M S, von Mentzer B, Geppetti P, Pothoulakis C, Bunnett N W (2014). Tachykinins and their receptors: contributions to physiological control and the mechanisms of disease. *Physiological Reviews*, 94(1):265-301.

Steven A C, Bisher M E, Roop D R, Steinert P M (1990). Biosynthetic pathways of filaggrin and loricrin - two major proteins expressed by terminally differentiated epidermal keratinocytes. *Journal of Structural Biology*, 104(1-3):150-162.

Stockinger B, Kassiotis G, Bourgeois C (2004). CD4 T-cell memory. *Seminars in Immunology*, 16(5):295-303.

Stoll S, Jonuleit H, Schmitt E, Muller G, Yamauchi H, Kurimoto M, Knop J, Enk AH (1998). Production of functional IL-18 by different subtypes of murine and human dendritic cells (DC): DC-derived IL-18 enhances IL-12-dependent Th1 development. *European Journal of Immunology*, 28(10):3231-3239.

Stott B, Lavender P, Lehmann S, Pennino D, Durham S, Schmidt-Weber C B (2013). Human IL-31 is induced by IL-4 and promotes T(H)2-driven inflammation. *Journal of Allergy and Clinical Immunology*, 132(2):446+.

Su P Y, Ko M C (2011). The Role of Central Gastrin-Releasing Peptide and Neuromedin B Receptors in the Modulation of Scratching Behavior in Rats. *Journal of Pharmacology and Experimental Therapeutics*, 337(3):822-829.

- Subramanian H, Gupta K, Guo Q, Price R, Ali H (2011). Mas-related gene X2 (MrgX2) is a novel G protein-coupled receptor for the antimicrobial peptide LL-37 in human mast cells: resistance to receptor phosphorylation, desensitization, and internalization. *Journal of Biological Chemistry*, 286(52):44739-44749.
- Subramanian H, Gupta K, Lee D, Bayir AK, Ahn H, Ali H (2013). Beta-Defensins Activate Human Mast Cells via Mas-Related Gene X2. *Journal of Immunology*, 191(1):345-352.
- Sugiura H, Maeda T, Uehara M (1992). Mast cell invasion of peripheral nerve in skin lesions of atopic dermatitis. *Acta Dermato-Venereologica*, 176:74-76.
- Sukhtankar D D, Ko M C (2013). Physiological Function of Gastrin-Releasing Peptide and Neuromedin B Receptors in Regulating Itch Scratching Behavior in the Spinal Cord of Mice. *PLoS ONE*, 8(6):e67422.
- Sun Y G, Chen Z F (2007). A gastrin-releasing peptide receptor mediates the itch sensation in the spinal cord. *Nature*, 448(7154):700-U10.
- Sun S H, Xu Q, Guo C X, Guan Y, Liu Q, Dong X Z (2017). Leaky Gate Model: Intensity-Dependent Coding of Pain and Itch in the Spinal Cord. *Neuron*, 93(4):840+.
- Suzuki H, Kurosumi K (1972). Lamellar Granules and Keratohyalin Granules in the Epidermal Keratinocytes, with Special Reference to Their Origin, Fate and Function. *Journal of Electron Microscopy*, 21(4):285-292.
- Suzuki M, Mizuno A, Kodaira K, Imai M (2003). Impaired pressure sensation in mice lacking TRPV4. *Journal of Biological Chemistry*, 278(25):22664-22668.
- Szabo S J, Kim S T, Costa G L, Zhang X K, Fathman C G, Glimcher L H (2000). A novel transcription factor, T-bet, directs Th1 lineage commitment. *Cell*, 100(6):655-669.
- Szegedi K, Kremer A E, Kezic S, Teunissen M B M, Bos J D, Luiten R M, Res P C, Middelkamp-Hup M A (2012). Increased frequencies of IL-31-producing T cells are found in chronic atopic dermatitis skin. *Experimental Dermatology*, 21(6):431-436.
- Takano N, Sakurai T, Kurachi M (2005). Effects of anti-nerve growth factor antibody on symptoms in the NC/Nga mouse, an atopic dermatitis model. *Journal of Pharmacological Sciences*, 99(3):277-286.
- Tam W Y, Au N P B, Ma C H E (2016). The association between laminin and microglial morphology *in vitro*. *Scientific Reports*, 6:28580.
- Tanaka A, Matsuda H (2005). Expression of nerve growth factor in itchy skins of atopic NC/NgaTnd mice. *Journal of Veterinary Medical science*, 67(9):915-919.
- Tang M, Wu G Y, Wang Z L, Yang N N, Shi H, He Q, Zhu C, Yang Y, Yu G, Wang C M, Yuan X L, Liu Q, Guan Y, Dong X Z, Tang Z X (2016). Voltage-gated potassium channels involved in regulation of physiological function in MrgprA3-specific itch neurons. *Brain Research*, 1636:161-171.

Takeuchi T, Harris J L, Huang W, Yan K W, Coughlin S R, Craik C S (2000). Cellular localization of membrane-type serine protease 1 and identification of protease-activated receptor-2 and single-chain urokinase-type plasminogen activator as substrates. *Journal of Biological Chemistry*, 275(34):26333-26342.

Tashian R E (1989). The carbonic anhydrases: widening perspectives on their evolution, expression and function. *Bioessays*, 10(6):186-192.

Taylor A M W, Peleshok J C, Ribeiro-Da-Silva A (2009). Distribution of P2X(3)-Immunoreactive Fibers in Hairy and Glabrous Skin of the Rat. *Journal of Comparative Neurology*, 514(6):555-566.

Than J Y X L, Li L, Hasan R, Zhang X M (2013). Excitation and Modulation of TRPA1, TRPV1, and TRPM8 Channel-expressing Sensory Neurons by the Pruritogen Chloroquine. *Journal of Biological Chemistry*, 288(18):12818-12827.

Thepen T, LangeveldWildschut G, Bihari I C, vanWichen D F, vanReijssen F C, Mudde G C, BuijnzeelKoomen C A F M (1996). Biphasic response against aeroallergen in atopic dermatitis showing a switch from an initial T-H2 response to a T-H1 response in situ: An immunocytochemical study. *Journal of Allergy and Clinical Immunology*, 97(3):828-837.

Thier M, Marz P, Otten U, Weis J, Rose-John S (1999). Interleukin-6 (IL-6) and its soluble receptor support survival of sensory neurons. *Journal of Neuroscience Research*, 55(4):411-422.

Thomsen J S, Petersen M B, Benfeldt E, Jensen S B, Serup J (2001). Scratch induction in the rat by intradermal serotonin: a model for pruritus. *Acta Dermato-Venereologica*, 81(4):250-254.

Thomsen J S, Sonne M, Benfeldt E, Jensen S B, Serup J, Menne T (2002). Experimental itch in sodium lauryl sulphate-inflamed and normal skin in humans: a randomized, double-blind, placebo-controlled study of histamine and other inducers of itch. *British Journal of Dermatology*, 146(5):792-800.

Thoppil R J, Adapala R K, Cappelli H C, Kondeti V, Dudley A C, Meszaros J G, Paruchuri S, Thodeti C K (2015). TRPV4 channel activation selectively inhibits tumor endothelial cell proliferation. *Scientific Reports*, 5:14257.

Tirado-Sanchez A, Bonifaz A, Ponce-Oliviera R M (2015). Serum gastrin-releasing peptide levels correlate with disease severity and pruritus in patients with atopic dermatitis. *British Journal of Dermatology*, 173(1):298-300.

Tobin D, Nabarro G, Delafaille H B, Vanvloten W A, Vanderputte S C J, Schuurman H J (1992). Increased number of immunoreactive nerve fibers in atopic dermatitis. *Journal of Allergy and Clinical Immunology*, 90(4):613-622.

Tominaga M, Caterina M J, Malmberg A B, Rosen T A, Gilbert H, Skinner K, Raumann B E, Basbaum A I, Julius, D (1998). The cloned capsaicin receptor integrates multiple pain-producing stimuli. *Neuron*, 21(3):531-543.

Tominaga M, Ogawa H, Takamori K (2007). Possible roles of epidermal opioid systems in pruritus of atopic dermatitis. *Journal of Investigative Dermatology*, 127(9):2228-2235.

- Tominaga M, Ogawa H, Takamori K (2009). Histological Characterization of Cutaneous Nerve Fibers Containing Gastrin-Releasing Peptide in NC/Nga Mice: An Atopic Dermatitis Model. *Journal of Investigative Dermatology*, 129(12):2901-2905.
- Tordai A, Brass L F, Gelfand E W (1995). Tunicamycin inhibits the expression of functional thrombin receptors on human T-lymphoblastoid cells. *Biochemical and Biophysical Research Communications*, 206(3):857–862.
- Touw K, Chakraborty S, Zhang W W, Obukhov A G, Tune J D, Gunst S J, Herring B P (2012). Altered calcium signaling in colonic smooth muscle of type 1 diabetic mice. *American Journal of Physiology-Gastrointestinal and Liver Physiology*, 302(1):G66-G67.
- Towne J E, Renshaw B R, Douangpanya J, Lipsky B P, Shen M, Gabel C A, Sims J E (2011). Interleukin-36 (IL-36) Ligands Require Processing for Full Agonist (IL-36 alpha, IL-36 beta, and IL-36 gamma) or Antagonist (IL-36Ra) Activity. *Journal of Biological Chemistry*, 286(49):42594-42602.
- Toyoda M, Nakamura M, Makino T, Hino T, Kagoura M, Morohashi M (2002). Nerve growth factor and substance P are useful plasma markers of disease activity in atopic dermatitis. *British Journal of Dermatology*, 147(1):71-79.
- Trautmann A, Akdis M, Kleemann D, Altnauer F, Simon H U, Graeve T, Noll M, Brocker E B, Blaser K, Akdis CA (2000). T cell-mediated Fas-induced keratinocyte apoptosis plays a key pathogenetic role in eczematous dermatitis. *Journal of Clinical Investigation*, 106(1):25-35.
- Trautmann A, Akdis M, Schmid-Grendelmeier P, Disch R, Brocker E B, Blaser K, Akdis C A (2001). Targeting keratinocyte apoptosis in the treatment of atopic dermatitis and allergic contact dermatitis. *Journal of Allergy and Clinical Immunology*, 108(5):839-846.
- Trentin P G, Fernandes M B, D'Orleans-Juste P, Rae G A (2006). Endothelin-1 causes pruritus in mice. *Experimental Biology and Medicine*, 231(6):1146-1151.
- Tsuji K, Andoh T, Lee J B, Kuraishi Y (2008). Activation of Proteinase-Activated Receptors Induces Itch-Associated Response Through Histamine-Dependent and -Independent Pathways in Mice. *Journal of Pharmacological Sciences*, 108(3):385-388.
- Tsuji K, Andoh T, Ui H, Lee J B, Kuraishi Y (2009). Involvement of Tryptase and Proteinase-Activated Receptor-2 in Spontaneous Itch-Associated Response in Mice With Atopy-like Dermatitis. *Journal of Pharmacological Sciences*, 109(3):388-395.
- Tsukuba T, Okamoto K, Okamoto Y, Yanagawa M, Kohmura K, Yasuda Y, Uchi H, Nakahara T, Furue M, Nakayama K, Kadowaki T, Yamamoto K, Nakayama K I (2003). Association of cathepsin E deficiency with development of atopic dermatitis. *Journal of Biochemistry*, 134(6):893-902.
- Tuckett R P (1982). Itch evoked by electrical-stimulation of the skin. *Journal of Investigative Dermatology*, 79(6):368-373.
- Turk V, Stoka V, Vasiljeva O, Renko M, Sun T, Turk B, Turk D (2012). Cysteine cathepsins: From structure, function and regulation to new frontiers. *Biochimica et Biophysica Acta - Proteins and Proteomics*, 1824(1):68-88.

- Twycross R, Greaves M W, Handwerker H, Jones E A, Libretto S E, Szepietowski J C, Zyllicz Z (2003). Itch: scratching more than the surface. *Quarterly Journal of Medicine - An International Journal of Medicine*, 96(1):7-26.
- Uchytlova E, Spicarova D, Palecek J (2015). Single high-concentration capsaicin application prevents c-Fos expression in spinothalamic and postsynaptic dorsal column neurons after surgical incision. *European Journal of Pain*, 19(10):1496-1505.
- Ui H, Andoh T, Lee JB, Nojima H, Kuraishi Y (2006). Potent pruritogenic action of tryptase mediated by PAR-2 receptor and its involvement in anti-pruritic effect of nafamostat mesilate in mice. *European Journal of Pharmacology*, 530(1-2):172-178.
- Urashima R, Mihara M (1998). Cutaneous nerves in atopic dermatitis - A histological, immunohistochemical and electron microscopic study. *Virchows Archiv - An International Journal of Pathology*, 432(4):363-370.
- Urban J D, Clarke W P, von Zastrow M, Nichols D E, Kobilka B, Weinstein H, Javitch J A, Roth B L, Christophoulos A, Sexton P M, Miller K J, Spedding M, Mailman R B (2007). Functional selectivity and classical concepts of quantitative pharmacology. *Journal of Pharmacology and Experimental Therapeutics*, 320(1):1-13.
- Usoskin D, Furlan A, Islam S, Abdo H, Lonnerberg P, Lou D, Hjerling-Leffler J, Haeggstrom J, Kharchenko O, Kharchenko P V, Linnarsson S, Ernfors P (2015). Unbiased classification of sensory neuron types by large-scale single-cell RNA sequencing. *Nature Neuroscience*, 18(1):145-153.
- Valet M, Pfab F, Sprenger T, Woller A, Zimmer C, Behrendt H, Ring J, Darsow U, Tolle T R (2008). Cerebral processing of histamine-induced itch using short-term alternating temperature modulation - An fMRI study. *Journal of Investigative Dermatology*, 128(2):426-433.
- Valladeau J, Saeland S (2005). Cutaneous dendritic cells. *Seminars in Immunology*, 17(4):273-283.
- Valtcheva M V, Davidson S, Zhao C, Leitges M, Gereau R W (2015a). Protein kinase C delta mediates histamine-evoked itch and responses in pruriceptors. *Molecular Pain*, 11(1).
- Valtcheva M V, Samineni V K, Golden J P, Gereau R W, Davidson S (2015b). Enhanced Nonpeptidergic Intraepidermal Fiber Density and an Expanded Subset of Chloroquine-Responsive Trigeminal Neurons in a Mouse Model of Dry Skin Itch. *Journal of Pain*, 16(4):346-356.
- van der Fits L, Mourits S, Voerman J S A, Kant M, Boon L, Laman J D, Cornelissen F, Mus A M, Florencia E, Prens E P, Lubberts E (2009). Imiquimod-Induced Psoriasis-Like Skin Inflammation in Mice Is Mediated via the IL-23/IL-17 Axis. *Journal of Immunology*, 182(9):5836-5845.
- van Kasteren S I, Overkleeft H S (2014). Endo-lysosomal proteases in antigen presentation. *Current Opinion in Chemical Biology*, 23:8-15.
- Vasiljeva O, Dolinar M, Pungercar J R, Turk V, Turk B (2005). Recombinant human procathepsin S is capable of autocatalytic processing at neutral pH in the presence of glycosaminoglycans. *FEBS Letters*, 579(5):1285-1290.

Vellani V, Kinsey A M, Prandini M, Hechtfisher S C, Reeh P, Magherini P C, Giacomoni C, McNaughton P A (2010). Protease activated receptors 1 and 4 sensitize TRPV1 in nociceptive neurones. *Molecular Pain*, 6(61).

Veres-Szekely A, Pap D, Sziksz E, Javorszky E, Rokonay R, Lippai R, Tory K, Fekete A, Tulassay T, Szabo A J, Vannay A (2017). Selective measurement of a smooth muscle actin: why beta-actin can not be used as a housekeeping gene when tissue fibrosis occurs. *BMC Molecular Biology*, 18:12.

Verge V M K, Richardson P M, Wiesenfeldhallin Z, Hokfelt T (1995). Differential Influence of Nerve Growth-Factor on Neuropeptide Expression in-vivo - a Novel Role in Peptide Suppression in Adult Sensory Neurons. *Journal of Neuroscience*, 15(3):2081-2096.

Vergnolle N, Bunnett N W, Sharkey K A, Brussee V, Compton S J, Grady E F, Cirino G, Gerard N, Basbaum A I, Andrade-Gordon P, Hollenburg M D, Wallace J L (2001). Proteinase-activated receptor-2 and hyperalgesia: a novel pain pathway. *Nature Medicine*, 7(7):821-826.

Villadsen L S, Schuurman J, Beurskens F, Dam T N, Dagnaes-Hansen F, Skov L, Rygaard J, Voorhorst-Ogink M M, Gerritsen A F, van Dijk M A, Parren P W H I, Baadsgaard O, van de Winkel J G J (2003). Resolution of psoriasis upon blockade of IL-15 biological activity in a xenograft mouse model. *Journal of Clinical Investigation*, 112(10):1571-1580.

Villanova F, Flutter B, Tosi I, Gryk K, Sreeneebus H, Perera G K, Chapman A, Smith C H, Di Meglio P, Nestle F O (2014). Characterization of Innate Lymphoid Cells in Human Skin and Blood Demonstrates Increase of NKp44+ILC3 in Psoriasis. *Journal of Investigative Dermatology*, 134(4):984-991.

Vilotti S, Marchenkova A, Ntamati N, Nistri A (2013). B-Type Natriuretic Peptide-Induced Delayed Modulation of TRPV1 and P2X₃ Receptors of Mouse Trigeminal Sensory Neurons. *PLoS ONE*, 8(11):e81138.

Viodé C, Lejeune O, Turlier V, Rouquier A, Casas C, Ménégaud V, Redoulès D, Schmitt A M (2014). Cathepsin S, a new pruritus biomarker in clinical dandruff/seborrheic dermatitis evaluation. *Experimental Dermatology*, 23(4):274-275.

Vogelsang M, Heyer G, Hornstein O P (1995). Acetylcholine induces different cutaneous sensations in atonic and non-atopic subjects. *Acta Dermato-Venereologica*, 75(6):434-436.

Voets T, Prenen J, Vriens J, Watanabe H, Janssens A, Wissenbach U, Boddling M, Droogmans G, Nilius B (2002). Molecular determinants of permeation through the cation channel TRPV4. *Journal of Biological Chemistry*, 277(37):33704-33710.

Vu T K H, Hung D T, Wheaton V I, Coughlin S R (1991). Molecular-cloning of a functional thrombin receptor reveals a novel proteolytic mechanism of receptor activation. *Cell*, 64(6):1057-1068.

Wahlgren C F, Hägermark O, Bergström R (1990). The antipruritic effect of a sedative and a non-sedative antihistamine in atopic dermatitis. *British Journal of Dermatology*, 122(4):545-551.

Wan L, Jin H, Liu X Y, Jeffry J, Barry D M, Shen K F, Peng J H, Liu X T, Jin J H, Sun Y, Kim R, Meng Q T, Mo P, Yin J, Tao A L, Bardoni R, Chen Z F (2017). Distinct roles of NMB and GRP in itch transmission. *Scientific Reports*, 7:15466.

Wang Y Y, Chang R B, Waters H N, Mckemy D D, Liman E R (2008). The Nociceptor Ion Channel TRPA1 Is Potentiated and Inactivated by Permeating Calcium Ions. *Journal of Biological Chemistry*, 283(47):32691-32703.

Wang N, Gibbons C H, Freeman R (2011). Novel Immunohistochemical Techniques Using Discrete Signal Amplification Systems for Human Cutaneous Peripheral Nerve Fiber Imaging. *The Journal of Histochemistry and Cytochemistry*, 59(4):382-390.

Wang H, Wu X, Li J Y, Chai B X Wang J, Mulholland M W, Zhang W (2010). Functional protease-activated receptors in the dorsal motor nucleus of the vagus. *Neurogastroenterology and Motility*, 22:431–438.

Wang X D, Xiong L, Yu G T, Li D D, Peng T, Luo D Q, Xu J (2015). Cathepsin S silencing induces apoptosis of human hepatocellular carcinoma cells. *American Journal of Translational Research*, 7(1):100-110.

Wang X D, Zhang J, Eberhart D, Urban R, Meda K, Solorzano C, Yamanaka H, Rice D, Basbaum A I (2013). Excitatory Superficial Dorsal Horn Interneurons Are Functionally Heterogeneous and Required for the Full Behavioral Expression of Pain and Itch. *Neuron*, 78(2):312-324.

Ward C, Kuehn D, Burden R E, Gormley J A, Jaquin T J, Gazdoui M, Small D, Bicknell R, Johnston J A, Scott C J, Olwill S A (2010). Antibody Targeting of Cathepsin S Inhibits Angiogenesis and Synergistically Enhances Anti-VEGF. *PLoS ONE*, 5(9):e12543.

Watabe A, Sugimoto Y, Honda A, Irie A, Namba T, Negishi M, Ito S, Narumiya S, Ichikawa A (1993). Cloning and expression of cDNA for a mouse EP1 subtype of prostaglandin E receptor. *Journal of Biological Chemistry*, 268(27):20175–20178.

Watanabe T K, Katagiri T, Suzuki M, Shimizu F, Fujiwara T, Kanemoto N, Nakamura Y, Hirai Y, Maekawa H, Takahashi E (1996). Cloning and characterization of two novel human cDNAs (NELL1 and NELL2) encoding proteins with six EGF-like repeats. *Genomics*, 38(3):273-276.

Watari M, Watari H, Nachamkin I, Strauss J F (2000). Lipopolysaccharide induces expression of genes encoding pro-inflammatory cytokines and the elastin-degrading enzyme, cathepsin S, in human cervical smooth-muscle cells. *Journal of the Society for Gynecologic Investigation*, 7(3):190-198.

Weber H C (2015). Gastrointestinal peptides and itch sensation. *Current Opinion In Endocrinology Diabetes and Obesity*, 22(1):29-33.

Wedi B, Raap U, Lewrick H, Kapp A (1998). IL-4-induced apoptosis in peripheral blood eosinophils. *Journal of Allergy and Clinical Immunology*, 102(6):1013-1020.

Werfel T (2009). The Role of Leukocytes, Keratinocytes, and Allergen-Specific IgE in the Development of Atopic Dermatitis. *Journal of Investigative Dermatology*, 129(8), 1878-1891.

Wertz P W, van den Bergh B (1998). The physical, chemical and functional properties of lipids in the skin and other biological barriers. *Chemistry and Physics of Lipids*, 91(2):85-96.

White J P M, Cibelli M, Fidalgo A R, Paule C C, Anderson P J, Jenes A, Rice A S C, Nagy I (2010). Sensitization of the transient receptor potential vanilloid type 1 ion channel by isoflurane or sevoflurane does not result in extracellular signal-regulated kinase 1/2 activation in rat spinal dorsal horn neurons. *Neuroscience*, 166(2):633-638.

White J P M, Cibelli M, Urban L, Nilius B, McGeown J G, Nagy I (2016). Trpv4: molecular conductor of a diverse orchestra. *Physiological Reviews*, 96(3):911-973.

Wickett R R, Visscher M O (2006). Structure and function of the epidermal barrier. *American Journal of Infection Control*, 34(10):S98-S110.

Wiederanders B, Bromme D, Kirschke H, Vonfigura K, Schmidt B, Peters C (1992). Phylogenetic Conservation of Cysteine Proteinases - Cloning and Expression of a cDNA Coding for Human Cathepsin-S. *Journal of Biological Chemistry*, 267(19):13708-13713.

Willcockson H, Valtschanoff J (2008). AMPA and NMDA glutamate receptors are found in both peptidergic and non-peptidergic primary afferent neurons in the rat. *Cell and Tissue Research*, 334(1):17-23.

Wilson S R, Gerhold K A, Bifolck-Fisher A, Liu Q, Patel K N, Dong X, Bautista D M (2011). TRPA1 is required for histamine-independent, Mas-related G protein-coupled receptor-mediated itch. *Nature Neuroscience*, 14(5):595 -602.

Wilson S R, The L, Batia L M, Beattie K, Katibah G E, McClain S P, Pellegrino M, Estandian D M, Bautista D M (2013). The Epithelial Cell-Derived Atopic Dermatitis Cytokine TSLP Activates Neurons to Induce Itch. *Cell*, 155(2):285-295.

Wolfe B L, Marchese A, Trejo J (2007). Ubiquitination differentially regulates clathrin-dependent internalization of protease-activated receptor-1. *Journal of Biological Chemistry*, 177(5):905-916.

Woo D H, Jung S J, Zhu M H, Park C K, Kim Y H, Oh S B, Lee C J (2008). Direct activation of Transient Receptor Potential Vanilloid 1 (TRPV1) by Diacylglycerol (DAG). *Molecular Pain*, 4:42.

Woolf C J, Mannion R J, Neumann S (1998). Null mutations lacking substance: elucidating pain mechanisms by genetic pharmacology. *Neuron*, 20(6):1063-1066.

Xia Y P, Li B S, Hylton D, Detmar M, Yancopoulos G D, Rudge J S (2003). Transgenic delivery of VEGF to mouse skin leads to an inflammatory condition resembling human psoriasis. *Blood*, 102(1):161-168.

Xu W F, Andersen H, Whitmore T E, Presnell S R, Yee D P, Ching A, Gilbert T, Davie E W, Foster D C (1998). Cloning and characterization of human protease-activated receptor 4. *Proceedings of the National Academy of Sciences of the United States of America*, 95(12):6642-6646.

Xu P, Hall A K (2007). Activin Acts with Nerve Growth Factor to Regulate Calcitonin Gene-Related Peptide mRNA in Sensory Neurons. *Neuroscience*, 105(3):665-674.

Yagi R, Nagai H, Iigo Y, Akimoto T, Arai T, Kubo M (2002). Development of atopic dermatitis-like skin lesions in STAT6-deficient NC/Nga mice. *Journal of Immunology*, 168(4):2020-2027.

- Yamaguchi J, Aihara M, Kobayashi Y, Kambara T, Ikezawa Z (2009). Quantitative analysis of nerve growth factor (NGF) in the atopic dermatitis and psoriasis horny layer and effect of treatment on NGF in atopic dermatitis. *Journal of Dermatological Science*, 53(1):48–54.
- Yamaguchi Y, Hayashi Y, Sugama Y, Miura Y, Kasahara T, Kitamura S, Torisu M, Mita S, Tominaga A, Takatsu K, Suda T (1988). Highly Purified Murine Interleukin-5 (IL-5) Stimulates Eosinophil Function and Prolongs *in vitro* Survival - IL-5 as an Eosinophil Chemotactic Factor. *Journal Of Experimental Medicine*, 167(5):1737-1742.
- Yamaguchi T, Nagasawa T, Satoh M, Kuraishi Y (1999). Itch-associated response induced by intradermal serotonin through 5-HT₂ receptors in mice. *Neuroscience Research*, 35(2):77-83.
- Yan D Y, Wang H W, Bowman R L, Joyce J A (2016). STAT3 and STAT6 Signaling Pathways Synergize to Promote Cathepsin Secretion from Macrophages via IRE1 alpha Activation. *Cell Reports*, 16(11):2914-2927.
- Yarbrough K B, Neuhaus K J, Simpson E L (2013). The effects of treatment on itch in atopic dermatitis. *Dermatologic Therapy*, 26(2):110-119.
- Yaron J R, Gangaraju S, Rao M Y, Kong X, Zhang L, Su F, Tian Y, Glenn H L, Meldrum D R (2015). K⁺ regulates Ca²⁺ to drive inflammasome signaling: dynamic visualization of ion flux in live cells. *Cell Death and Disease*, 6:e1954.
- Yin H B, Tian Y, Luo R Y, Deng Y P (2017). Thymic Stromal Lymphopoietin Is Expressed in Human Corneal Stromal Cells and Secreted upon Protease-Activated Receptor 1 Activation. *IUBMB Life*, 69(8):606-610.
- Yoneda K, Nakagawa T, Lawrence O T, Huard J, Demitsu T, Kubota Y, Presland R B (2012). Interaction of the Profilaggrin N-Terminal Domain with Loricrin in Human Cultured Keratinocytes and Epidermis. *Journal of Investigative Dermatology*, 132(4):1206-1214.
- Yoo J, Omori M, Gyarmati D, Zhou B H, Aye T, Brewer A, Comeau M R, Campbell D J, Ziegler S F (2005). Spontaneous atopic dermatitis in mice expressing an inducible thymic stromal lymphopoietin transgene specifically in the skin. *Journal of Experimental Medicine*, 202(4):541-549.
- Yoshimoto T, Takeda K, Tanaka T, Ohkusu K, Kashiwamura S, Okamura H, Akira S, Nakanishi K (1998). IL-12 up-regulates IL-18 receptor expression on T cells, Th1 cells, and B cells: synergism with IL-18 for IFN-gamma production. *Journal of Immunology*, 161(7):3400-3407.
- Yoshioka T, Imura K, Asakawa M, Suzuki M, Oshima I, Hirasawa T, Sakata T, Horikawa T, Arimura A (2009). Impact of the Gly573Ser Substitution in TRPV3 on the Development of Allergic and Pruritic Dermatitis in Mice. *Journal of Investigative Dermatology*, 129(3):714-722.
- Yoshizawa Y, Nomaguchi H, Izaki S, Kitamura K (2002). Serum cytokine levels in atopic dermatitis. *Clinical and Experimental Dermatology*, 27(3):225-229.
- Yosipovitch G, Ansari N, Goon A, Chan Y H, Goh C L (2002). Clinical characteristics of pruritus in chronic idiopathic urticaria. *British Journal of Dermatology*, 147(1):32-36.

- Yosipovitch G, Goon A, Wee J, Chan Y H, Goh C L (2000). The prevalence and clinical characteristics of pruritus among patients with extensive psoriasis. *British Journal of Dermatology*, 143(5):969-973.
- Yosipovitch G, Zucker I, Boner G, Gafter U, Shapira Y, David M (2001). A questionnaire for the assessment of pruritus: Validation in uremic patients. *Acta Dermato-Venereologica*, 81(2):108-111.
- Yung K K (1998). Localization of glutamate receptors in dorsal horn of rat spinal cord. *Neuroreport*, 9(7):1639-1644.
- Zaba L C, Fuentes-Duculan J, Steinman R M, Krueger J G, Lowes M A (2007). Normal human dermis contains distinct populations of CD11c(+)BDCA-1(+) dendritic cells and CD163(+)FXIIIa(+) macrophages. *Journal of Clinical Investigation*, 117(9):2517-2525.
- Zaid A, Mackay L K, Rahimpour A, Braun A, Veldhoen M, Carbone F R, Manton J H, Heath W R, Mueller S N (2014). Persistence of skin-resident memory T cells within an epidermal niche. *Proceedings of the National Academy of Sciences of the United States of America*, 111(14):5307-5312.
- Zania P, Gourni D, Aplin A C, Nicosia R F, Flordellis C S, Maragoudakis M E, Tsopanoglou N E (2009). Parstatin, the cleaved peptide on proteinase-activated receptor 1 activation, is a potent inhibitor of angiogenesis. *Journal of Pharmacology and Experimental Therapeutics*, 328(2):378-389.
- Zhan I, Yang Y, Ma T T, Huang C, Meng X M, Zhang L, Li J (2015). Transient receptor potential vanilloid 4 inhibits rat HSC-T6 apoptosis through induction of autophagy. *Cell and Molecular Biology*, 402:9-22.
- Zhang X M, Huang J H, McNaughton P A (2005). NGF rapidly increases membrane expression of TRPV1 heat-gated ion channels. *EMBO Journal*, 24(24):4211-4223.
- Zhang L, Jiang G Y, Song N J, Huang Y, Chen J Y, Wang Q X, Ding Y Q (2014). Extracellular signal-regulated kinase (ERK) activation is required for itch sensation in the spinal cord. *Molecular Pain*, 7:25.
- Zhang F X, Liu X J, Gong L Q, Yao J R, Li K C, Li Z Y, Lin L B, Lu Y J, Xiao H S, Bao L, Zhang X H, Zhang X (2010). Inhibition of Inflammatory Pain by Activating B-Type Natriuretic Peptide Signal Pathway in Nociceptive Sensory Neurons. *Journal of Neuroscience*, 30(32):10927-10938.
- Zhang Q, Putheti P, Zhou Q, Liu Q S, Gao W D (2008). Structures and biological functions of IL-31 and IL-31 receptors. *Cytokine and Growth Factor Reviews*, 19(5-6):347-356.
- Zhao Z Q, Huo F Q, Jeffry J, Hampton L, Demehri S, Kim S, Liu X Y, Barry D M, Wan L, Liu Z C, Li H, Turkoz A, Ma K J, Cornelius L A, Kopan R, Battey J F, Zhong J, Chen Z F (2013). Chronic itch development in sensory neurons requires BRAF signaling pathways. *Journal of Clinical Investigation*, 123(11):4769-4780.
- Zhao P S, Lieu T, Barlow N, Metcalf M, Veldhuis N A, Jensen D D, Kocan M, Sostegni S, Haerteis S, Baraznenok V, Henderson I, Lindstrom E, Guerrero-Alba R, Valdez-Morales E E, Liedtke W, McIntyre P, Vanner S J, Korbmayer C, Bunnett N W (2014a). Cathepsin S Causes Inflammatory Pain via Biased Agonism of PAR(2) and TRPV4. *Journal of Biological Chemistry*, 289(39):27215-27234.

Zhao P S, Metcalf M, Bunnett N W (2014b). Biased signaling of protease-activated receptors. *Frontiers in Endocrinology*, 5(67).

Zhao Z Q, Wan L, Liu X Y, Huo F Q, Li H, Barry D M, Krieger S, Kim S, Liu Z C, Xu J B, Rogers B E, Li Y Q, Chen Z F (2014c). Cross-Inhibition of NMBR and GRPR Signaling Maintains Normal Histaminergic Itch Transmission. *Journal of Neuroscience*, 34(37):12402-12414.

Zheng T, Oh M H, Oh S Y, Schroeder J T, Glick A B, Zhu Z (2009). Transgenic expression of interleukin-13 in the skin induces a pruritic dermatitis and skin remodeling. *Journal of Investigative Dermatology*, 129(3):742-751.

Zheng T, Zhu Z, Wang Z D, Homer R J, Ma B, Riese R J, Chapman H A, Shapiro S D, Elias J A (2000). Inducible targeting of IL-13 to the adult lung causes matrix metalloproteinase-and cathepsin-dependent emphysema. *Journal of Clinical Investigation*, 106(9):1081-1093.

Zhong J, Li X Y, McNamee C, Chen A P, Baccarini M, Snider W D (2007). Raf kinase signaling functions in sensory neuron differentiation and axon growth *in vivo*. *Nature Neuroscience*, 10(5):598-607.

Zhu Y, Pan W H, Wang X R, Liu Y, Chen M, Xu X G, Liao W Q, Hu J H (2015). Tryptase and protease-activated receptor-2 stimulate scratching behavior in a murine model of ovalbumin-induced atopic-like dermatitis. *International Immunopharmacology*, 28(1):507-512.

Zhu Y, Peng C, Xu J G, Liu Y X, Zhu Q G, Liu J Y, Li F Q, Wu J H, Hu J H (2009). Participation of Proteinase-Activated Receptor-2 in Passive Cutaneous Anaphylaxis-Induced Scratching Behavior and the Inhibitory Effect of Tacrolimus. *Biological and Pharmaceutical Bulletin*, 32(7):1173-1176.

Zhu W J, Yamanaka H, Obata K, Dai Y, Kobayashi K, Kozai T, Tokunaga A, Noguchi K (2005). Expression of mRNA for four subtypes of the proteinase-activated receptor in rat dorsal root ganglia. *Brain Research*, 1041(2):205-211.

Zhu K J, Ye J, Wu M A, Cheng H (2010). Expression of Th1 and Th2 cytokine-associated transcription factors, T-bet and GATA-3, in peripheral blood mononuclear cells and skin lesions of patients with psoriasis vulgaris. *Archives of Dermatological Research*, 302(7):517-523.

Zhuo R G, Ma X Y, Zhou P L, Liu X Y, Zhang K, Wei X L, Yan H T, Xu J P, Zheng J Q (2014). Mas-related G protein-coupled receptor D is coupled to endogenous calcium-activated chloride channel in *Xenopus* oocytes. *Journal of Physiology and Biochemistry*, 70(1):185-191.

Zoudilova M, Min J, Richards H L, Carter D, Huang T, Defea K A (2010). Beta-Arrestins Scaffold Cofilin with Chronophin to Direct Localized Actin Filament Severing and Membrane Protrusions Downstream of Protease-activated Receptor-2. *Journal of Biological Chemistry*, 285(19):14318-14329.

Zygmunt P M, Ermund A, Movahed P, Andersson D A, Simonsen C, Jonsson B A G, Blomgren A, Birnir B, Bevan S, Eschalier A, Mallet C, Gomis A, Hogestatt E D (2013). Monoacylglycerols Activate TRPV1-A Link between Phospholipase C and TRPV1. *PLoS ONE*, 8(12):e81618.

Zylka M J, Rice F L, Anderson D J (2005). Topographically distinct epidermal nociceptive circuits revealed by axonal tracers targeted to MrgprD. *Neuron*, 45(1):17-25.